AFIT/GAE/ENY/92D-25

# SHOCK TUBE STUDY OF THE EFFECTS OF LARGE DENSITY DIFFERENCES AND BLOWING RATIO ON HEAT TRANSFER TO A FILM-COOLED FLAT PLATE

THESIS

Thomas A. Eads, Captain, USAF

AFIT/GAE/ENY/92D-25



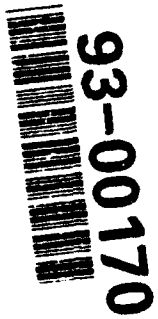



Approved for public release; distribution unlimited

AFIT/GAE/ENY/92D-25

# SHOCK TUBE STUDY OF THE EFFECTS OF LARGE DENSITY DIFFERENCES AND BLOWING RATIO ON HEAT TRANSFER TO A FILM-COOLED FLAT PLATE

THESIS

Presented to the Faculty of the School of Engineering

of the Air Force Institute of Technology

Air University

In Partial Fulfillment of the

Requirements for the Degree of

Master of Science in Aeronautical Engineering





Thomas A. Eads, B.S.

Captain, USAF

December 1992

## Preface

This study continues the film cooling research done in the AFIT Low Speed Shock Tube by previous researchers. Most of this research focused on building a reconfigurable test plate, calibration of thin-film heat flux gages, and verifying and extending previous researchers' work to include inclined holes and a greater density ratio. A more capable data acquisition system is in place with an associated data reduction program written in Fortran 77. Much effort was required to improve the shock tube so that gases other than dry filtered air could be used for studies.

Acknowledgements are in order, for completion of a project this size cannot be done without the help of many people. Thanks go to my advisor Dr. William C. Elrod, Major Jerry R. Bowman, and Dr. Paul I. King who were there to answer my questions. I thank Mr. John Brohas of the AFIT Model Fabrication shop for his extremely prompt and precise machining work. Also, I thank Mr. Andrew Pitts, Mr. Jay Anderson, and the AFIT/ENY Laboratory staff and previous students, for without their help completion of this thesis would have been impossible. They have spent untold hours preparing the instrumentation and shock tube for calibration and experimentation.

Finally, my special thanks go to my dear wife, Penni, and my four little children, Michael, Perry, Malena, and James, for their love, patience, and support of this undertaking while enduring the long hours I was gone.

Thomas A. Eads

Table of Contents


Page

Preface . . . . . ii

Table of Contents . . . . . iii

List of Figures . . . . . v

List of Tables . . . . . viii

List of Symbols . . . . . ix

Abstract . . . . . xiii

I. Introduction . . . . . 1.1

1.1 Background . . . . . 1.1
1.2 Problem . . . . . 1.2
1.3 Summary of Current Knowledge . . . . . 1.2
1.4 Objectives and Scope . . . . . 1.7
1.5 Methodology . . . . . 1.8

II. Theory . . . . . 2.1

2.1 The Shock Tube . . . . . 2.1
2.2 Mixtures of Gases . . . . . 2.4
2.3 Flat Plate Boundary Layer and Heat Transfer in the Shock Tube . . . 2.5
2.4 Electrical Analog For Heat Transfer . . . . . 2.9

III. Experimental Apparatus . . . . . 3.1

3.1 Shock Tube . . . . . 3.2
3.2 Instrumented Flat Plate . . . . . 3.3
3.3 Film Cooling System . . . . . 3.3
3.4 Shock Tube Gas Control System . . . . . 3.4
3.5 Data Acquisition System . . . . . 3.4
3.6 Instrumentation . . . . . 3.5
3.6.1 Pressure Transducers . . . . . 3.5
3.6.2 Thin-Film Resistance Gauges . . . . . 3.6

3.6.3 Bridge/Amplifier/Analog . . . . . 3.6

IV. Experimental Procedure . . . . . 4.1

4.1 Instrument Calibrations . . . . . 4.1
4.1.1 Calibration for Thin-Film Gauge Temperature Coefficient . . 4.1
4.1.2 Calibration of Heat Flux Gauges for $\sqrt{\rho C_p k}$ . . . . . 4.2
4.1.3 Calibration of Heat Flux Analog . . . . . 4.5
4.1.4 Calibration of Pressure Measuring Instruments . . . . . 4.7
4.2 Preparing the Shock Tube . . . . . 4.8
4.3 Shock Generation . . . . . 4.8
4.4 Data Collection . . . . . 4.10
4.5 Film Cooling . . . . . 4.11

V. Results and Discussion . . . . . 5.1

5.1 Heat Transfer Results Without Film Cooling . . . . . 5.4
5.2 Heat Transfer Results With Film Cooling . . . . . 5.6

VI. Conclusions . . . . . 6.1

VII. Recommendations . . . . . 7.1

Appendix A: Calibration of Thin-Film Resistance Gauges for Temperature Coefficient . . . . . A.1

Appendix B: Calibration of Thin-Film Resistance Gauges for Substrate Bulk Thermal Diffusivity $\sqrt{\rho C_p k}$ . . . . . B.1

Appendix C: Calibration of Pressure Measuring Instruments . . . . . C.1

Appendix D: Heat Flux Analog Circuit Calibration . . . . . D.1

Appendix E: Shock Tube Film Cooling Computer Program . . . . . E.1

Appendix F: Data Summary Worksheets . . . . . F.1

Bibliography . . . . . Bib.1

Vita . . . . . Vita.1

## List of Figures


| Figure | | Page |
|---|---|---|
| 1.1 | Film Cooling Effectiveness for Single Hole and Multiple Hole Injection at 35° for various blowing rates $M_b$ (Goldstein, 1971:373) | Fig.1 |
| 1.2 | Effect of Coolant Density on Film Effectiveness (from Pederson, 1977:626; Suo, 1985:299) | Fig.2 |
| 2.1 | (a) Simple shock tube<br>(b) An (x-t) diagram showing progress of the shock wave, the rarefaction fan and the contact surface separating driver and experimental gases<br>(c) The pressure distribution along the tube at time $t_1$<br>(d) The temperature distribution at time $t_1$<br>(Gaydon and Hurle, 1963:1) | Fig.3 |
| 2.2 | Boundary Layer Formation on a Flat Plate Behind a Shock Wave (combining Schlichting, 1979, 1979:440; Mirels, 1956:53) | Fig.4 |
| 2.3 | Derivation of the Electrical Analog of Heat Conduction (Schultz and Jones, 1973:37,38,111) | Fig.5 |
| 2.4 | The Heat Flux Analog (Rockwell, 1989) | Fig.6 |
| 3.1 | Test Plate in Low Pressure Shock Tube | Fig.7 |
| 3.2 | Instrumented Flat Plate | Fig.8 |
| 3.3 | Film Cooling Supply and Control System | Fig.9 |
| 3.4 | Shock Tube Gas Fill and Control, Driven Section | Fig.10 |
| 3.5 | Pressure Transducer and Thin-Film Gauge Locations in the Shock Tube | Fig.11 |
| 3.6 | Platinum Thin-Film Resistance Heat Transfer Gauge, Medtherm Instruments Model PTF-100-20293 | Fig.12 |
| 3.7 | Schematic of Heat Flux Analog Circuit and Bridge Connections | Fig.13 |
| 4.1 | Comparison of Measured and Theoretical Values of Bulk Thermal Diffusivity $\sqrt{\rho C_p k}$ for Corning Pyrex 7740 (Taken from Schultz and Jones, 1973:99) | Fig.14 |
| 4.2 | Gauge Holder for Calibration of Thin-Film Gauges | Fig.15 |
| 4.3 | Data Acquisition Set-up | Fig.16 |
| 5.1 | Output of Forward and Rear Pressure Transducers for Test T10 | Fig.17 |
| 5.2 | Temperature Output of Gauge No. 4 (in Volts), Test T10 | Fig.18 |
| 5.3 | Heat Flux Output, Test T10, Gauge 7 | Fig.19 |
| 5.4 | Heat Flux Output, Test T10, Gauge 3 | Fig.20 |
| 5.5 | Heat Flux Output, Test T10, Gauge 5 | Fig.22 |
| 5.6 | Flat Plate Turbulent Air Flow, St vs. $Re_x$ | Fig.22 |
| 5.6.1 | Flat Plate Turbulent Air Flow, St vs. $Re_x$ | Fig.23 |
| 5.6.2 | Flat Plate Turbulent Flow, Showing Effect of Uncovered Holes on Heat | |

| | | |
|---|---|---|
| | Transfer | Fig.24 |
| 5.7 | Air/Helium Flow, St vs. $Re_x$ | Fig.25 |
| 5.8 | Combined Results for Air and Air/Helium, St v. $Re_x$ | Fig.26 |
| 5.9 | Heat Flux and Film Cooling Pressure Output, Test T15 | Fig.27 |
| 5.10 | Film-Cooling Heat Transfer vs. Blowing Ratio (D.R. = 1.2, $M_2$ = 0.37) | Fig.28 |
| 5.11 | Film-Cooling Heat transfer vs. Blowing Ratio (D.R. = 2.1, $M_2$ = 0.34) | Fig.29 |
| 5.12 | Film-Cooling Heat Transfer vs. Velocity Ratio Parameter (D.R. = 2.1, $M_2$=0.34) | Fig.30 |
| 5.13 | Film-Cooling Heat Transfer vs. Velocity Ratio Parameter (D.R.=1.2 and 2.1, $M_2$=0.37 and 0.34) | Fig.31 |
| 5.14 | Correlation of Data for Four Injection-to-Mainstream Temperature Ratios, Single row of 30 deg Inclined Holes (Forth and Jones, 1986:1276) | Fig.32 |

| | | |
|---|---|---|
| A.1 | Heat Flux Gauge Temperature Coefficient Calibration Set-up | A.3 |
| A.2 | Calibration Curve for Gauge No. 1 | A.4 |
| A.3 | Calibration Curve for Gauge No. 2 | A.5 |
| A.4 | Calibration Curve for Gauge No. 3 | A.6 |
| A.5 | Calibration Curve for Gauge No. 4 | A.7 |
| A.6 | Calibration Curve for Gauge No. 5 | A.8 |
| A.7 | Calibration Curve for Gauge No. 6 | A.9 |
| A.8 | Calibration Curve for Gauge No. 7 | A.10 |

| | | |
|---|---|---|
| B.1 | Sqrt (rho$C_p$k) Calibration Output for Gauge No. 1 | B.5 |
| B.2 | Sqrt (rho$C_p$k) Calibration Curves for Gauge No. 1 (S/N 702) | B.6 |
| B.3 | Sqrt (rho$C_p$k) Calibration Output for Gauge No. 2 | B.7 |
| B.4 | Sqrt (rho$C_p$k) Calibration Curves for Gauge No. 2 (S/N 705) | B.8 |
| B.5 | Sqrt (rho$C_p$k) Calibration Output for Gauge No. 3 | B.9 |
| B.6 | Sqrt (rho$C_p$k) Calibration Curves for Gauge No. 3 (S/N 706) | B.10 |
| B.7 | Sqrt (rho$C_p$k) Calibration Output for Gauge No. 4 | B.11 |
| B.8 | Sqrt (rho$C_p$k) Calibration Curves for Gauge No. 4 (S/N 710) | B.12 |
| B.9 | Sqrt (rho$C_p$k) Calibration Output for Gauge No. 5 | B.13 |
| B.10 | Sqrt (rho$C_p$k) Calibration Curves for Gauge No. 5 (S/N 768) | B.14 |
| B.11 | Sqrt (rho$C_p$k) Calibration Output for Gauge No. 6 | B.15 |
| B.12 | Sqrt (rho$C_p$k) Calibration Curves for Gauge No. 6 (S/N 703) | B.16 |
| B.13 | Sqrt (rho$C_p$k) Calibration Output for Gauge No. 7 | B.17 |
| B.14 | Sqrt (rho$C_p$k) Calibration Curves for Gauge No. 7 (S/N 824) | B.18 |

| | | |
|---|---|---|
| C.1 | Calibration Curve for Forward Pressure Transducer | C.3 |
| C.2 | Calibration Curve for Rear Pressure Transducer | C.4 |
| C.3 | Calibration Curve for Film Cooling Pressure Transducer | C.5 |
| C.4 | Calibration of Bourdon Tube Pressure Gauge ($P_4$) | C.6 |

| | | |
|---|---|---|
| D.1 | Sample Output of Analog Circuit Calibration | D.2 |
| D.2 | Calibration of Heat Flux Analog Circuit No. 1 (31-820) | D.3 |

D.3 Calibration of Heat Flux Analog Circuit No. 2 (32-200) . . . . . D.4
D.4 Calibration of Heat Flux Analog Circuit No. 3 (31-850) . . . . . D.5
D.5 Calibration of Heat Flux Analog Circuit No. 4 (31-105) . . . . . D.6
D.6 Calibration of Heat Flux Analog Circuit No. 5 (31-790) . . . . . D.7
D.7 Calibration of Heat Flux Analog Circuit No. 6 (31-870) . . . . . D.8
D.8 Calibration of Heat Flux Analog Circuit No. 7 (32-100) . . . . . D.9

E.1 Calculated Density Ratio Versus Partial Pressure of Helium in Shock Tube for Min. Blowing (from Fortran Program STFCRT) . . . . . E.11

## List of Tables


| Table | | Page |
|---|---|---|
| 4.1 | Temperature Coefficients of the Heat Flux Gauges . . . . . | 4.2 |
| 4.2 | Bulk Thermal Diffusivity of the Heat Flux Gauges . . . . . | 4.5 |
| 4.3 | Calibration Constant of Analog Circuits . . . . . | 4.7 |
| 5.1 | Summary of Film Cooling Data . . . . . | 5.7 |

## List of Symbols

| Symbol | Description | Units |
|---|---|---|
| a | Sonic velocity | m/sec |
| c | Capacitance per unit length | μFarad/m |
| $C_p$ | Specific heat at constant pressure | J/kg-K |
| d | Diameter of cooling holes | mm (in.) |
| D | Diameter of flat plate leading edge | cm (in.) |
| D.R. | Density ratio ($\rho_c/\rho_\infty$) | |
| G | Electrical analog amplifier gain | |
| h | Convective heat transfer coefficient | $W/m^2$-K |
| HFC | Heat flux calibration constant | $W/m^2$/Volt |
| i | Current flow into analog circuit | Amperes |
| I | Momentum flux ratio ($\rho_c U_c^2/\rho_\infty U_\infty^2$) | |
| k | Thermal Conductivity | W/m-K |
| L | Hole length | mm (in.) |
| m | Slope of a calibration curve | |
| M | Mach number (U/a) | |
| $M_b$ | Mass flux (blowing ratio) parameter ($\rho_c U_c/\rho_\infty U_\infty$) | |
| MW | Molecular weight | kg/kmol |
| Nu | Nusselt number (hX/k) | |

| Symbol | Description | Units |
|---|---|---|
| p | Pitch or lateral hole-to-hole spacing | mm (in.) |
| P | Pressure | kPa (psi or in. Hg) |
| Pr | Prandtl number ($\mu C_p/k$) | |
| q | Heat flux | $W/m^2$ |
| r | Resistance per unit length | Ohm/m |
| $r_c$ | Recovery factor | |
| R | Gas constant ($\bar{R}$/MW) | J/kg-K |
| | Resistance | Ohm |
| $\bar{R}$ | Universal gas constant (8314.34) | J/kmol-K |
| Re | Reynolds number ($\rho U/\mu$) | 1/m |
| s | Laplace transform variable | |
| S | Sutherland constant | |
| St | Stanton number ($h/\rho UC_p$) | |
| t | Time | sec |
| T | Temperature | K (°R), °C (°F) |
| Tu | Turbulence intensity (longitudinal) | percent |
| U | Velocity | m/sec |
| u' | Velocity fluctuation (longitudinal direction) | m/sec |
| V | Electrical voltage or potential | Volt |
| V' | Voltage across resistor $R_1$ in analog circuit | Volt |
| x | Length, and distance from center of cooling hole | mm (in.) |

| Symbol | Description | Units |
|---|---|---|
| X | Distance from leading edge of flat plate | m (in.) |

Greek Letters

| | | |
|---|---|---|
| $\alpha$ | Thin film gauge temperature coefficient | $K^{-1}$ ($^{\circ}R^{-1}$) |
| $\gamma$ | Ratio of specific heats ($C_p/C_v$) | |
| $\Delta$ | Change in | |
| $\eta_f$ | Adiabatic film-cooling efficiency | |
| $\rho$ | Density | $kg/m^3$ |
| $\mu$ | Dynamic viscosity | Pa-sec |
| $\pi$ | Arithmetic constant (3.14159265359) | |
| $\Phi$ | Semi-empirical parameter for mixture viscosity or conductivity | |
| $\chi$ | Mole fraction | |
| $\omega$ | Frequency | rad/sec, Hz |
| $\sqrt{\rho C_p k}$ | Bulk thermal diffusivity | $J/m^2\text{-}K\text{-}sec^{1/2}$ |

Subscripts

| | |
|---|---|
| $_{air}$ | Air |
| $_{atm}$ | Atmospheric |
| $_{c}$ | Coolant |
| $_{avg}$ | Average |
| $_{gly}$ | Glycerin USP, 95% |

| | |
|---|---|
| He | Helium |
| mix | Mixture of gases |
| o | Without film cooling, or output (for voltage) |
| pyrex | Corning Pyrex®7740 |
| s | Shock, or Series, shunt (for Wheatstone bridge resistor) |
| subs | Substrate of thin-film gauge |
| v | Variable (potentiometer) |
| w | Wall |
| x | Local, or based on distance |
| 0 | Stagnation condition |
| 1 | Shock tube driven section (before shock) |
| 2 | Driven section (after shock), test mainstream condition |
| 4 | Driver section |
| ∞ | Free-stream or test mainstream condition |
| - | Average, or denoting Laplace transform variable |

## Abstract

The effects of coolant-to-mainstream density ratio (D.R.) and mass flux (blowing) ratio ($M_b$) on flat plate heat transfer were investigated in a shock tube. The round-nosed plate has a single row of holes inclined 35 deg downstream with two-diameter lateral spacing and a length-to-diameter ratio of three. Helium was mixed with air in the shock tube to produce a D.R. range of 1.2 to 2.1. The parameters studied represent operating conditions of film-cooled gas turbine engine components. For an $M_b$ range of 0.4 to 3 and 10% mainstream turbulence, surface temperature was measured with thin-film resistance gauges located 4 to 30 hole diameters downstream and converted to heat flux using an electrical analog.

Shock tube driver-to-driven pressure ratios were varied to produce different flow conditions over the flat plate. The "steady" portion of turbulent flow heat transfer test data compared within 20% of the theoretical flat plate solution. Ratios of heat flux with film cooling to heat flux without cooling versus $M_b$ and D.R. were determined.

Analysis of the results suggests film cooling heat transfer is correlated by the parameter involving coolant-to-mainstream velocity ratio and non-dimensional downstream distance $x/d(U_c/U_\infty)^{-4/3}$ proposed for "strong injection" through inclined holes by Forth and Jones (1986). However, comparison with their results showed effectiveness of cooling was reduced, or heat transfer increased, due to high mainstream turbulence.

# SHOCK TUBE STUDY OF THE EFFECTS OF LARGE DENSITY DIFFERENCES AND BLOWING RATIO ON HEAT TRANSFER TO A FILM-COOLED FLAT PLATE

## I. Introduction

### 1.1 Background

The Air Force and industry desire efficient and high performance aircraft engines. More efficient engines save fuel, and better performance leads to smaller engines with higher thrust. The demands for increased performance have required researchers and gas turbine designers to better understand the complex flow in gas turbine engines.

The improved performance of increasing the inlet temperature of the turbine has led to designs of turbines that can withstand the hotter gases. Turbine blades are cooled by using relatively cooler air drawn from the compressor. In practice, the cooling air is introduced through small holes on the blade surfaces forming a protective film. This practice is called film cooling.

In new aircraft engines, up to 20% of the compressor discharge airflow may be required for sufficient cooling (Suo, 1985:278), significantly reducing the hot-gas mass flow through the combustor. Such a substantial fraction of mass flow causes losses of turbine work and engine efficiency; however, Hill and Peterson (1986:394) state that losses are much smaller than the gains from operating the engine at much higher turbine inlet temperature.

## 1.2 Problem

An estimate of heat transfer to film-cooled blades, or film-cooling effectiveness, is required to determine how much cooling airflow is needed to keep the blade temperature acceptable, i.e. allowing the blade to remain structurally sound. Although film cooling has been used in modern turbine engines for many years, the parameters that maximize film-cooling effectiveness are not well understood and have vexed gas turbine designers and motivated researchers.

The flow in a turbine is highly turbulent with large temperature gradients. This flow, combined with film cooling and turbine blade geometry, makes analytical modeling of the heat transfer extremely difficult. "Analytical and computational models of film cooling do not represent the complex flow field with enough accuracy to provide reliable film-cooling data to design with." (Forth and Jones 1986:1271) Experimental research is required to analyze the phenomena, and many experimental investigations have been undertaken in order to produce design data. This requirement is typical of heat transfer problems.

## 1.3 Summary of Current Knowledge

In solving the problem of optimizing film-cooling effectiveness, simpler geometries such as the flat plate are studied to reduce the complexity of the flow and to determine the factors affecting heat transfer.

According to Kays and Crawford (1980:224-225) the major parameters affecting film-cooling effectiveness $\eta_f$ on a two dimensional (slot injection) adiabatic surface are blowing ratio $M_b$, slot height, and the distance downstream from the injection location x. The defining equation for $\eta_f$ is

$$\eta_f = \frac{T_{aw}-T_\infty}{T_c-T_\infty} \qquad (1.1)$$

where $T_{aw}$ is the adiabatic wall temperature, $T_\infty$ is the free-stream temperature, and $T_c$ is the cooling-fluid temperature; and the blowing parameter (or mass flux ratio) $M_b$ is defined as

$$M_b = \frac{\rho_c U_c}{\rho_\infty U_\infty} \qquad (1.2)$$

Further, for flow from rows of holes on a flat plate, Hill and Peterson (1992:397) state that $\eta_f$ (and Stanton number, or non-dimensional heat transfer) is a function of Pr, $Re_x$, p/d, and $M_b$, where $Re_x$ is the Reynolds number based on X, the distance from the leading edge of the flat plate, and p is the "pitch" or hole-to-hole spacing and p/d is the pitch-diameter ratio.

Goldstein (1971:321-379) consolidated the work of many researchers. He provided correlations from experimental studies of the effects of film-cooling on heat transfer. For inclined holes, a relationship of film-cooling effectiveness versus blowing ratio was established giving a maximum effectiveness at $M_b = 0.5$ (see Figure 1.1). However, few of the studies involved the high velocities, temperature ratios, and turbulence experienced in modern gas turbine engines. Also, he stated that much work still needed to "be done

experimentally to understand the effects of hole geometry, density differences, and the interaction of individual jets on the adiabatic wall temperature distribution. In addition, information on the effect of the mass addition on the local heat transfer is required." (Goldstein 1971:375)

Besides mass flux ratio and cooling hole geometry other fluid mechanical parameters governing the cooling interaction include coolant-to-freestream ratios of density, velocity, and momentum flux defined as

$$D.R. = \frac{\rho_c}{\rho_\infty} \qquad V.R. = \frac{U_c}{U_\infty} \qquad I = \frac{\rho_c U_c^2}{\rho_\infty U_\infty^2} \tag{1.3}$$

and curvature, rotation, and mainstream turbulence also have significant effects (Suo, 1985:300-303,322).

Pederson et. al (1977:620-627) used a mass transfer analogy on a plate with 35° inclined holes, p/d = 3, $M_b$= 0.2 to 2., D.R.=.75 to 4.17, and showed the density ratio has a strong effect on film effectiveness for injection through inclined holes. Qualitatively, film effectiveness increased with D.R., and the $M_b$ giving maximum effectiveness moved to higher values (see Figure 1.2).

Forth and Jones (1986:1271-1276) performed experiments in an Isentropic Light Piston Tunnel. They identified two flow regimes--a "weak" injection and a "strong" injection regime. For a single row of 30° inclined holes, strong injection was associated with jet lift off, occurring at I ≈ 0.1. Correlation of data for four injection-to-mainstream temperature ratios (or density ratios) was found for strong injection. Film-cooling data

collapsed when plotting ratio of Nusselt number with and without film cooling versus a scaling parameter of V.R. and non-dimensional distance given as

$$\frac{x/d}{(U_o/U_\infty)^{4/3}}$$

Data was for Mach 0.55 flow over an isothermal plate, more closely resembling that on a turbine blade.

Ammari et. al (1990:444-450) successfully correlated data to the same parameter of velocity ratio for heat transfer coefficients at density ratios of 1.0 and 1.51 on an isothermal plate in a mainstream velocity of 25 m/s. It was noted that for normal injection the heat transfer coefficient was insensitive to the variation of density ratios and scaled better with a blowing ratio distance parameter.

MacMullin (1989) and other researchers have shown that free-stream turbulence intensity increases heat transfer. Longitudinal turbulence intensity Tu is given by

$$Tu = (\overline{u'^2})^{1/2}/U_\infty$$

where u' is the longitudinal velocity fluctuation from the rms average velocity, $U_\infty$. Levels of 10 to 20 percent occur in a turbine engine (Rivir, 1987). The higher free-stream turbulence also causes a faster decay in film-cooling effectiveness down the plate (Jumper, 1987).

Researchers have used the shock tube to study high-temperature-ratio, high-turbulence-intensity flows. However, little research has been done on film-cooling using shock tubes.

At AFIT Jurgelewicz (1989) obtained heat transfer data on a film-cooled flat plate in a shock tube. He developed a numerical technique to obtain heat flux from thin-film heat-flux gauges mounted on the plate behind normal-injection cooling holes. Rockwell (1989) built analog electrical circuits to convert the gauge output voltage directly to wall heat flux potential. Gul (1991) expanded the data of Jurgelewicz to lower blowing ratios. Using the electrical analog circuits built by Rockwell, he studied the effect of varying blowing ratio and mainstream conditions. During the film-cooling studies, critical parameters of adiabatic wall temperature and/or heat transfer coefficient could not be determined due to the transient nature of the flow and the experimental setup.

The film-cooled flat plate of Jurgelewicz and Gul had a round leading edge and one row of 90° 1-mm-diameter film-cooling holes at 5.08 cm (2 in.) downstream of the leading edge with a lateral spacing p/d of two. Thin-film heat flux gauge spacing had low resolution and the limited operating gauges and data recording channels limited measurements to three or four locations downstream. A film cooling pressure transducer, located outside the test section, upstream of the chamber, may have influenced their calculation of blowing rates. Also, the cooling flow ran the length of the 25.5 in. aluminum plate arrangement essentially disallowing any difference between the cooling air temperature and the plate temperature. Measured background turbulence was high ranging from 9.4 to 9.6 percent by Gul (1991) and Rockwell (1989), respectively.

## 1.4 Objectives and Scope

The research goal was to determine the effectiveness of inclined-hole film cooling in reducing the heat transfer to the flat plate. The effect of varying cooling flow and mainstream flow parameters such as the velocity and density (and, thus, blowing rate) was determined with a coolant-to-freestream density ratio greater than one.

An attempt was made to determine a correlation between the measured flow parameters and a dimensionless heat transfer or film cooling effectiveness. Such a comparison is very important for any work in the heat transfer field, since most of the relations or equations used in this field are empirically derived.

Using the shock tube to induce high temperature turbulent flow over a flat plate, research was conducted to determine the effectiveness of film cooling on heat transfer in high free-stream turbulence and coolant-to-freestream density ratios greater than one.

The effect of film cooling on downstream heat transfer for different free-stream conditions was determined by varying the flow parameters of velocity, temperature, and density. Pressure regulation provided the velocity and density variation in the cooling flow. Shock speed was varied to provided a range of mainstream conditions, and the gas mixture in the shock tube was also varied to establish a greater density ratio between the cooling flow and free-stream flow. A cooling hole angle of 35° relative to the plate was used to be consistent with the literature and give a difference of data compared to Jurgelewicz (1989) and Gul (1991).

## 1.5 Methodology

In the pressurized driver section of the shock tube a diaphragm is ruptured generating a shock wave. The shock wave propagates down the tube (or tunnel) at supersonic speed into the driven section which is at a pressure lower than that of the driven section. It passes by the round leading edge of the flat plate, inducing a short-duration turbulent flow across the plate in the driven test section. The temperature suddenly rises causing heat to be transferred to the plate.

The transient nature of the shock tube can be a detriment. Because the flow lasts only a small fraction of a second, wide use of the shock tube as a research tool in fluid mechanics and heat transfer was limited until fast response instrumentation was developed. An advantage of the short-duration tests in the shock tube is elimination of the environmental cooling flow required to run similar tests in hot tunnel facilities.

For short-duration test conditions, fast response instrumentation is required to measure the flow and heat transfer. Medtherm thin-film resistance gauges made of a platinum film deposited on a Corning Pyrex 7740 substrate and Endevco Models 8530A-100 and 8510B-50 piezoresistive pressure transducers were used to meet this fast response requirement. The pressure transducers measure shock tube test section and film cooling cavity pressures and are used to determine the speed of the shock wave which is then used to calculate the velocity and temperature of the air behind the shock wave.

The test model is a blunt body with a semi-cylinder leading edge and a flat afterbody, simulating the leading edge of a gas turbine vane. The 1.905 cm (3/4 in.) diameter leading edge and the two 1.27 cm (1/2 in.) diameter instrumentation tubes in this

study create a flow area blockage of 20.7% in the shock tube. The cooling flow is dry filtered air supplied through a row of 1 mm diameter holes 5.08 cm (2 in.) from the round leading edge of the test model and inclined 35 degrees from the downstream direction.

The test model and area blockage compares to a study done by Mehendale, Han, and Ou (1991:843-850) in a wind tunnel which showed no influence of mainstream turbulence of up to 15% on the downstream turbulent flat plate heat transfer due to turbulence decay for $Re_D$ (based on leading edge diameter) up to 100,000. The point of interest is that a separation and reattachment location exists where the leading edge semi-cylinder merges with the flat plate (at X = 0.8 D). Laminar flow exists on the round nose and turbulent flow occurs upon reattachment of the boundary layer. Heat transfer is increased about 50% at the reattachment location but relaxes to the turbulent flat plate correlation by a downstream distance X = 1.4 D. This lends confidence to locating the film cooling holes at X = 3.0 D, as in this and past studies, to avoid leading edge effects and ensure turbulent flow. Nevertheless, a typical $Re_D$ in this study is 250,000, well above that studied by Mehendale.

# II. Theory

## 2.1 The Shock Tube

The shock tube is an apparatus used to produce a moving shock wave of desired strength by pressurizing one side of a diaphragm and rupturing it. The high pressure side is called the driver section and the low pressure side is the driven section. Figure 2.1 (a) shows a simple shock tube. The pressure wave moves into the driven section at a speed determined by the pressure ratio across the diaphragm and the properties of the gases in the two sections of the shock tube. Higher shock strengths are attained for higher driver-to-driven pressure ratios and "lighter" gases in the driver section. The driven section is typically labeled '1' and the driver section '4' depicting the separate regions after shock initiation. Referring to Figure 2.1 (b)-(d), the four conditions are discernible from patterns indicated by location versus time.

Upon rupturing the diaphragm, compression waves move into the driven section and coalesce to form a normal shock wave, while expansion waves move into the driver section. A contact discontinuity of temperature (and composition, if different gases are used) separates region 2 and 3. The higher pressure and temperature flow behind the shock wave, condition 2, is of prime interest as it established the conditions in the test section for this investigation. The test time is terminated when a fifth region occurs following a second passage of the shock after it reflects off the end wall.

Determination of the pressure, temperature, and velocity of the test condition is found from normal shock theory for ideal gases. Derivation of the equations is straight forward and can be found in many gas dynamics texts. It is useful to calculate the shock velocity from the pressure ratio across the diaphragm from John (1984: 114), Gaydon and Hurle (1963: 20), Glass (1958: 78), and Hall (1958: 142).

$$\frac{P_4}{P_1} = \frac{2\gamma_1 M_s^2 - \gamma_1 + 1}{\gamma_1 + 1} \left[ 1 - \frac{\gamma_4 - 1}{\gamma_1 + 1} \frac{a_1}{a_4} \left( M_s - \frac{1}{M_s} \right) \right]^{-\frac{2\gamma_4}{\gamma_4 - 1}} \qquad (2.1)$$

$M_s$ is the Mach number of the shock wave ($U_s/a_1$) and equals $M_1$, the Mach number of the gas upstream of the shock taken relative to the shock. $U_s$ is the velocity of the shock wave and $a_1$ is the velocity of sound in the driven section computed as $(\gamma_1 R_1 T_1)^{1/2}$. $\gamma$ is the ratio of specific heats, R is the gas constant, and T is the absolute static temperature. For a given pressure ratio $P_4/P_1$ across the diaphragm a theoretical $M_s$ can be computed by iteration of equation (2.1).

The actual value of $M_s$ decreases from the theoretical value as the shock wave propagates down the tube due to viscous interaction with the walls and real gas effects (small for low speeds). The measured $U_s$ may also vary from run to run if the diaphragm does not burst ideally. For more in-depth discussion of these effects the text by Gaydon (1963) or the references Glass (1958) and Hall (1958) can be referred to.

Given the theoretical $M_s$ or the measured $U_s$ and the gas composition, and knowing the driven section pressure $P_1$ and temperature $T_1$, the test condition pressure $P_2$, temperature $T_2$, and velocity $U_2$ may be computed.

For pressure, from Gaydon (1963:72)

$$\frac{P_2}{P_1} = \frac{2\gamma_1 M_s^2 - (\gamma_1 - 1)}{\gamma_1 + 1} \tag{2.2}$$

or from John (1984:114)

$$\frac{P_2}{P_1} = 1 + \frac{2\gamma_1}{\gamma_1 + 1}\left(\frac{U_s^2}{\gamma_1 R_1 T_1} - 1\right) \tag{2.3}$$

For temperature, from Gaydon (1963:17) or John (1984:42)

$$\frac{T_2}{T_1} = \frac{(\gamma_1 M_s^2 - \frac{\gamma_1 - 1}{2})(\frac{\gamma_1 - 1}{2} M_s^2 + 1)}{(\frac{\gamma_1 + 1}{2} M_s)^2} \tag{2.4}$$

For velocity, from Gaydon (1963:25)

$$U_2 = \frac{2a_1}{\gamma_1 + 1}\left(M_s - \frac{1}{M_s}\right) \tag{2.5}$$

or, similarly, from John (1984:114)

$$U_2 = \frac{2}{\gamma_1 + 1}\left(U_s - \frac{\gamma_1 R_1 T_1}{U_s}\right) \tag{2.6}$$

Density has similar relationships, but the same results come from the ideal gas law $\rho_2 = P_2/(R_1 T_1)$.

## 2.2 Mixtures of Gases

For accurate shock tube calculations the ratio of specific heats and gas constant must be known. These values can be found in tables for individual dilute gases (and air of standard composition) at atmospheric conditions. The values $\gamma_{mix}$ and $R_{mix}$ for mixtures of gases can be computed based on the mole fractions or partial pressures of the gases. The molecular weight of the mixture is computed from (White, 1991:32)

$$MW_{mix} = \sum_i \chi_i MW_i \tag{2.7}$$

where $\chi_i$ and $MW_i$ are the mole fraction and molecular weight of a component of the mixture, respectively. Mixture gas constant is then computed by $R_{mix} = \bar{R}/MW_{mix}$ where $\bar{R}$ is the universal gas constant. The mass averaged weighted specific heat is computed from

$$C_{p_{mix}} = \sum_i \chi_i C_{p_i} \frac{MW_i}{MW_{mix}} \tag{2.8}$$

Finally, mixture ratio of specific heats is now easily determined from

$$\gamma_{mix} = C_{p,\,mix}/(C_{p,\,mix} - R_{mix}).$$

Properties of viscosity and conductivity for the mixture are needed for later calculations. These properties are given by a semi-empirical formula derived from the kinetic theory of gases by C. R. Wilke and quoted as follows by Bird, et al (1960:24) and White (1991:35)

$$\mu_{mix} \approx \sum_i \frac{\chi_i \mu_i}{\sum_j \chi_j \Phi_{ij}} \tag{2.9}$$

where

$$\Phi_{ij} = \frac{\left[1 + \left(\frac{\mu_i}{\mu_j}\right)^{1/2} \left(\frac{MW_j}{MW_i}\right)^{1/4}\right]^2}{\sqrt{8}\left(1 + \frac{MW_i}{MW_j}\right)^{1/2}} \tag{2.10}$$

Bird states that this formula has "shown to reproduce measured values of $\mu_{mix}$ within an average deviation of two per cent." Also, the dependence on composition is extremely nonlinear, but calculation is good above 100 K for nonpolar gases and gas mixtures at low density.

For thermal conductivity, $k_{mix}$, equations (2.9) and (2.10) are used, but $\mu_i$ is replaced by $k_i$ (White, 1991:36).

## 2.3 Flat Plate Boundary Layer and Heat Transfer in the Shock Tube

As the shock wave passes through the shock tube test section, the flow induced behind the shock causes a boundary layer to develop on the test plate due to friction, or viscous interaction. The layer begins to develop at different moments (Schlichting, 1979:439-443; Mirels, 1956), as depicted by Figure 2.2 shown highly exaggerated. At time t the flow is unsteady for locations between $X = U_2 t$ and $X = U_s t$. The flow is steady between $X = 0$ and $X = U_2 t$, ignoring the shock reflection from the leading edge of the plate and the boundary layer developing on the shock tube walls.

The two-dimensional bounded flow, due to Prandtl, assumes the viscous effects are confined to a thin layer at the boundary. Outside the boundary layer the shearing effects of viscosity have negligible effect on the flow and potential flow solutions are adequate. Additionally, boundary layer theory gives constant pressure through the layer, being imposed by the free-stream.

The profile of velocity and temperature are depicted in Figure 2.2, also. The velocity decreases from the mainstream value to zero at the wall. The temperature varies from the freestream value to the wall temperature. The momentum or velocity boundary layer and thermal boundary layer thicknesses are not necessarily equal in a laminar flow, being dependent on the ratio of viscous to thermal diffusion, or Prandtl number. However, for turbulent flow the eddies feeding from the mainstream dissipate toward the wall causing mixing in the boundary layer and making the momentum and thermal thicknesses essentially the same.

At a given location X on the plate, laminar flow is initiated as the shock passes. The flow quickly transitions to turbulent flow which becomes steady by time $t \approx X/U_2$ at which time there is no memory of the shock passage. The steady portion is of interest in this study.

The wall temperature is dependent on the temperature gradient, the flow conditions, and the wall heat flux. For an insulated wall the heat flux is zero, and the wall would assume an adiabatic wall temperature $T_{aw}$ which is close to the stagnation temperature of the freestream for low speed flow. For high speed flow the temperature

does not recover to the freestream stagnation value. A recovery factor $r_c$ accounts for this in the equation (Eckert, 1955:586)

$$T_{aw} = T_\infty + r_c \frac{U_\infty^2}{2C_p}$$

or equally

$$T_{aw} = T_\infty [1 + r_c \frac{(\gamma_1 - 1)}{2} M_\infty^2] \tag{2.11}$$

A local heat transfer coefficient without film cooling $h_o$ is defined by (Eckert, 1955:586)

$$h_o = \frac{q_w}{T_{aw} - T_w} \tag{2.12}$$

where $q_w$ is the wall heat flux, and $T_w$ is the wall temperature.

The standard turbulent flat plate correlation for heat transfer with constant wall temperature, no film cooling, and no free-stream turbulence is (Kays and Crawford, 1980:213)

$$St\ Pr^{0.4} = 0.0287\ Re_x^{-0.2} \tag{2.13}$$

where St is the Stanton number, or non-dimensional heat transfer, defined by

$$St = \frac{h_o}{\rho_\infty U_\infty C_{p_\infty}} \tag{2.14}$$

Pr is the Prandtl number, and $Re_x$ is the Reynolds number based on distance from the leading edge and mainstream conditions.

In a high velocity flow and/or large temperature gradient the fluid properties vary through the boundary layer. Eckert (1955:585,586) found that using the relationships for constant property fluids and introducing properties at a proper reference temperature described friction factors and heat transfer coefficients on a flat plate with constant wall temperature with satisfactory agreement with measurements on supersonic turbulent boundary layers. The proposed reference temperature is

$$T^* = 0.5(T_\infty + T_w) + 0.22 r_c \frac{\gamma_1 - 1}{2} M_\infty^2 T_\infty \tag{2.15}$$

The recovery factor for turbulent flow is given by (White, 1991:556; Mirels, 1956:23; Eckert, 1955:587)

$$r_c = \sqrt[3]{Pr^*} \tag{2.16}$$

where Pr is evaluated at the reference temperature. An iteration is implied here, but since Pr is not a strong function of temperature convergence is rapid. In this study, the recovery factor used in the reference temperature equation is calculated from a Prandtl number based on $\gamma_1$ given by White (1991:31) as $Pr = 4\gamma_1 / (7.08\gamma_1 - 1.8)$.

With high mainstream turbulence the heat transfer is increased through the turbulent boundary layer. Simonich and Bradshaw (1978:676) gave the correlation such that heat transfer increases 5% for each 1% of turbulence intensity, Tu.

$$\frac{St}{St_{(Tu=0)}} = 1 + 5\,Tu \qquad (2.17)$$

## 2.4 Electrical Analog For Heat Transfer

Processing surface temperature information is required to determine the flow of heat into the surface, or wall heat flux. The flow of heat into the semi-infinite material is analogous to the current flow into a transmission line or a medium containing distributed capacity and resistance. The derivation here is taken from Schultz and Jones (1973:37,38,111) and Rockwell (1989:2.6-2.9).

By paralleling the equations governing the one-dimensional heat flow and current flow, the analogy may be seen (Figure 2.3). Thus, the heat conduction partial differential equation

$$\frac{\partial T}{\partial t} = \frac{k}{\rho C_p}\frac{\partial^2 T}{\partial x^2} \qquad (2.18)$$

and the current transmission partial differential equation

$$\frac{\partial V}{\partial t} = \frac{1}{rc}\frac{\partial^2 V}{\partial x^2} \qquad (2.19)$$

can be combined. In practice, the combination of the thin-film gauge and electrical analog circuit (Figure 2.4) obtains wall heat flux $q_w$ proportional to the output voltage of the electrical analog $V_{out}$ as

$$q_w = \sqrt{\rho C_p k}_{probe} \sqrt{\frac{r}{c}} \frac{1}{V_o \alpha} \frac{V_{out}}{GR_1} \qquad (2.20)$$

where $\rho$, $C_p$, and $k$ are properties of the thin-film gauge substrate; $r$ and $c$ are analog block resistor and capacitor values; $V_o$ is the applied voltage to the thin film of temperature coefficient $\alpha$; and $R_1$ is a resistor through which the current flows and across which the output voltage $V'_{out}$ is taken and amplified by the factor $G$ to obtain $V_{out}$.

## III. Experimental Apparatus

The facilities and equipment are similar to that used by Gul and Jurgelewicz (Gul, 1991; Jurgelewicz, 1989). Differences include (1) A different test plate with 35 deg inclined holes and pressure transducer at film cooling cavity, (2) Removal of turbulence generator between last two four-foot sections of the shock tube, (3) Use of test section with window at leading edge of test plate, (4) Installation of helium lines, (5) Removal of dump tank to reduce amount of helium required, and (6) Use of a new data acquisition system with more data channels.

A test plate was fabricated for 35° inclined holes with length-to-diameter ratio of 3 and a lateral hole spacing of 2 diameters. Heat flux gauges were located closer to the cooling holes to achieve higher resolution than previous studies. The instrumentation leads were removed from the path of shock impact. The plate was made reconfigurable to allow for different hole geometries.

The available support equipment and circuitry allowed seven thin-film resistance gauges to be mounted on the test plate. Much data reduction time was saved by using the heat transfer analog circuits built by Rockwell (1989) to convert the amplified output of the gauges into voltage proportional to heat flux. This electrical analog circuit has proven to be useful and accurate in the research done by Rockwell (1989) and Gul (1991).

A Nicolet data acquisition system was employed to increase the range of data that can be taken in a test run, thus helping to ensure all gauge information can be recorded and stored. This also required development of a data reduction program different from the program POST used with the Datalab DL1200 recorder by Rockwell and Gul.

A shock tube gas control system was developed to adjust a helium and air mixture to give repeatable results at the desired density ratios.

## 3.1 Shock Tube

The AFIT low-pressure shock tube is used in this research (Figure 3.1). The shock tube has two main sections: a four-foot-long driver section, and a 16-foot-long-driven section which includes a four-foot test section. The driver and driven sections are separated by a mylar diaphragm. Only 0.005 inch thick mylar was used for test runs in this study.

The driven section is movable in the horizontal plane to facilitate diaphragm changing and removal of expended mylar pieces. The driver and driven sections are locked together by hand pump-driven hydraulic actuators.

Driver pressure ($P_4$) is measured using a calibrated bourdon tube pressure gauge. After pressurizing the driver section to the desired pressure from the 100 psi-maximum facility air compressor, the diaphragm is ruptured using a pneumatically actuated/controlled plunger to initiate the shock.

The test plate is located at the mid-line of the 8-inch-inside-height of the shock tube with the leading edge 12 ft. 2.8 in. from the diaphragm interface (see Figure 3.1).

## 3.2 Instrumented Flat Plate

The test model used in this study is a flat plate with a round leading edge and 41 1-mm-diameter cooling holes (see Figure 3.2). The o-ring-sealed plate insert is instrumented with seven platinum thin-film resistance heat flux gauges, and a 50-psig pressure transducer in the film-cooling chamber. The heat flux gauges were surface mounted in the middle of the plate downstream of and laterally centered on cooling holes. The instrument leads exit the plate through either of two 1/2-inch-O.D. tubes leading down through the shock tube wall.

The test plate is 1.915 cm (0.750 in.) thick, 10.16 cm (4.00 in.) wide, and 64.8 cm (25.5 in.) long. Cooling flow is supplied through two 3/8-inch-O.D. x 5/16-inch-I.D. tubes to the cooling chamber and issues at 35 deg from horizontal through one laterally-centered row of 1-mm (0.040 in.) holes. At the hole exit the center is located 5.08 cm (2.00 in.) from the leading edge of the plate. The holes are spaced at two diameters and have a length-to-diameter ratio of 3.05. The cooling flow consists of dry filtered air.

## 3.3 Film Cooling System

The film-cooling supply and control system is depicted in Figure 3.3. Control pressure is set with the regulator on the high pressure cylinder. The control pressure is applied to a Grove Instruments dome valve by switching 120-Volt power to the solenoid valve, which switching turns on the cooling flow.

A 1/4-turn hand-operated valve is located downstream of the dome valve to close off the line when the shock tube is evacuated below atmospheric pressure. When the

solenoid valve is de-energized, atmospheric pressure is applied to the dome valve control side allowing flow through the dome valve if vacuum pressure is allowed at the outlet.

## 3.4 Shock Tube Gas Control System

The gas fill and control system for the driven section is depicted in Figure 3.4. The W. C. Heraeus type E-70 vacuum pump is driven by a 3-phase motor and controlled with a push on/push off control switch mounted on the shock tube control panel (containing control valves, $P_4$ gauge, and plunger pressure regulator, gauge and actuator lever). The two-inch line between the pump and the driven section contains a 1/4-turn valve to close the pump off from the shock tube and to seal the pump from leaking back into the evacuated driven section upon turning it off for helium fill.

The helium fill control switch, mounted near the control panel, switches 120 Volt to the 3/32-inch orifice solenoid valve to allow helium to flow through the lines into the shock tube at three locations. Upon raising the pressure with helium to give the desired partial pressure a valve above the test section was quickly opened to purge the remaining helium from the lines with room air and promote mixing as the pressure was raised to the atmospheric level.

## 3.5 Data Acquisition System

The Nicolet System 500 Data Acquisition System is a high-speed analog/digital recorder and is used to record the voltage outputs from the instruments. This recorder can receive up to twenty channels of data simultaneously.

The Data Acquisition Unit Pedestal has a Nicolet model 540 CPU and five model 514 digitizer boards with four channels each. The data is acquired, stored, and analyzed with Nicolet System 500 software version 6.1 running on a DTK model KEEN-2000 80386 computer with Windows®3.0.

Data can be acquired by triggering automatically, continuously, by individual board trigger levels, or by all boards triggering off of a bus trigger set by one or a combination of other channels. Each channel input voltage level can be selected individually, labeled with units, and multiplied by a scalar and added to an offset, giving output in actual calibrated engineering units. Pre-triggering can be selected, and rates as fast as one μsec per data point for up to 66,295 data points can be taken. This study used 2 μsec per point for 5000 data points or 10 msec of acquisition time for test runs to have good resolution between points yet limit the size of files.

## 3.6 Instrumentation

3.6.1 Pressure Transducers. Endevco Models 8530A-100 and 8510B-50 pressure transducers are used for measuring shock tube driven section and film cooling pressures, respectively. The transducers are connected to Endevco Model 4423 Signal Conditioner and power supply modules with four-wire shielded cable. Location of transducers and gauges in the shock tube can be seen in Figure 3.5.

3.6.2 Thin-Film Resistance Gauges. The Medtherm thin-film resistance gauges are made of a platinum film, ~0.4 mm wide and 0.1 μm thick, vapor deposited on a Corning Pyrex 7740 substrate (see Figure 3.6). The copper leads are coated in an insulating enamel. The gauges are flush-mounted in the middle of the test plate with small 1-72 UNF-3A nuts and connected in a constant voltage Wheatstone bridge through shielded, twisted-wire cable.

3.6.3 Bridge/Amplifier/Analog. The thin-film heat flux gages were connected to the Transamerica Model PSC 8115 bridge supply modules with 2.5 V dc voltage applied to the bridge (see Figure 3.7). The output of these bridge modules is amplified (required due to the low output) and filtered (to increase the signal-to-noise ratio) by the programmable PSC 8015-1 high gain differential DC amplifier modules. The amplified output is converted into voltage proportional to heat flux using the heat transfer analog circuits designed by Rockwell (1989). Figure 3.7 and Appendix D give some details on the analog circuits, but a full description of the construction is given by Rockwell (1989). Seven sets of the bridge supply modules, amplifier modules, and analog circuits are available, which allow seven thin-film gauges to be mounted on the test plate.

# IV. Experimental Procedure

As in most experimental work, much time was spent becoming familiar with the equipment. To ensure accurate data, time consuming calibrations were performed for the gauges and transducers used in the shock tube. Past research (Gul, 1991:45; Rockwell, 1989:5.11) showed that errors as high as 20% can be introduced by using values from properties tabulated in the literature for the thin-film gauges. Figure 4.1 shows a comparison of theoretical properties for Corning Pyrex 7740 to those measured by Hartunian and Varwig, as presented by Schultz and Jones (1973:99).

## 4.1 Instrument Calibrations

Standardized calibration procedures were followed for each instrument calibration. These calibrations provide a measure of confidence in the experimental measurements.

4.1.1 Calibration for Thin-Film Gauge Temperature Coefficient. The calibration method used allows calibration of all gauges at one time, using a gauge holder, a thermal mixer, and the Nicolet System 500. Figure 4.2 shows a drawing of the gauge holder apparatus used to secure the gauges during the calibration. Appendix A describes the setup and procedure in detail, and the desired temperature coefficients are summarized in Table 4.1 for the seven heat flux gauges.

Table 4.1

Temperature Coefficients of the Heat Flux Gauges

| Gauge Number | Gauge Serial Number | $V_o \alpha$ mVolt/°R | Temp. Coeff Volt/K |
|---|---|---|---|
| 1 | 702 | 22.32 | 0.04017 |
| 2 | 705 | 17.57 | 0.03162 |
| 3 | 706 | 17.65 | 0.03176 |
| 4 | 710 | 18.82 | 0.03387 |
| 5 | 768 | 26.12 | 0.04701 |
| 6 | 703 | 16.22 | 0.02919 |
| 7 | 824 | 30.92 | 0.05566 |

4.1.2 Calibration of Heat Flux Gauges for $\sqrt{\rho C_p k}$. The bulk thermal diffusivity ($\sqrt{\rho C_p k}$) calibration technique given by Schultz and Jones (1973:23-25) and used by Gul (1991) is also used in this study. The technique consists of passing a constant current through the gauge for a short time so that ohmic heating within the film produces a change in resistance. Serious errors (approx. 15%) can result if only a single calibration in vacuum

is performed, due to a requirement to measure the film surface area; so, to avoid this error, a double calibration is performed (Schultz and Jones 1973:24).

The gauge is first pulse calibrated in air. Then, the film is immersed in a fluid of known thermal properties, such as glycerin, and pulse calibrated identically to that in air. Using this technique Gul found that the $\sqrt{\rho C_p k}$ values for the heat flux gauges were higher than the theoretical value for the gauge substrate (Corning Pyrex 7740) and that the $\sqrt{\rho C_p k}$ values varied from gauge to gauge. The difference of values compares well to Figure 4.1, taken from Schultz and Jones (1973:99). Also, the variance of $\sqrt{\rho C_p k}$ for Pyrex is given by Scott (1976:388) as

$$\sqrt{\rho C_p k} = 1520 \frac{W}{m^2 \cdot K \cdot sec^{1/2}} \pm 5\%$$

Details of the calibration done in this study are found in Appendix B. Plots of the parabolic voltage output versus time for the seven gauges calibrated and the linear change in voltage output versus the square root of time are provided. The slopes of the change in voltage versus the square root of the time for the cases of air and glycerin are then used in the following equation to determine the $\sqrt{\rho C_p k}$ value of the gauge substrate (Schultz and Jones, 1973:24; Gul, 1991:28, 29, App. A):

$$\sqrt{(\rho C_p k)}_{sub} = \frac{\sqrt{(\rho C_p k)}_{gly}}{\frac{(\Delta V/\sqrt{t})_{air}}{(\Delta V/\sqrt{t})_{gly}} - 1}$$

where the bulk thermal diffusivity for glycerin is (Schultz and Jones, 1973:25; Incropera and DeWitt, 1981:780):

$$\sqrt{(\rho C_p k)}_{gly} = 925 \frac{J}{m^2 K \sqrt{sec}} \pm 4\%$$

Nominally a value of 930 $J/m^2Ksec^{1/2}$ was used for the temperature at which calibrations were performed. Table 4.2 shows the values of the bulk thermal diffusivity for the Pyrex substrate along with the slopes of the change in voltage versus square root of time for the seven gauges used in this research.

Table 4.2

Bulk Thermal Diffusivity of the Heat Flux Gauges

| Gauge Number | Serial Number | $\Delta V_{air}/\sqrt{t}$ Volt/sec$^{1/2}$ | $\Delta V_{gly}/\sqrt{t}$ Volt/sec$^{1/2}$ | $\sqrt{\rho C_p k}$ J/m$^2$Ksec$^{1/2}$ |
|---|---|---|---|---|
| 1 | 702 | 12.802 | 8.027 | 1563 |
| 2 | 705 | 8.678 | 5.402 | 1534 |
| 3 | 706 | 11.689 | 7.258 | 1525 |
| 4 | 710 | 12.780 | 8.028 | 1571 |
| 5 | 768 | 11.390 | 7.118 | 1551 |
| 6 | 703 | 11.906 | 8.309 | 2151 |
| 7 | 824 | 23.387 | 14.229 | 1447 |

All values compare well to the 1520 J/m$^2$Ksec$^{1/2}$ ± 5% value except for gauge No. 6. Its value seems high, but later we'll see that the measurements of heat transfer fall in line with that of the other gauges.

4.1.3 Calibration of Heat Flux Analog. Recalling that the output of the electrical analog is proportional to the heat flux seen by the thin-film gauge, equation (2.20), we see the proportionality is not complete without the value $\sqrt{r/c}\,/(R_1G)$ from the analog circuits.

A calibration of the electrical analog circuits provides the necessary information. The following derivation for calibration comes from Schultz and Jones (1973:38) and Rockwell (1989).

In Figure 2.3, the solution of equation (2.19) is an equation for the Laplace transform of current $\bar{i}$. Taking the inverse Laplace transform of this equation applied to the input of the electrical analog (figure 2.4) obtains

$$i_{input} = \sqrt{\frac{c}{r}}\,\sqrt{\omega}\; V_{input}$$

where $\omega$ is frequency in rad/sec. Since $V'_{out} = i_{input}\, R_1$ and $V_{out} = G\, V'_{out}$ it follows that

$$\frac{V_{out}}{V_{input}} = G\, R_1 \sqrt{\frac{c}{r}}\,\sqrt{\omega}$$

An electrical calibration of the analog circuit with a gain measurement $V_{out}/V_{in}$ at known frequencies gives the parabolic relationship to $\omega$ for the working frequency range of the circuit. Thus, the slope m of the linear curve plotting $V_{out}/V_{in}$ vs. $\sqrt{\omega}$ gives the values needed for equation (2.20) which becomes

$$q_w = \frac{\sqrt{\rho\, C_p\, k_{probe}}}{m\, V_o \alpha}\, V_{out} \qquad (4.1)$$

Appendix D further describes the calibration of the heat flux analog circuits and gives the associated plots. Table 4.3 gives the determined values of $m = (R_1 G)\sqrt{c/r}$

with the correlation coefficient and associated top frequency for working range of each analog circuit. [Note: Designed values were r/c = $1.9\times10^{10}$ , $R_1$ = 100 Ω , G = 300 Rockwell (1989)]

Table 4.3

Calibration Constant of Analog Circuits

| Circuit No. | Serial Number | Slope m $Hz^{-1/2}$ | Correlation Coefficient | Top Freq. kHz | Slope m $(rad/s)^{-1/2}$ |
|---|---|---|---|---|---|
| 1 | 31-820 | 0.7245 | 0.9994 | 40 | 0.2890 |
| 2 | 32-200 | 0.6958 | 0.9991 | 25 | 0.2776 |
| 3 | 31-850 | 0.7312 | 0.9992 | 35 | 0.2917 |
| 4 | 31-105 | 0.7401 | 0.9994 | 40 | 0.2953 |
| 5 | 31-790 | 0.7865 | 0.9991 | 40 | 0.3138 |
| 6 | 31-870 | 0.8030 | 0.9993 | 15 | 0.3204 |
| 7 | 32-100 | 0.7319 | 0.9991 | 35 | 0.2920 |

4.1.4 Calibration of Pressure Measuring Instruments. Each instrument for measuring pressure used in calculations was calibrated. Appendix C describes the calibrations with

a dead-weight tester in detail. Plots of output voltage versus input pressure are included. The transducers and bourdon tube pressure gauge were calibrated in positive gauge pressure.

## 4.2 Preparing the Shock Tube

The shock tube driven section was evacuated using the vacuum pump, but would leak (or draw in air) upon turning off the pump. In order to have reasonable control over the amount of each gas in the tube the shock tube system needed to be capable of holding the vacuum with a relatively small amount of leakage. The shock tube system consists of multiple sections, composed of multiple plates, with numerous screws and attachments in these plates. This means literally hundreds of places had to be checked for leaks. An ultrasonic air leak detector was used to find the leaks with the shock tube under vacuum pressure. After tightening connections and applying modeling clay to leaking plate interfaces, the shock tube system began to hold vacuum pressure better. The minimum pressure attained was 0.25 psia, measured using the MKS Baratron Portable Vacuum Standard Type PVS-2 which has a temperature controlled pressure transducer and bridge (warm-up time is 4 hours).

## 4.3 Shock Generation

Attaining a repeatable flow condition is important for the comparison of data runs. Precise control and accurate measurement of driver and driven pressures takes the major role in repeatability, since a given shock strength is determined by the pressure ratio

$P_4/P_1$. The burst characteristics of the mylar diaphragm also plays a part. Inconsistent stretching, such as raising pressure too much above the desired pressure in the driver section then reducing it, may alter

the shock characteristics. An inaccurate measurement of temperature $T_1$ could account for some non-repeatability, as sonic velocity depends on it.

Consistent shock Mach numbers could be attained within 0.3 % even at different ambient conditions (pressure and temperature). A higher pressure $P_4$ was set for higher barometric pressure readings to maintain the same $P_4/P_1$.

The stretching of the diagram was allowed for in all tests, and the same diaphragm thickness (0.005 in) was used. Pressure would be raised to about .4 inches mercury (Hg) above the desired pressure then allowed to decrease as the diaphragm stretched. Then the pressure was adjusted to a stable value within 0.02 in. Hg of the desired pressure. When the driven section was not open to the atmosphere, a rise in pressure $P_1$ of approx. 0.04 in. Hg was measured. Therefore, pressure $P_1$ was measured just prior to shock initiation. This was especially important for test runs when helium was added to the driven section.

Since all initial temperatures were allowed to stabilize at room temperature, temperature $T_1$ was measured, to an accuracy of 0.1 deg C, at the upper outside wall of the test section using the same temperature calibrator used for heat flux gauge calibration. Temperature varied less than 0.5 deg C over a series of tests (i.e. Tests T01 to T03, or Tests T09 to T12 [see Chap.5 and Appendix F]).

For test runs with film cooling, cooling air was begun just prior to shock initiation (within 0.5 sec) to avoid raising the pressure in the driven section.

## 4.4 Data Collection and Reduction

All data was acquired using the Nicolet Data Acquisition System (see Figure 4.3), and the programmable Transamerica PSC 8015-1 amplifiers were set at the same signal conditioning settings that were used for calibration of the heat flux gauges (mode = AMPD, filter = 10 kHz, gain = 250). Sample interval was 2 μsec, and a pre-trigger of 10 %, or 1 msec, was used to see reference levels and the rise in voltage of the forward pressure transducer, from which data collection was triggered (at a level of 0.2 Volts). Data channels A1 to B3 (or digitizer boards one and two) were used for heat flux gauge input from the analog circuits. Channels C1 to C3 were used for pressure transducer input, and channels D1 to D4 were connected to output directly from the PSC amplifiers for wall temperature input (gauges 1, 4, 6, and 7).

The bridge supply modules were re-balanced between calibrations and flat plate test runs, and between the test runs and film cooling runs. This would not affect the results since zero references were not used in the data reduction. Only differences of voltage output were used, which when multiplied by the slopes of calibration curves attained differences in engineering measurement units. Stable, initial reference levels of pressure and temperature were taken from the calibration instruments used.

Data was reduced using the fortran computer program STFCRT (Shock Tube Film Cooling - Reference Temperature) on the AFIT VAX/VMS mainframe and the Nicolet 500 software (see Appendix E and Figure 4.3). Only heat flux voltage output data needed to be transferred to the the VAX (using file transfer program "ftp"), since the program only uses this data to compute average heat flux (with subroutine QAVE). Pressure and

temperature voltage levels could be multiplied by the respective calibration constants using the Nicolet software. This reduction process was also used for heat flux for comparison to QAVE calculations.

## 4.5 Film Cooling

Isentropic compressible flow relations, based on chamber stagnation conditions $P_{0c}$ and $T_{0c} = T_1$, neglecting chamber flow velocity, were used to calculate static temperature, density, and velocity of the coolant air exiting the holes. Choked flow conditions were not achieved due to the low blowing rates used. Coolant density, velocity, and temperature are given by the following:

$$\rho_c = \frac{P_{0c}}{R_{air} T_{0c}} \left(\frac{P_{0c}}{P_2}\right)^{\frac{-1}{\gamma_{air}}} \tag{4.2}$$

$$U_c = \left\{ \frac{2\gamma_{air} R_{air} T_{0c}}{\gamma_{air} - 1} \left[ 1 - \left(\frac{P_2}{P_{0c}}\right)^{\frac{\gamma_{air}-1}{\gamma_{air}}} \right] \right\}^{1/2} \tag{4.3}$$

$$T_c = T_{0c} \left(\frac{P_2}{P_{0c}}\right)^{\frac{\gamma_{air}-1}{\gamma_{air}}} \tag{4.4}$$

## V. Results and Discussion

Heat transfer results are presented for flat plate test runs without film cooling at four different flow conditions, or driver pressures, and for test runs with film cooling at two density ratios and one flow condition each (similar flow Mach numbers $M_2 = M_\infty$). The heat transfer with film cooling is presented for different blowing rates and downstream distance compared to the flat plate heat transfer.

For tests without film cooling, the cooling holes were covered with black electrical tape of thickness 0.009 inches. The tape needed to be strong yet easy to apply and remove. For tests with helium in the driven section, the vacuum applied would draw a small amount of air through the o-ring seal between the instrumentation and cooling cavities from the room through the cooling holes into the driven section. That is to say, the tape would not hold the seal under vacuum and would lift up from the plate on both ends of the cooling hole row until the driven section pressure was increased to atmospheric pressure. Then the tape would re-seal before running a test. This warranted use of the tape, but the thickness may have affected the flat plate results, as will be shown.

Figure 5.1 shows typical outputs of forward and rear pressure transducers (test T10 shown). The difference in times between shock passage is accurately discernible within 2 μsec sample time. The shock velocity $U_s = \Delta x/\Delta t$ is easily calculated knowing the distance between the two transducers (Figure 3.5). Although the Nicolet can sample at

1 μsec the larger data files and slightly better accuracy of shock velocity are not warranted due to the decay of shock velocity as the shock moves down the shock tube.

Better determination of shock velocity at the plate (the pressure transducers being located upstream) could be made using the rear transducer and a heat flux gauge, since the fast response of the gauge compares to that of the transducers (see Figures 5.2 and 5.3). Test T01, at $P_4 = 60$ in. Hg, gave a 4.8 m/sec shock velocity decay analyzed this way. This equates to a difference of 1.2% in shock Mach number. Nonetheless, data was reduced using the pressure transducers. Later, this may slightly account for a higher Stanton number calculated from measured heat flux, due to the resulting higher $T_2$ temperature deduced.

The average deduced pressure $P_2$ of the rear transducer (1 msec after shock passage) compares well to the theoretical value based on measured shock Mach number (within 1 kPa). From Figure 5.1, the pressure trace of the rear transducer (closest to plate leading edge) is steady for about 3 msec then rises quickly, indicating passage of the shock reflecting off the flat plate leading edge.

The shock reflection phenomena is described well by Jurgelewicz (1989:66-72). The reflection propagates out from the leading edge analogous to the wave off the bow of a ship or a pebble dropped in a pond. The reflected shock repeatedly reflects between the shock tube upper wall and the plate surface, decreasing in strength at each reflection due to viscous dissipation. Schlieren and high speed photography could verify this phenomena.

Finally, the latter time of Figure 5.1 indicates passage of expansion waves in steadily decreasing pressure. A longer test time would show passage of the shock reflected off the shock tube end wall giving the sharp rise in pressure similar to the initial shock passage, but superimposed on the higher pressure already present.

Figure 5.2 gives the typical temperature trace (gauge 4 shown), from test T10, and the second sharp increase in temperature shows the reflected shock passage. Digitized output is discernible in this amplified view; temperature rise is a small 2.4 deg C. Just before the end-wall shock reflection, a change in slope is noticed, taken to be passage of the contact surface. Different shock speeds and gauge location determine whether the contact surface arrives first.

Figures 5.3 to 5.5 show typical surface heat flux output, from test T10. The unsteady laminar, transition, and turbulent flow regions are indicated, and compare to plots from Jurgelewicz (1989). After the steady condition occurs, Figures 5.4 and 5.5 show the steady increase of heat transfer indicating presence of leading edge shock reflections, and arrival of the contact surface shows as a reduction in heat flux (negative slope) just before the end-wall shock reflection. Figure 5.3 has the end-wall shock (region 5) wall heat flux removed. No reduction in heat transfer appears, due to its location closer to the end wall.

Tests at lower shock Mach numbers show a relatively faster arrival of the contact surface or expansion waves (see Figure 2.1) in relation to the reflected shock. For higher shock Mach numbers, region 2 conditions end upon arrival of the reflected shock, and test time is shorter.

Introducing helium with the air greatly reduces the test time. The much higher gas constant and sonic velocity in helium greatly increase the shock speed, however the shock Mach number is somewhat reduced for a comparable driver-to-driven pressure ratio.

## 5.1 Heat Transfer Results Without Film Cooling

The non-dimensional heat transfer results are shown in Figure 5.6 for one series of tests (T09 to T12) with air in the driven section. A fair comparison to the theoretical turbulent flat plate correlation in 9.5% turbulence is attained using equations (2.13) and (2.17) for theoretical results. The slope of the data is slightly different and the data generally higher. Results of a second series of tests is added to the first on Figure 5.6.1 to show the results are repeatable.

A close look at the data points for a given test run reveals a consistent pattern. The first data point in a given test corresponds to heat flux gauge number 1, the second data point to gauge 2, etc. The consistent pattern indicates inaccuracy of calibration (likely the bulk thermal diffusivity calibration). Gauge number 1 consistently gives higher heat flux output than the other gauges with respect to the theoretical line. This may have resulted from its proximity to the tape covering the cooling holes.

A test run, X11, was done to compare heat transfer results without the holes covered to a similar test, T11, with covered holes. The comparison is shown in Figure 5.6.2. With the holes uncovered the boundary layer would be bled off to the lower pressure cooling chamber, causing an increase in heat transfer, as the results verify. Heat flux output of gauges 1, 4, 6, and 7 increases approximately 10% by uncovering the holes

(these gauges are all located downstream of the same cooling hole). Gauge number 2 output increases substantially, 40%, and gauge 3, 30%, and gauge 5, 20%. These three gauges are all located behind different cooling holes.

Figure 5.7 shows heat transfer results for two tests (P09 and T13) with air and helium mixture in the driven section. Test P09 has lower velocity, or Reynolds numbers, and quite high Stanton numbers compared to the theoretical results. The correlation equation (2.13) is stated only to be good down to a Reynolds number of $5\times10^5$ (Kays and Crawford, 1980:213), and test P09 is below that range. Nevertheless, this test seems high. Part of the difference may be the uncertainty of the viscosity of the mixture and the slight error in measured partial pressure of helium in the mixture, but these differences would also apply to test T13.

Figure 5.8 shows the combined heat transfer results of Figures 5.6 and 5.7 for flows of air and air/helium mixture (without test T09 and P09). The difference between measured and theoretical St versus $Re_x$ slope may be attributed to the assumption of a thermal boundary layer for an isothermal surface. The boundary layer develops from the leading edge over an aluminum surface; whereas, the measurement of the surface temperature is done on the Pyrex substrate of the gauge. The Pyrex is close to an adiabatic surface compared to the aluminum. The temperature of the aluminum surface changes more quickly and affects the thermal boundary layer profile. The correction of the slope will be seen only by using a test plate with a similar material to the heat flux gauge substrate.

The generally higher Stanton numbers must be attributed to the difference in background turbulence intensity from the value previously measured (9.5%). Measurements by Rockwell (1989) and Gul (1991) had probe vibration problems associated with them. A measurement of Tu with a more accurate procedure may show higher values with the present set-up.

The presence of shock reflections complicates the data reduction for the comparison of heat flux with film cooling to heat flux without film cooling. The film cooling chamber pressure increases to the test condition value after the higher back pressure occurs following the passage of the shock wave (see Figure 5.9). The heat flux comparison has to compare heat transfer for the later test times, due to pressure not coming to equilibrium fast enough and the slightly higher heat flux from the shock reflections. The film cooling chamber pressure trace shows two steps of pressure adjustment. The second rise may be due to the delay in reaction of the dome valve, which is located approximately 35 inches upstream of the cooling chamber. The average heat flux is taken from 0.3 msec to 1.2 msec after the film cooling chamber pressure levels off.

## 5.2 Heat Transfer Results With Film Cooling

Film cooling tests T14 to T20 were run with air in the driven section (at a density ratio of 1.2 to 1.3) and increasing film cooling chamber pressure or blowing rate. Table 5.1 gives the film cooling test results. Figure 5.10 presents the results of heat flux for each gauge divided by the heat flux without film cooling, $q/q_o$, versus mass flux ratio,

Table 5.1

Summary of Film Cooling Data

| Test No. | D.R. | V.R. | $M_b$ | $q/q_o$ Gauge No. 1 | 2 | 3 | 4 | 5 | 6 | 7 |
|---|---|---|---|---|---|---|---|---|---|---|
| T14 | 1.18 | 0.33 | 0.39 | 1.00 | 1.25 | 1.19 | 1.10 | 1.13 | 1.09 | 1.09 |
| T15 | 1.19 | 0.61 | 0.73 | 0.90 | 1.12 | 1.11 | 1.00 | 1.06 | 1.02 | 1.05 |
| T16 | 1.20 | 0.88 | 1.05 | 0.70 | 0.85 | 0.87 | 0.88 | 0.93 | 0.96 | 0.87 |
| T17 | 1.22 | 1.16 | 1.42 | 0.80 | 0.94 | 0.92 | 0.92 | 0.96 | 0.98 | 0.93 |
| T18 | 1.24 | 1.34 | 1.66 | 0.85 | 1.08 | 1.00 | 0.91 | 0.88 | 0.97 | 0.86 |
| T19 | 1.28 | 1.61 | 2.06 | 1.01 | 1.25 | 1.16 | 0.93 | 0.84 | 0.91 | 0.83 |
| T20 | 1.31 | 1.81 | 2.36 | 1.12 | 1.24 | 1.14 | 1.06 | 0.98 | 1.05 | 0.87 |
| H01 | 2.10 | 0.39 | 0.81 | 0.86 | 1.09 | 1.02 | 1.03 | 1.07 | 1.01 | 1.04 |
| H02 | 2.12 | 0.52 | 1.10 | 0.78 | 0.93 | 0.89 | 0.97 | 1.03 | 0.92 | 1.08 |
| H03 | 2.03 | 0.66 | 1.40 | 0.71 | 0.93 | 0.84 | 0.91 | 1.01 | 0.97 | 1.01 |
| H04 | 2.13 | 0.94 | 2.00 | 0.80 | 0.89 | 0.89 | 0.89 | 0.97 | 0.95 | 1.00 |
| H06 | 2.17 | 1.12 | 2.43 | 0.84 | 1.05 | 0.97 | 0.88 | 0.91 | 0.84 | 0.95 |
| H05 | 2.20 | 1.27 | 2.82 | 0.98 | 1.19 | 1.14 | 0.97 | 0.98 | 1.00 | 0.95 |

$M_b$. Generally, heat transfer decreases with increasing blowing to some point, after which heat transfer begins to increase.

Qualitatively, the minimum heat transfer occurs at different points depending on the downstream distance, x/d, from the cooling holes. The increase in heat transfer can be attributed to film-cooling jet lift-off as the jet penetrates further into the mainstream flow with increasing blowing. With low blowing the jet is turned quickly into the direction of mainstream flow and forms a cool film at the boundary.

Increasing blowing rate into the "strong injection" regime causes the jet to lift off, but it quickly reattaches at the lower blowing rates. All testing was done in the "strong injection" regime, or a momentum flux ratio, I, greater than 0.1. [See Forth and Jones (1986).]

Thus, results from Figure 5.10 show the reattachment point moves downstream with increasing blowing. Also, the effectiveness of the film in reducing heat transfer is low at the downstream distance of x/d = 30.3 (gauge 7 location). This reduced effectiveness is due to increased mixing with the freestream for increasing downstream distance.

Figure 5.11 gives results of heat transfer versus blowing ratio with helium added to the driven section to give a density ratio between 2.1 and 2.2 (see Table 5.1, Tests H01 to H06). Qualitative results similar to the lower density ratio tests are attained, but there are some notable differences. The blowing ratio giving the minimum heat transfer (or maximum effectiveness) has shifted to higher rates for each downstream distance. The range of effectiveness is generally broader, noted from the smaller slopes on either side

of the data point giving maximum effectiveness compared to the lower density ratio tests. Gauges 1, 2, and 3 (x/d less than 10) show increased effectiveness at the higher density ratio for blowing ratios greater than one. Also, the increase of density ratio from 1 to 2 shows no significant effect for gauges 4 to 7 (x/d greater than or equal to 10) and blowing ratios up to 2.4.

The quantitative values are probably in error, noting the increase in heat transfer ($q/q_o > 1.0$) with the small blowing rates, more so at the lower density ratio. The values of $q_o$ are apparently low, and the deduced values of blowing rate appear high compared to results of other studies.

Comparing the set of data points for the lowest blowing rate ($M_b = 0.4$) on Figure 5.10 (Test T14) to the results of Figure 5.6.2 with no blowing, we see a similarity. Uncovering the holes increased heat transfer significantly (suction of boundary layer), and in a similar proportion to the $M_b = 0.4$ data points, except for gauge number 1. The $M_b = 0.4$ heat transfer increase for gauge 2 is 25%; for gauge 3, 19%; for gauge 5, 13%; for gauges 4, 6, and 7, 9-10%; and for gauge 1, 0%. This similarity indicates that the low blowing may actually be no blowing or even a low suction (except for gauge 1 results, which indicate the low blowing).

This error could be accounted for by noting that equations (4.2) and (4.3) were used to compute the density and velocity for the coolant in the mass flux ratio, equation (1.2). No accounting for friction or entrance losses was made, which would decrease the coolant exit velocity and mass flux ratio for a given coolant chamber stagnation pressure, $P_{0c}$. This would have the effect of shifting all the curves in figures 5.10 and 5.11 to the

left. This brings the results for blowing ratio giving maximum effectiveness closer to that of other studies in the literature. Pederson (1977) showed the effects of density ratio giving $M_{b,\,max}$ = 0.5 to 0.8 at x/d = 10.3 (see Figure 1.2); and Jumper (1987) gave the effects of mainstream turbulence intensity of 17%, i.e. $M_{b,max}$ = 0.5 to 0.7 at x/d = 5.5, $M_{b,max}$ = 1.5 at x/d = 10.5, and $M_{b,max}$ = 2.0 at x/d = 20.5. The exact difference of the combined effects in this study remains to be deduced.

Correlating the data in a similar manner to that of Forth and Jones (1986) gives Figures 5.12 and 5.13, with heat flux ratio $q/q_o$ plotted versus the velocity ratio and distance parameter $x/d\ (V.R.)^{-4/3}$ proposed for "strong injection" through inclined holes. For values of the parameter greater than or equal to 10, most of the data tends toward a pattern similar to that of Forth and Jones (1986) (see Figure 5.14). For values of the parameter below 10 the data tends to increase again as the parameter approaches zero or the velocity ratio increases. Forth and Jones used a ratio of Nusselt numbers with and without film cooling, but the definition used makes the ratio similar to the heat flux ratio used in this study.

The heat transfer values are all higher in this study, and would still be higher even taking into account the inaccurate $q_o$ values used. Figure 5.12 only includes the data for a density ratio of 2, more closely resembling the flow in a turbine, and the data tends to correlate with the velocity ratio. The higher heat transfer would be the effect of higher mainstream turbulence intensity, i.e. the higher mainstream turbulence increases heat transfer or reduces effectiveness of film cooling.

## VI. Conclusions

The calibration of the thin-film heat flux gauges for bulk thermal diffusivity is required, noting the substantial difference of gauge number 6 from the established experimental level of $\sqrt{\rho C_p k}$ = 1520 J/m$^2$Ksec$^{1/2}$ ± 5%. The range of error of the calibration technique established in this study needs to be determined, but is estimated at 10% noting the flat plate heat transfer results.

Turbulent flat plate heat transfer in the shock tube still needs to be fine tuned to obtain results closer to the mainstream turbulence adjusted turbulent heat transfer correlation.

For film cooling tests accurate determination of the coolant exit velocity and density is required.

Results from film cooling tests shows that increasing the density ratio from 1 to 2 has the following effects:

(1) Increases the $M_b$ that gives maximum effectiveness of cooling (min. heat transfer).

(2) Generally broadens range of effectiveness.

(3) Increases effectiveness for $M_b$ greater than 1 and x/d less than 10.

(4) No effect for $M_b$ less than 2.4 and x/d greater than or equal to 10.

Increasing $M_b$ increases cooling effectiveness to a point (attributed to jet lift-off) then decreases. Maximum effectiveness occurred at values higher than for other similar studies without high mainstream turbulence or without high density ratio. The actual increase in the optimum blowing ratio with combined effects of density ratio and turbulence intensity still needs to be determined accurately.

Generally, higher mainstream turbulence increases heat transfer, or decreases cooling effectiveness.

Thus, the results from studies done at a coolant-to-mainstream density ratio of one and low turbulence intensity levels need to be corrected for application to design of film-cooled turbine components.

## VII. Recommendations

The recommendations from this experimental investigation are as follows:

Fabricate a test plate with a more adiabatic test surface similar to the gauge substrate, or use a different surface temperature measurement technique such as a thin-film ribbon applied to a styrofoam surface to achieve an adiabatic wall temperature for film-cooling effectiveness measurements. The correlation between measurable quantities and the adiabatic film cooling effectiveness parameter or non-dimensional heat transfer is important. This correlation would allow the data of Jurgelewicz, Gul, and this research to be compared more effectively to studies done at other facilities. This determination would not be possible by insulating the plate alone.

Seal the test plate and shock tube better to gain better control of the experimental gas mixture.

Use a test plate without holes for flat plate tests to avoid the roughness effects of tape covered holes.

Use larger holes and a wider lateral hole spacing of three to achieve a better resolution on the close-to-hole cooling effectiveness. Higher resolution means more gauges; therefore, more analog circuits and signal conditioning equipment need to be acquired.

Measure turbulence intensity at the test location, or at multiple locations, with a probe that won't be affected by vibration from passage of the shock wave. Also, do studies of film cooling with the previous researchers' turbulence generator to better quantify the effects of mainstream turbulence on cooling effectiveness.

Locate pressure transducers at the test location to better correlate the heat transfer results with the reflected shocks from the leading edge of the plate and to measure shock speed more accurately at the test location. Measurement of test condition temperature would increase the accuracy of determining the density or film-cooling effectiveness and determine arrival of the contact surface.

Use high speed photography to greatly enhance the understanding of the boundary layer development and reflected shock interactions. Relating development of the boundary layer to the measured heat transfer is necessary. Schlieren photography can be employed to some degree of success, but due to the slight variance of shock speed for a given set-up high speed photography would be required to effectively visualize the flow and qualitatively determine the conditions of the boundary layer. A high speed camera is available, but past attempts to use it suggest a great amount of time would be required to set up, test, and employ it.

Study 90 degree, inclined hole, and multiple row film cooling for the effects of density ratio, turbulence intensity, and flow conditions (only one flow condition was used in this study). Increase the number of blowing rates studied, especially in the lower range.

Calculate and/or measure coolant exit density and velocity more accurately to account for friction and entrance losses. Measure coolant chamber pressure with an absolute measurement or a differential across the cooling holes (i.e. connect the transducer reference tube to a tap on the test plate surface).

Automate the shock and film cooling initiation and the helium fill processes to obtain more consistent results.

Cool the coolant supply and measure temperature at the cooling chamber for a more realistic film-cooling boundary layer and for film-cooling effectiveness measurements.

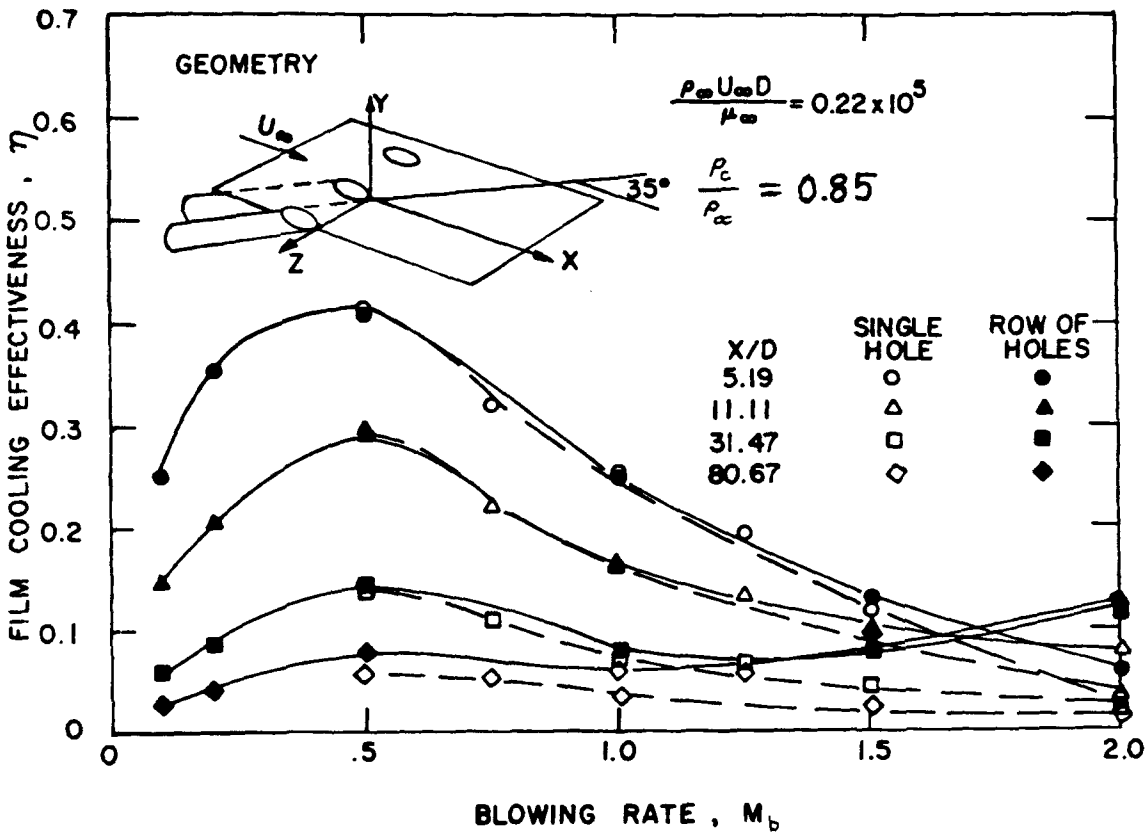


Figure 1.1 Film Cooling Effectiveness for Single Hole and Multiple Hole Injection at 35° for various blowing rates $M_b$ (Goldstein, 1971:373)

Fig.1

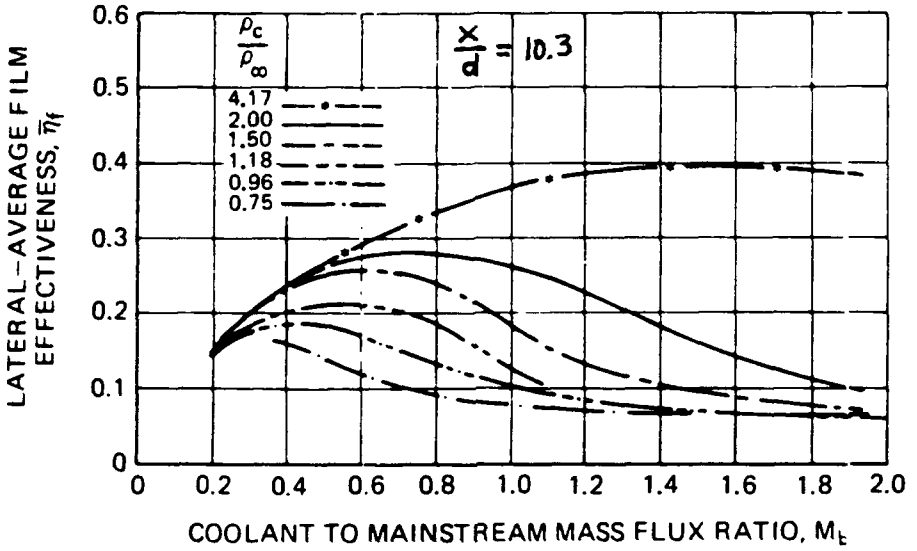


Figure 1.2 Effect of Coolant Density on Film Effectiveness (from Pederson, 1977:626; Suo, 1985:299)

Fig.2

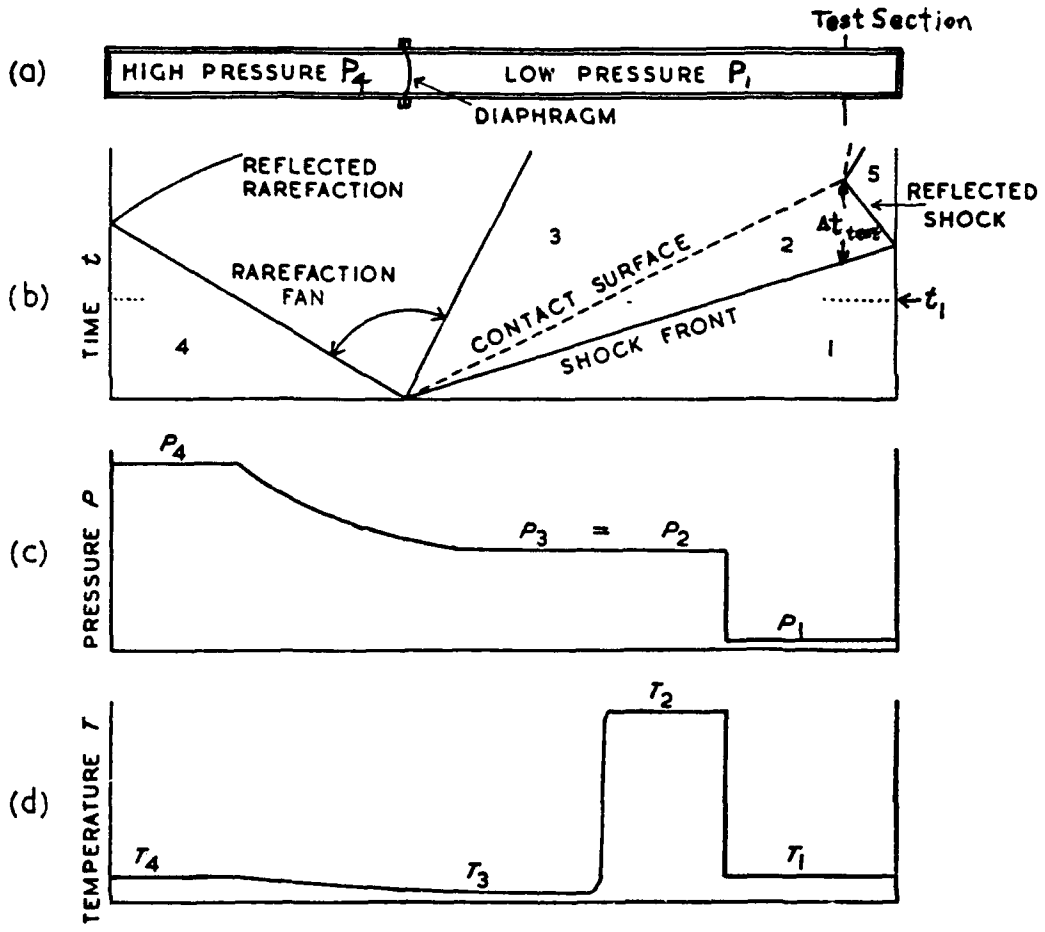


Figure 2.1 (a) Simple shock tube
(b) An (x-t) diagram showing progress of the shock wave, the rarefaction fan and the contact surface separating driver and experimental gases
(c) The pressure distribution along the tube at time $t_1$
(d) The temperature distribution at time $t_1$
(Gaydon and Hurle, 1963:1)

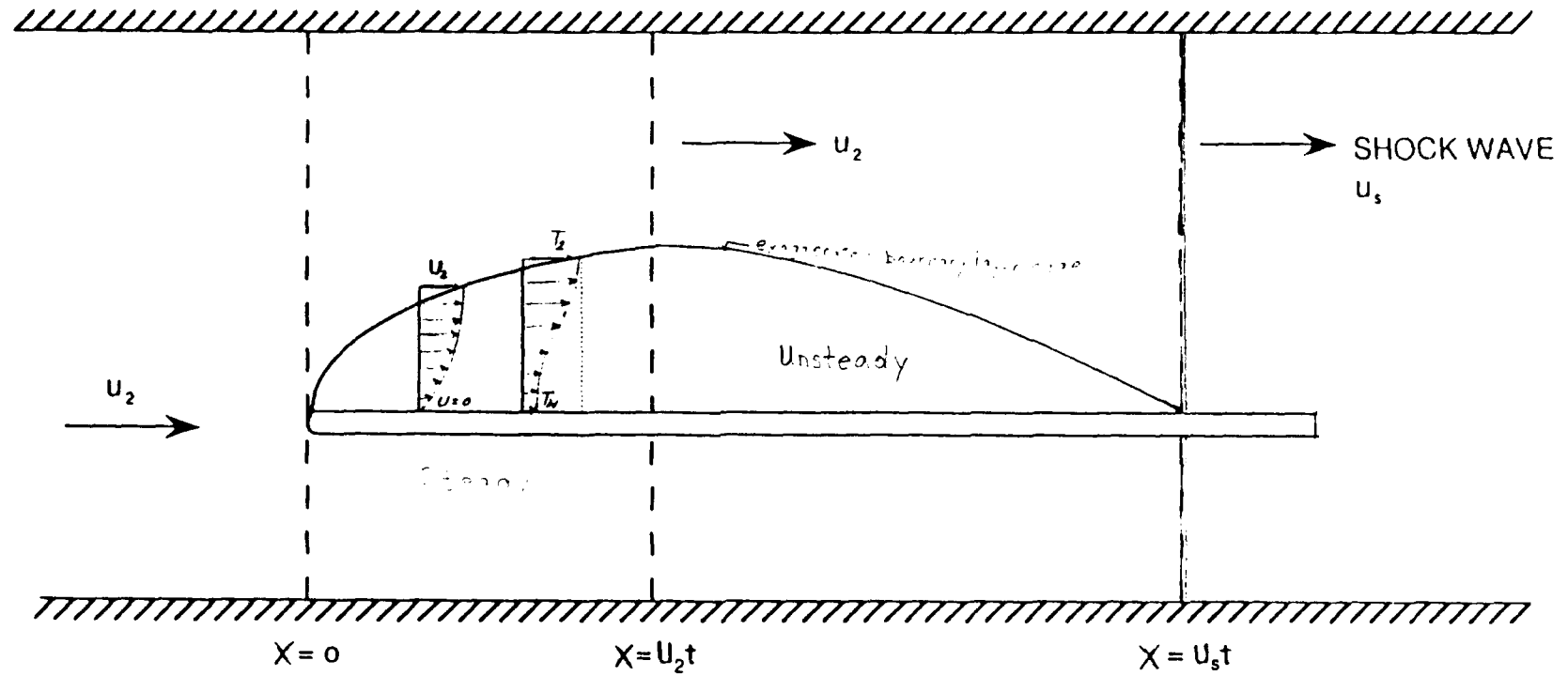


Fig.4

Figure 2.2 Boundary Layer Formation on a Flat Plate Behind a Shock Wave (combining Schlichting, 1979, 1979:440; Mirels, 1956:53)

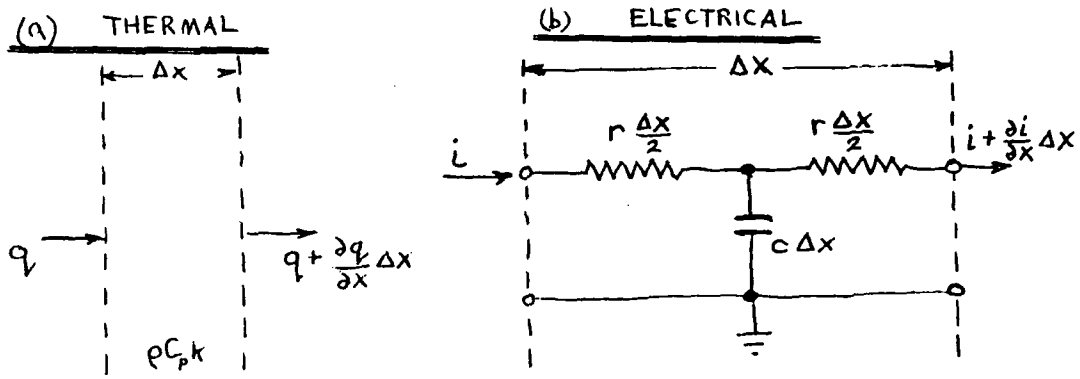


Rate of gain of energy in element $\Delta x$

$$= -\frac{\partial q}{\partial x}\Delta x$$

which by conservation of energy

$$= \rho C_p \Delta x \frac{\partial T}{\partial t}$$

Thus

$$\frac{\partial q}{\partial x} = -\rho C_p \frac{\partial T}{\partial t}$$

Fourier's Law is

$$q = -k\frac{\partial T}{\partial x}$$

Combining these two equations we obtain the diffusion equation

$$\boxed{\frac{\partial^2 T}{\partial x^2} = \frac{\rho C_p}{k}\frac{\partial T}{\partial t}}$$

Solving using Laplace transforms obtains (see Rockwell 1989: App. B)

$$\boxed{\bar{q} = \sqrt{\rho C_p k}\sqrt{s}\,\bar{T}} \quad \text{for} \quad \begin{matrix} T=0 \ @ t=0 \\ T=0 \ @ x=\infty \end{matrix}$$

Rate of gain of charge in element $\Delta x$

$$= -\frac{\partial i}{\partial x}\Delta x$$

which by conservation of charge

$$= c\,\Delta x \frac{\partial V}{\partial t}$$

Thus

$$\frac{\partial i}{\partial x} = -c\frac{\partial V}{\partial t}$$

Ohm's Law is $V = iR$ or

$$i = -\frac{1}{r\Delta x}\frac{\partial V}{\partial x}\Delta x = -\frac{1}{r}\frac{\partial V}{\partial x}$$

Combining these two equations we obtain the transmission line equation

$$\boxed{\frac{\partial^2 V}{\partial x^2} = rc\frac{\partial T}{\partial t}}$$

Solving using Laplace transforms obtains

$$\boxed{\bar{i} = \sqrt{\frac{c}{r}}\sqrt{s}\,\bar{V}} \quad \text{for} \quad \begin{matrix} V=0 \ @ t=0 \\ V=0 \ @ x=\infty \end{matrix}$$

(c) Combining in a practical circuit: Output $V_o \propto T$ from thin film heat transfer gauge is applied to input of electrical analog RC blocks as $\bar{V}_{in} = \bar{V}_o \propto \bar{T}$ giving $\bar{i}_{in} = \sqrt{\frac{c}{r}}\sqrt{s}\,\bar{V}_o \propto \bar{T}$. Solving for $\bar{T}$ and substituting in $\bar{q}$ equation obtains $\bar{q} = \sqrt{\rho C_p k}\sqrt{\frac{r}{c}}\frac{1}{\bar{V}_o \propto}\bar{i}_{in}$. Taking inverse Laplace transform (s does not appear) and taking $i_{in} = \frac{V'_{out}}{R_1}$ for output across analog circuit input resistor $R_1$ we obtain

$$\boxed{q = \sqrt{\rho C_p k}\sqrt{\frac{r}{c}}\frac{1}{V_o \propto}\frac{V'_{out}}{R_1}}$$

and $V'_{out} = \frac{V_{out}}{G}$ for amplified output of gain G.

Figure 2.3 Derivation of the Electrical Analog of Heat Conduction (Schultz and Jones, 1973:37,38,111)

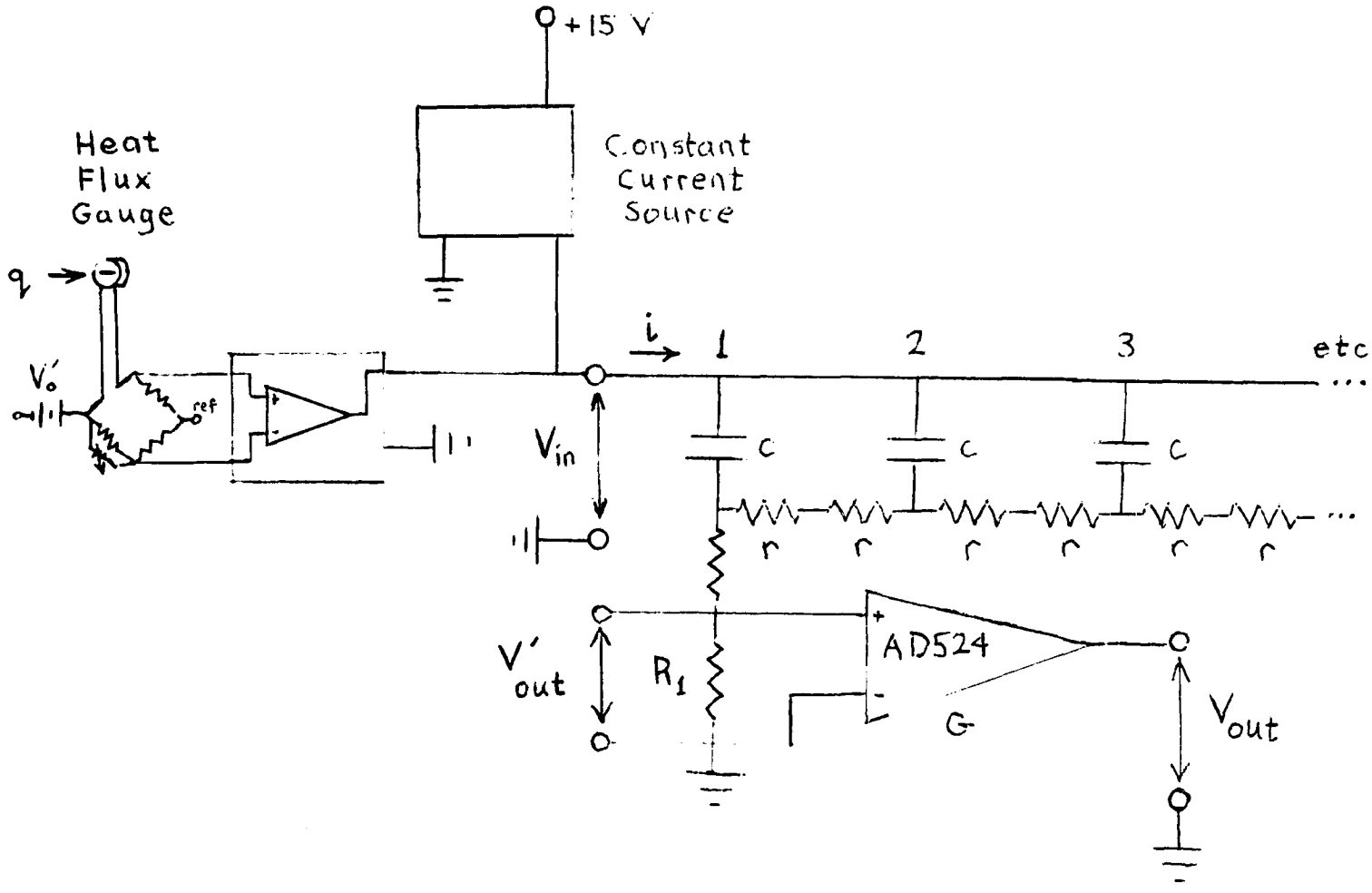


Fig.6

Figure 2.4 The Heat Flux Analog (Rockwell, 1989)

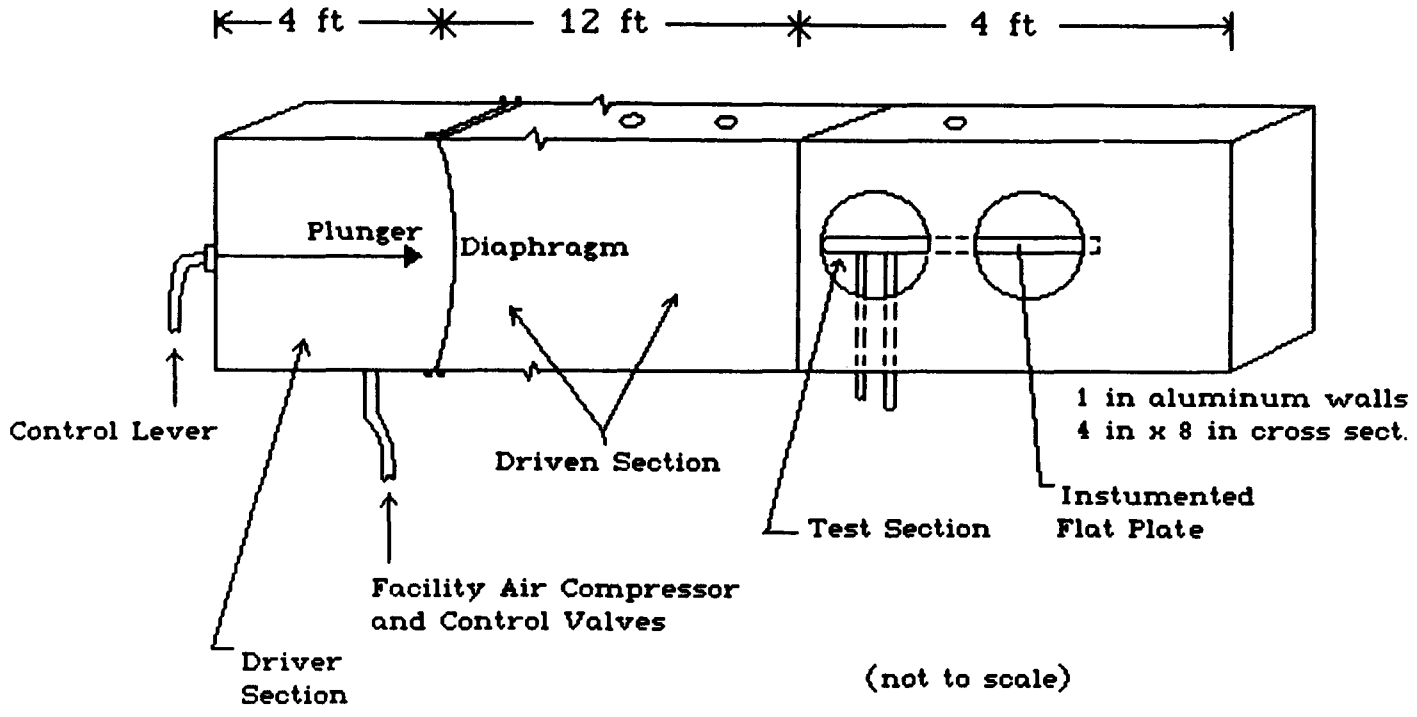


Fig.7

Figure 3.1 Test Plate in Low Pressure Shock Tube

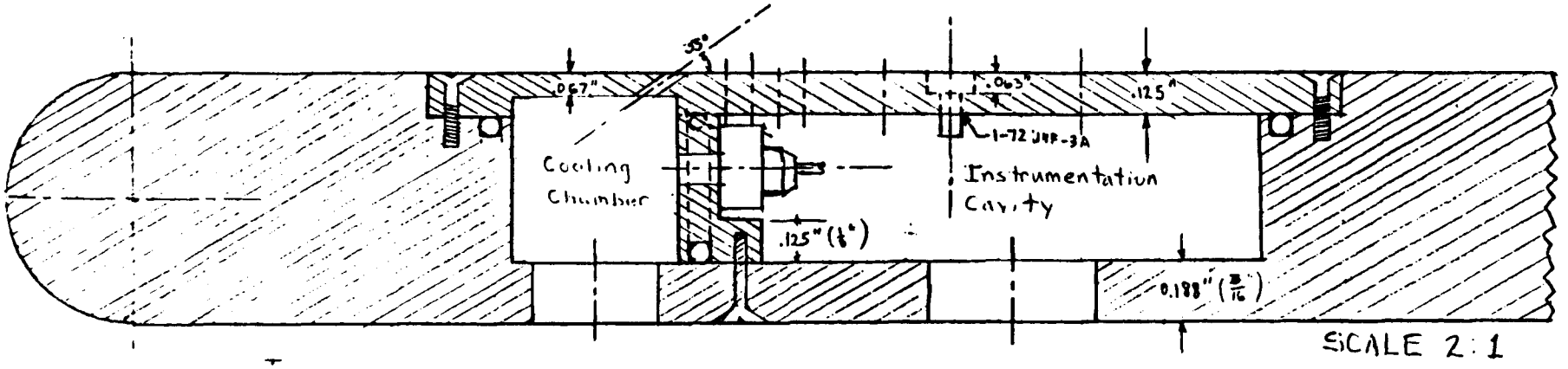


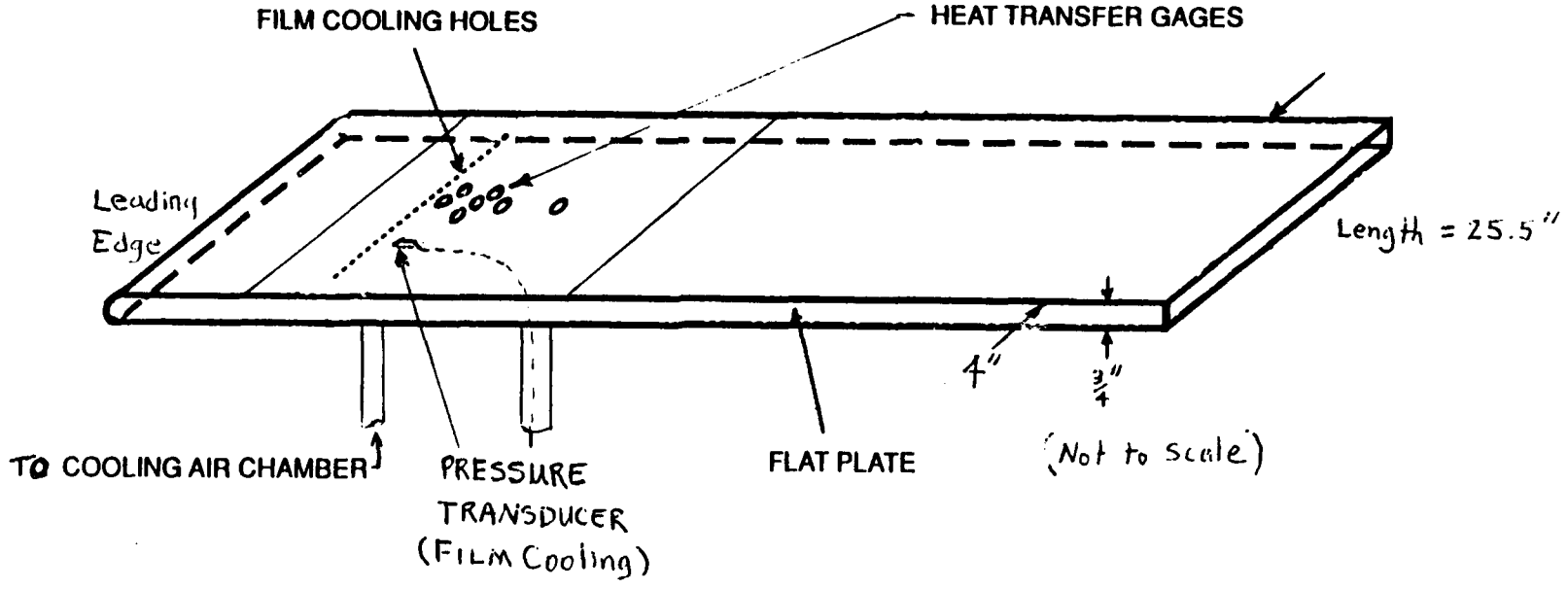


Fig.8

Figure 3.2 Instrumented Flat Plate

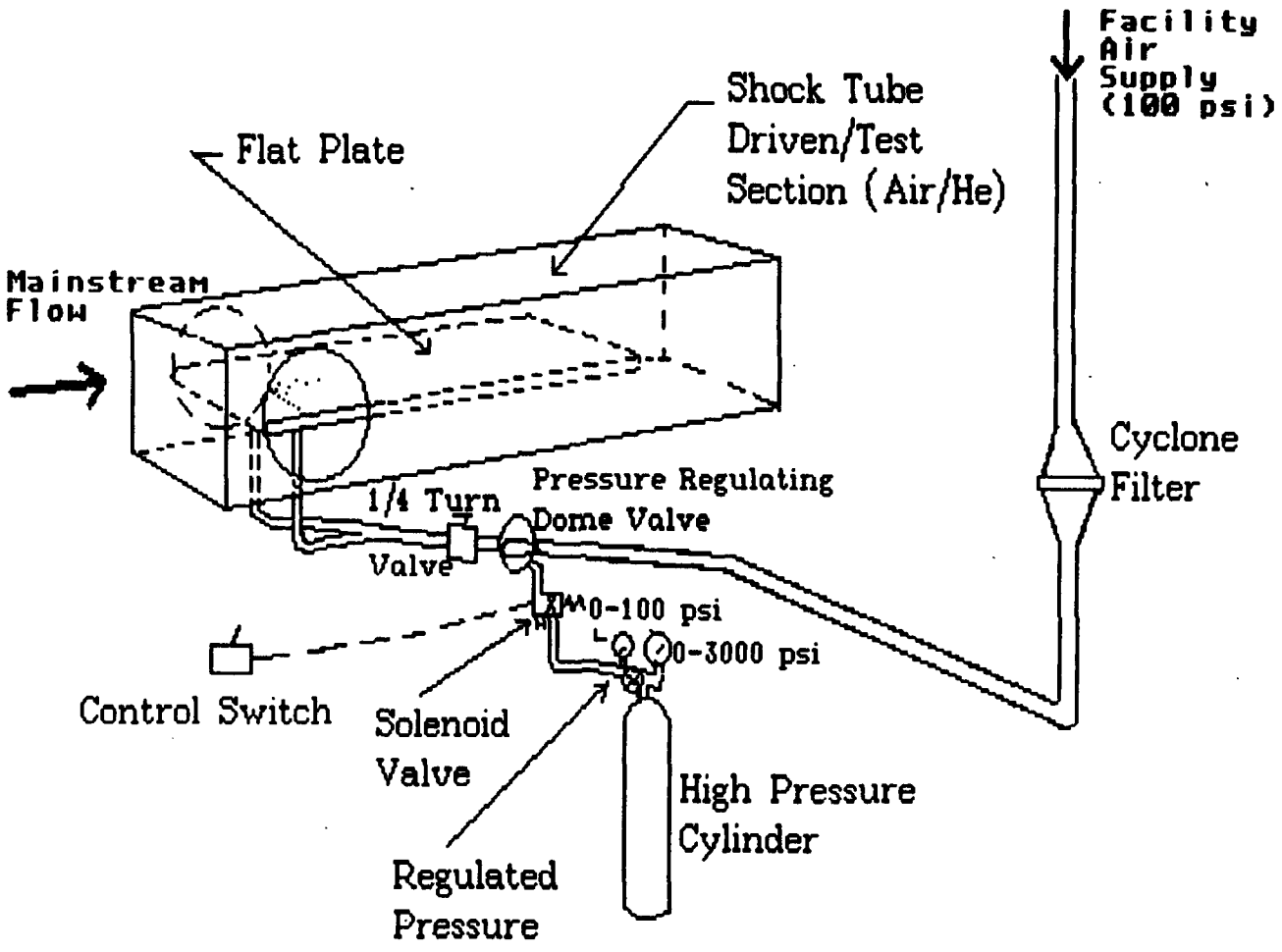


Figure 3.3 Film Cooling Supply and Control System

Fig.9

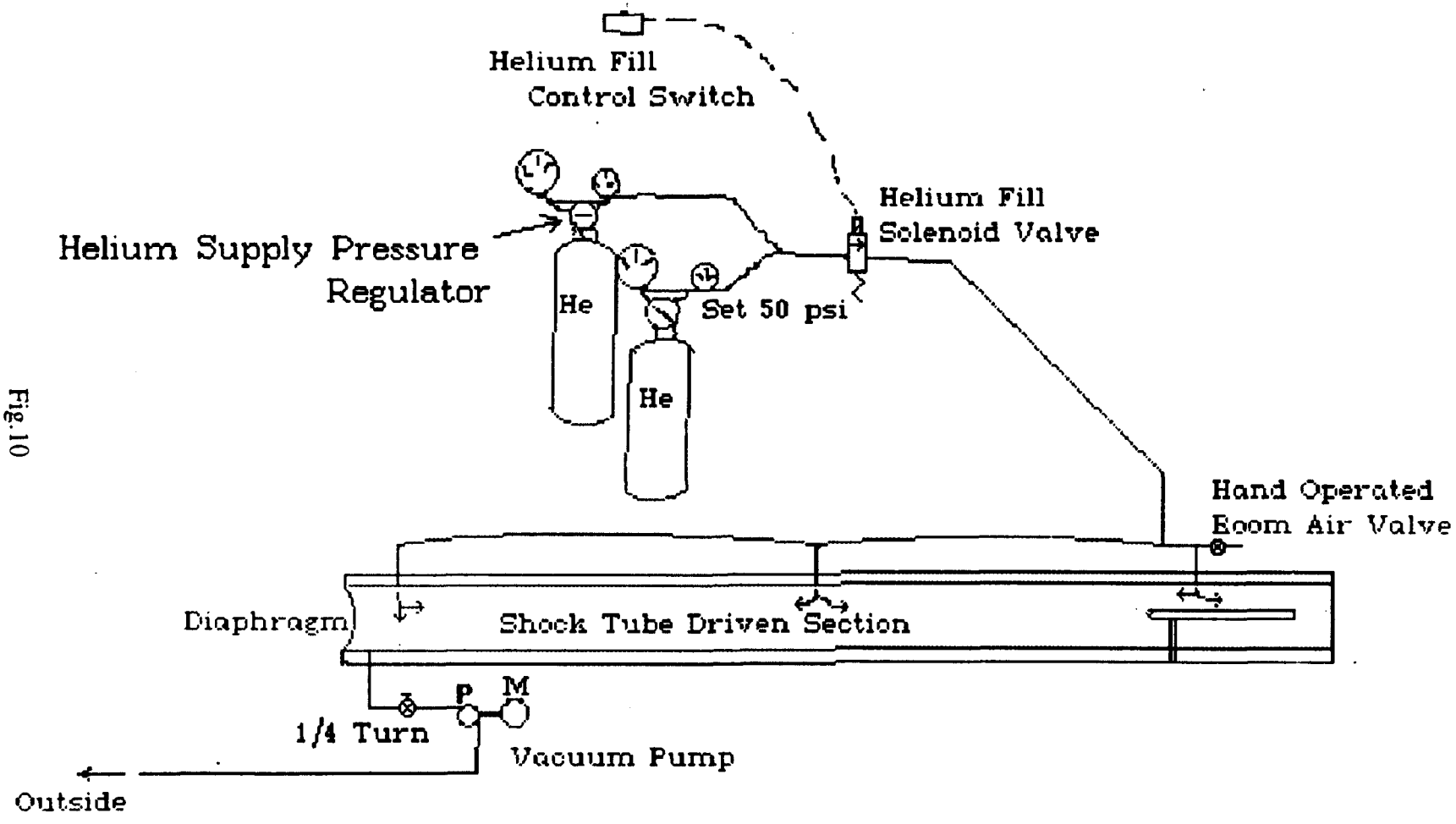


Fig.10

Figure 3.4 Shock Tube Gas Fill and Control, Driven Section

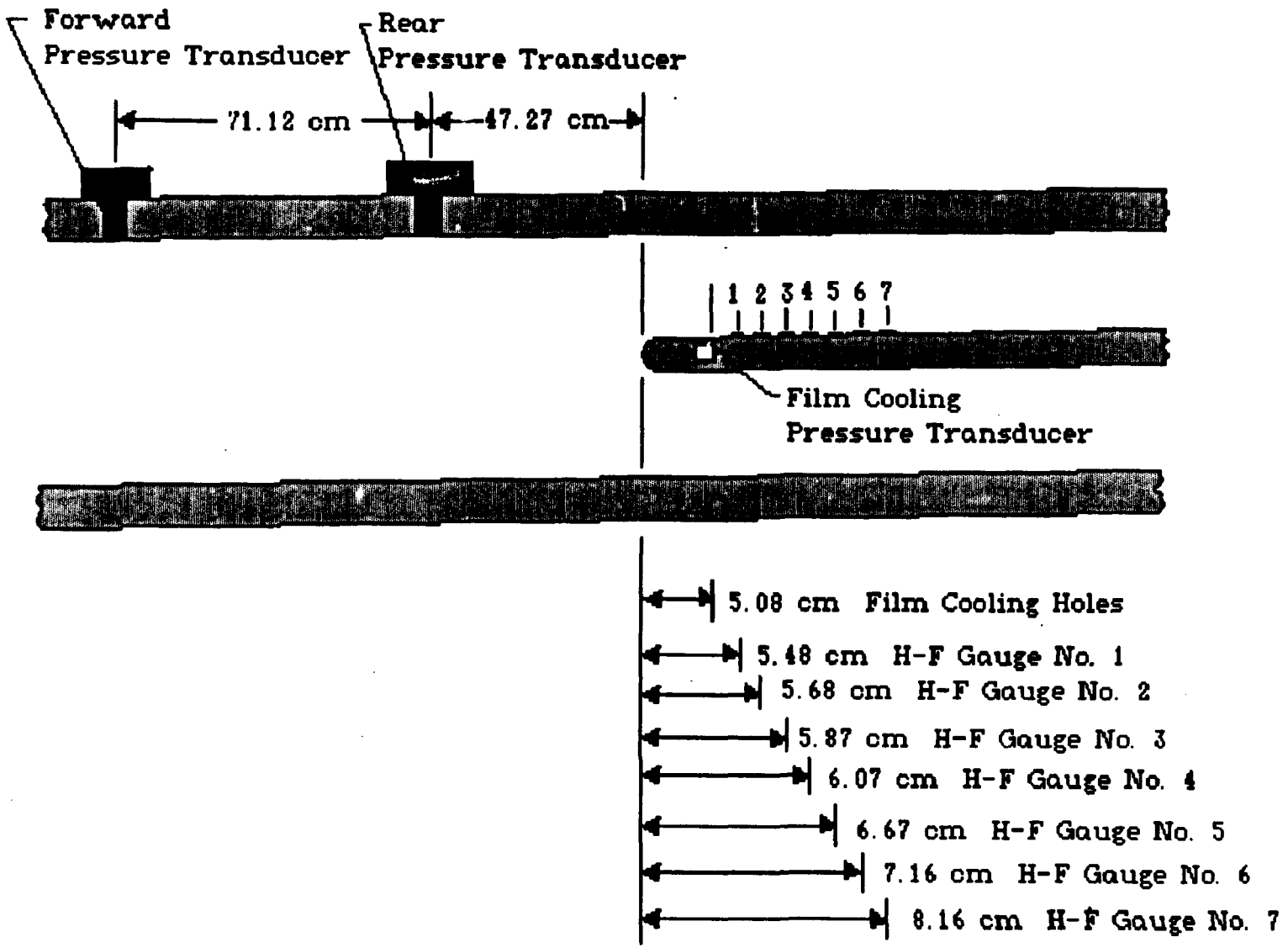


Fig.11

Figure 3.5 Pressure Transducer and Thin-Film Gauge Locations in the Shock Tube

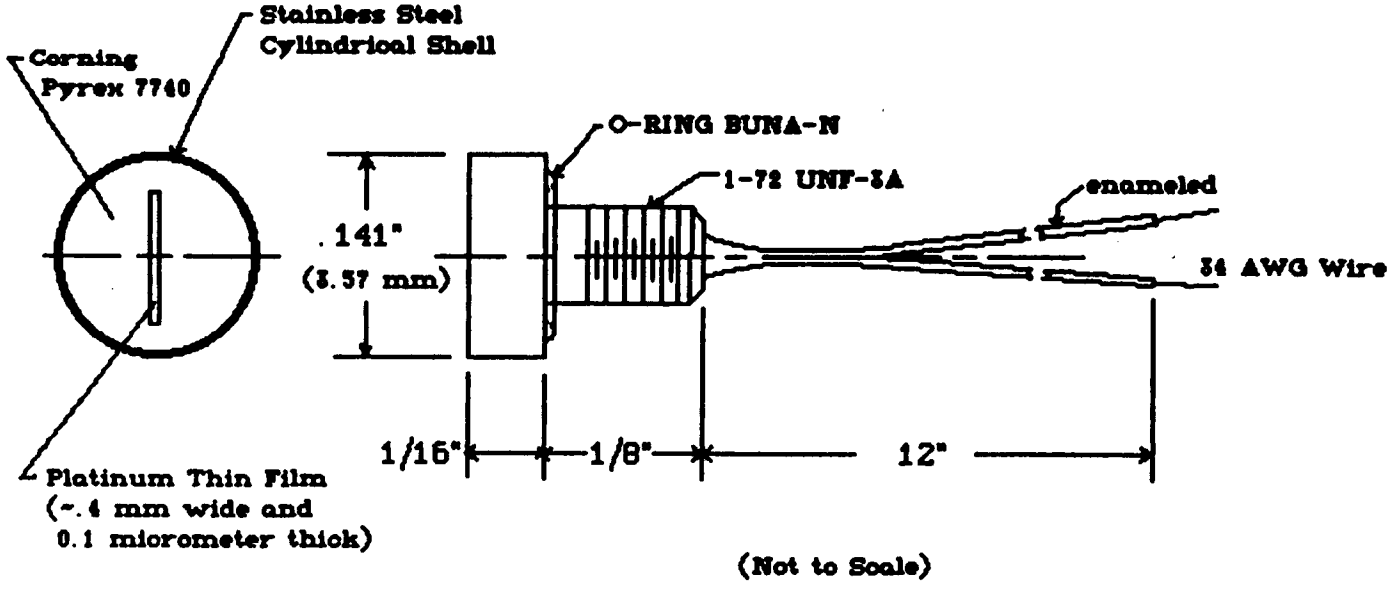


Fig.12

Figure 3.6 Platinum Thin-Film Resistance Heat Transfer Gauge, Medtherm Instruments Model PTF-100-20293

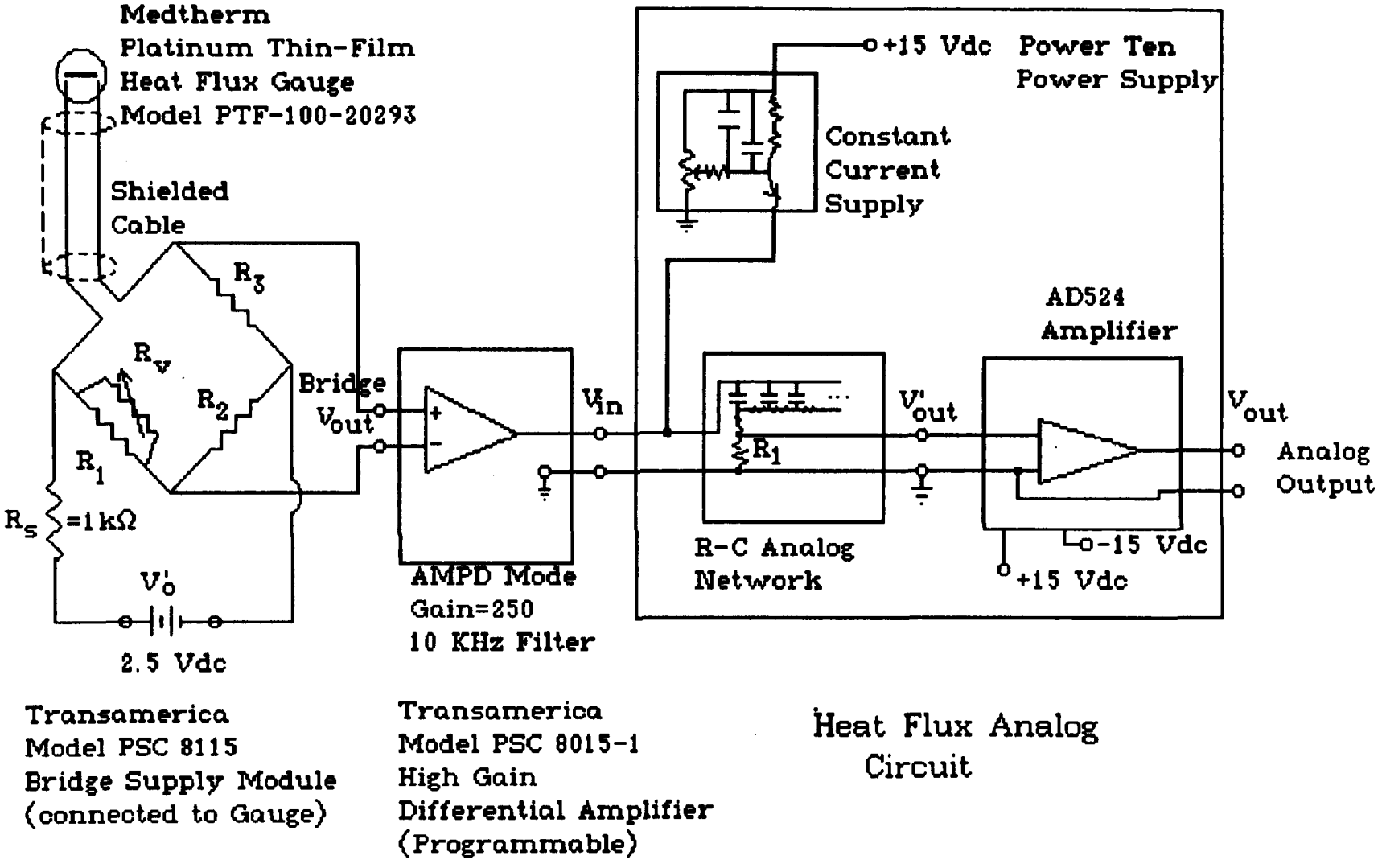


Fig.13

Figure 3.7 Schematic of Heat Flux Analog Circuit and Bridge Connections

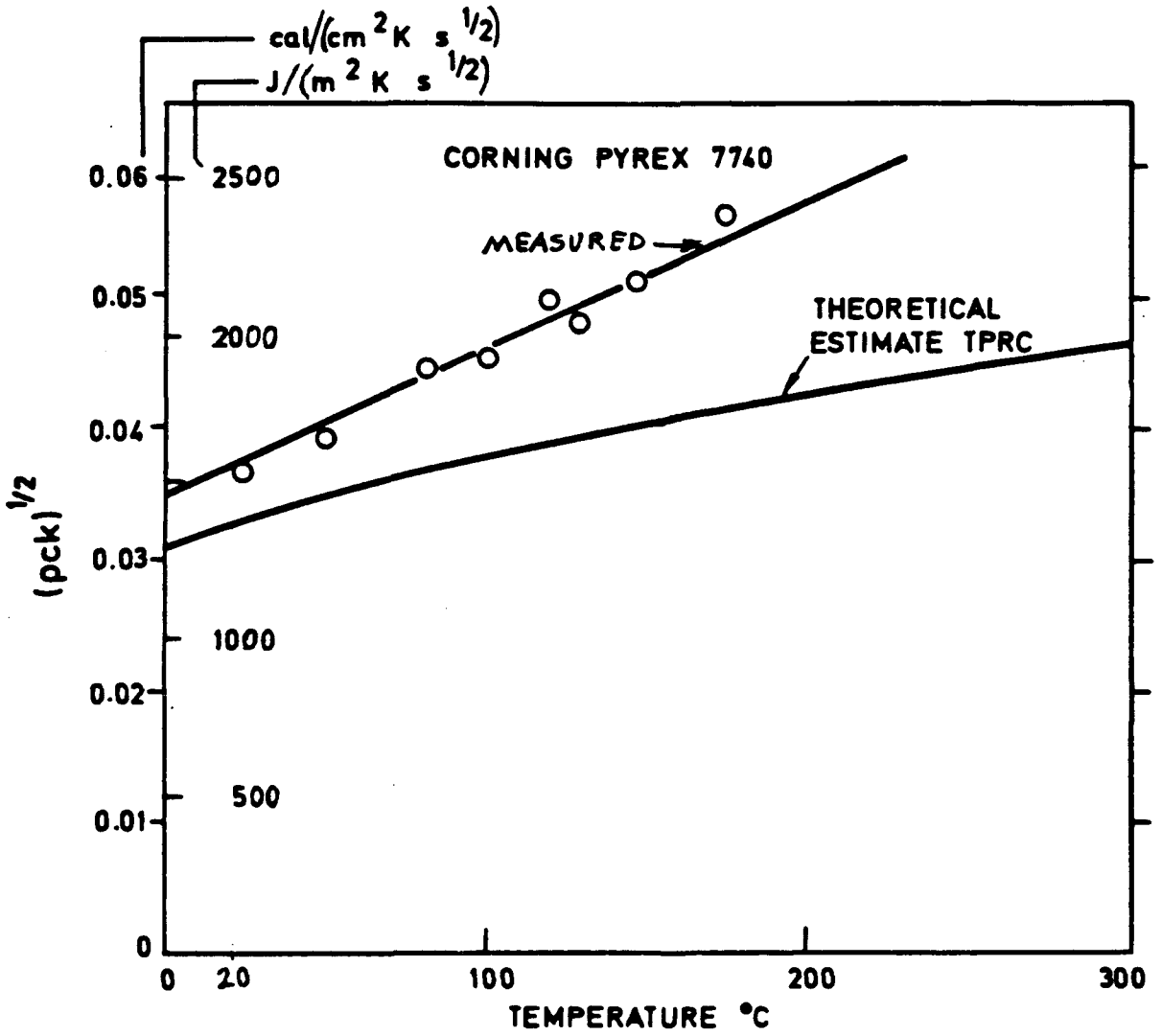


Figure 4.1 Comparison of Measured and Theoretical Values of Bulk Thermal Diffusivity $\sqrt{\rho C_p k}$ for Corning Pyrex 7740 (Taken from Schultz and Jones, 1973:99)

Fig.14

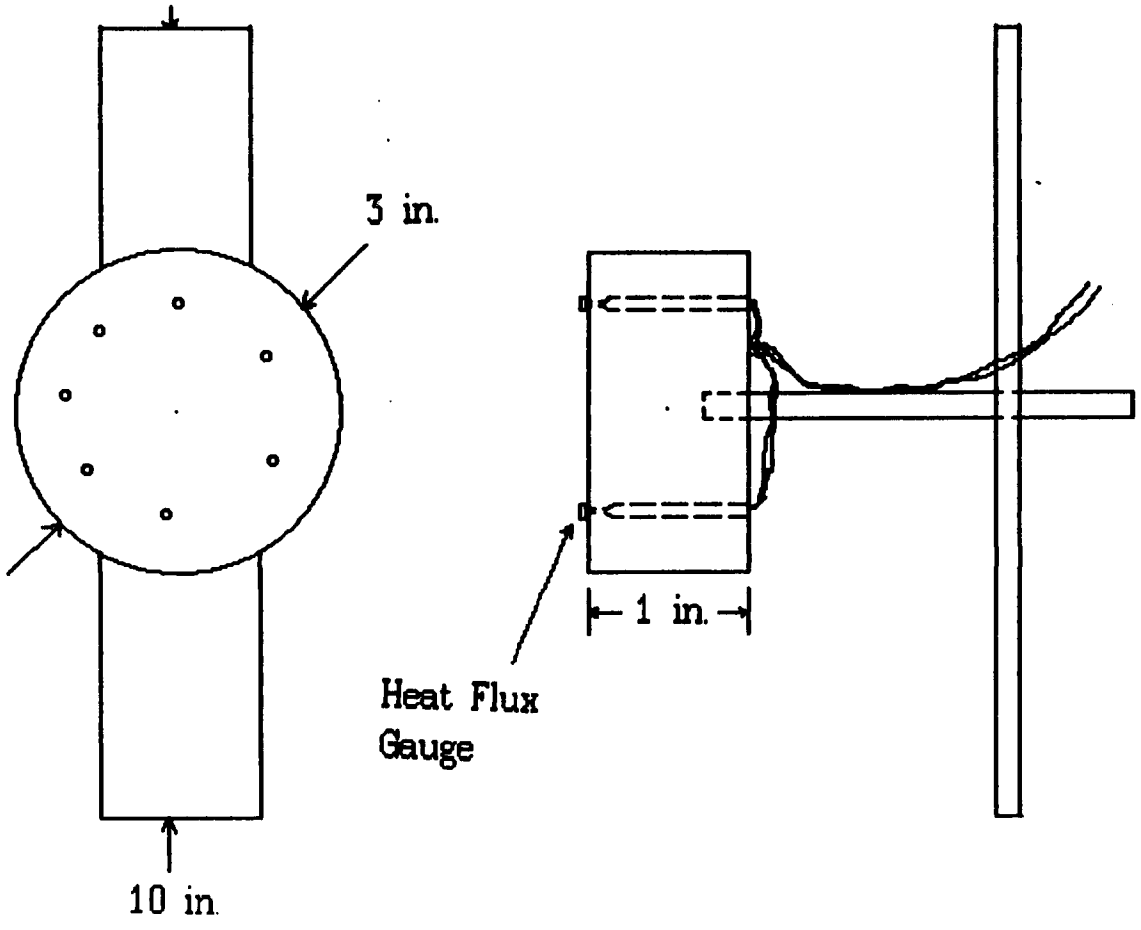


Fig.15

Figure 4.2 Gauge Holder for Calibration of Thin-Film Gauges

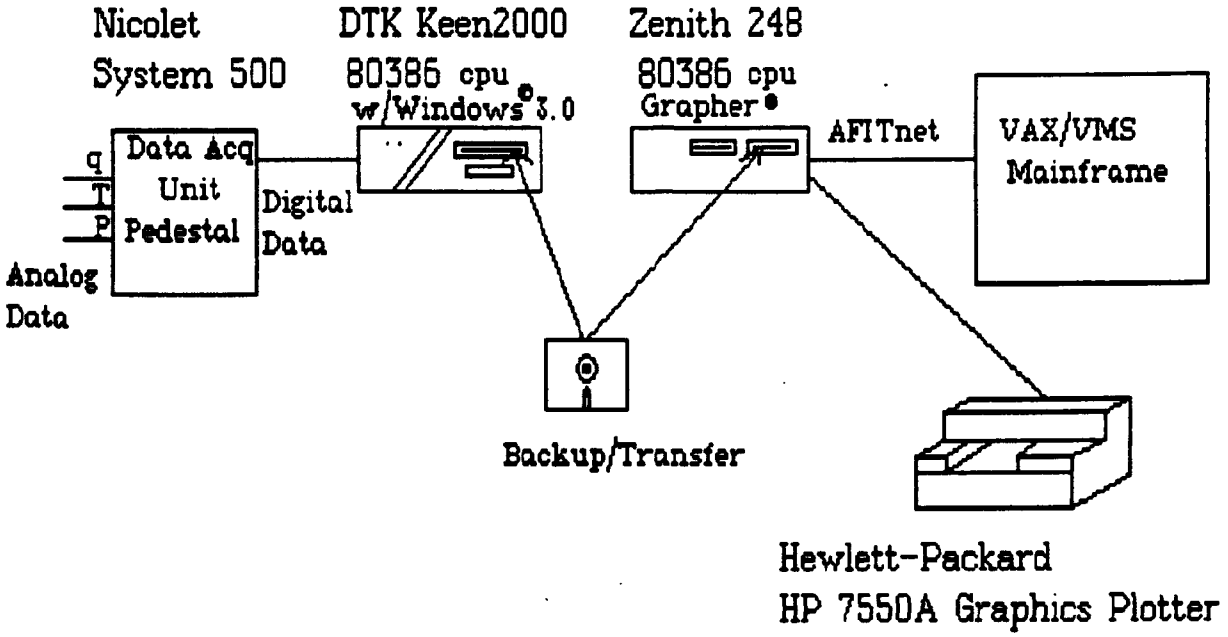


Figure 4.3 Data Acquisition Set-up

Fig.16

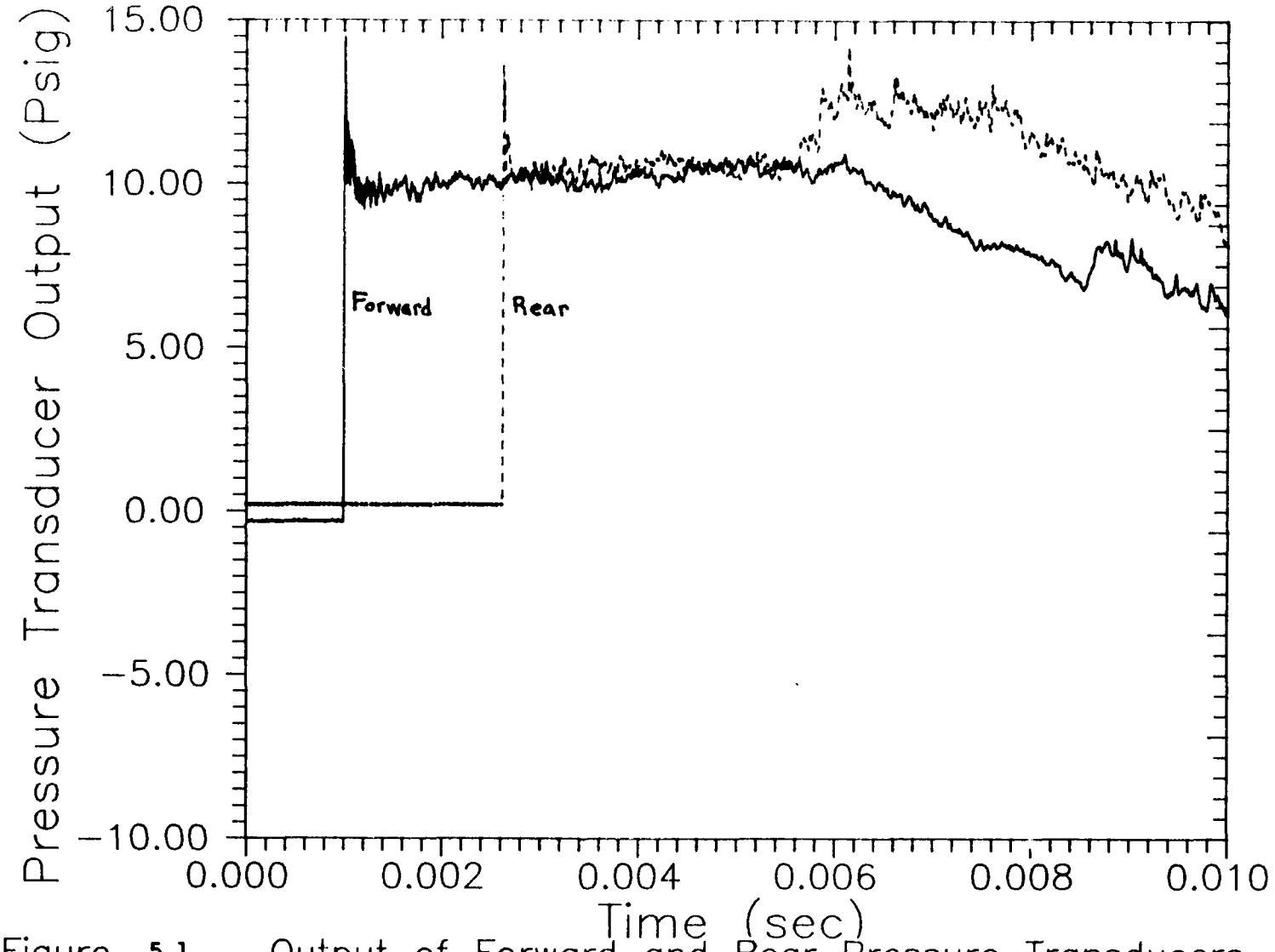


Figure 5.1 Output of Forward and Rear Pressure Transducers for Test T10

Fig.17

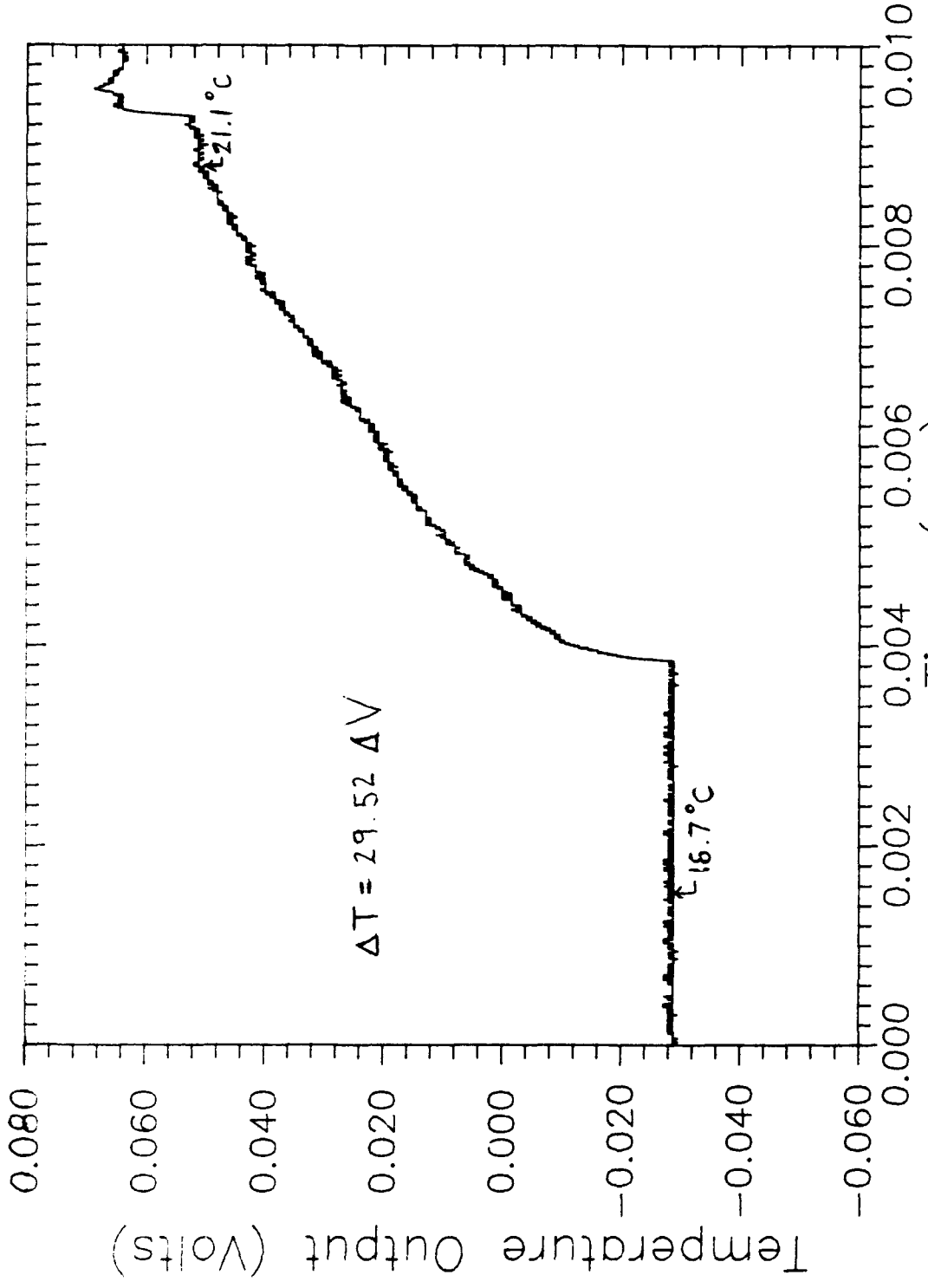


Figure 5.2 Temperature Output of Gauge No. 4 (in Volts), Test T10

Fig. 18

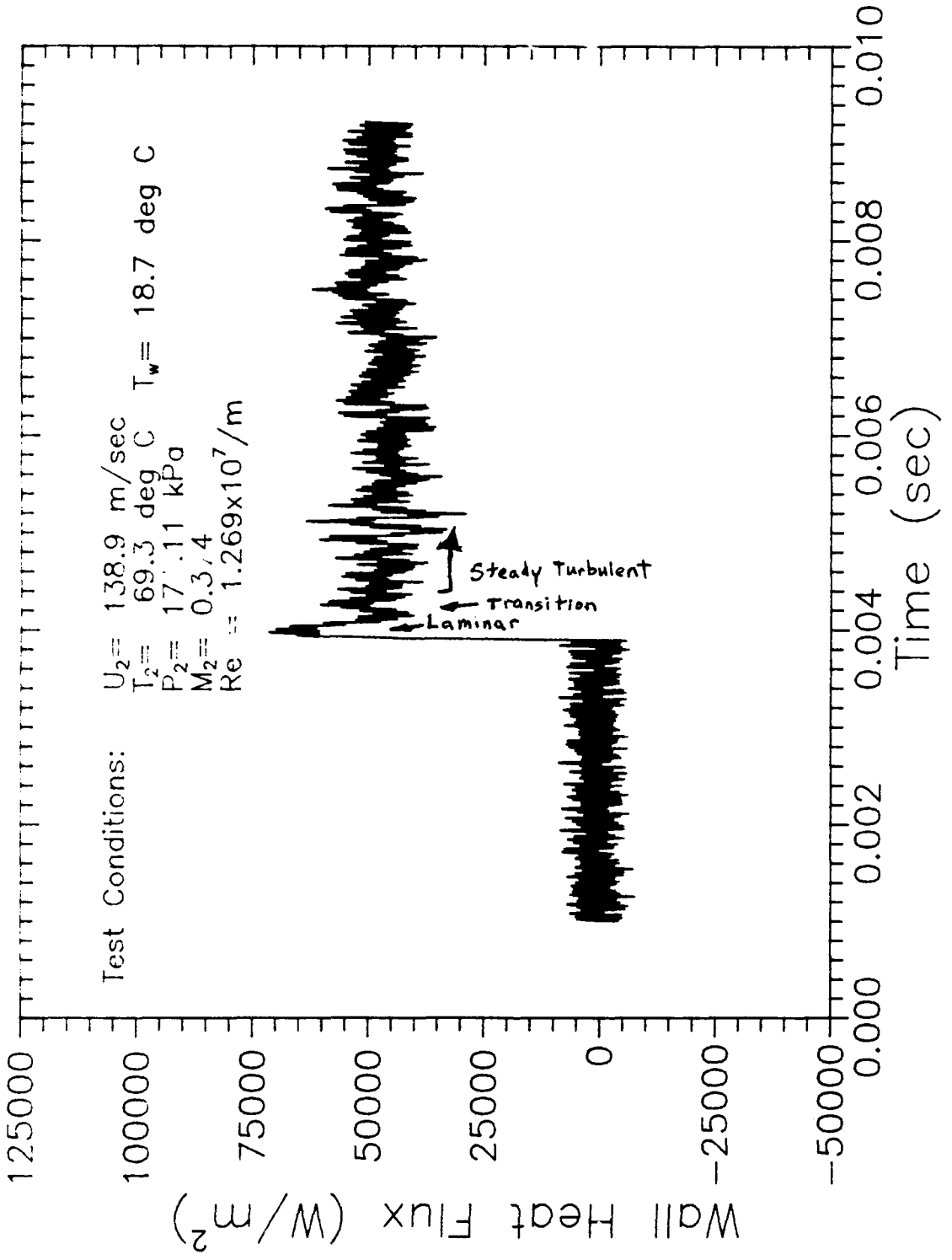


Figure 5.3 Heat Flux Output, Test T10, Gauge 7

Fig.19

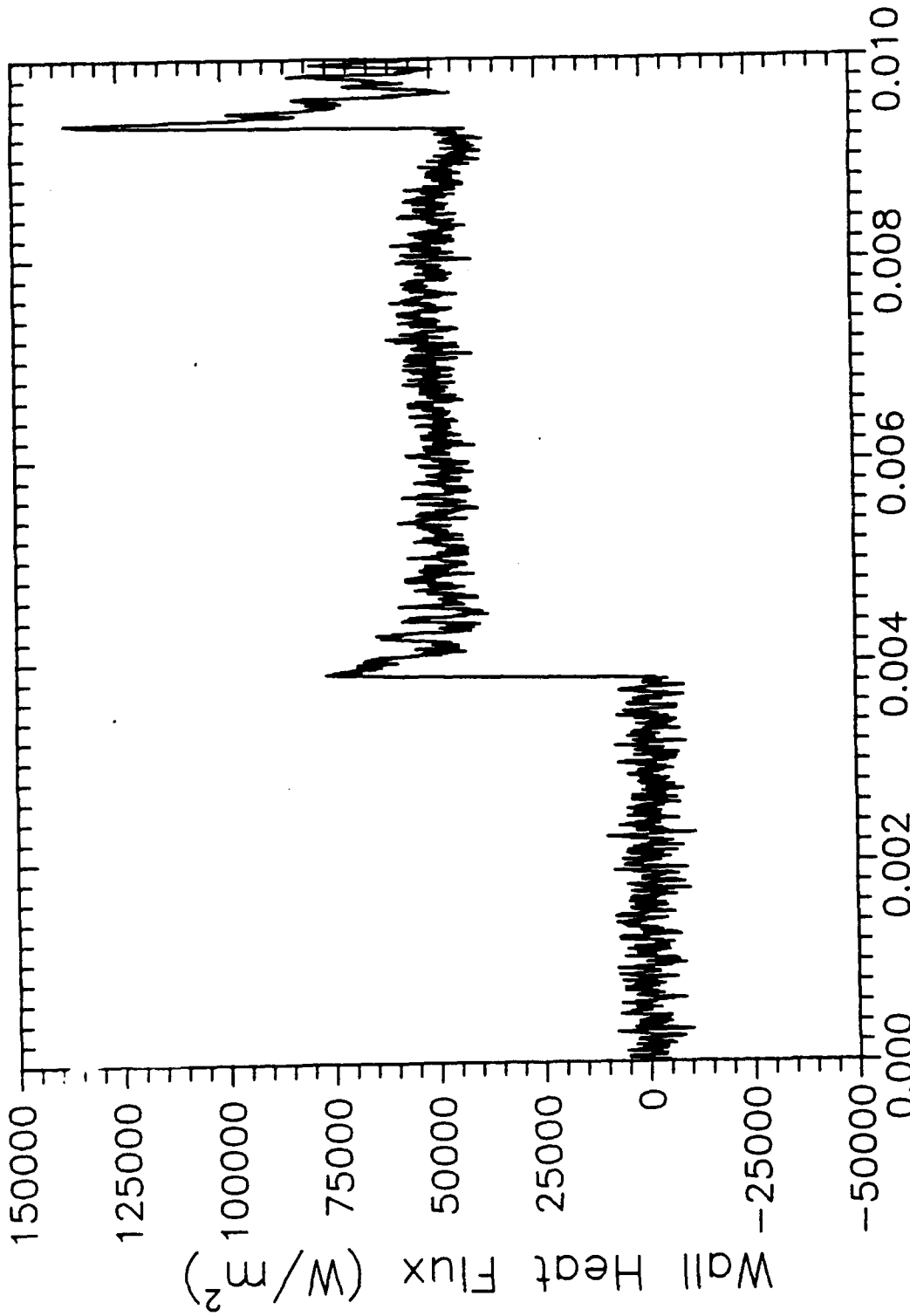


Figure 5.4 Heat Flux Output, Test T10, Gauge 3

Fig.20

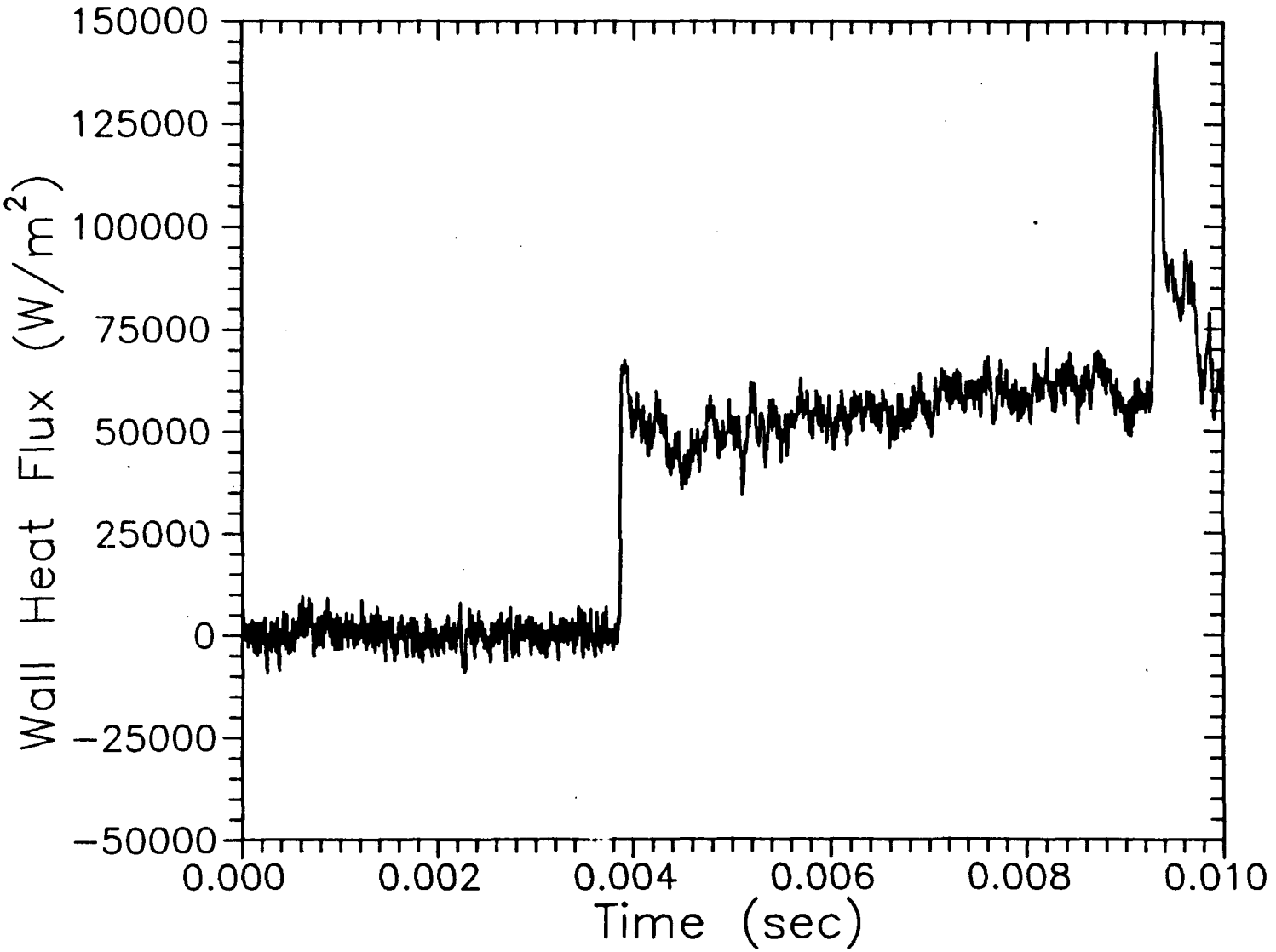


Figure 5.5 Heat Flux Output, Test T10, Gauge 5

Fig.21

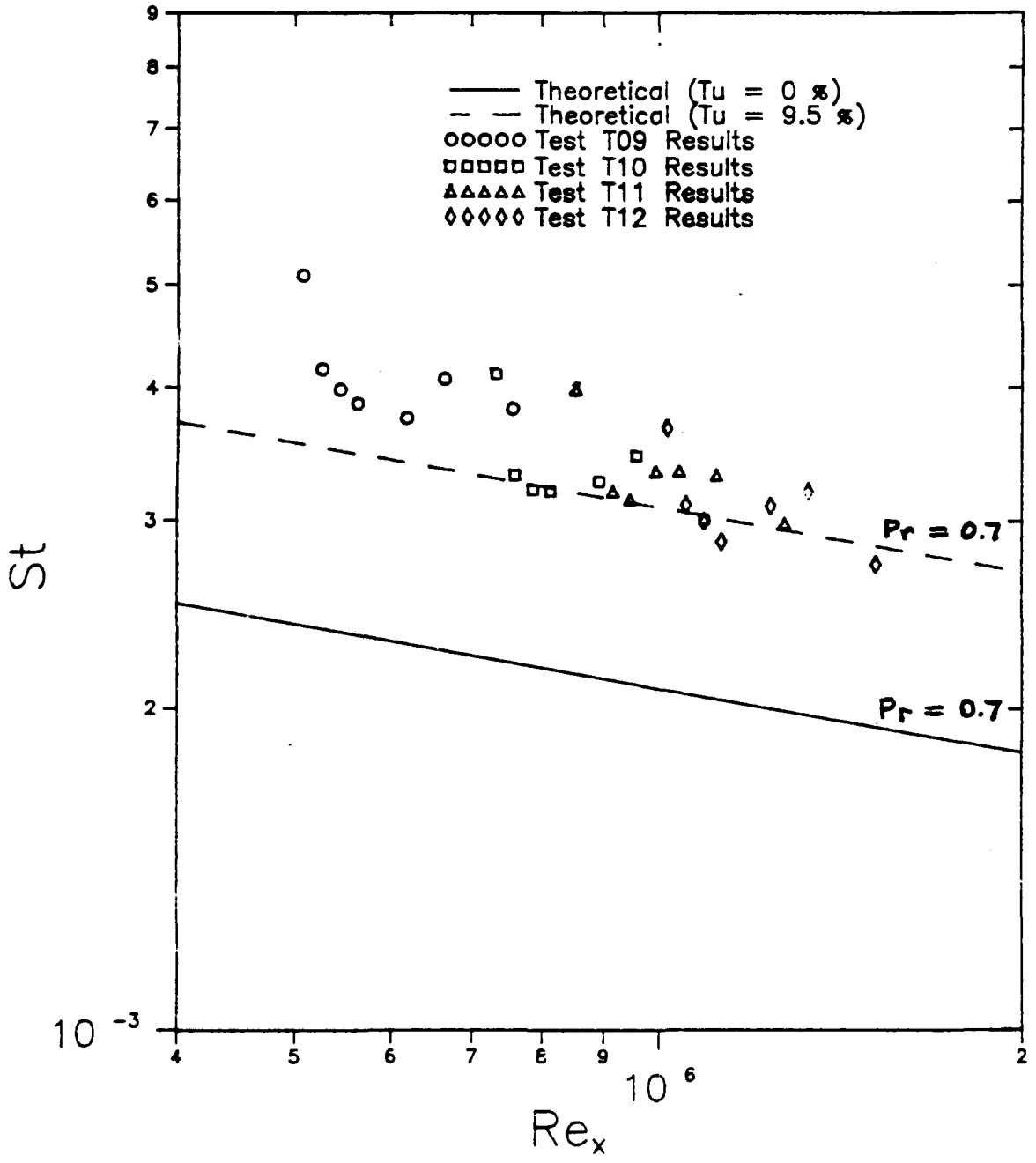


Figure 5.6 Flat Plate Turbulent Air Flow, St vs. $Re_x$

Fig.22

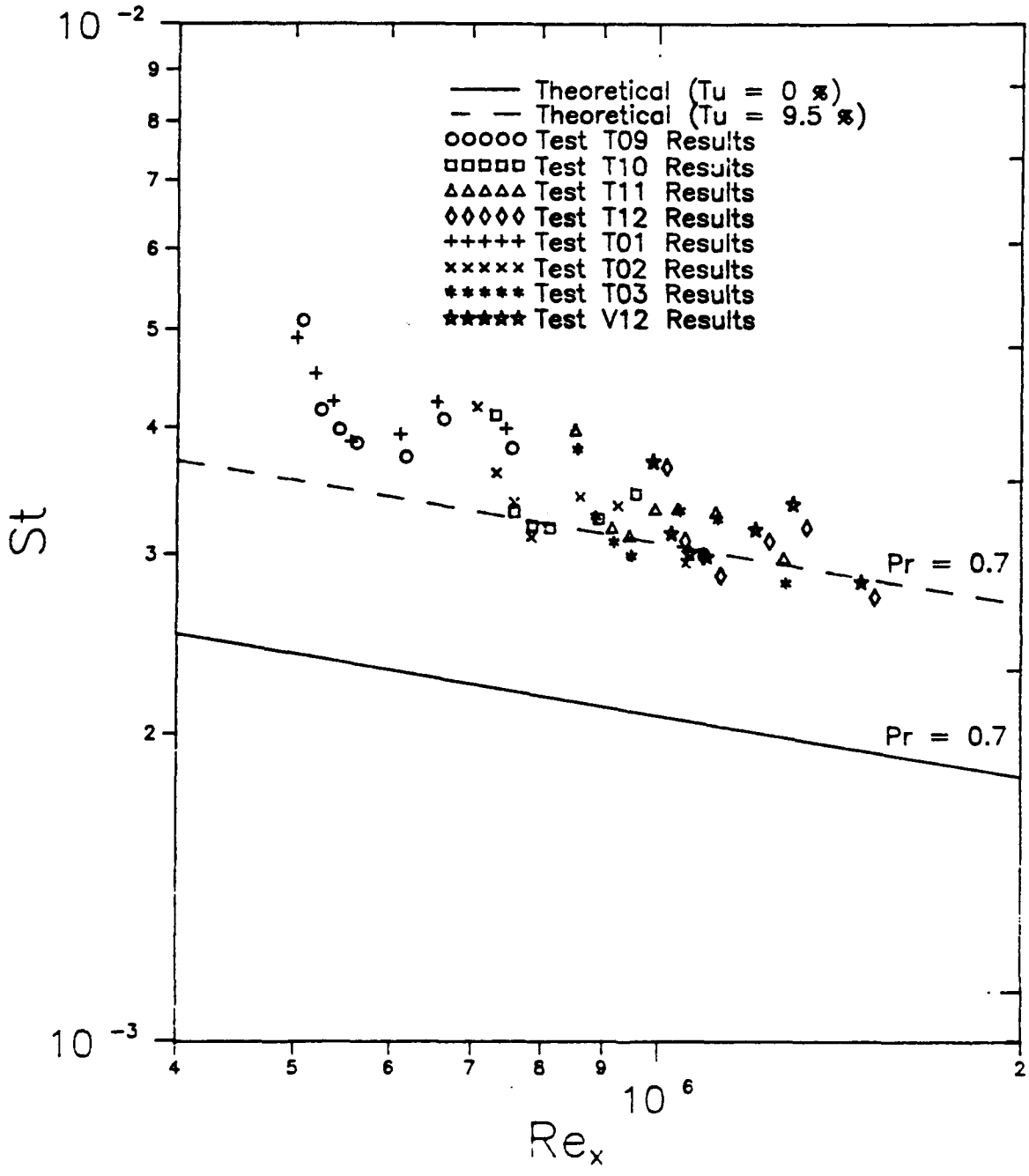


Figure 5.6.1 Flat Plate Turbulent Air Flow, St vs. $Re_x$

Fig.23

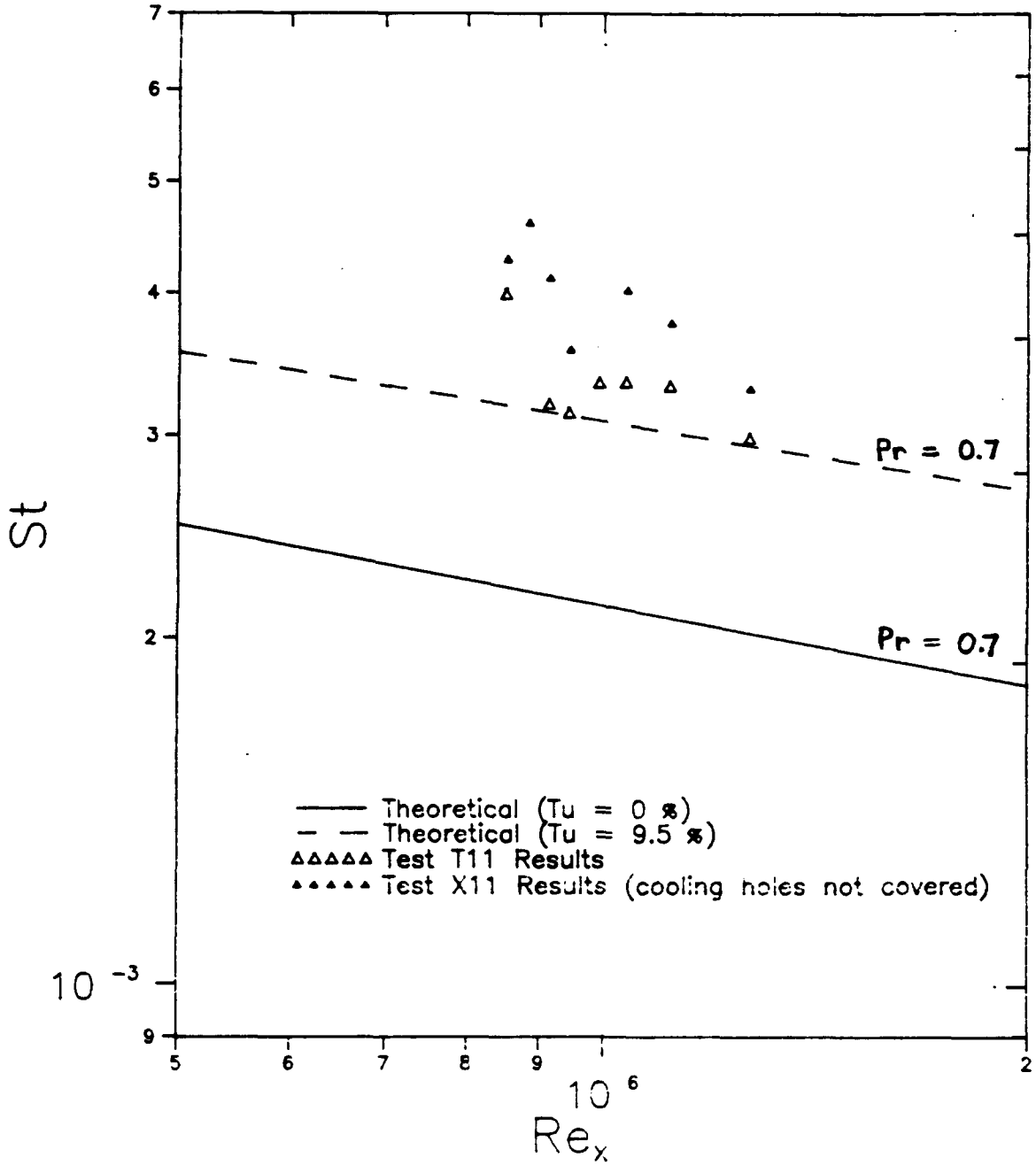


Figure 5.6.2 Flat Plate Turbulent Flow, Showing Effect of Uncovered Holes on Heat Transfer

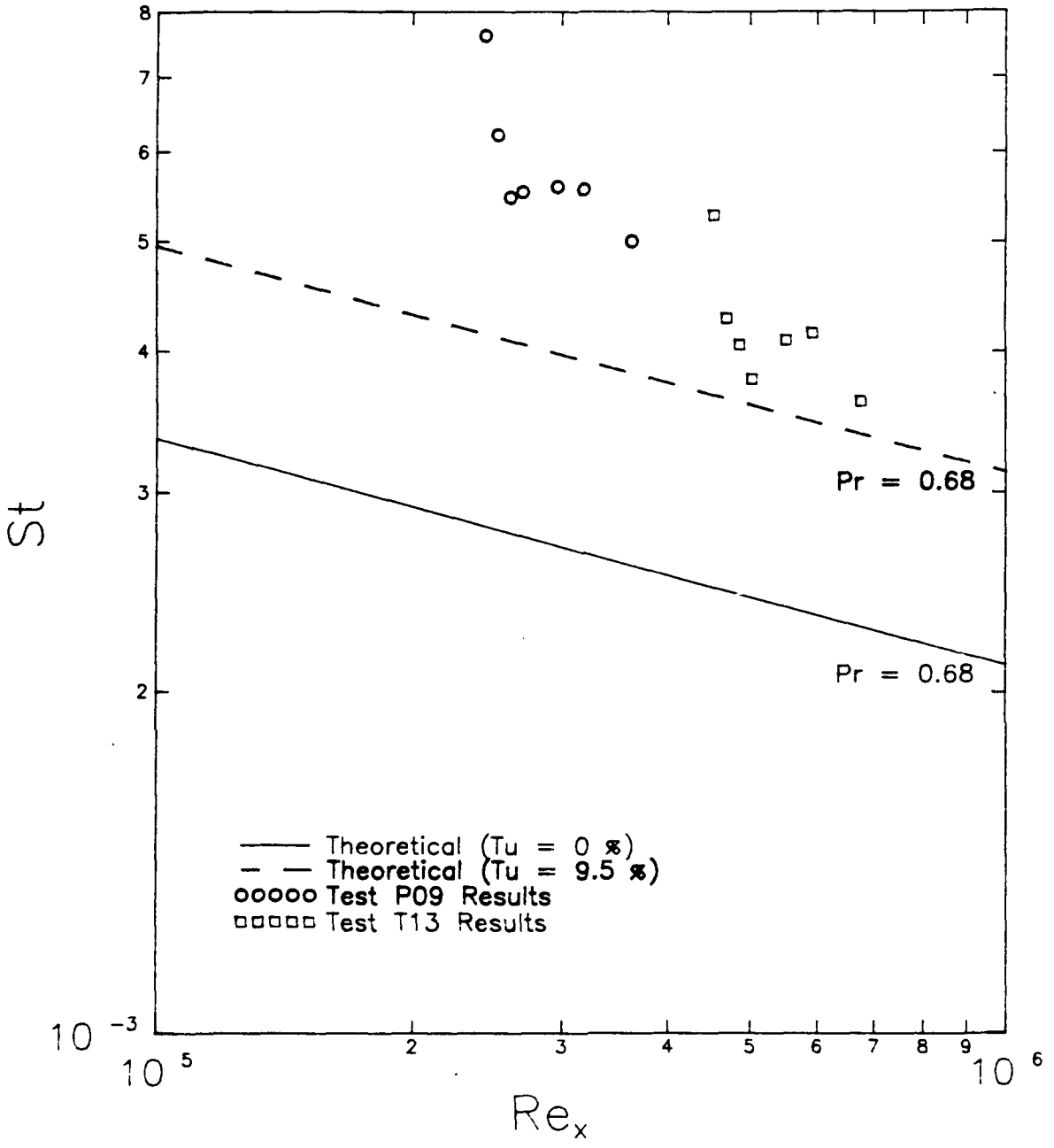


Figure 5.7 Air/Helium Flow, St vs. $Re_x$

Fig.25

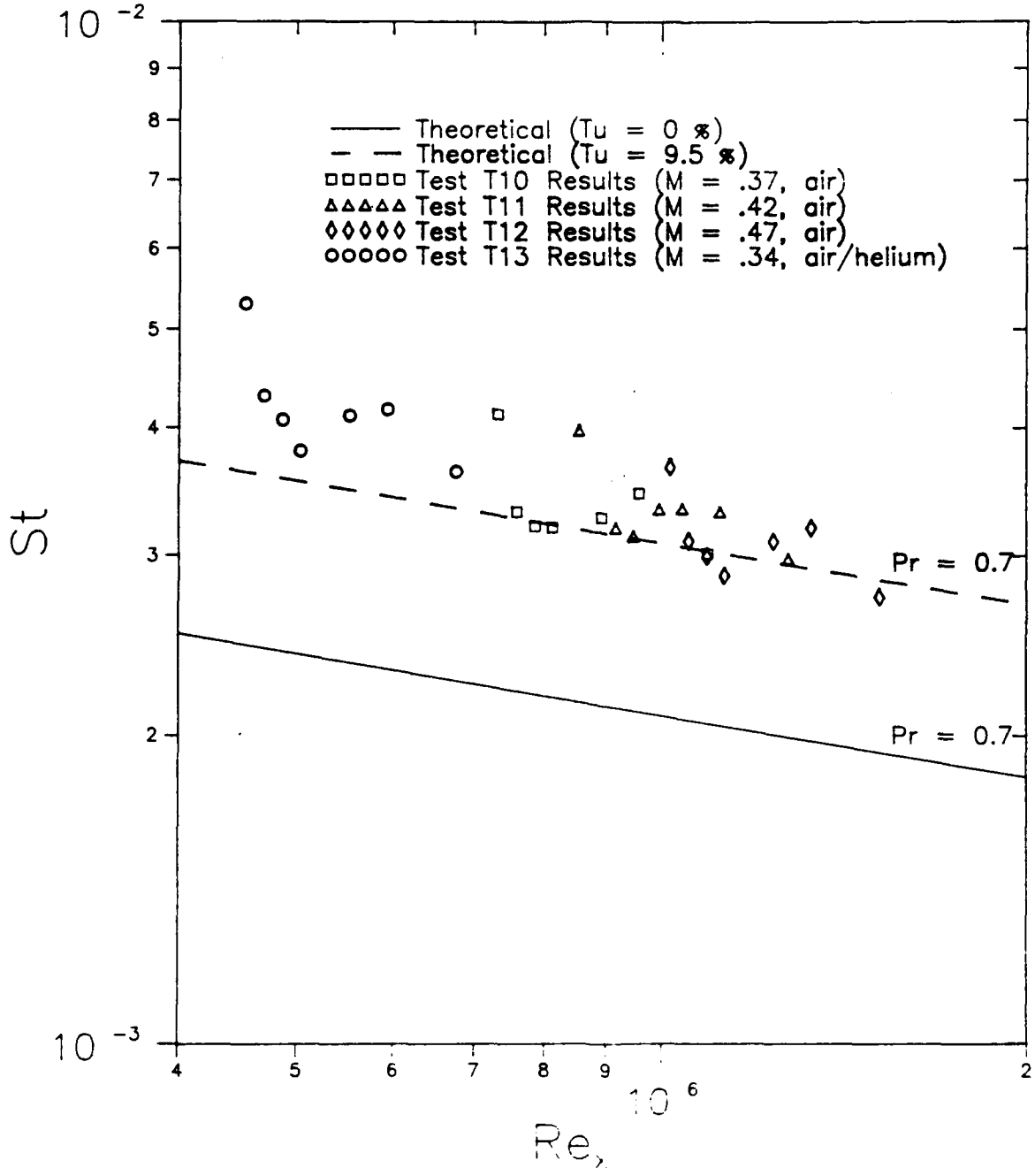


Figure 5.8 Combined Results for Air and Air/Helium, St v. $Re_x$

Fig.26

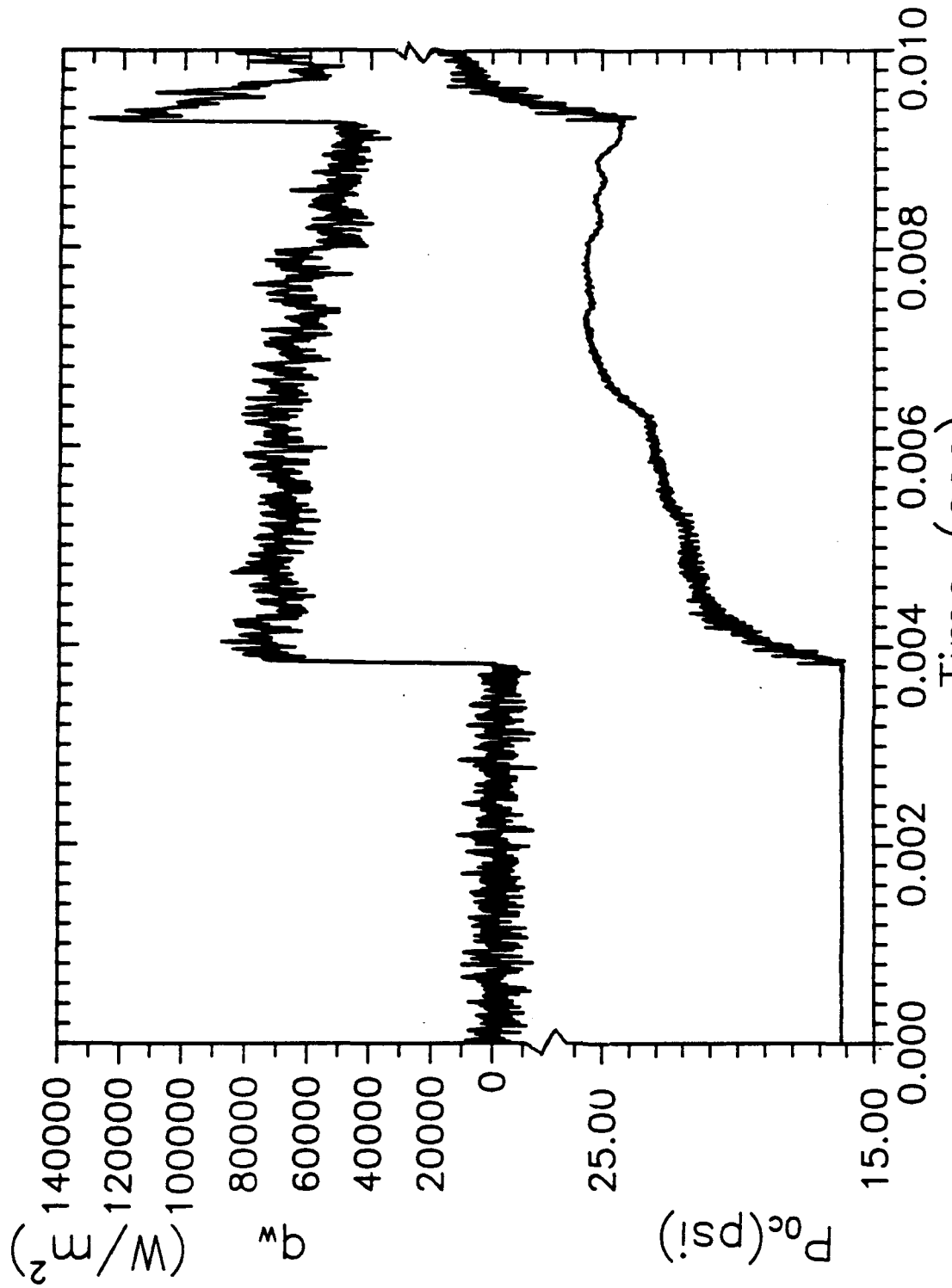


Figure 5.9 Heat Flux and Film Cooling Pressure Output, Test T15

Fig.27

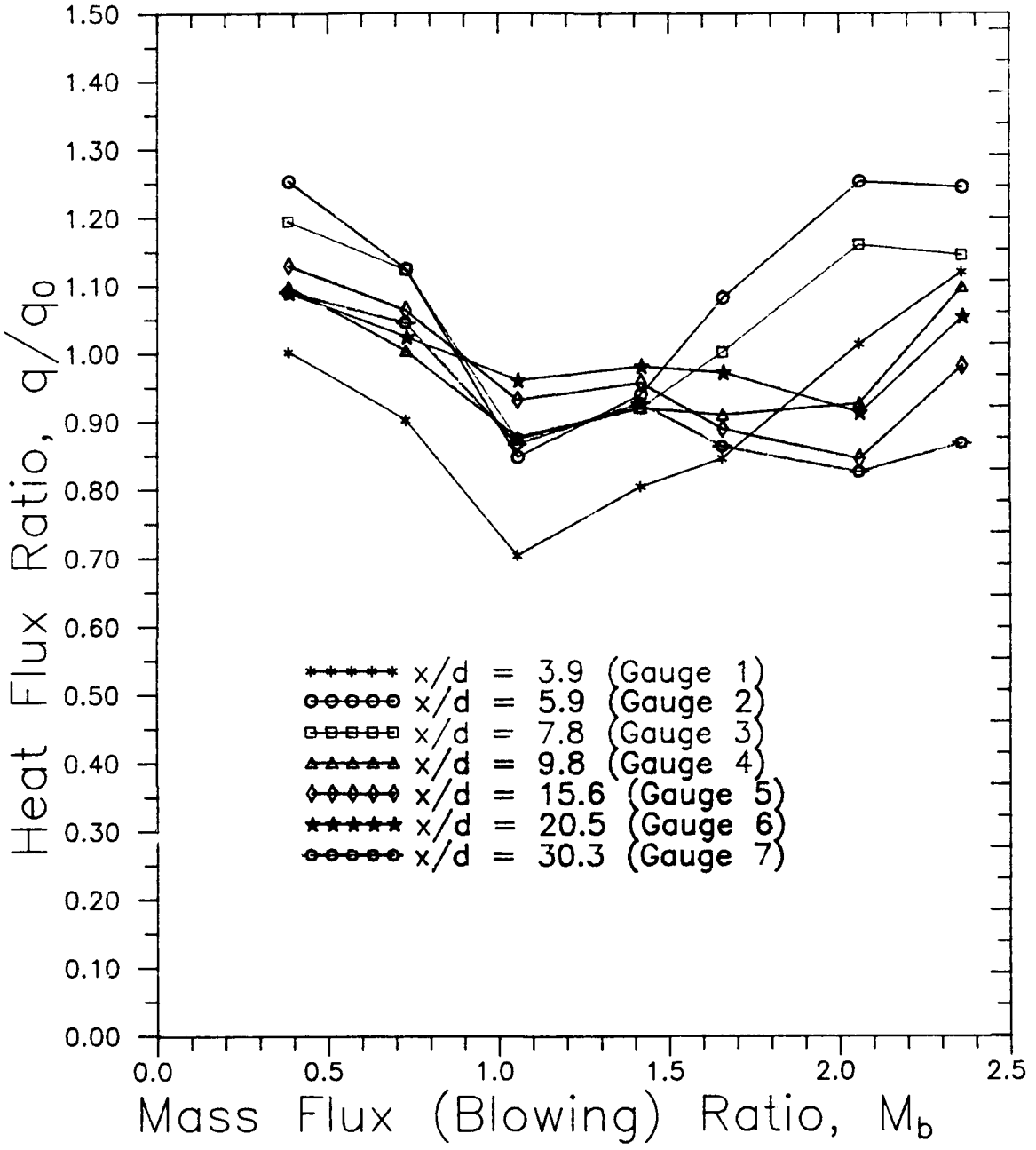


Figure 5.10 Film-Cooling Heat Transfer vs. Blowing Ratio (D.R. = 1.2, $M_2$ = 0.37)

Fig.28

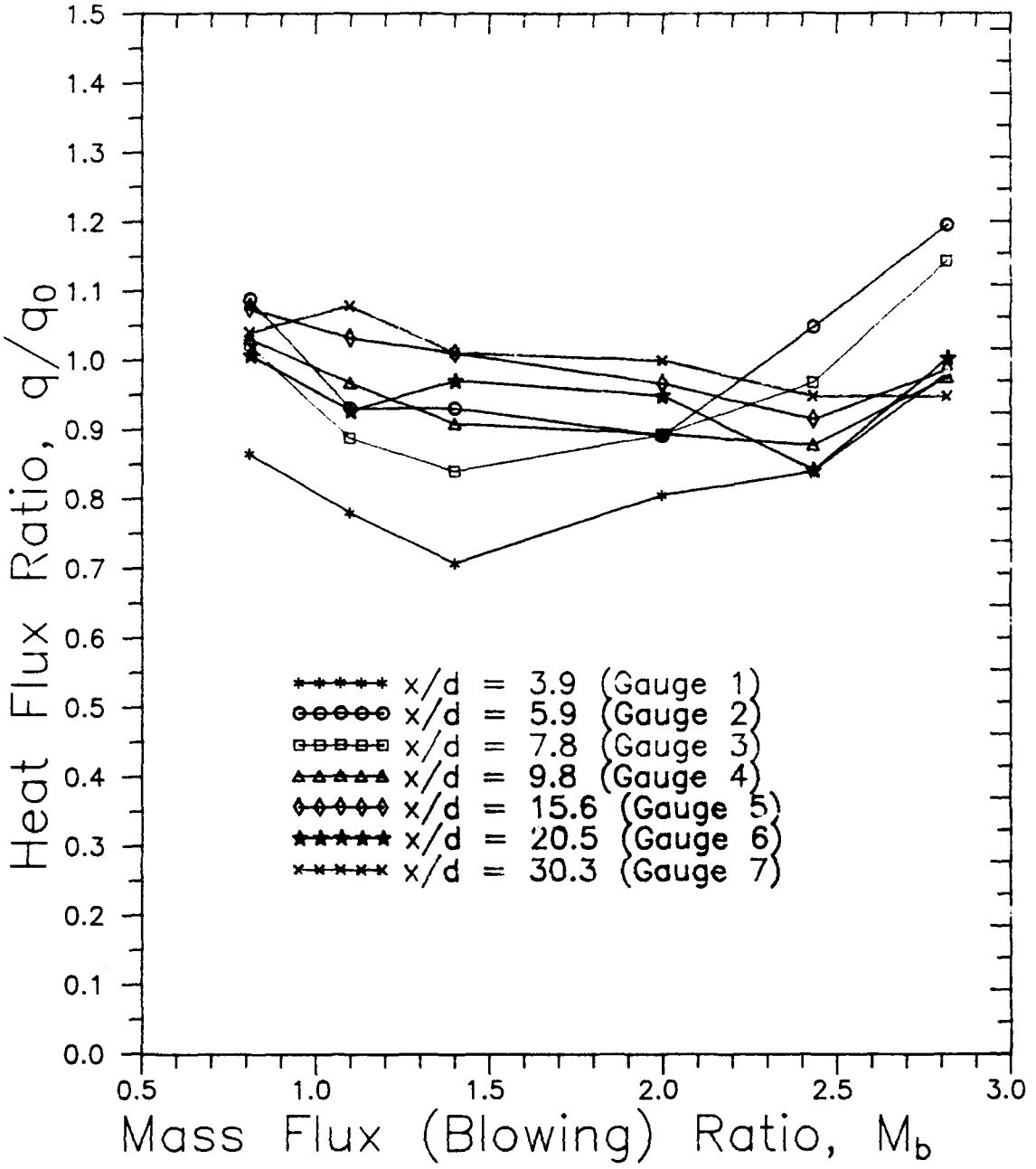


Figure 5.11 Film-Cooling Heat transfer vs. Blowing Ratio (D.R. = 2.1, $M_2$ = 0.34)

Fig.29

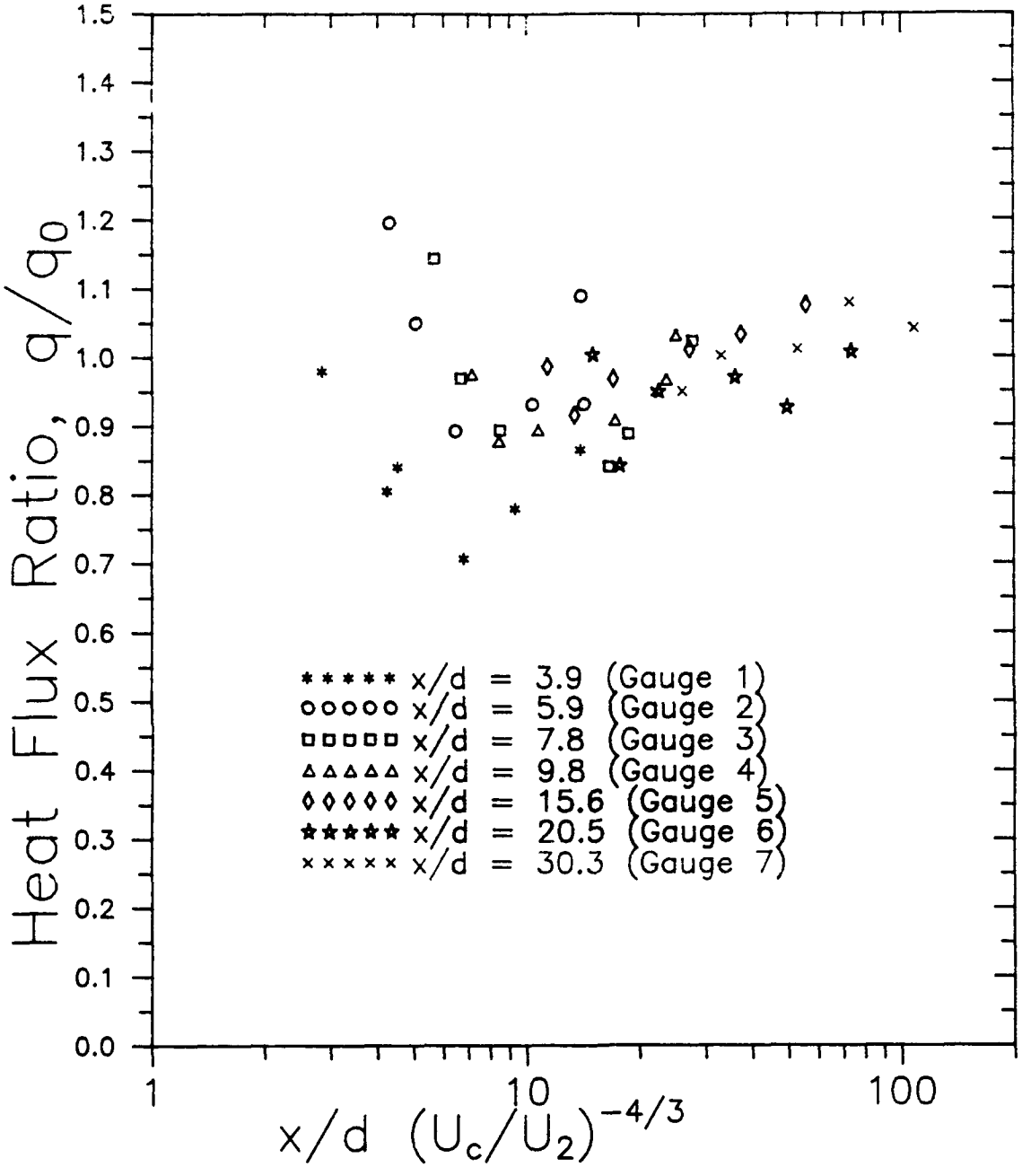


Figure 5.12 Film-Cooling Heat Transfer vs. Velocity Ratio Parameter (D.R. = 2.1, $M_2$=0.34)

Fig.30

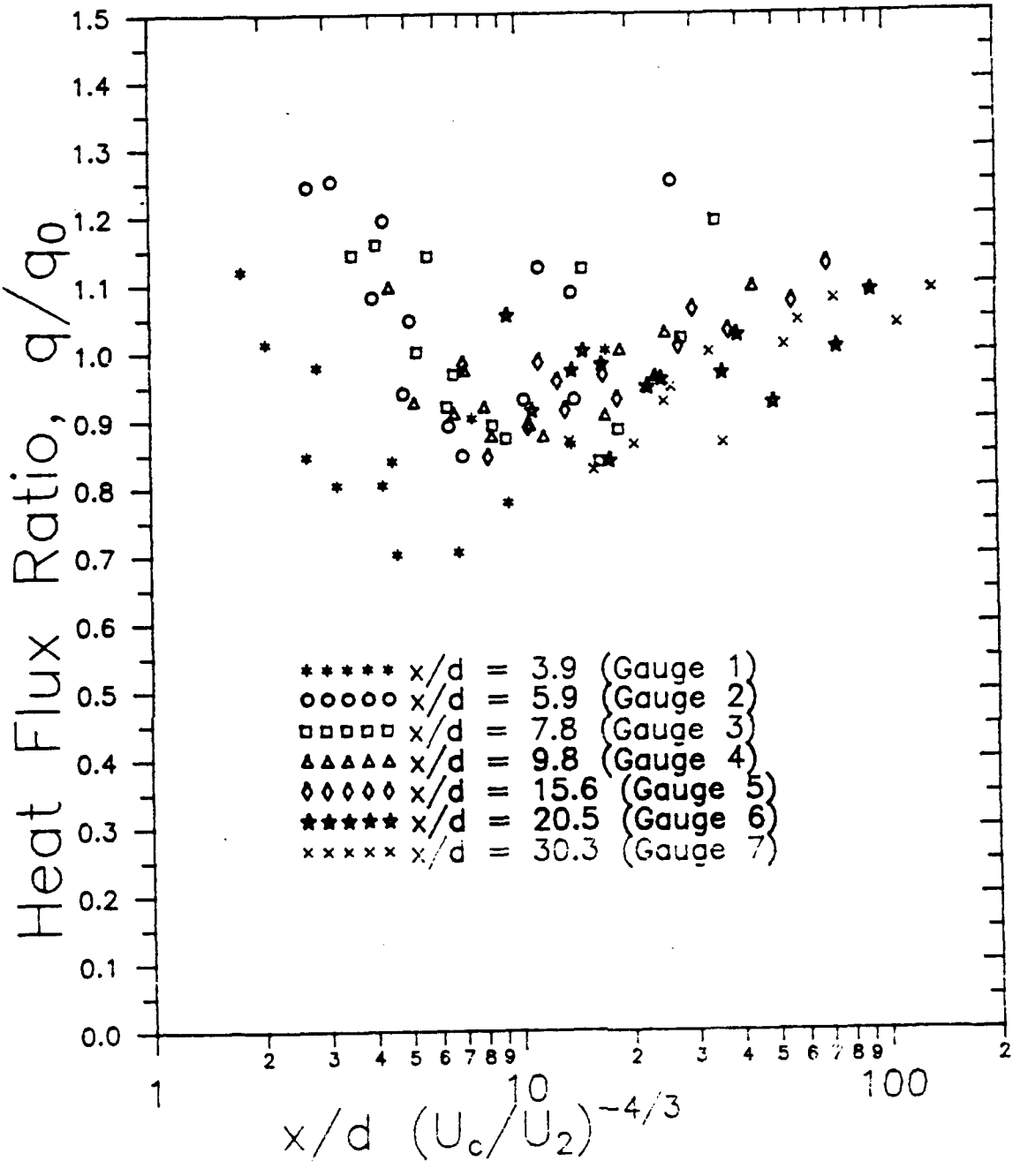


Figure 5.13 Film-Cooling Heat Transfer vs. Velocity Ratio Parameter (D.R.=1.2 and 2.1, $M_2$=0.37 and 0.34)

Fig.31

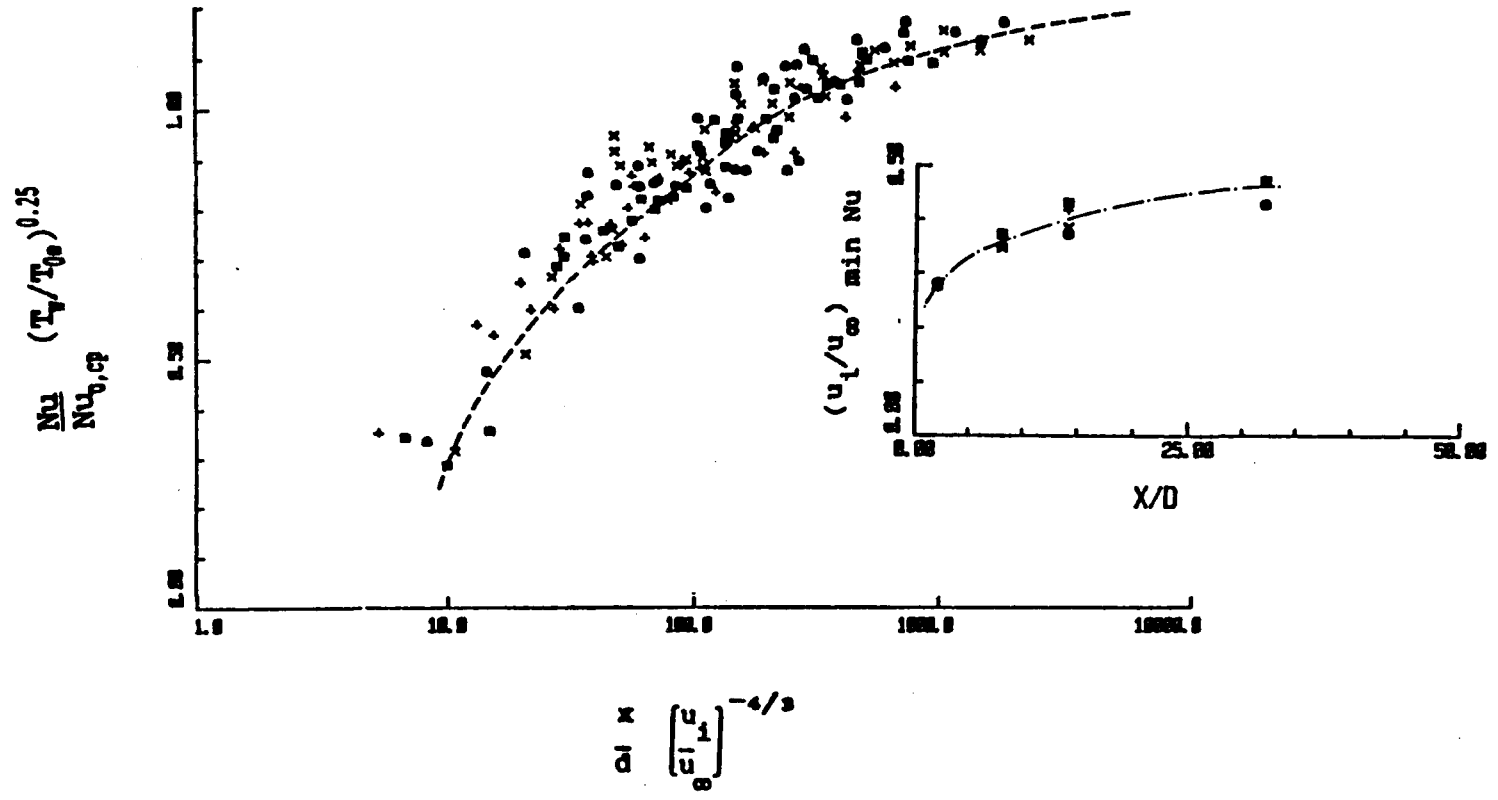


Fig.32

Figure 5.14 Correlation of Data for Four Injection-to-Mainstream Temperature Ratios, Single Row of 30 deg Inclined Holes (Forth and Jones, 1986: 1276). Inset shows scaling of condition of minimum Nusselt number at each downstream position with velocity ratio.
[Nusselt number defined by $Nu = q\ x/\ k_{0\infty}(T_{0\infty}-T_w)$ ]

## Appendix A: Calibration of Thin-Film Resistance Gauges for Temperature Coefficient

Using a gauge holder for all seven thin-film gauges and the Nicolet System 500, calibration for all gauge temperature coefficients $V_o\alpha$ was accomplished simultaneously.

The gauge wires were inserted through the face of the holder and attached to a terminal strip (see Figure A.2). (Note: After installing gauges on the test plate with the small nuts, the attachment of connectors to the gauge leads will not allow the gauges to be removed without cutting the wire at the connectors to remove the nuts.) From the terminal strip a short length of shielded cable connected the gauges to the normal test cable for data collection. After the gauge leads were carefully pulled to set the gauges flush with the face of the holder, a latex sheet (surgical glove) was pulled taut around the holder to ensure good contact of all gauge faces. The holder was adjusted in height and set in the water and on the 4000 ml beaker and thermal mixer combination as shown in the diagram.

Allowing the water to stand over night ensured a constant temperature at which to balance all the gauge/bridge circuits. The calibrator thermocouple was placed in the water next to the gauges and taped to the holder to maintain its location when the mixer was stirring the water. After allowing the gauge/bridge circuits to achieve their equilibrium balance following the last adjustment, the calibration began. The Nicolet system 500 read all the voltage levels output from the amplifiers using "one shot" with

"auto trigger" setting. The acquisition settings were 0.5 sec, 1000 points, at 1.2 Volt dc range. Each data point was saved before acquiring the next one.

The thermal plate and mixer were turned on to mid-range to heat the water uniformly. The calibrator temperature was monitored. As soon as the temperature readout stabilized at the 1/10th of 1 deg F temperature desired, a "one shot" was selected to read all voltage levels input to the seven channels used. The temperature was recorded and the data saved to the next file. Temperature increase was at the rate of approximately 0.5 deg F per minute.

Upon completing the highest temperature point, the average voltage level was noted for each channel/gauge for each temperature. This procedure produced very good results, achieving a minimum correlation coefficient of 0.9997 (gauge 6) for the least squares fit of the data. Figures A.2 to A.8 show plots of the calibration data.

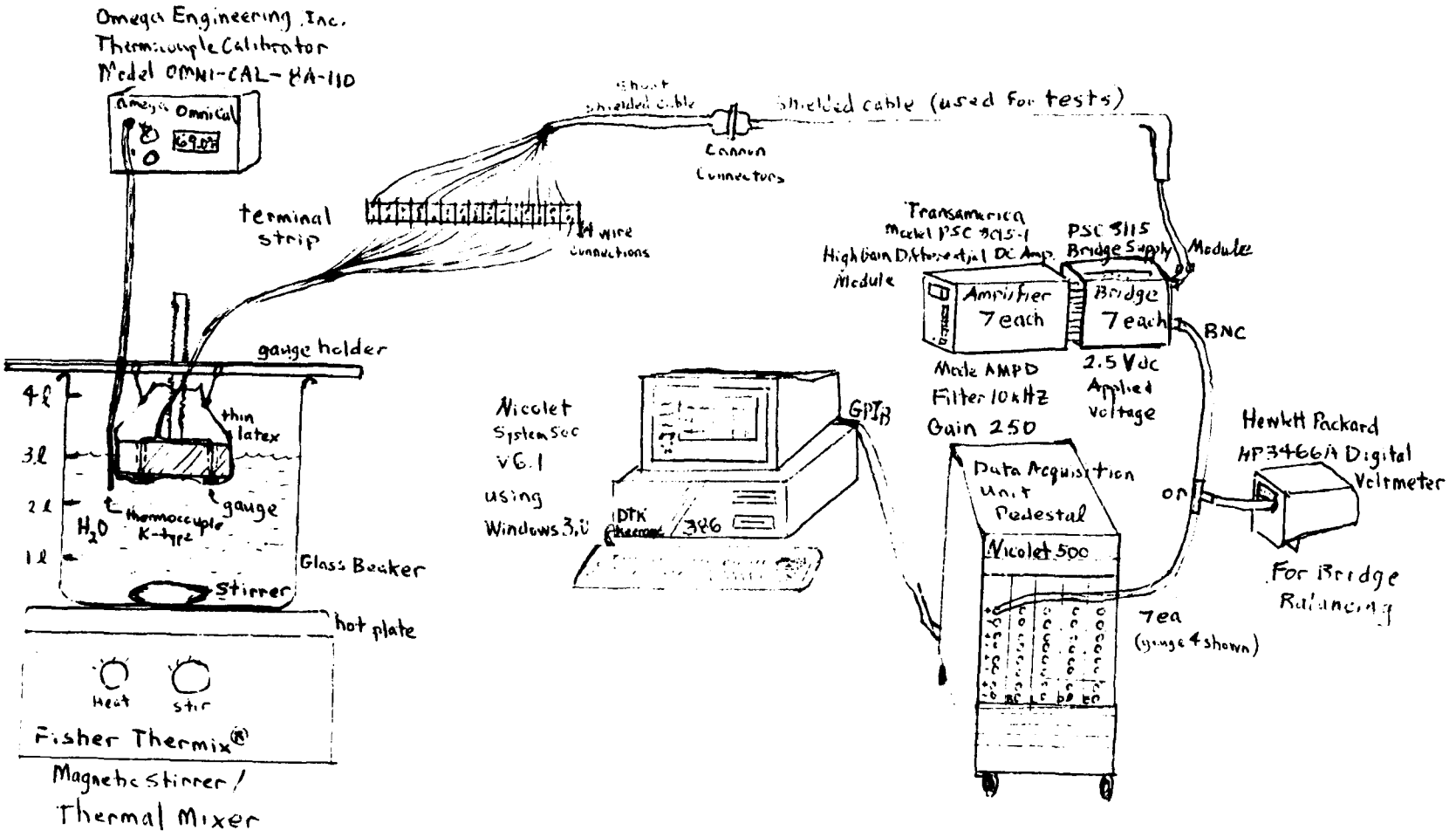


Figure A.1 Heat Flux Gauge Temperature Coefficient Calibration Set-up

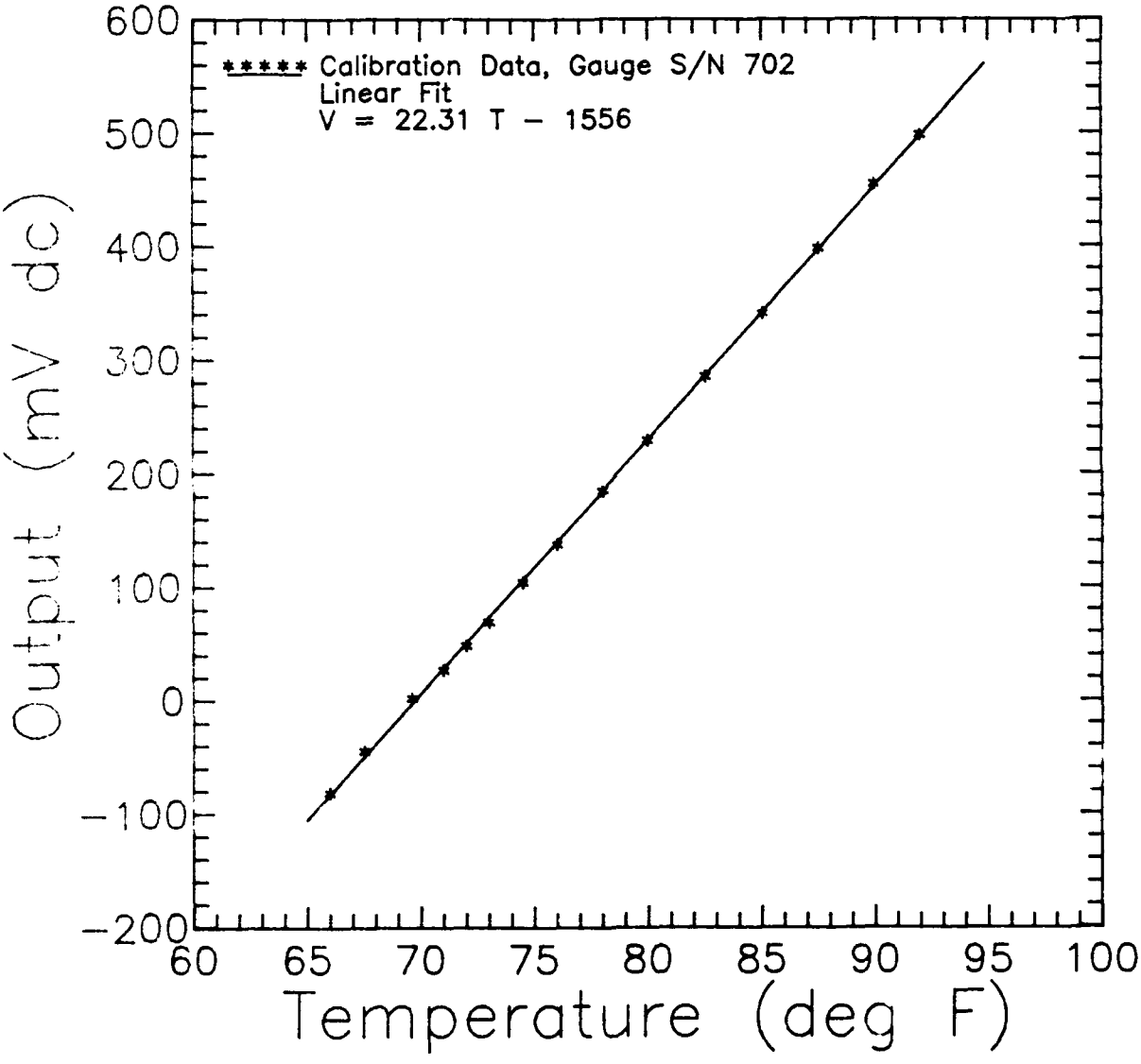


Figure A.2 Calibration Curve for Gauge No. 1

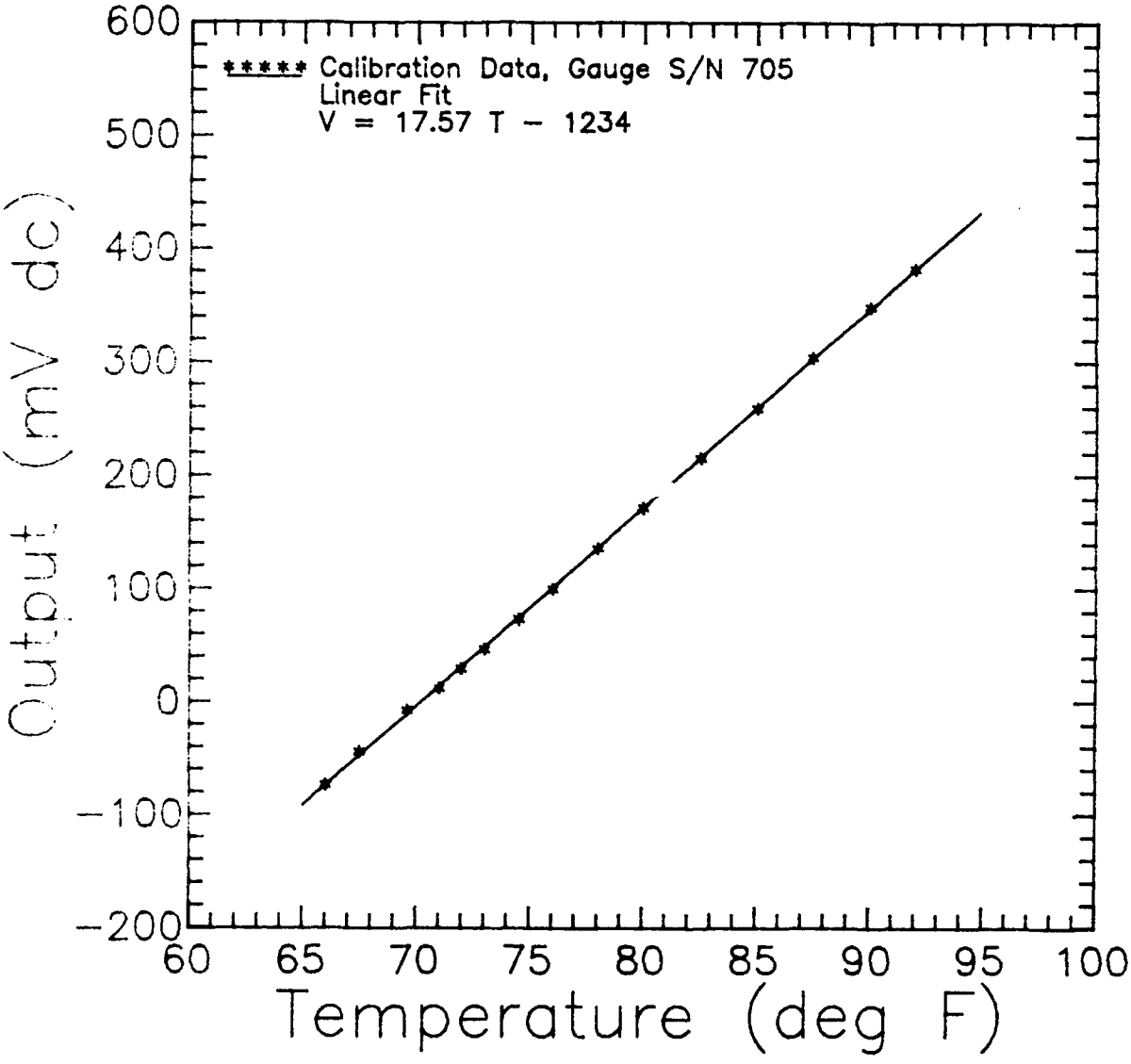


Figure A.3 Calibration Curve for Gauge No. 2

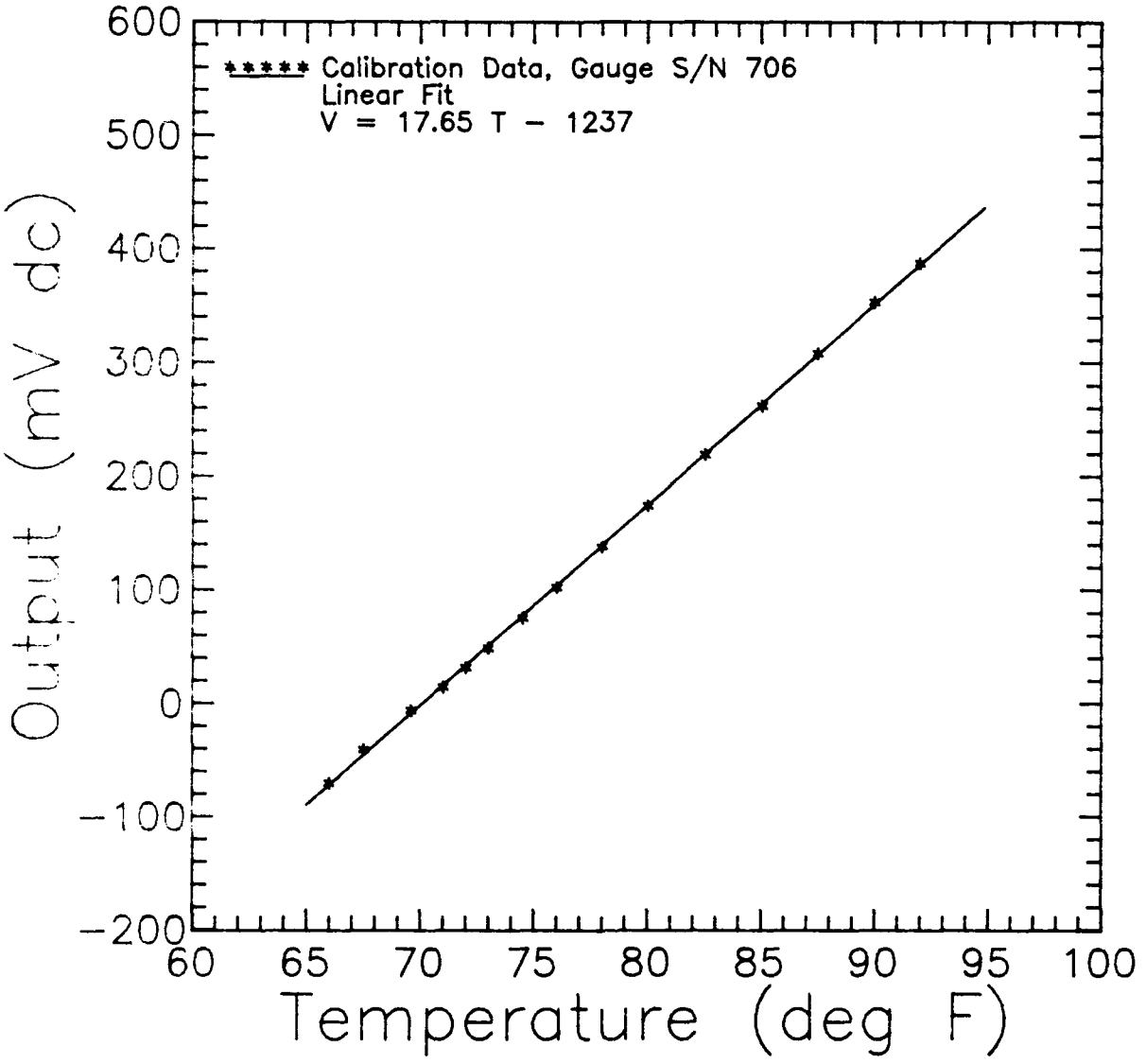


Figure A.4 Calibration Curve for Gauge No. 3

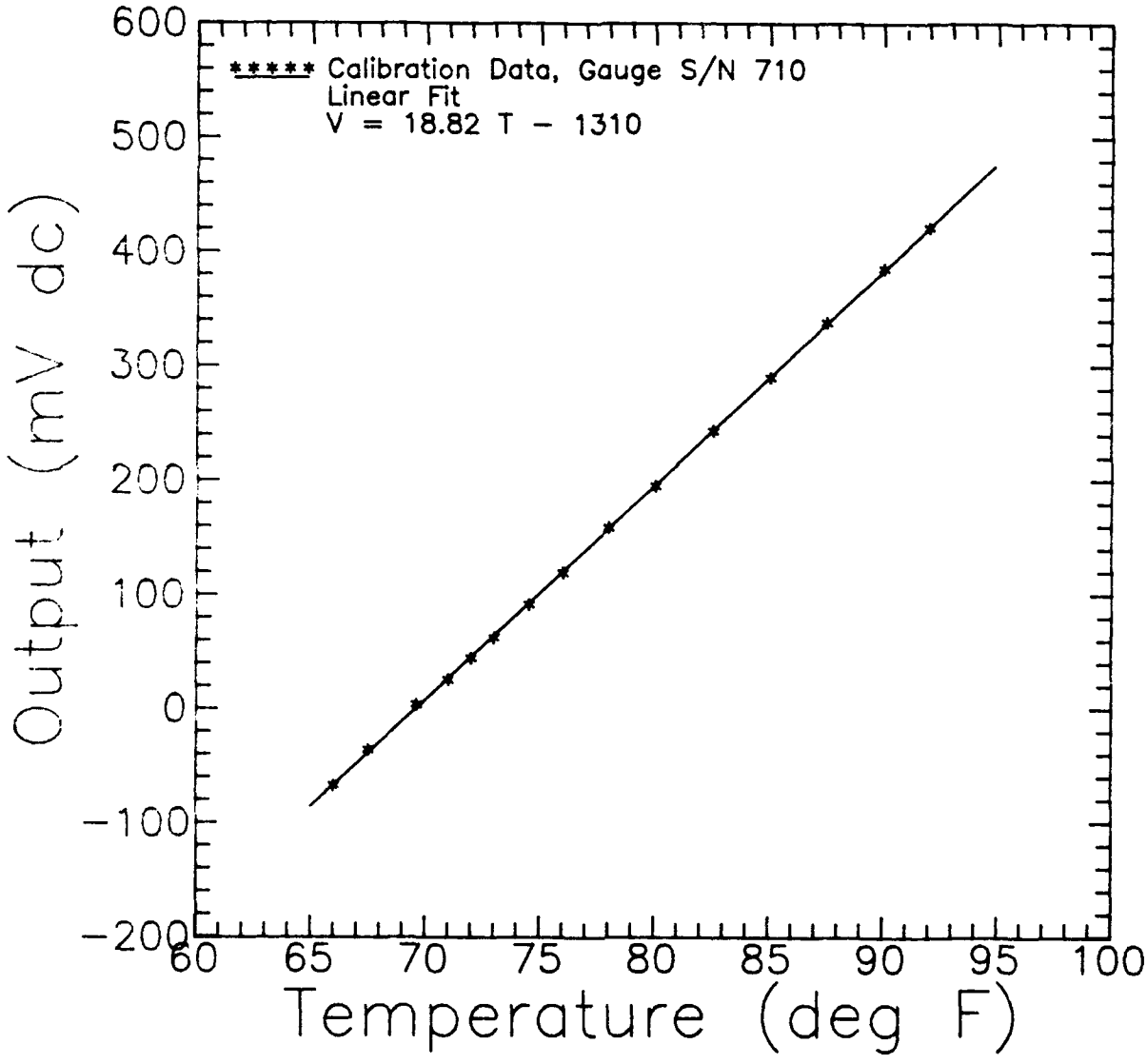


Figure A.5 Calibration Curve for Gauge No. 4

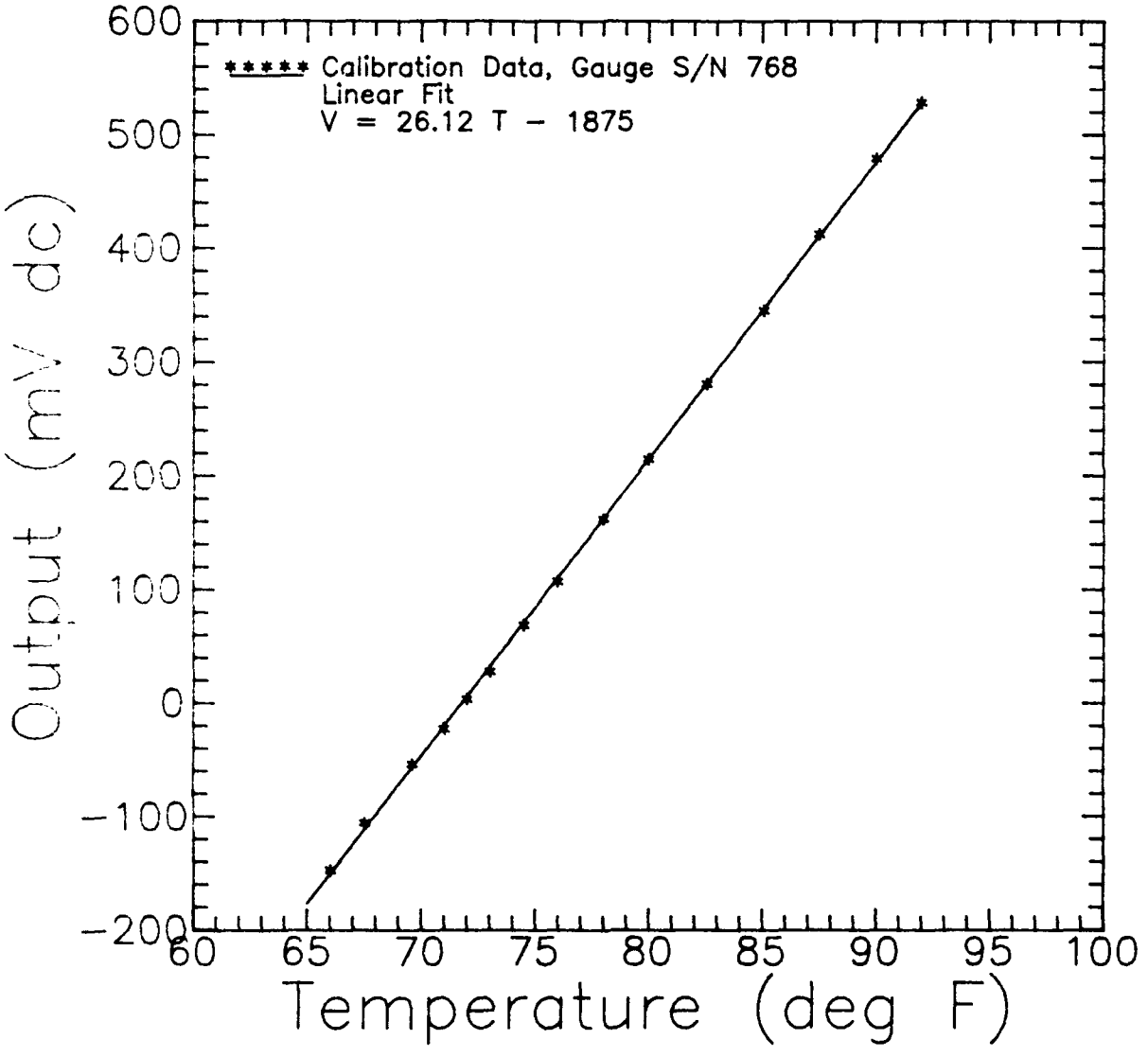


Figure A.6 Calibration Curve for Gauge No. 5

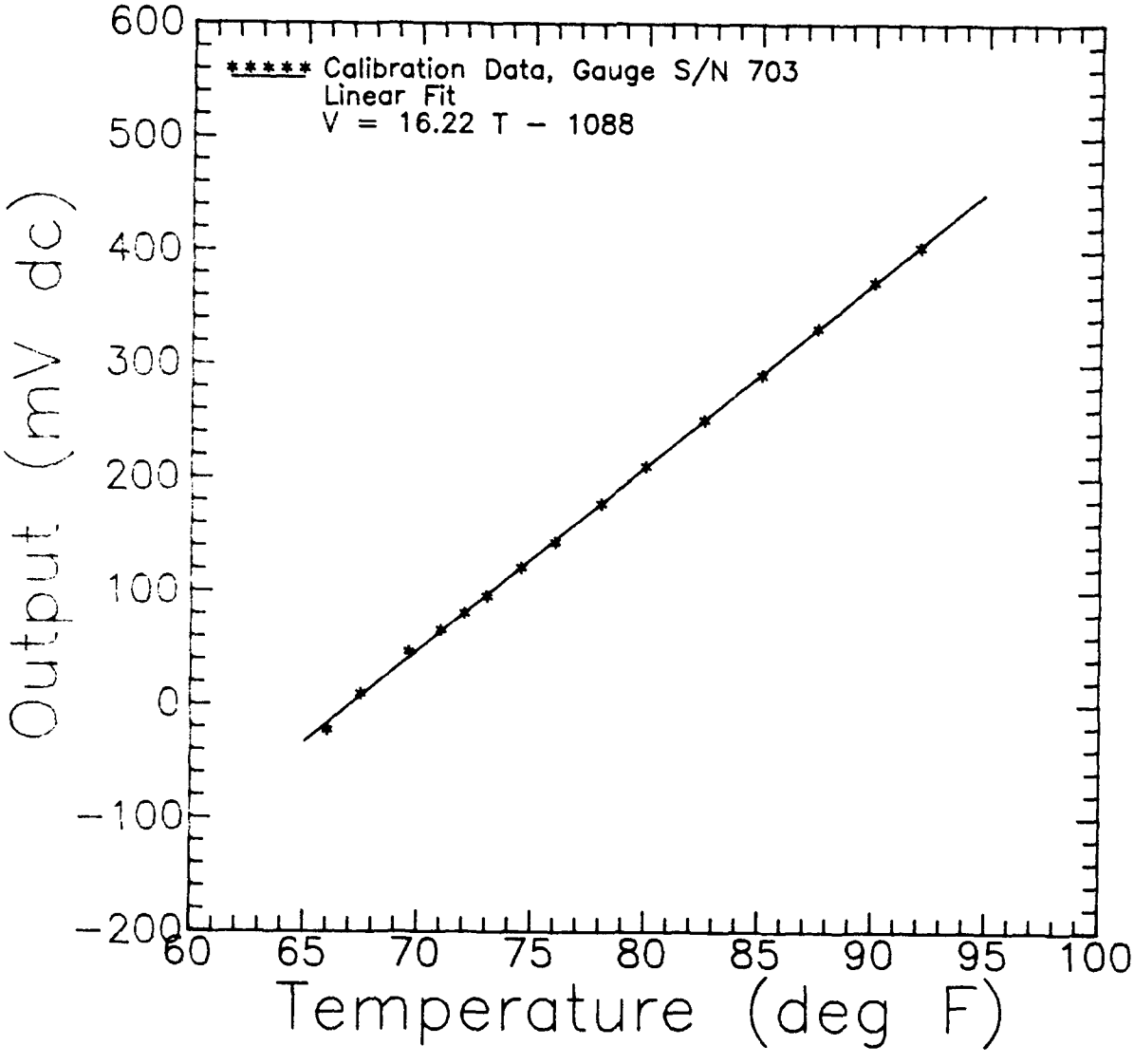


Figure A.7 Calibration Curve for Gauge No. 6

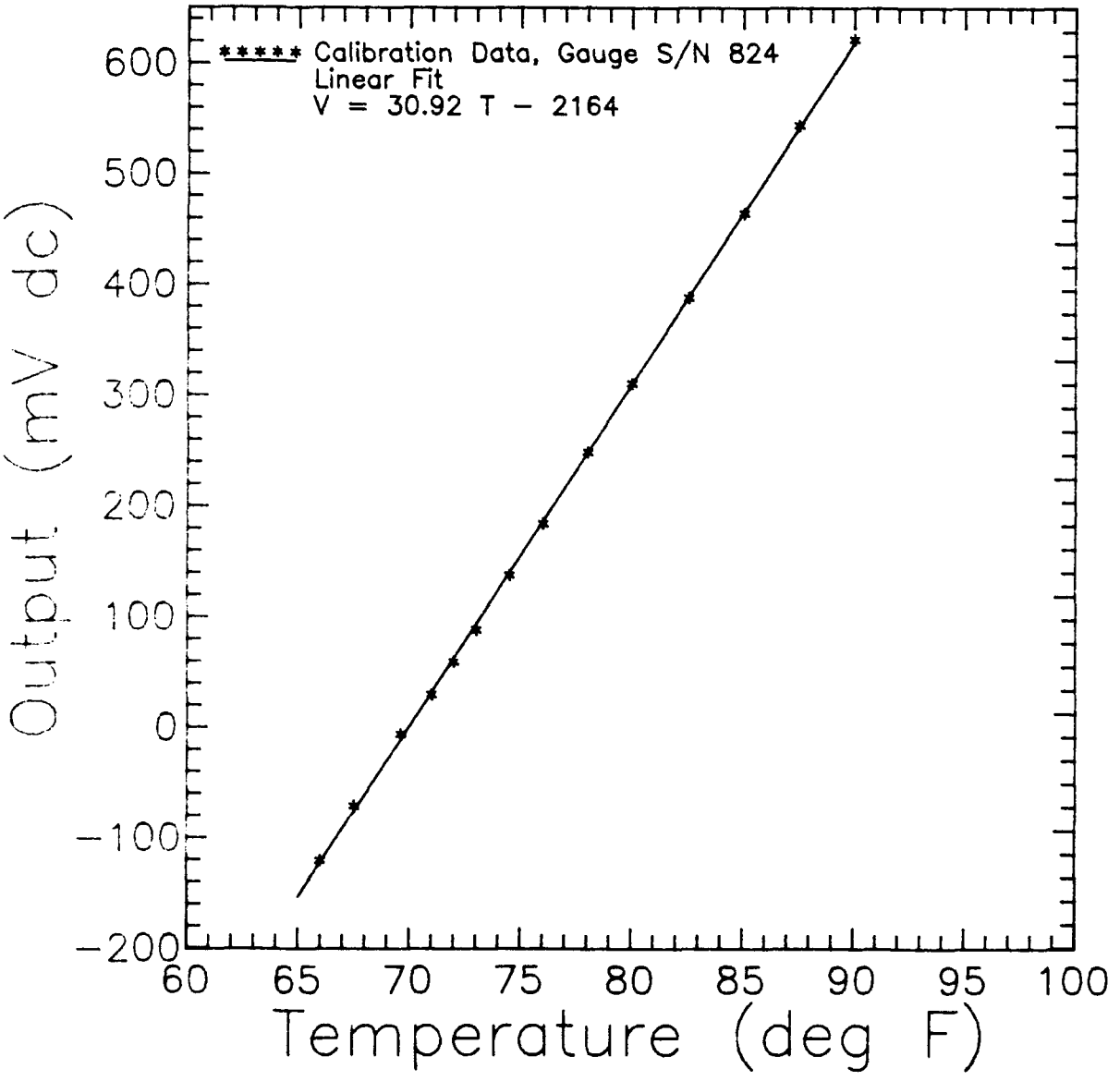


Figure A.8 Calibration Curve for Gauge No. 7

## Appendix B: Calibration of Thin-Film Resistance Gauges for Substrate Bulk Thermal Diffusivity $\sqrt{\rho C_p k}$

The thin-film resistance gauge substrate (Corning Pyrex 7740) bulk thermal diffusivity, $\sqrt{\rho C_p k}$, values vary from gauge to gauge. The determination of the gauge substrate properties is done using a double pulse calibration technique (Schultz and Jones 1973:24). The gauge is first pulse calibrated in air. Then, the gauge surface is covered with fluid of known thermal properties, such as glycerin, and pulse calibrated identically to that in air. The voltage output versus time is parabolic giving a linear change in voltage output versus the square root of time. The slope of the change in voltage versus the square root of the time for the cases of air and glycerin are then used in the following equation to determine the $\sqrt{\rho C_p k}$ value of the gauge substrate (Schultz and Jones, 1973:24; Gul, 1991:28, 29, App. A):

$$\sqrt{(\rho C_p k)}_{subs} = \frac{\sqrt{(\rho C_p k)}_{gly}}{\dfrac{(\Delta V/\sqrt{t})_{air}}{(\Delta V/\sqrt{t})_{gly}} - 1}$$

where the bulk thermal diffusivity for glycerin is (Schultz and Jones, 1973:25; Incropera and DeWitt, 1981:780):

$$\sqrt{(\rho C_p k)}_{sty} = 925 \frac{J}{m^2 K \sqrt{sec}} \pm 4\%$$

A value of 930 to 931.5 $J/m^2Ksec^{1/2}$ was used for the temperatures at which calibrations were performed.

For this calibration a bridge was built on a breadboard for each gauge using a matched set of 350 Ω resistors as two legs, the gauge (installed in the gauge holder) as a third, and another resistor in parallel with a 10 kΩ ten-turn variable resistor as the fourth leg of the bridge (see Figure 3.7 and the similar set-up on page A.3 ignoring the thermal mixer and using a relatively short 4-ft shielded cable for connection of the gauge). Between attempts in glycerin then air, the applied bead of glycerin was removed with a cloth then the surface cleaned with a cotton swab and denatured alcohol.

A Wavetek Model 278 signal generator was used to supply a 5 Volt pulse with a width of 5 milliseconds. Too high of a pulse voltage applied to the bridge could overpower the gauge film by creating too much ohmic heating; whereas, too little voltage would not give high enough output resolution. In order to avoid these problems the bridge was pulsed with different shunt resistors $R_s$ in series with the bridge, starting with a 1 kΩ resistor then working down into lower shunt resistor values until the desired output (a change of about 500 mV for the 5 msec period) was obtained. The final values of the shunt resistors varied from gauge to gauge because of the varying temperature coefficients. The bridge balance was easier to do with the higher shunt resistor values.

The bridge was balanced with the 2.5 Volt dc source from the PSC 8115/PSC 8015-1 combination applied to the bridge and then the source was disconnected and re-

applied briefly. The bridge would immediately be out of balance when the constant voltage source was removed since the gauge would begin cooling down from the equilibrium temperature it was heated up to by ohmic heating. Re-balancing the bridge after it cooled down was found to give a better balanced bridge. The bridge output would be quickly noted on the voltmeter, then the variable resistor would be adjusted to balance the bridge as well as possible (between 1 and 10 mVolt output, after multiple adjustments). Then the 2.5 Vdc source and voltmeter were disconnected and the Wavetek and Nicolet were quickly connected and the 5 Volt pulse was applied to the bridge. Any initial bridge imbalance is amplified due to the difference in applied voltage, showing as an immediate jump in the output voltage of the bridge when the pulse was applied. This jump is in addition to the sharp spikes which could not be accounted for, but appeared to be characteristic of the gauge/bridge combination.

This technique generally required 5 to 10 attempts in order to balance the unloaded bridge and give the desired output so as to have minimal initial jump in the voltage output when the pulse was applied to the bridge. Switching the value of $R_1$ (slightly higher value than the gauge room temperature resistance) could aid in bridge balancing and would change the spike height slightly.

Gul (1991) normalized the data from the top of a voltage jump (or beginning of the parabolic curve), and used the output voltage change from this point to determine the $\Delta V/\sqrt{t}$ for the data. In this study the normalization was accomplished by a program called GANORM.FOR with which the user could choose the time reference and length of time (e.g. 0.5 msec) from the data to normalize (change time to $\sqrt{t}$ and change V to

$\Delta V$). The program was used in conjunction with the Nicolet system on the DTK computer to choose the initial reference point. For the gauges with a spike in the direction of the parabolic output, e.g. gauge 1, a close look in an amplified view on the computer screen revealed the change in slope from the spike to the parabolic output. This point was taken as the reference zero point for normalization.

Figures B.1 to B.14 show plots of the voltage output versus time in air and glycerin for each gauge followed by the plot of the change in voltage versus the square root of time with the value of bulk thermal diffusivity calculated from the relative slopes of the least squares fit equations. It should be noted that the output from the GANORM program was edited, removing the first 25 microsec of the initial 500 microsec used of the parabolic curve to determine the slope more accurately. Taking more than 0.5 msec of the data showed a greater curvature in the "linear" curves and resulted in higher values for the bulk thermal diffusivity.

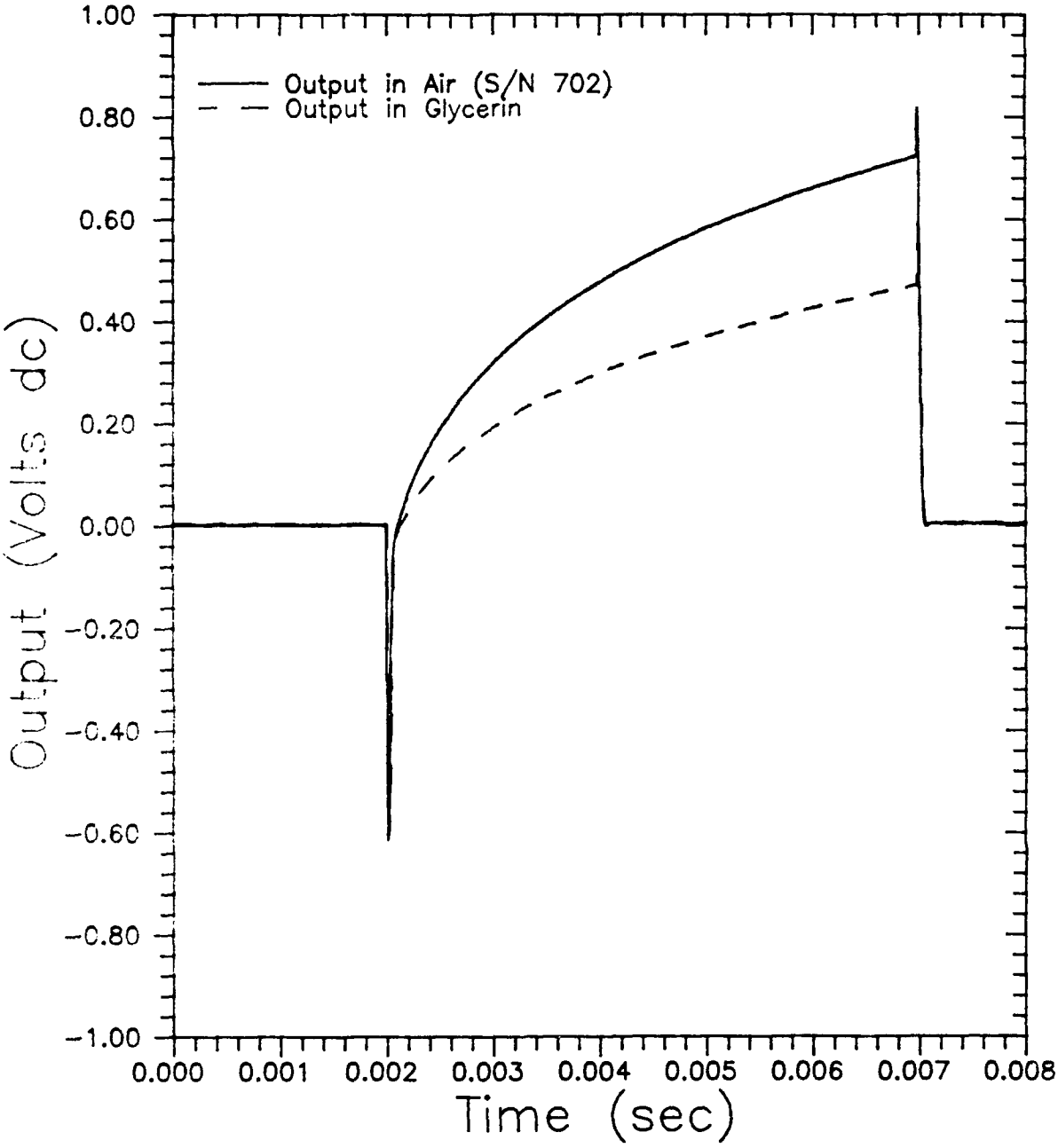


Figure B.1 Sqrt(rho$C_p$k) Calibration Output for Gauge No. 1

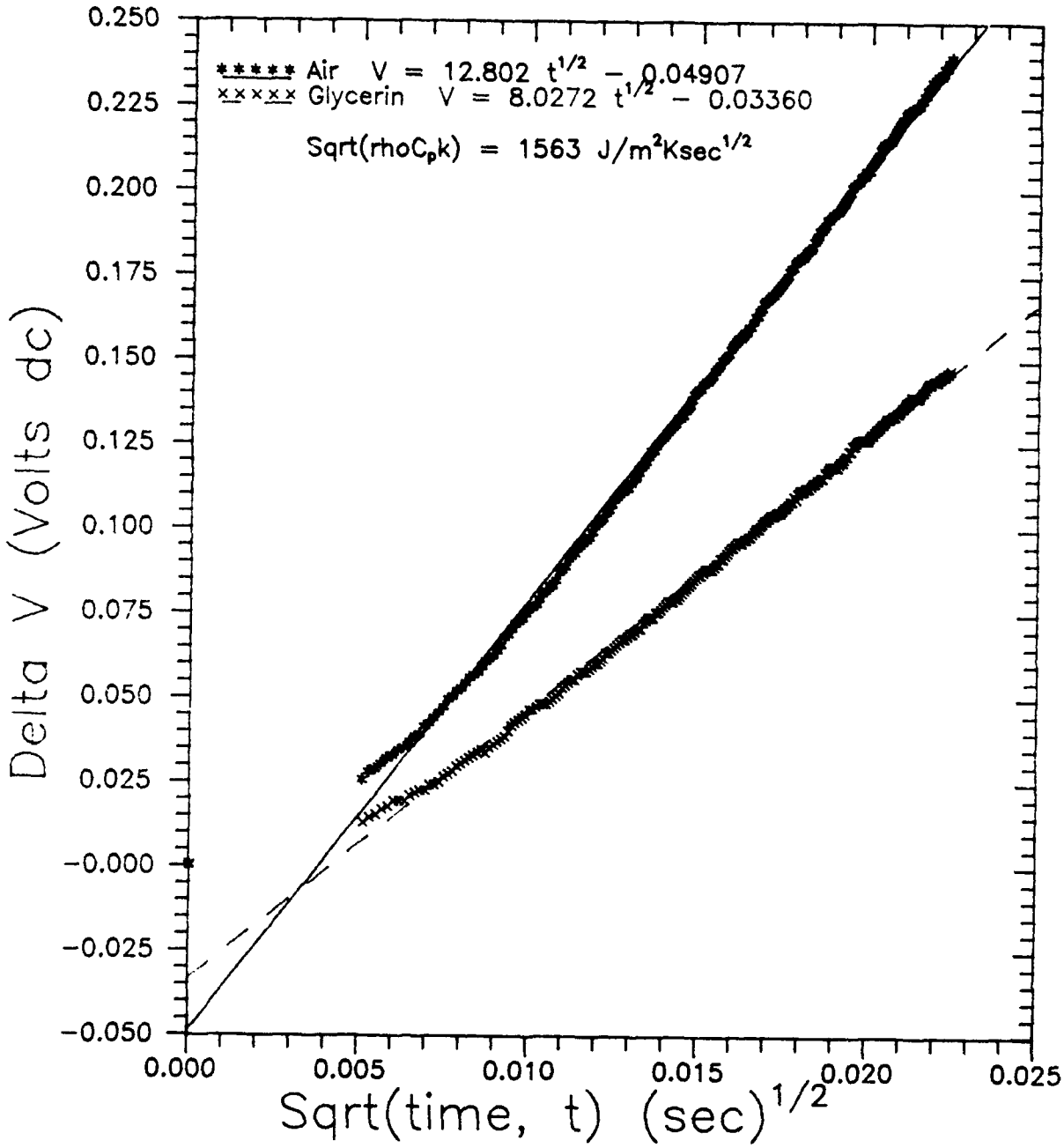


Figure B.2 Sqrt($rhoC_pk$) Calibration Curves for Gauge No. 1 (S/N 702)

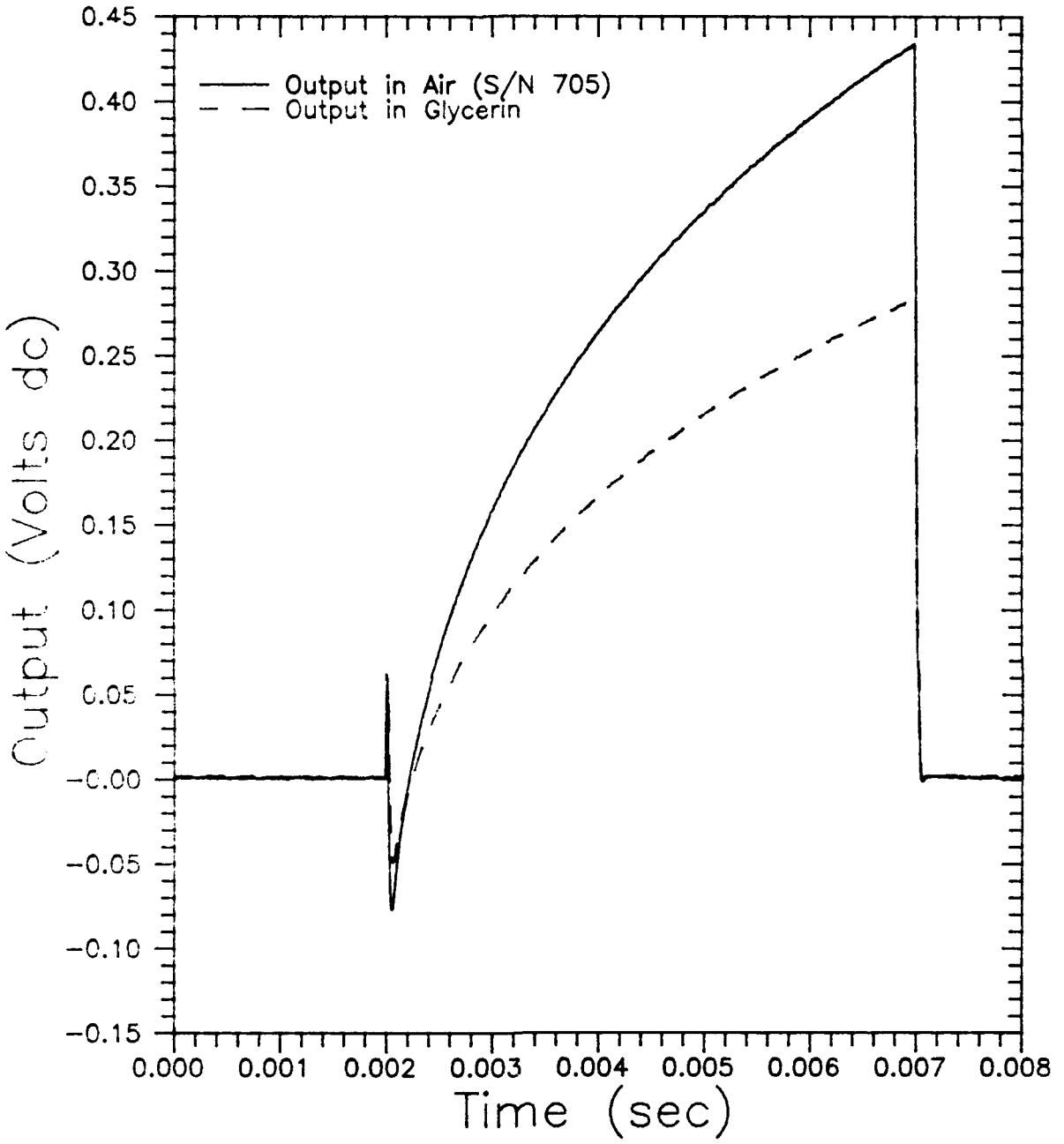


Figure B.3 $\sqrt{\rho C_p k}$ Calibration Output for Gauge No. 2

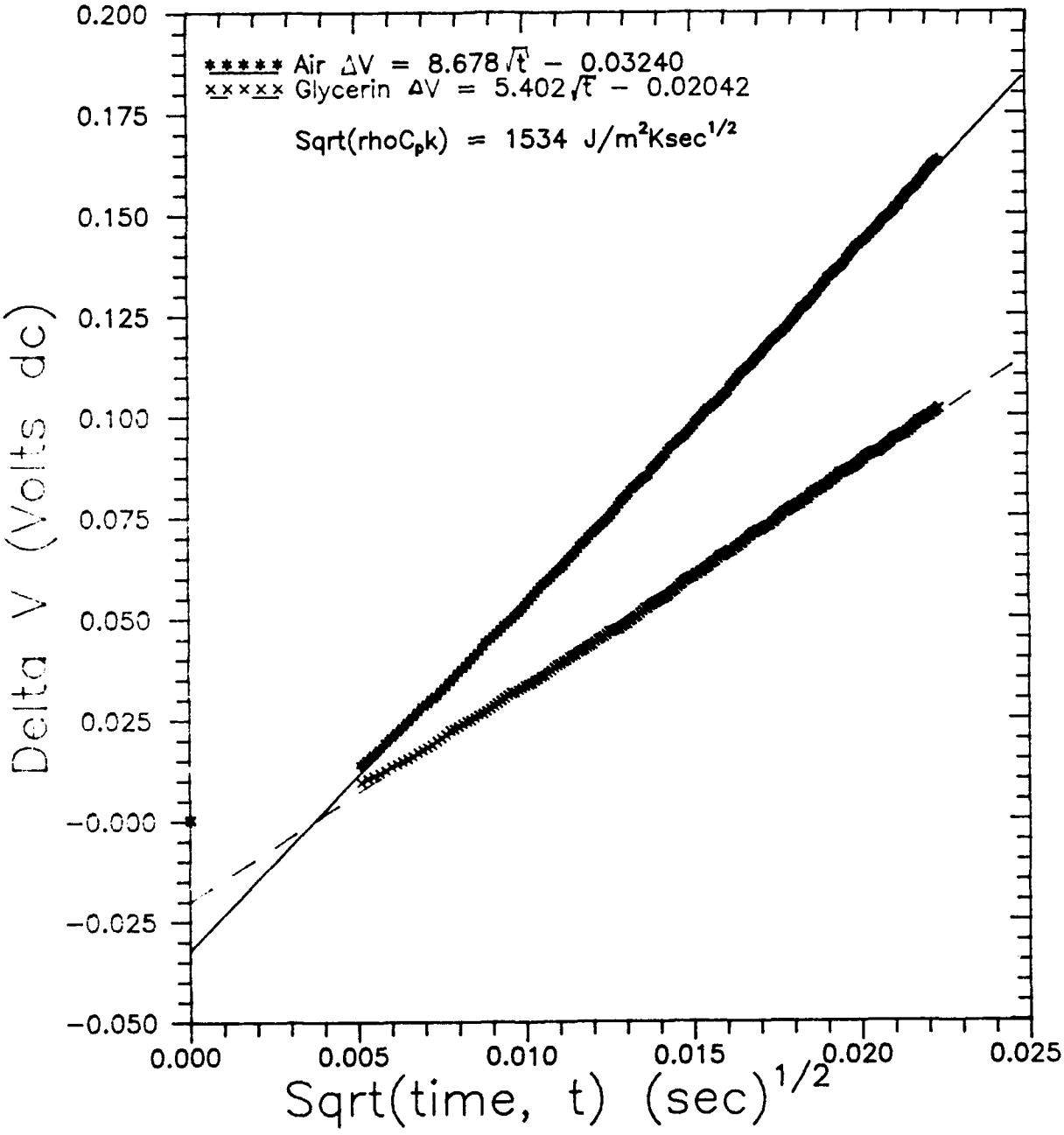


Figure B.4 Sqrt($rhoC_pk$) Calibration Curves for Gauge No. 2 (S/N 705)

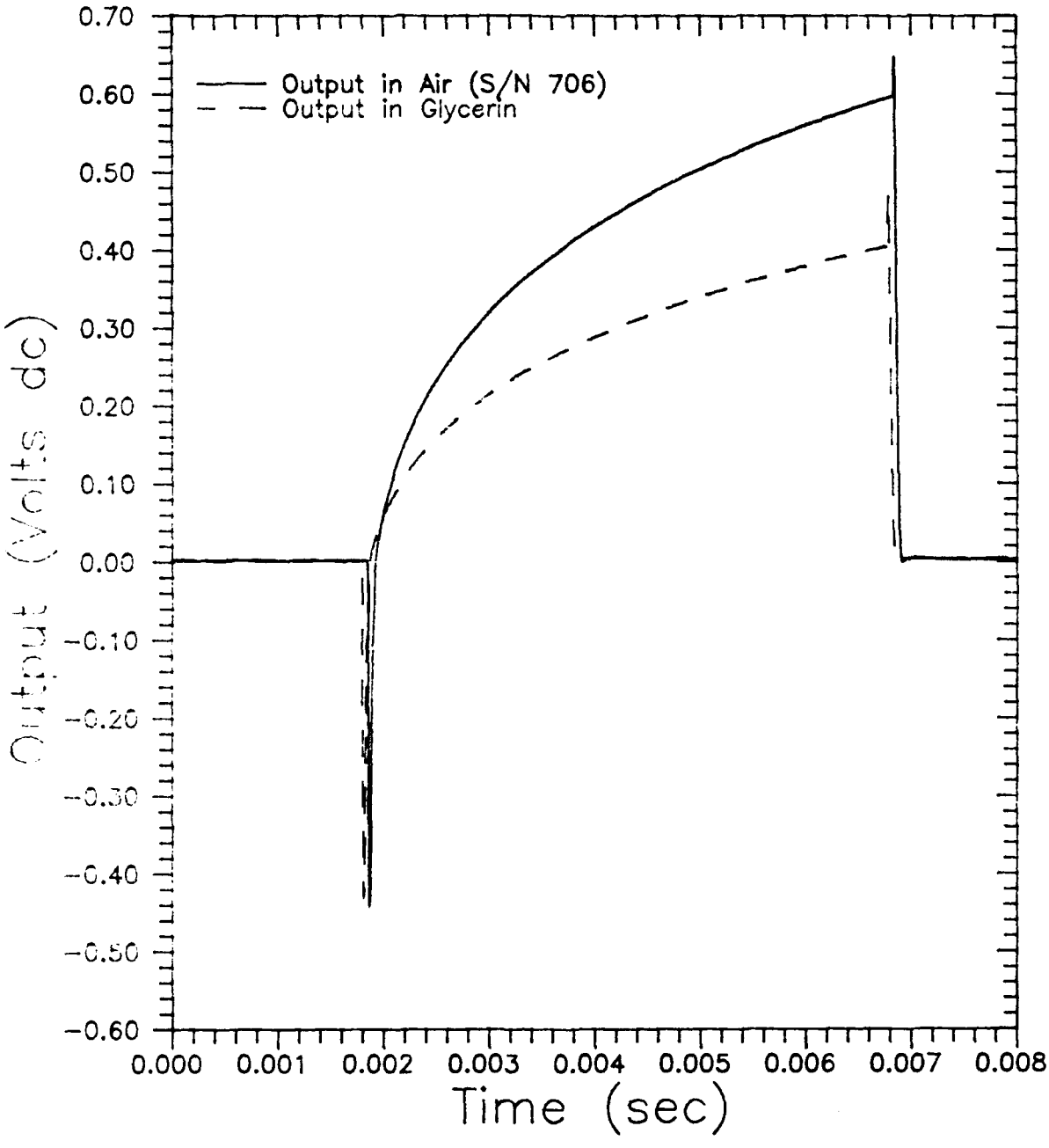


Figure B.5 Sqrt(rho$C_p$k) Calibration Output for Gauge No. 3

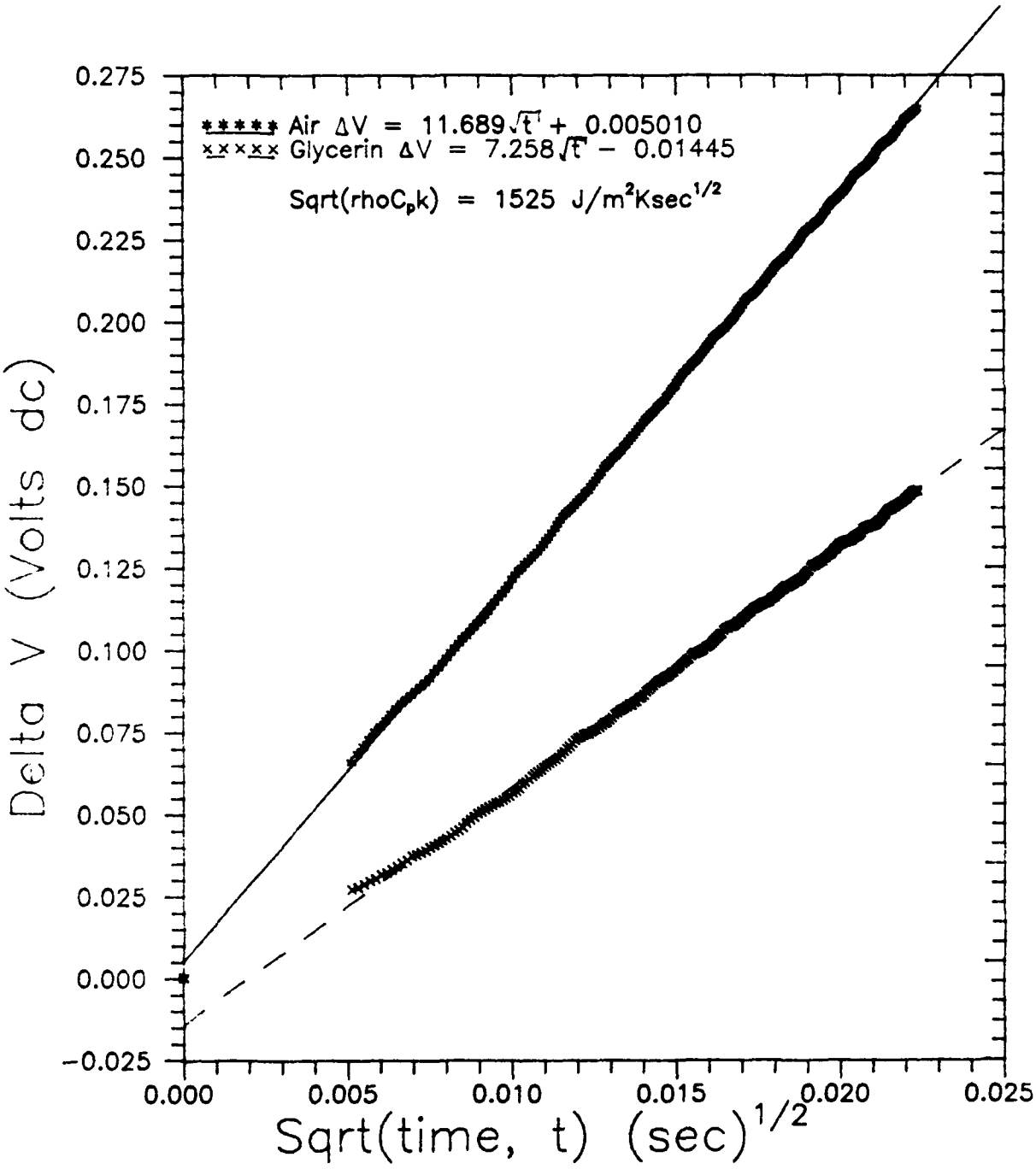


Figure B.6 Sqrt($rhoC_pk$) Calibration Curves for Gauge No. 3 (S/N 706)

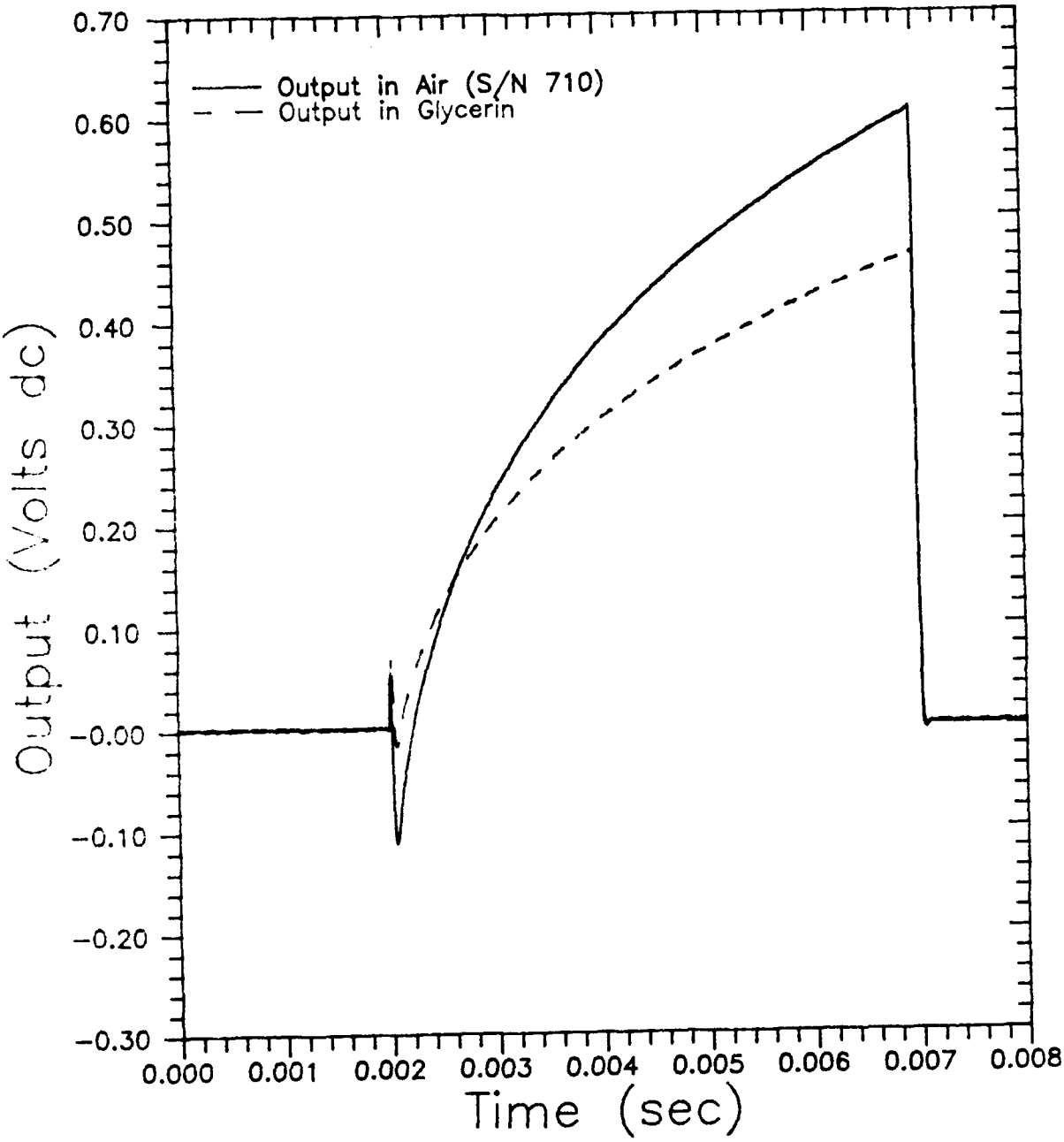


Figure B.7 Sqrt(rho$C_p$k) Calibration Output for Gauge No. 4

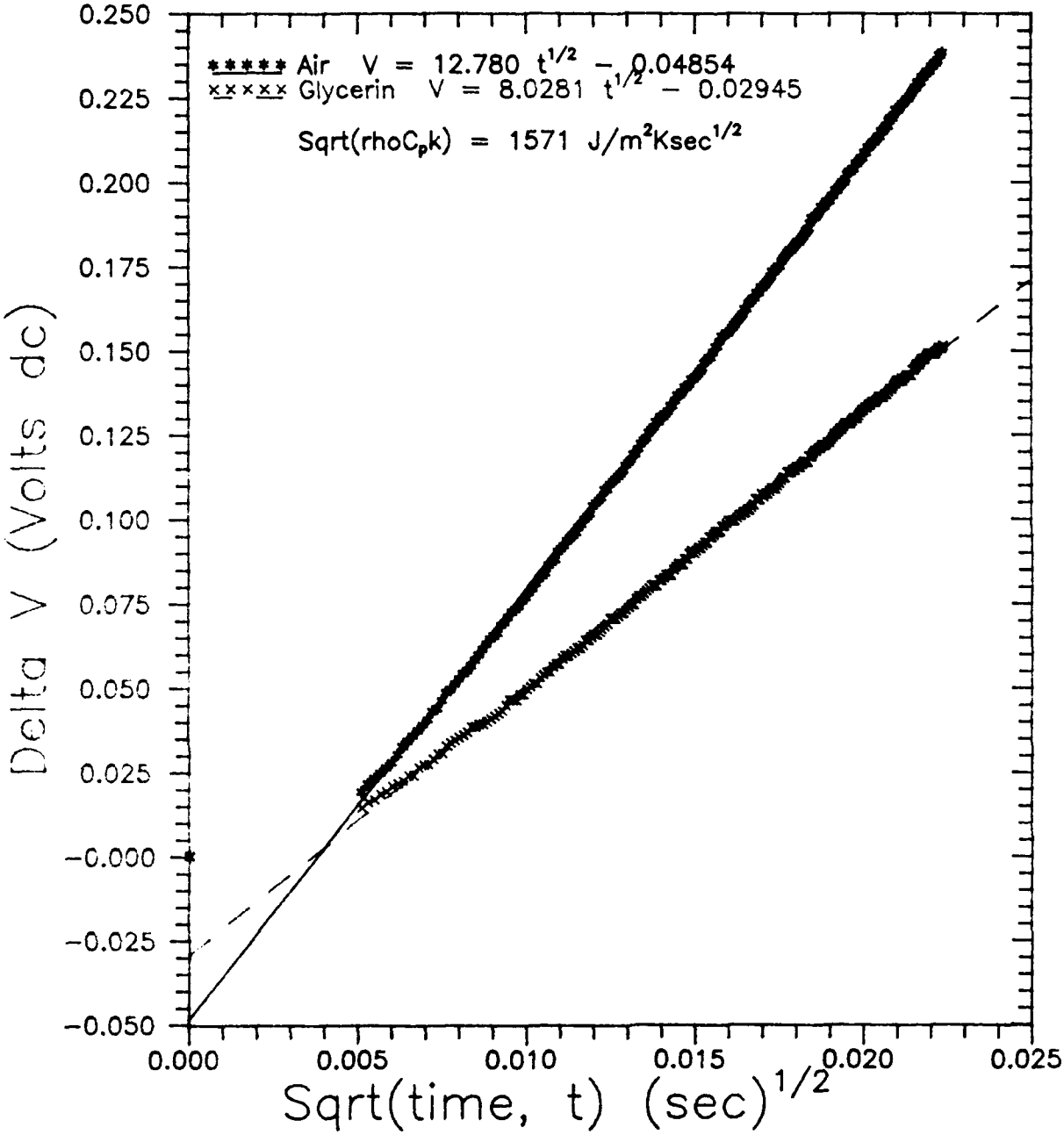


Figure B.8 Sqrt($rhoC_pk$) Calibration Curves for Gauge No. 4 (S/N 710)

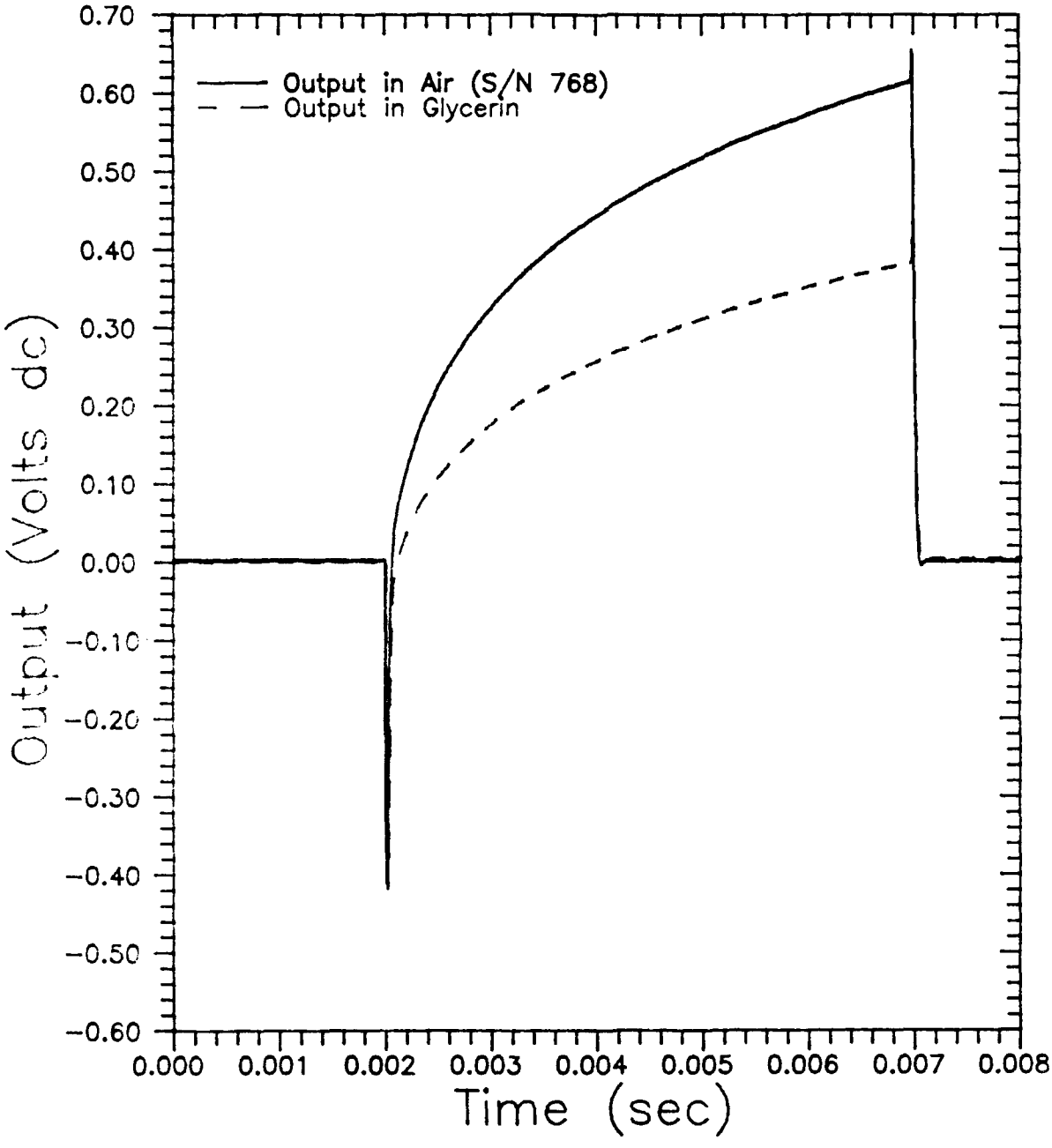


Figure B.9 Sqrt(rho$C_p$k) Calibration Output for Gauge No. 5

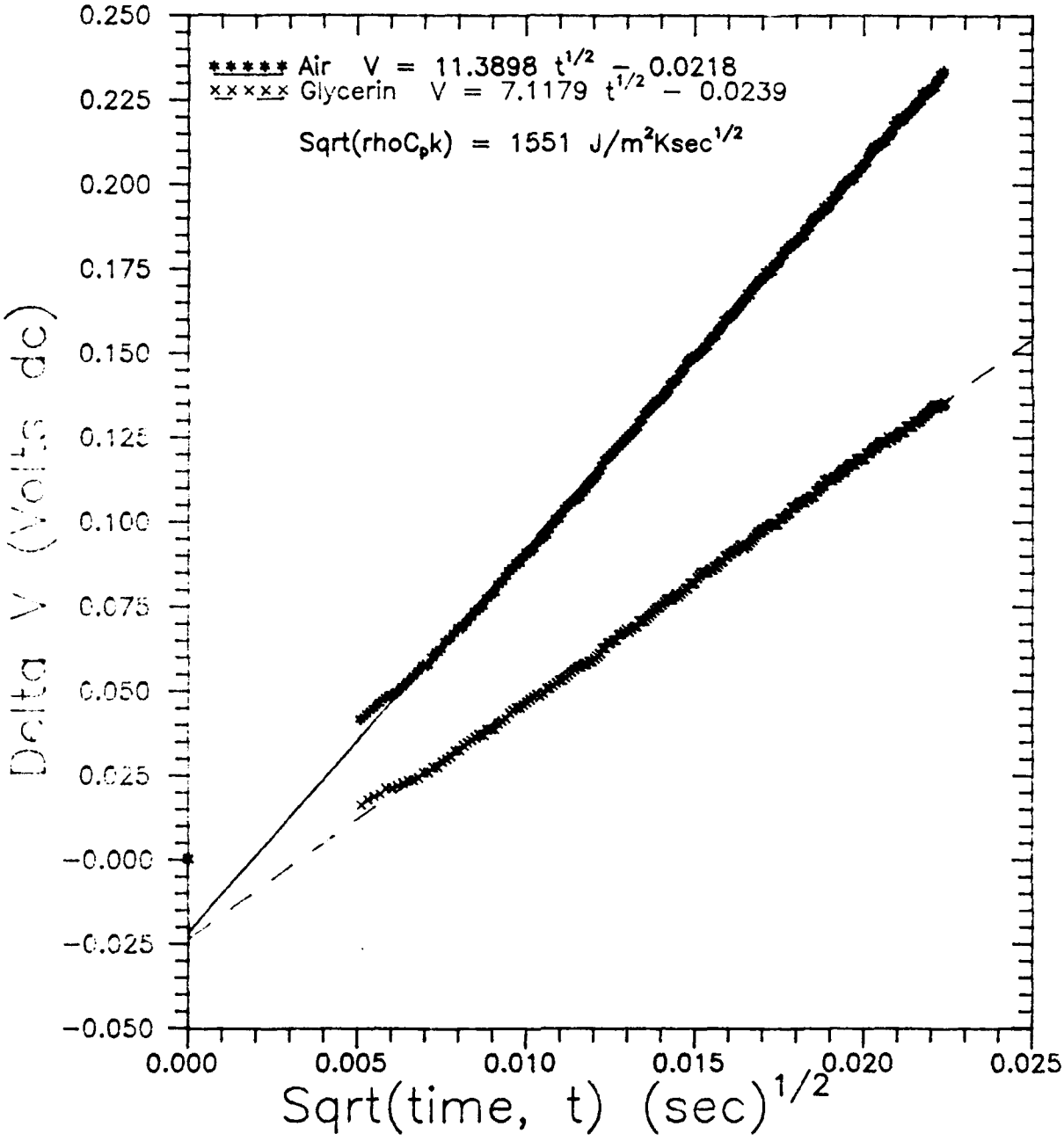


Figure B.10 Sqrt($rhoC_pk$) Calibration Curves for Gauge No. 5 (S/N 768)

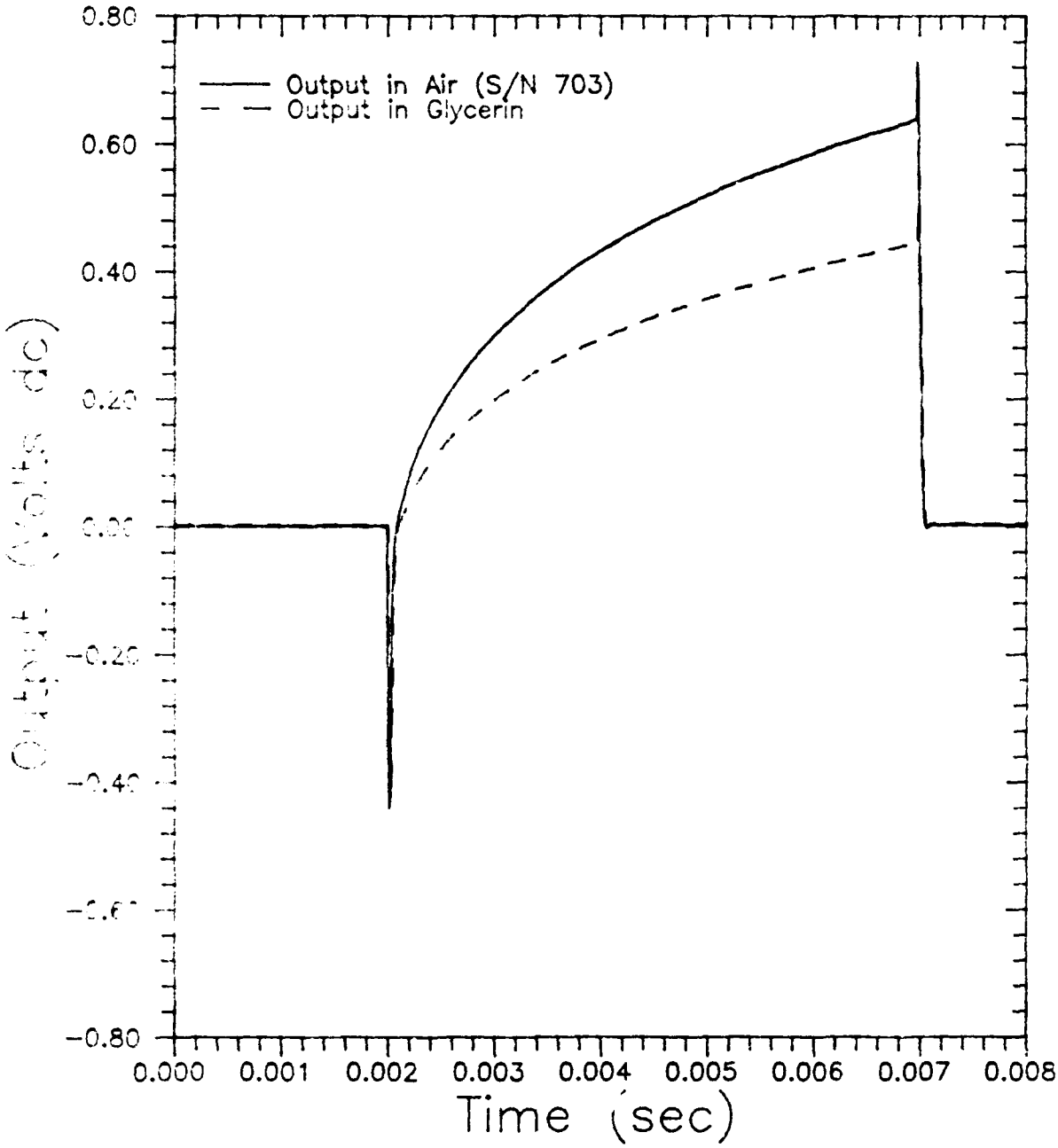


Figure B.11 Sqrt(rho$C_p$k) Calibration Output for Gauge No. 6

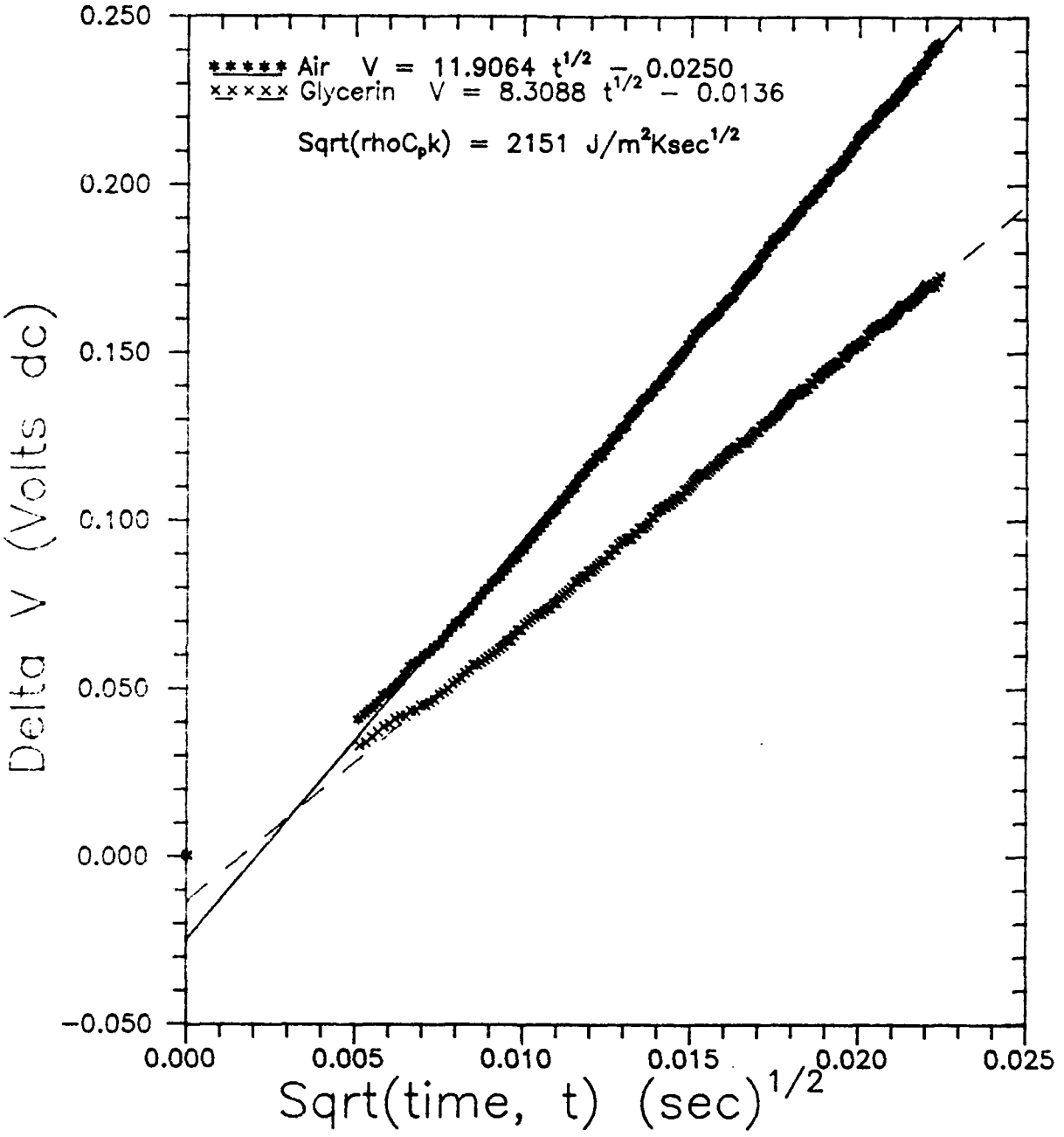


Figure B.12 Sqrt($rhoC_pk$) Calibration Curves for Gauge No. 6 (S/N 703)

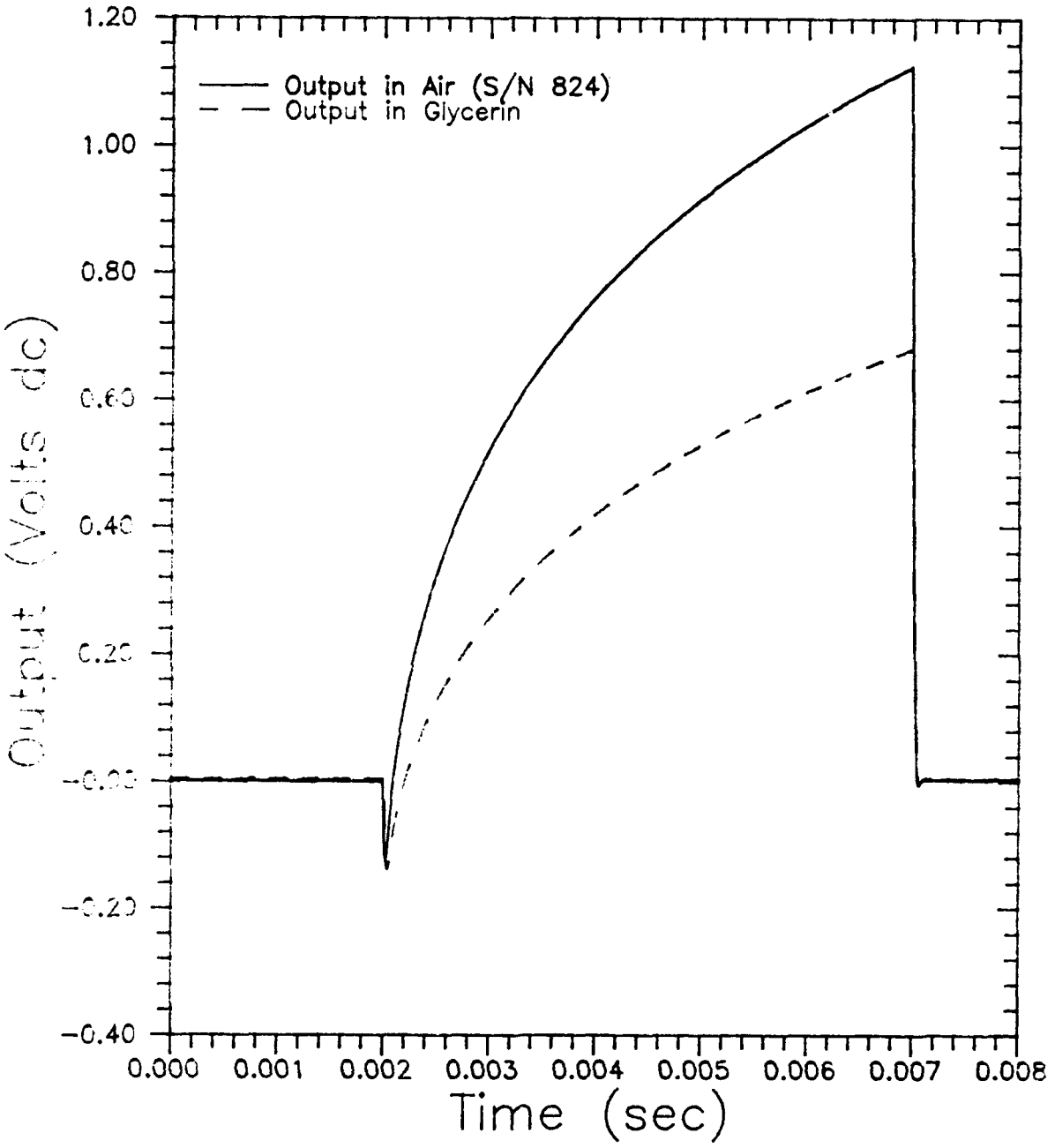


Figure B.13 Sqrt(rho$C_p$k) Calibration Output for Gauge No. 7

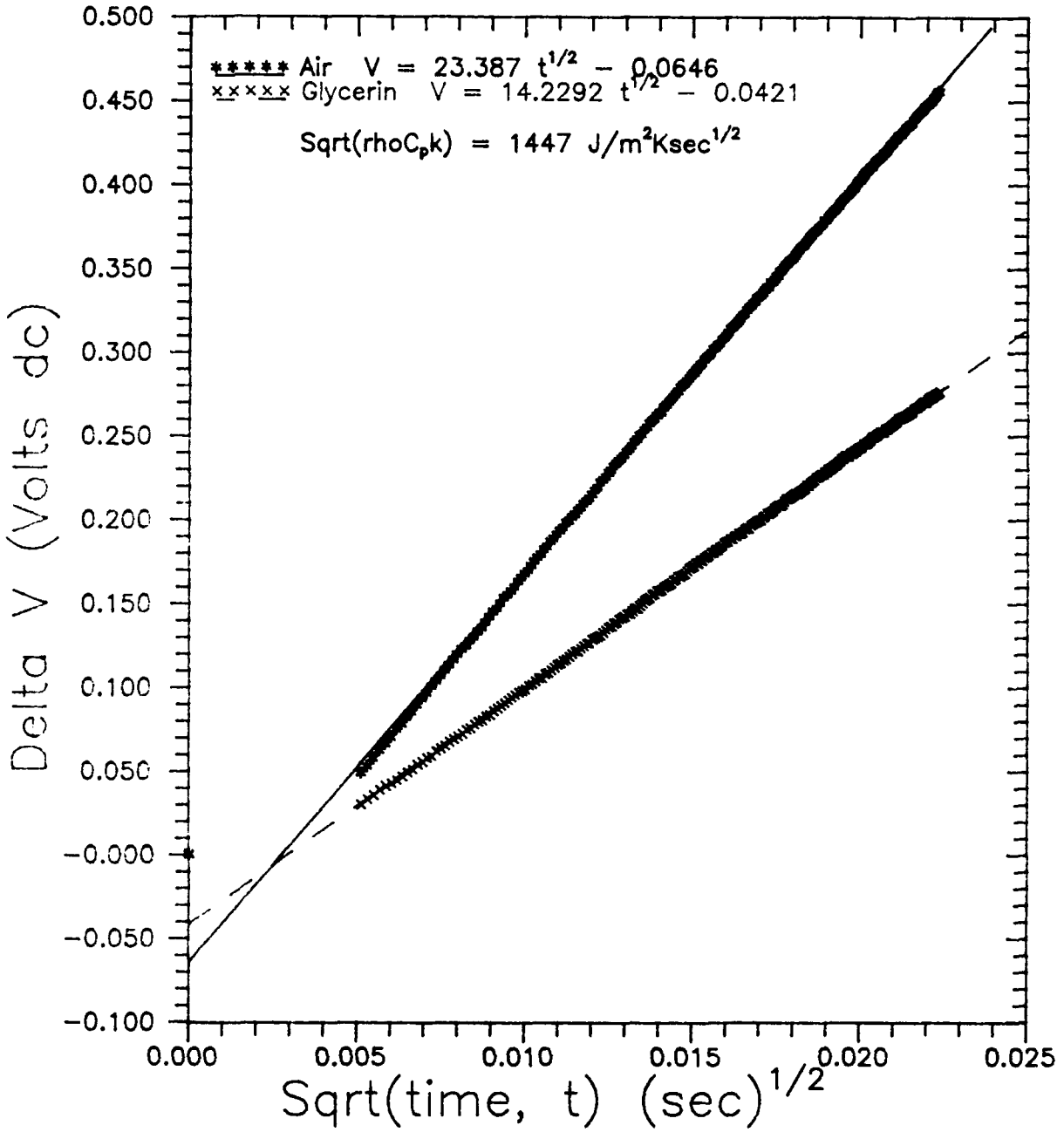


Figure B.14 Sqrt($\rho C_p k$) Calibration Curves for Gauge No. 7 (S/N 824)

## Appendix C: Calibration of Pressure Measuring Instruments

The Endevco Model 8530A-100 and Model 8510B-50 pressure transducers were calibrated for positive gauge pressures using an AMETEK Model HK-500 Pneumatic Pressure Tester. This tester uses an air supply and calibrated weights to supply a known pressure to a chamber to which the transducer is attached. The weight is spun to reduce misalignment and friction effects. Sufficient pressure is supplied to the tester to just raise the weight and avoid over-pressurization which causes vibration of the lower weights.

Each transducer was calibrated with its associated shielded cable and Endevco Model 4423 Signal Conditioner attached as in experimental measurements. The gain was set to not allow the maximum output of 10 Volts to be reached over the range of calibration. The output of the signal conditioner was read by an HP Model 3466A Digital Voltmeter.

Each transducer was cycled up to its maximum range before calibration. The output voltage is recorded as a function of the input gauge pressure in pounds per square inch (psig). The atmospheric pressure was measured at 14.20 psia using a fortin-type mercury barometer. The output was recorded for eleven pressures while increasing pressure, and the same pressures were input while decreasing pressure and recording output. The data points for each transducer are plotted with a least squares curve fit in Figures C.1 to C.3.

Results give the following equations for the three pressure transducers.

Forward Pressure Transducer, S/N 29BA, Gain = 50

$P = 15.3979$ (psi/Volt) $V + 0.050744$

Rear Pressure Transducer, S/N TM73, Gain = 20

$P = 14.7474$ (psi/Volt) $V + 0.043237$

Film Cooling Flow Pressure Transducer, S/N 07CY, Gain = 50

$P = 9.3559$ (psi/Volt) $V - 0.010390$

The bourdon tube pressure gauge used to measure pressure $P_4$ of the driver section was calibrated in a similar manner. Of course, the output is read from the face of the dial in inches of mercury (in. Hg gauge). The gauge was re-zeroed prior to calibration. The calibration curve is given in Figure C.4.

The instrument used to measure vacuum and atmospheric pressure in the driven section is an MKS Instruments Baratron Portable Vacuum Standard Model PVS-2. It had been calibrated before and our laboratory had no facility to re-calibrate it in vacuum. However, checks of atmospheric pressure measurements using the fortin-type mercury barometer compared to within 0.02 in. Hg or 0.07%.

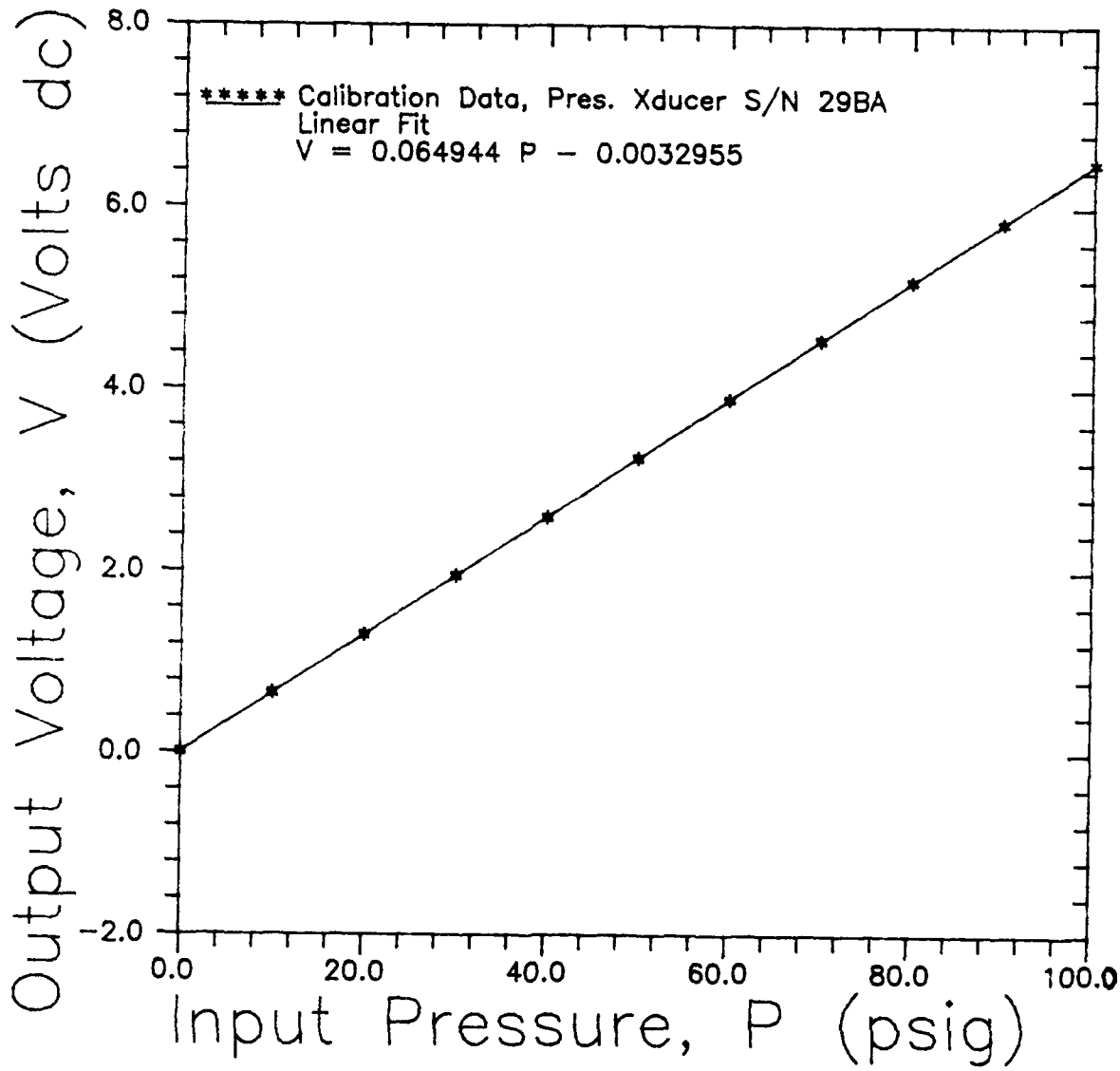


Figure C.1 Calibration Curve for Forward Pressure Transducer

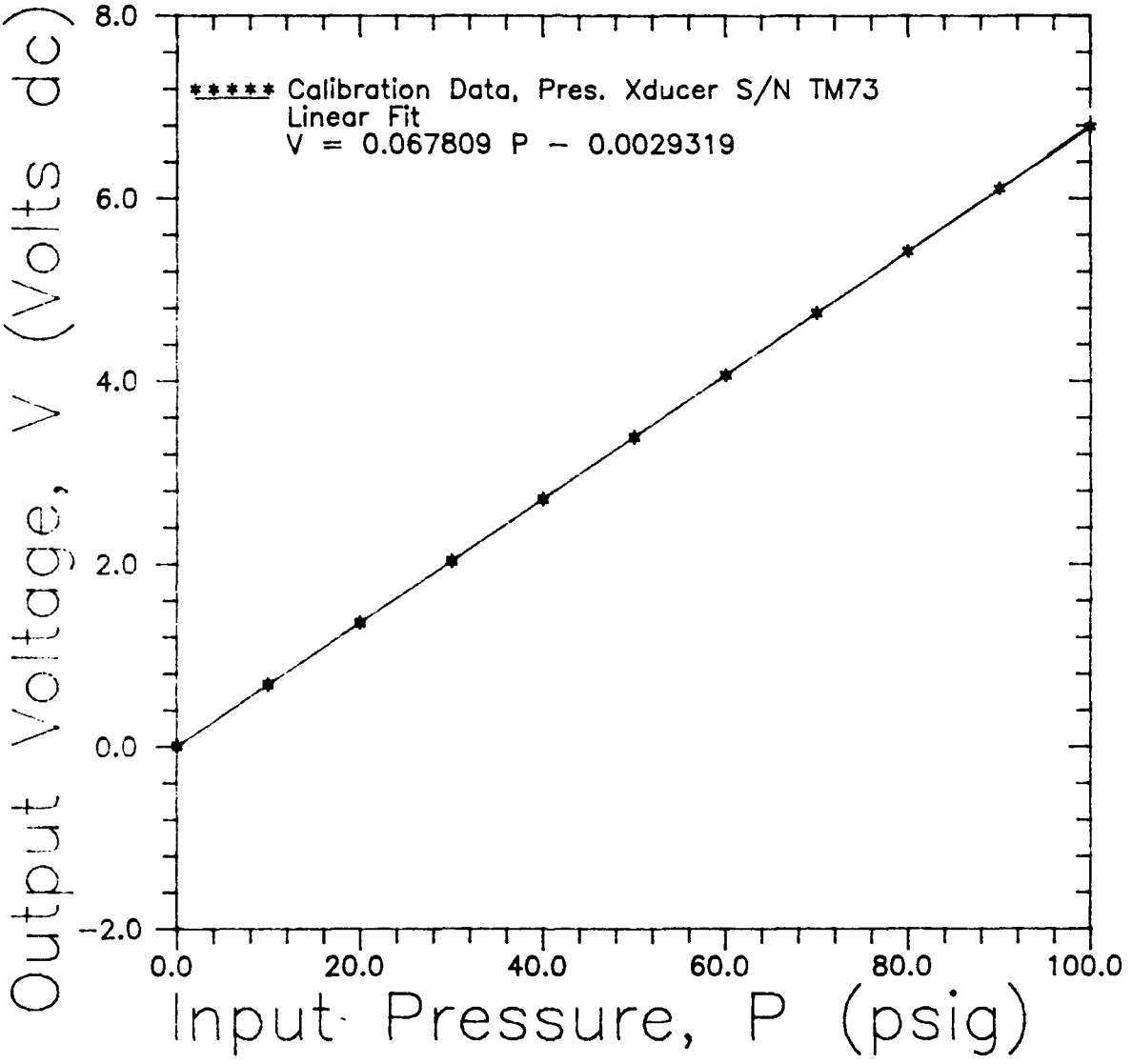


Figure C.2 Calibration Curve for Rear Pressure Transducer

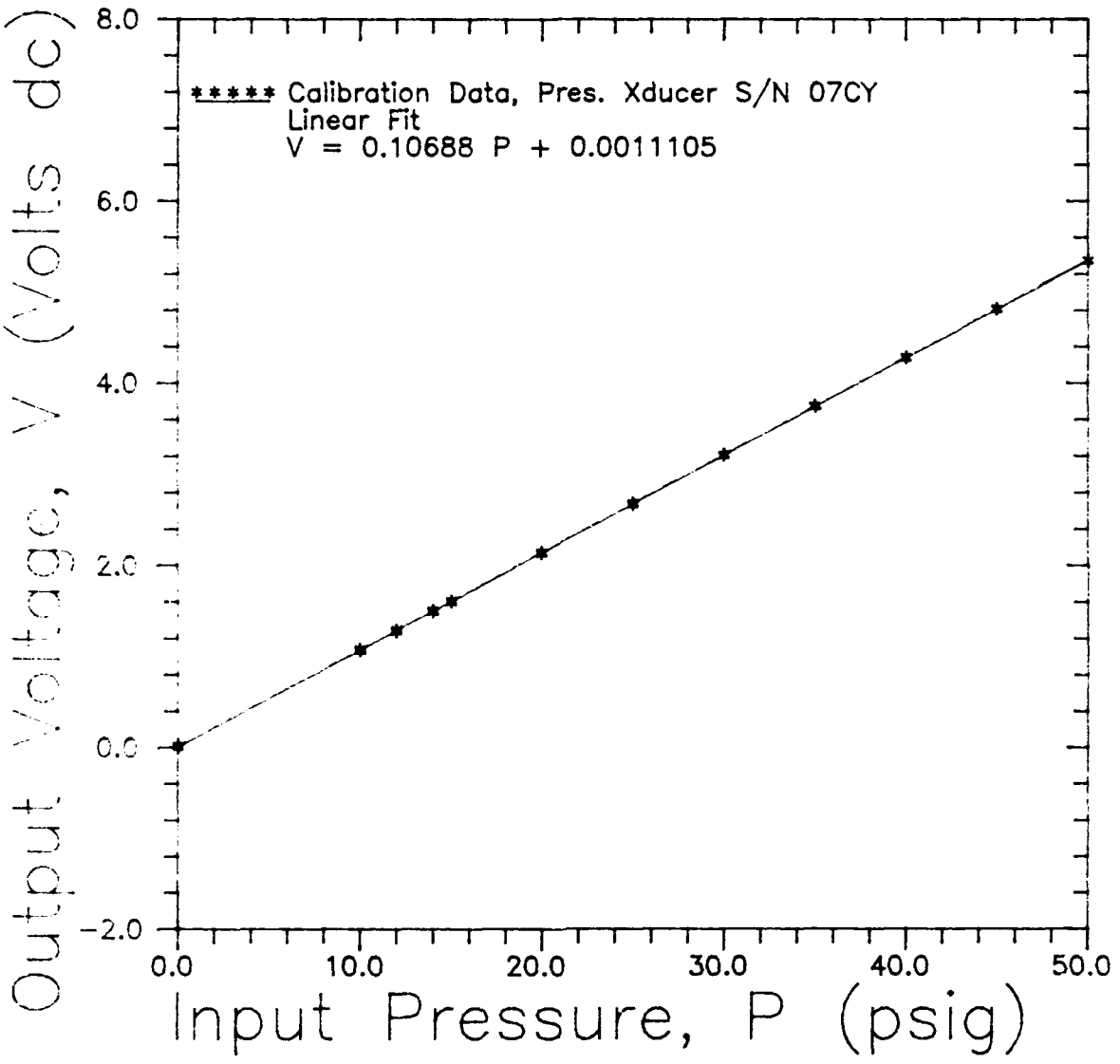


Figure C.3 Calibration Curve for Film Cooling Pressure Transducer

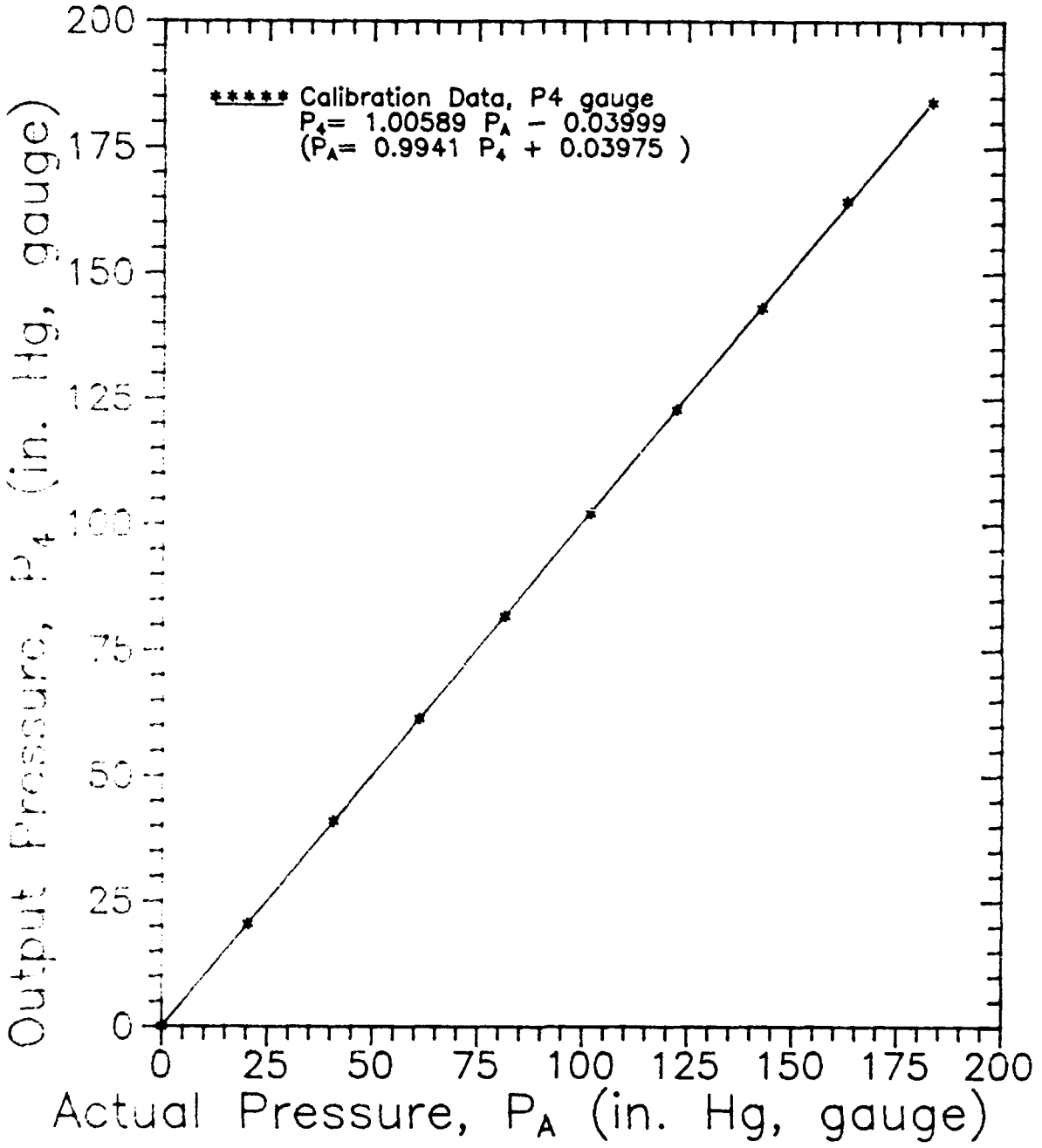


Figure C.4 Calibration of Bourdon Pressure Gauge (P4)
$P_{atm}$= 29.33 in. Hg

## Appendix D: Heat Flux Analog Circuit Calibration

A Hewlett-Packard Model HP 35660A Dynamic Signal Analyzer was used to determine the frequency response of each electrical analog circuit. The sketch below depicts the set-up. Random noise was input and the output over input rms voltage magnitude was measured then averaged over fifteen sets of random noise input. The averaged output vs. frequency up to 51.2 kHz is plotted to the analyzer screen continuously.

Figure D.1 gives a sample of the parabolic result of a circuit calibration, output to an HP Model 7470A plotter from the signal analyzer screen. Points along the curve were plotted versus the square root of frequency to give the linear plots on Figures D.2 to D.8. Points of increasing frequency were included until the correlation coefficient decreased below 0.9990. This determines the working range of the circuits, generally resulting in the range 512 Hz to 35 kHz. The slope of the lines is the desired calibration coefficient.

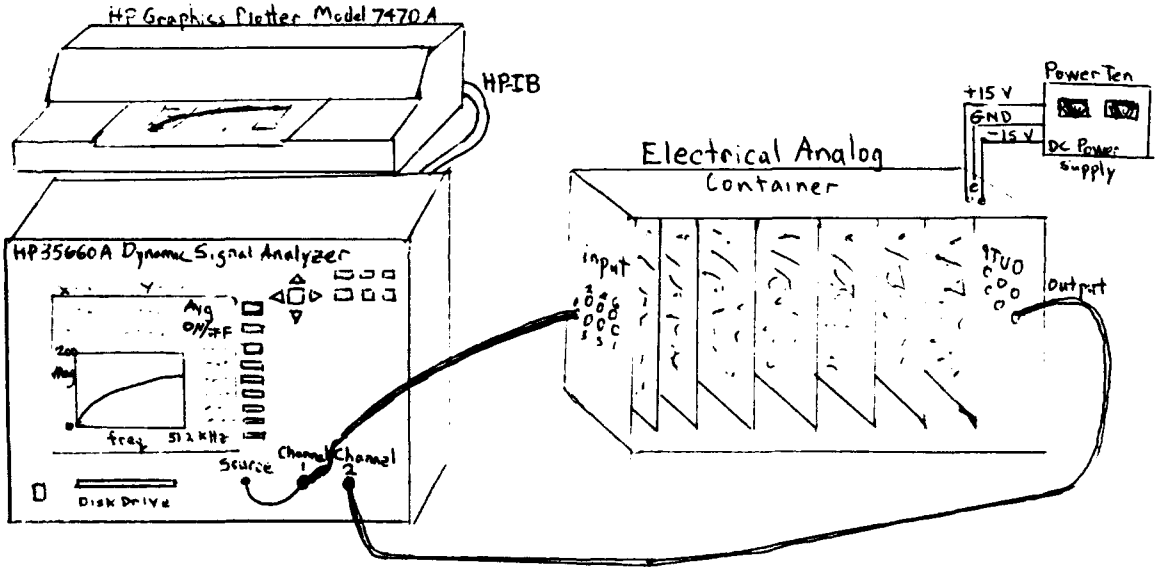

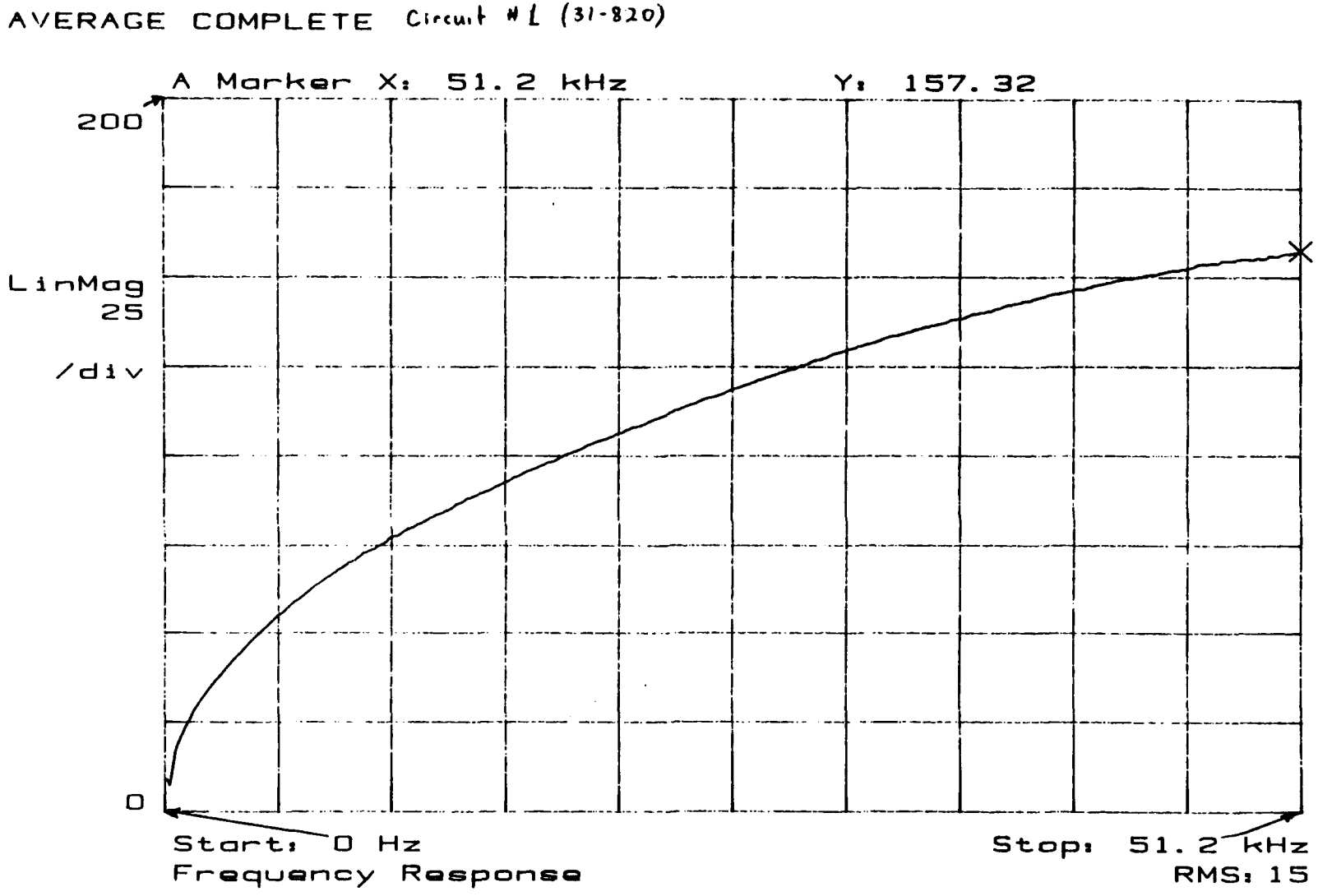


Figure D.1 Sample Output of Analog Circuit Calibration

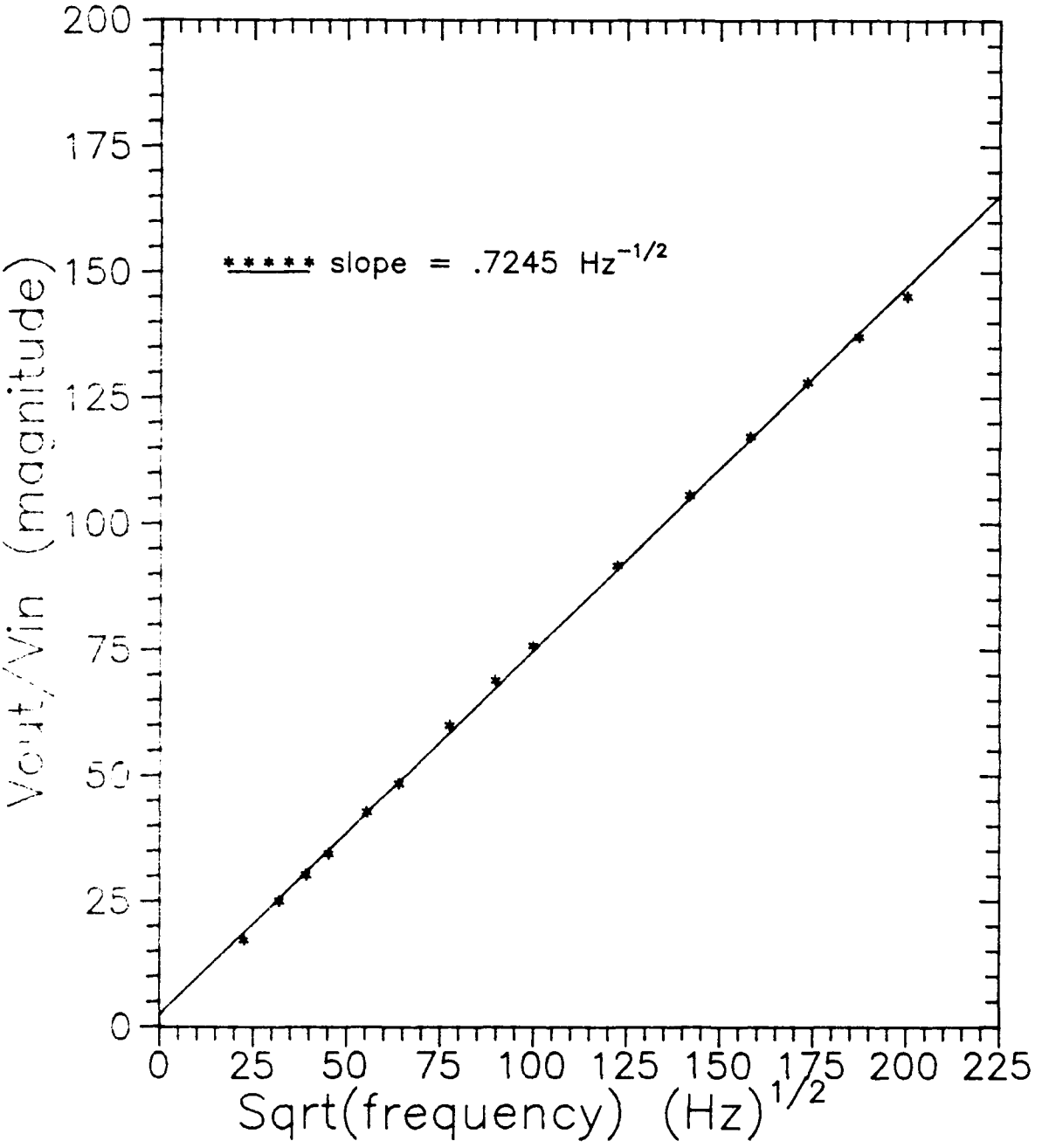


Figure D.2 Calibration of Heat Flux Analog Circuit No. 1 (31–820)

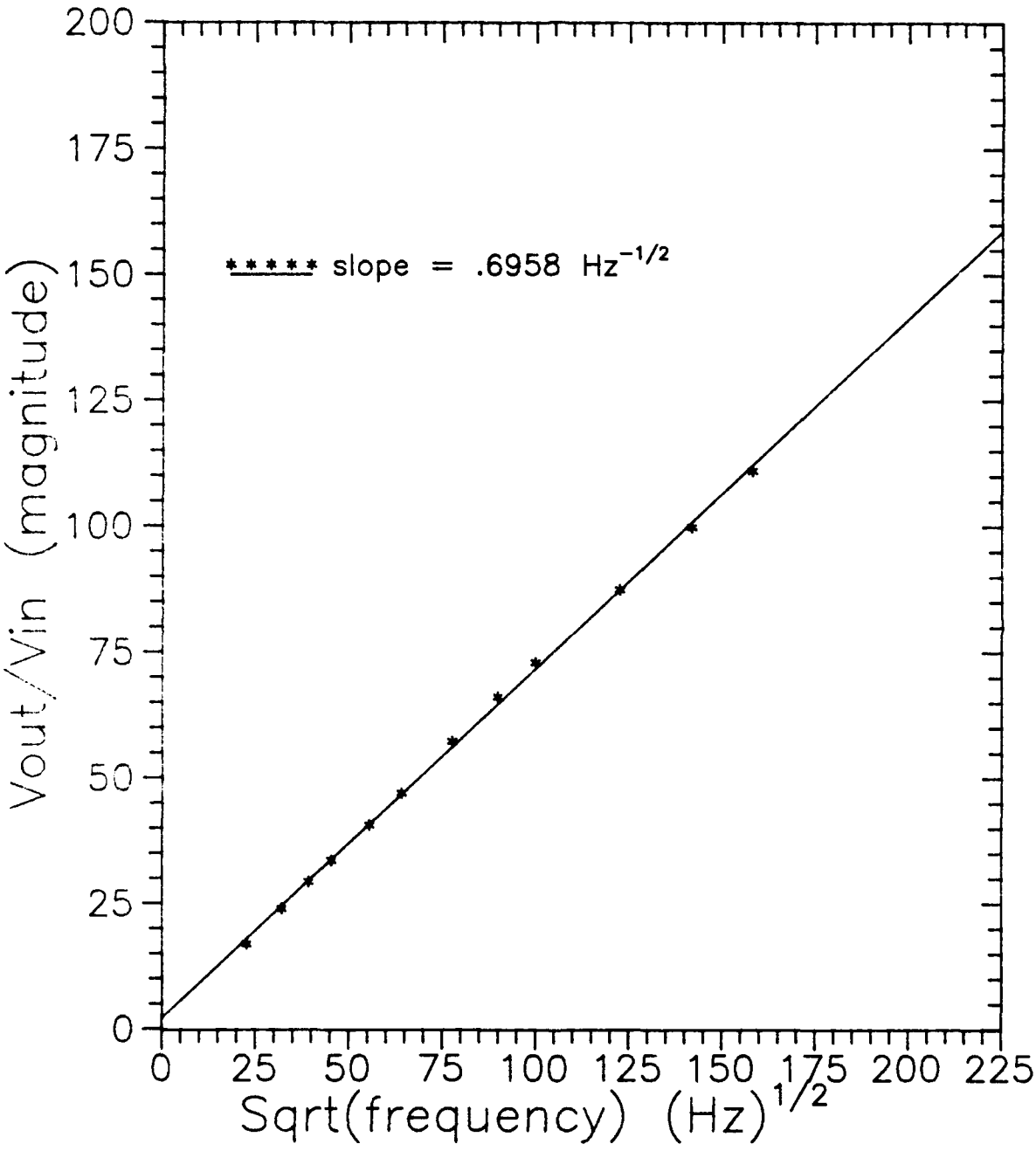


Figure D.3 Calibration of Heat Flux Analog Circuit No. 2 (32–200)

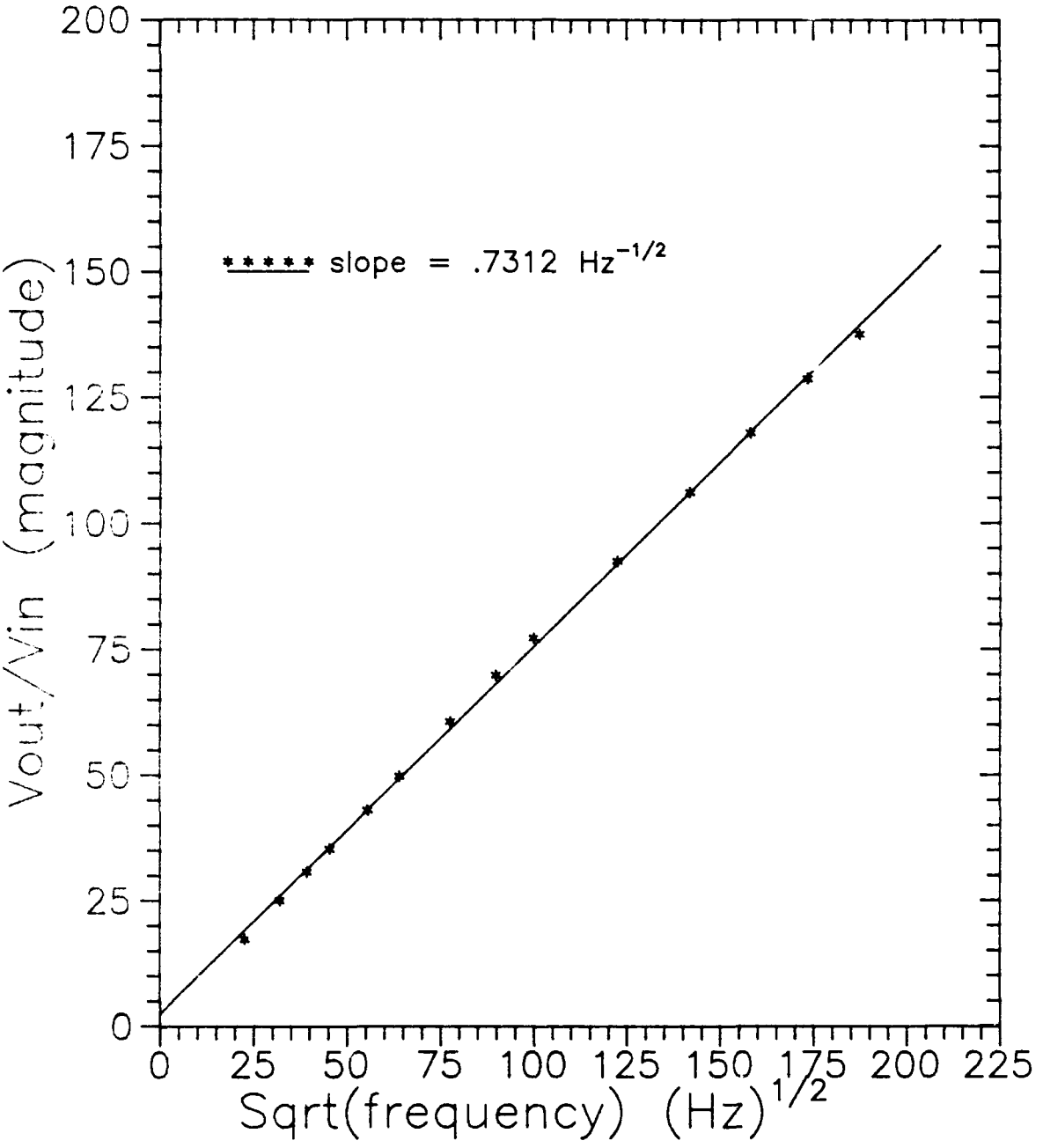


Figure D.4 Calibration of Heat Flux Analog Circuit No. 3 (31–850)

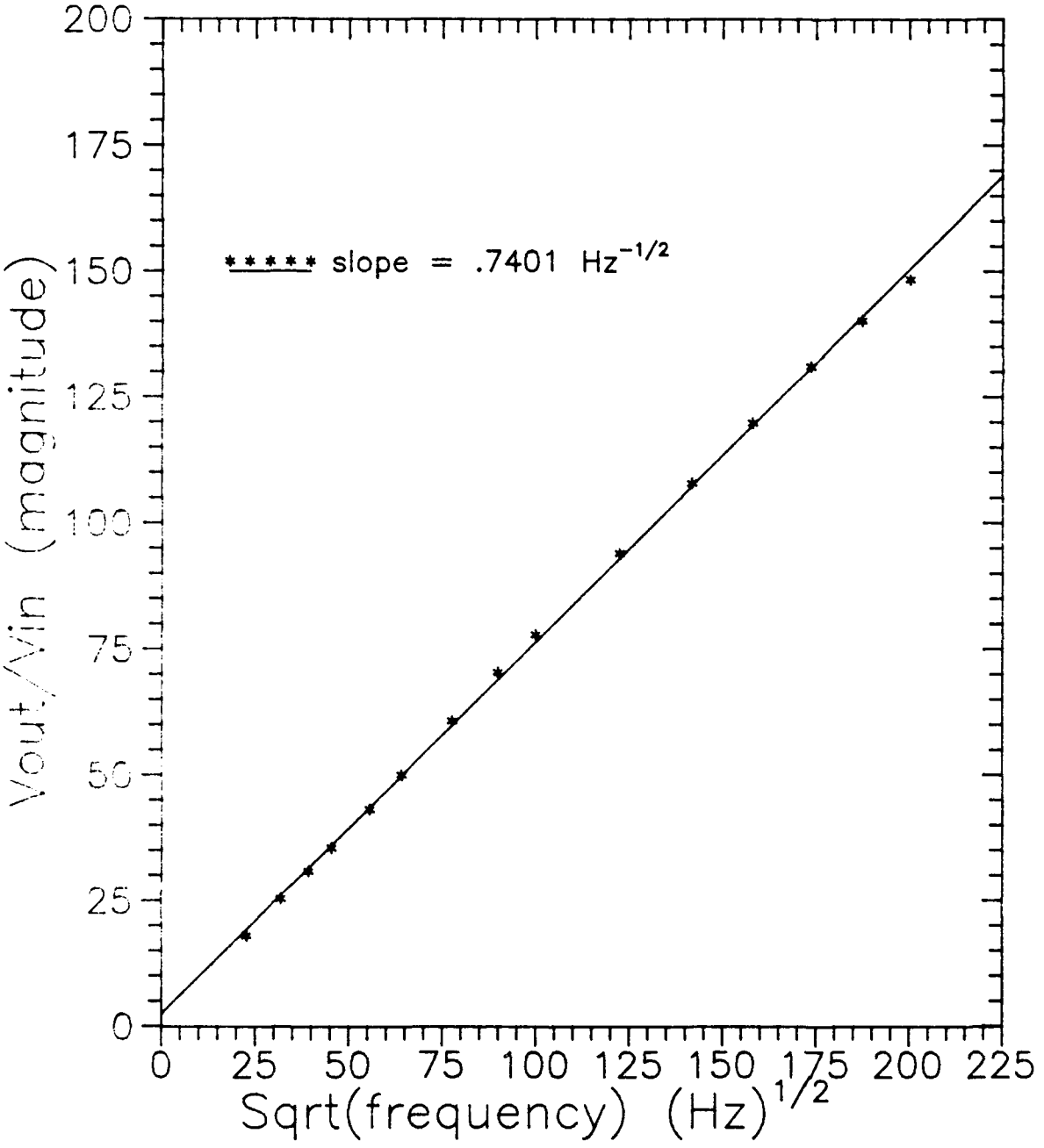


Figure D.5 Calibration of Heat Flux Analog Circuit No. 4 (31–105)

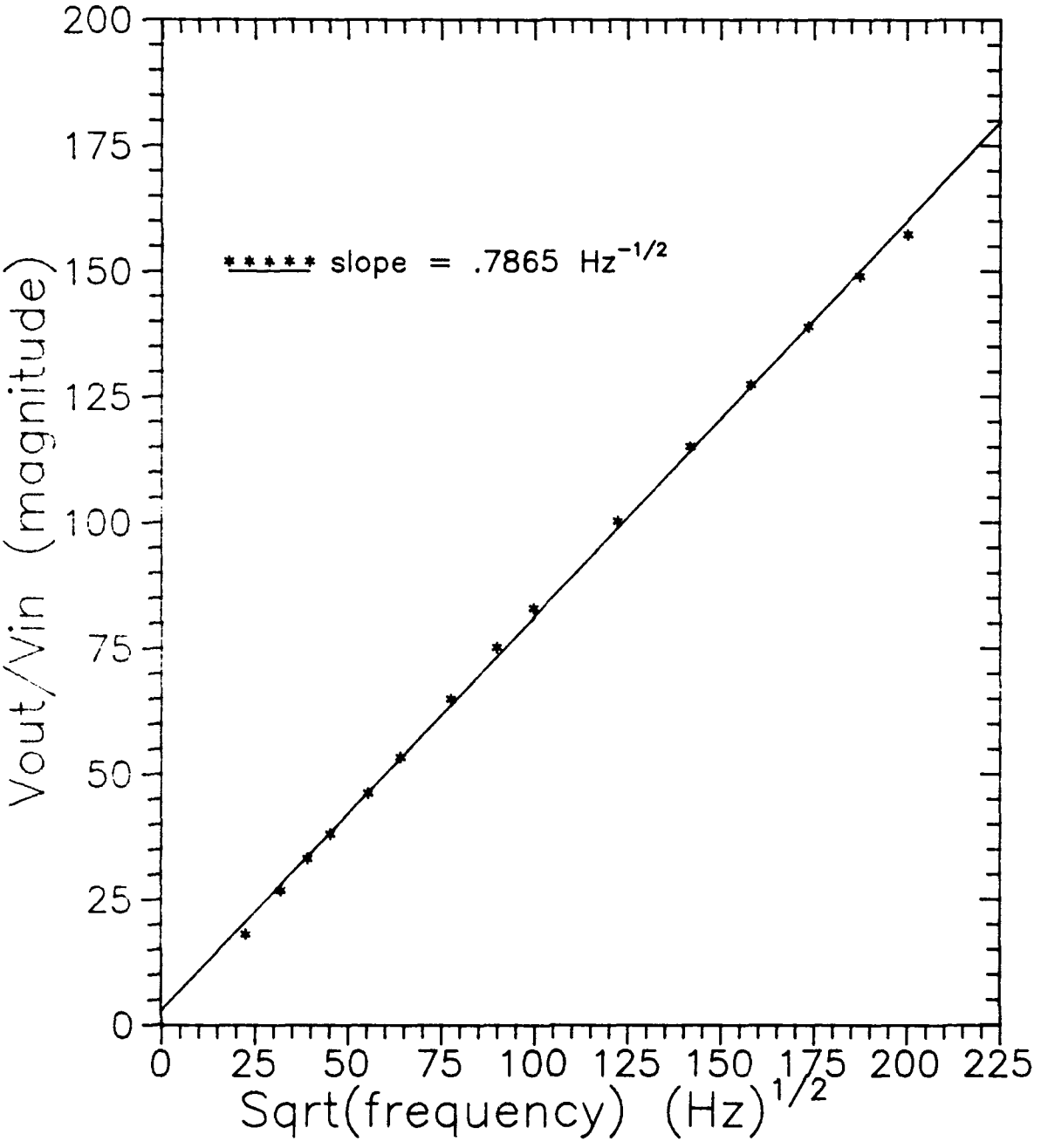


Figure D.6 Calibration of Heat Flux Analog Circuit No. 5 (31–790)

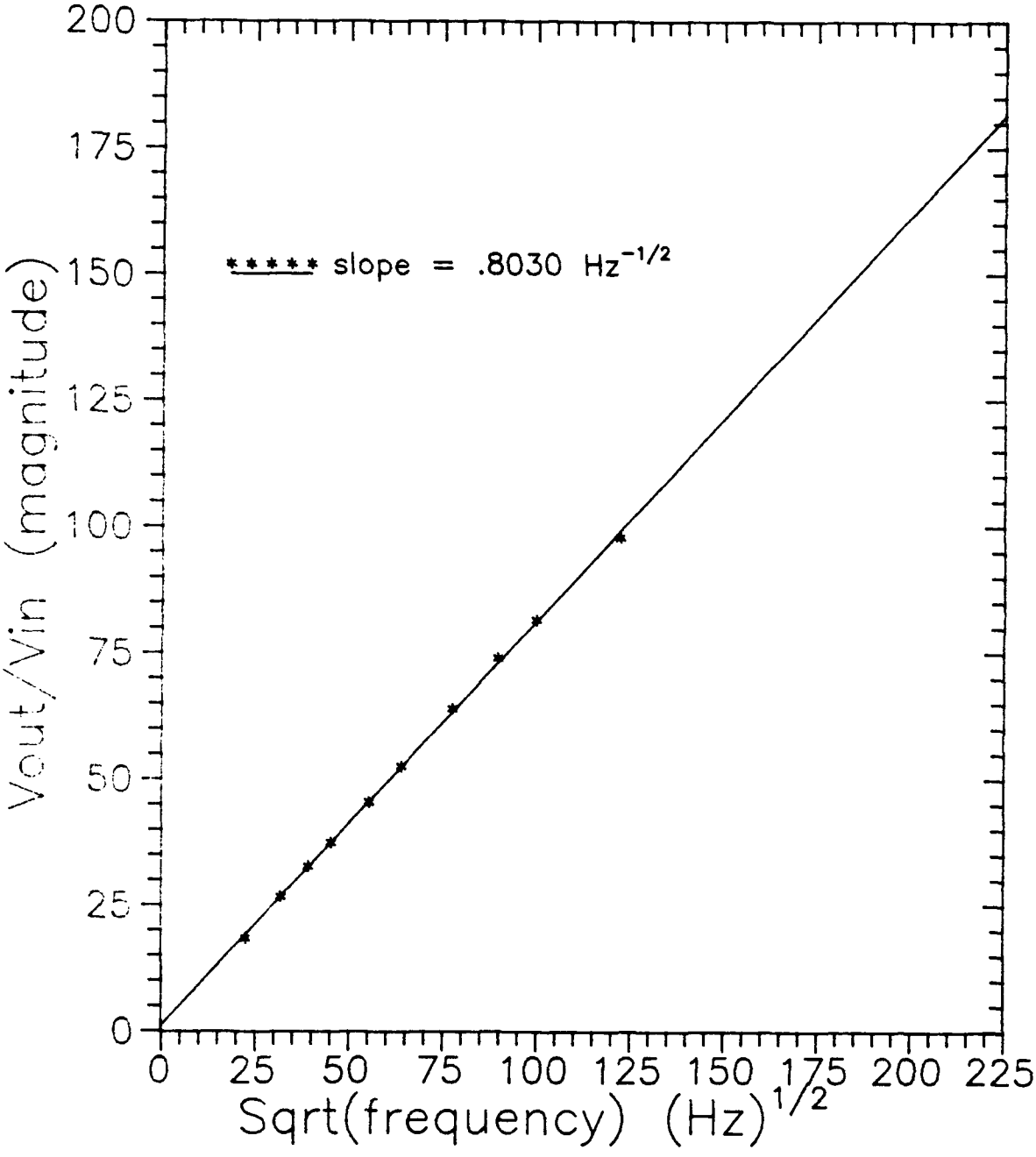


Figure D.7 Calibration of Heat Flux Analog Circuit No. 6 (31–870)

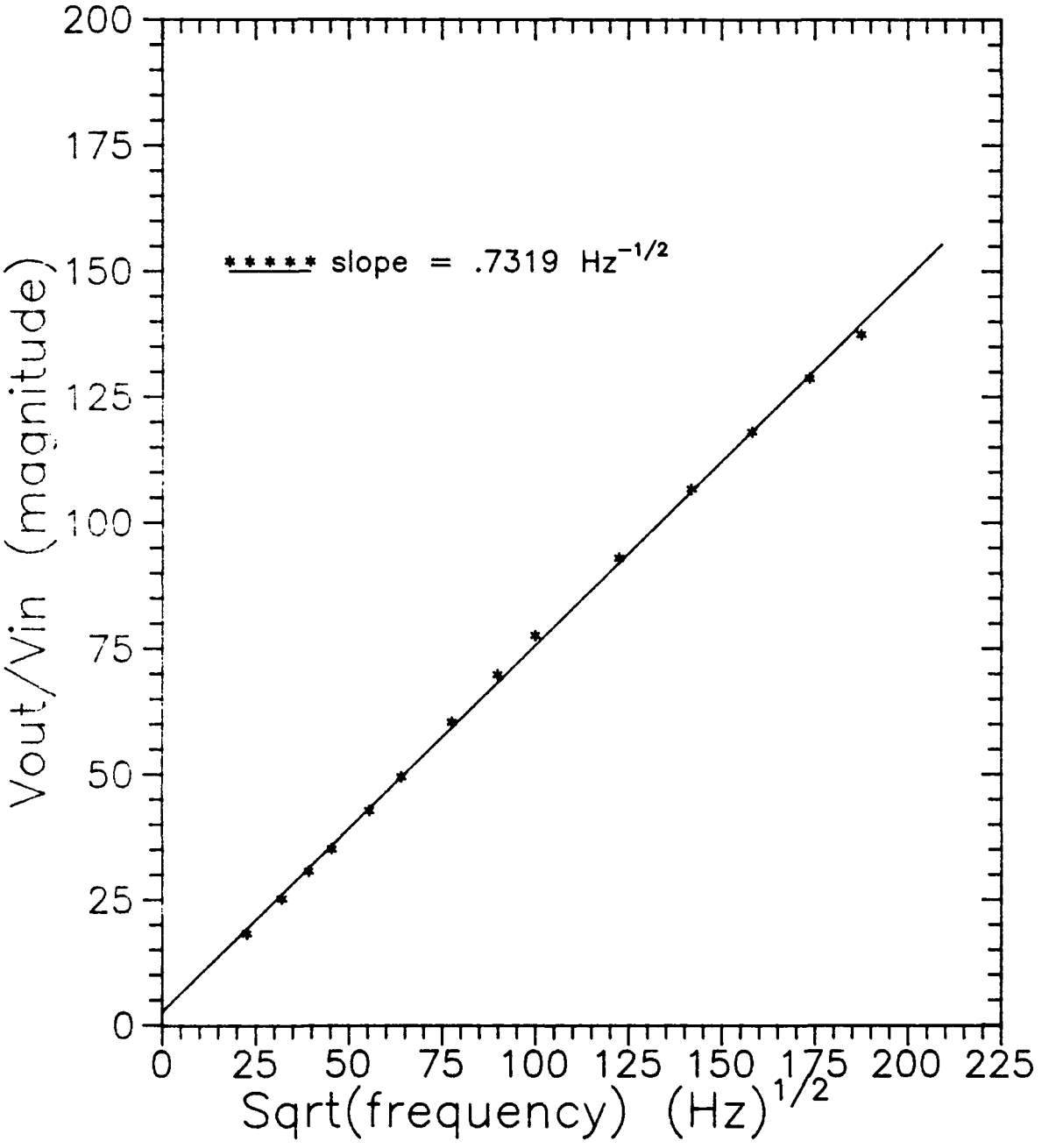


Figure D.8 Calibration of Heat Flux Analog Circuit No. 7 (32–100)

## Appendix E: Shock Tube Film Cooling Computer Program

The program STFCRT, written in Fortran 77, and compiled on the AFIT VAX/VMS mainframe, was used for data reduction for all tests, with and without film cooling. It incorporates mixtures of helium and air in the shock tube driven section. The main program is listed first, followed by a subroutine QAVE used to compute average heat flux.

Finally, a plot of theoretical points is included from calculations made by varying the partial pressure of helium and noting the calculated density ratio for minimum blowing, i.e. $P_{0c} = P_2$.

```
      PROGRAM STFCRT              !SHOCK TUBE FILM COOLING- REF. TEMP.
C  Written by Capt. Thomas A. Eads for Thesis 1992
C  THIS PROGRAM COMPUTES HEAT TRANSFER FOR A RANGE OF FILM COOLING-TO-
C  FREESTREAM DENSITY, VELOCITY, AND MASS FLUX RATIOS ON A FLAT PLATE IN
C  A SHOCK TUBE FOR A GIVEN DRIVER-TO-DRIVEN PRESS. RATIO (P4/P1) AND
C  VARYING HELIUM/AIR MIXTURES IN THE DRIVEN SECTION AND VARYING FILM
C  COOLING PRESSURES.
C     (Theoretical Shock Speed Ms can be solved for using a secant or
C     bisection method on P4/P1 equation, (2.25) of Gaydon 1963:20)
C
C     VARIABLES:
C     A             SPEED OF SOUND
C     CP            SPECIFIC HEAT, CONSTANT PRESSURE
C     DR            FILM COOLING-TO-MAINSTREAM DENSITY RATIO
C     H             HEAT TRANSFER COEFFICIENT
C     K             THERMAL CONDUCTIVITY
C     MB            MASS FLUX (BLOWING) RATIO
C     GAM           RATIO OF SPECIFIC HEATS
C     M             MACH NUMBER
C     IR            MOMENTUM FLUX RATIO (normally I)
C     MU            DYNAMIC VISCOSITY
C     P             PRESSURE
C     PR            PRANDTL NUMBER
C     Q             HEAT TRANSFER/UNIT AREA
C     REX           LOCAL REYNOLDS NUMBER
C     R             GAS CONSTANT
C     RC            RECOVERY FACTOR
C     RHO           DENSITY
C     ST            STANTON NUMBER
C     T             TEMPERATURE
C     TU            TURBULENCE
C     U             VELOCITY
C     VR            FILM COOLING-TO-MAINSTREAM VELOCITY RATIO
C     X             DISTANCE FROM PLATE L.E.
C
C     SUBSCRIPTS:
C     A             AIR
C     AW            ADIABATIC WALL
C     HE            HELIUM
C     E             ENGLISH UNITS
C     C             COOLING
C     TH            THEORETICAL
C     W             WALL
C     x             LOCAL
C     0             STAGNATION
C     1             DRIVEN SECTION
C     2             FREESTREAM (FOLLOWING SHOCK)
C     4             DRIVER SECTION
C
      IMPLICIT NONE
      REAL A1,A4,A14,CPA,CPHE,CP1,DR,GAM1,GAM4,MB,MS,MSOLD,MWA,MWHE,MW1
      REAL PA,PC,PCE,P1,P1E,P2,P4,P4E,P41,PHE,PHE1,PHE2,PHE1E,PHE2E
      REAL R,RA,R1,R2,R4,RHOC,RHO1,RHO2,TC,T1,T2,T4,U2,UC,A2,M2,MU,K
      REAL Patm, PatmE, PR, RC, X, TR, TU, REX, STTH, HTH, TAW, TW, QTH
      REAL CP, RHO, QW, H, ST, DRMIN, VR, IR, TOC, MUHE, KHE, MUA, KA
      INTEGER NG, NS, IFLAG
      CHARACTER*1 ANS
      CHARACTER*13 OUTPUT
      WRITE(6,*)'WELCOME TO THE SHOCK TUBE/FILM COOLING PROGRAM'
      WRITE(6,*)' '
```

```
      PRINT*,'THIS PROGRAM COMPUTES A RANGE OF FILM COOLING-TO-'
      PRINT*,'FREESTREAM DENSITY, VELOCITY, MASS FLUX, AND MOMENTUM'
      PRINT*,'RATIOS ON A FLAT PLATE IN A SHOCK TUBE FOR A GIVEN'
      PRINT*,'DRIVER-TO-DRIVEN PRESS. RATIO (P4/P1) AND VARYING'
      PRINT*,'HELIUM/AIR MIXTURES IN THE DRIVEN SECTION AND VARYING'
      PRINT*,'FILM COOLING PRESSURES (note: Ms is input by user)'
 5    WRITE(6,'(/,A)')' ENTER NAME OF OUTPUT FILE:'
      READ(5,'(A13)') OUTPUT
      IFLAG=1
      OPEN(13,FILE=OUTPUT,STATUS='UNKNOWN')
 10   WRITE(6,*)'ENTER NUMBER FOR CALCULATION FROM THE FOLLOWING'
      WRITE(6,*)'1)  INPUT TEST CONDITION, CALCULATE FLOW VALUES'
      WRITE(6,*)'2)  INPUT/CALCULATE ave. wall heat flux, q'
      WRITE(6,*)'3)  CALCULATE REx, St, h, q(th), ETC.'
      WRITE(6,*)'4)  DETERMINE D.R., MASS FLUX (BLOWING) RATIO (Mb),'
      WRITE(6,*)'    VELOCITY RATIO (VR), AND MOMENTUM RATIO (I) FOR'
      WRITE(6,*)'    INPUT FILM-COOLING PRESSURES'
      WRITE(6,*)'5)  CHANGE TEST/OUTPUT FILE NAME'
      WRITE(6,*)'6)  EXIT PROGRAM'
      READ(5,*) NS
      GO TO (100,200,300,400,5,500) NS
*
*  INPUT
*
 100  IFLAG=0
      WRITE(6,*)'ENTER DRIVER PRESSURE P4 (in. Hg, gauge)'
      READ(5,*) P4E
      WRITE(6,*)'ENTER DRIVEN PRESSURE P1 (in. Hg)'
      READ(5,*) P1E
      WRITE(6,*)'ENTER ATMOSPHERIC PRESSURE (in. Hg)'
      READ(5,*) PatmE
      WRITE(6,*)'ENTER TEMPERATURE T1 (deg C)'
      READ(5,*) T1
      WRITE(6,*)'ENTER FILM COOLING AIR TEMPERATURE T0c (Deg C)'
      READ(5,*) T0C
      WRITE(13,890)' For P4=',P4E,'("Hg) P1=',P1E,' T1=',T1,'K  Tc=',T0C
 890  FORMAT(/,A,F10.6,A,F10.6,/,A,F10.6,A,F10.6,/,' PHe',13X,'D.R.',
     &7X,'Ms')
*
*  INITIALIZE
*
      T1=T1+273.15
      T0C=T0C+273.15
      P4= (P4E+PatmE) * 3386.388158          !Convert to Pa
      P1= P1E * 3386.388158
      Patm=PatmE * 3386.388158
      P41=P4/P1
      CPA=1005.
      CPHE=5193.
      R=8314.34
      MWA=28.966
      MWHE=4.003
      RA=R/MWA
      GAM4=CPA/(CPA-RA)              !=1.400
      R4=RA                          !Air in driver section
      T4=T1
C     TU=9.5                        ! % Turbulence (from Gul, Rockwell ave)
 150  WRITE(6,*)'ENTER He PARTIAL PRESSURE (psi)'
      READ(5,*) PHE1E
      PHE= PHE1E * 6894.757293                !Convert to Pa
```

```
      PA=P1-PHE              !Determine Part. Pres. of air
      IF (PA.LT.0.) THEN
         PRINT*,'HELIUM PRESSURE EXCEEDS DRIVEN PRESSURE!'
         IFLAG=1
         GO TO 10
      ENDIF
*
*  CALCULATIONS
*
      MW1=PA/P1*MWA + PHE/P1*MWHE
      CP1=(PA*MWA*CPA + PHE*MWHE*CPHE)/P1/MW1
      R1=R/MW1
      GAM1=CP1/(CP1-R1)
      A1=(GAM1*R1*T1)**.5
      A4=(GAM4*R4*T4)**.5
      A14=A1/A4
      PRINT*,'PHe=',PHE,'(Pa)'
      PRINT*,'P4=',P4/1000.,' kPa   P1=',P1/1000.,' kPa '
      PRINT*,'GAM1=',GAM1,' a14=',A14,' P4/P1=',P41
      PRINT*,'a1=',A1,'m/s  R1=',R1,'J/kg-K  MW1=',MW1,'kg/kmol'
*
*  INPUT COMPUTED SHOCK VELOCITY AND CONTINUE CALCULATIONS
*       Us= dist. between press. xducers (.7112 m) / Delta t
      WRITE(6,*)'Calculate / ENTER Ms (Measured Us/a1 or Theor.)'
      READ(5,*) MS
      P2=P1*(2.*GAM1*MS**2.-GAM1+1.)/(GAM1+1.)
      T2=T1*(1+(GAM1-1.)/2.*MS**2.)*(2.*GAM1*MS**2./(GAM1-1.)
     &-1.)/MS**2./(2*GAM1/(GAM1-1.)+(GAM1-1.)/2.)
      A2=(GAM1*R1*T2)**.5
      U2=2.*A1/(GAM1+1.)*(MS-(1./MS))
      M2=U2/A2
*
*     INPUT Wall Temp, CALCULATE  Reference Temp., recov. fact., Taw
*
      WRITE(6,*)'Wall Temp., Tw = T1 = ',T1,'K.  Change? (Y or N)'
      READ(5,'(A1)') ANS
      IF (ANS.EQ.'Y'.OR.ANS.EQ.'y') THEN
        WRITE(6,*)'ENTER WALL TEMP(deg C) FOR TIME INTERVAL OF q (ave)'
        READ(5,*)TW
        TW=TW+273.15
      ELSE
         TW=T1
      ENDIF
*  Approximate Prandtl Number from (White, 1991:31)
      PR=4.*GAM1/(7.08*GAM1-1.8)
*  Reference Temperature
      TR=0.5*(T2+TW) + PR**(1./3.)*(GAM1-1.)/2.*M2**2.*T2
      WRITE(6,*)'Ref. Temp. = ',TR,'K    (',TR-273.15,'deg C)'
*  Density
      RHO=P2/R1/TR
*  Option for more accurate Specific Heat
      WRITE(6,*)'Specific Heat, Cp = ',CP1,'J/kg-K.  Change? (Y or N)'
      READ(5,'(A1)') ANS
      IF (ANS.EQ.'Y'.OR.ANS.EQ.'y') THEN
         WRITE(6,*)'ENTER Cp'
         READ(5,*) CP
      ELSE
         CP=CP1
      ENDIF
*  Evaluate viscosity and thermal conductivity
```

```
      CALL MUMIX(TR,P1,PA,PHE,MWA,MWHE,MU)
      CALL KMIX(TR,P1,PA,PHE,MWA,MWHE,K)
*  Prandtl Number for air (He/Air mixture approximated above)
      IF(PHE.LE.1) PR=MU*CP/K
*  Recovery Factor
      RC=PR**(1./3.)
*  Adiabatic Wall Temp.
      TAW=T2*(1+RC*(GAM1-1.)*M2**2/2.)
*
*  FOR FILM COOLING, min blowing
*
      PCE=(P2-Patm)/6894.757293
      RHOC=P2/RA/T0C
      RHO2=P2/R1/T2
      DRMIN=RHOC/RHO2
*
*  OUTPUT
*
      PRINT*,'P2=',P2,' Pa  T2=',T2,' K  RHO2=',RHO2,' kg/m^3'
      PRINT*,'U2=',U2,'m/s  a2=',A2,'m/s  M2=',M2
      PRINT*,'RHO (at Tref)=',RHO
      PRINT*,'MU=',MU,' Pa-sec   k=',K,' W/m^2-K'
      PRINT*,'Pr=',PR,'  rc=',RC
      PRINT*,'Taw=',TAW,'K   (',TAW-273.15,'deg C)'
      PRINT*,'FOR FILM COOLING'
      PRINT*,'Pc,min=',PCE,'psig'
      WRITE(6,900) PHE1E, DRMIN
 900  FORMAT(1X,'He PART. PRESS.=',F11.6,' (psi), D.R.min= ',F11.6)
      WRITE(13,901) PHE1E, DRMIN, MS
 901  FORMAT(1X,F11.6,2X,F11.6,2X,F8.5,/)
      WRITE(13,*)'Patm = ',PatmE,' in Hg   Pc,min = ',PCE,'psig'
      WRITE(6,*)'Continue with a new Press.(He)? (Y or N)'
      READ(5,'(A1)') ANS
      IF (ANS.EQ.'Y'.OR.ANS.EQ.'y') GOTO 150
      GO TO 10
*
*  COMPUTE AVERAGE HEAT FLUX, MEASURED
*
 200  WRITE(6,*)'ENTER (1) FOR HAND ENTRY, (2) GO TO PROGRAM QAVE'
      READ(5,*) NS
      GO TO (225,250) NS
 225  WRITE(6,*)'ENTER Gauge # '
      READ(5,*) NG
      WRITE(6,*)'ENTER heat flux q (ave) (kW/m^2) FROM PROGRAM QAVE'
      READ(5,*) QW
      QW=QW*1000.
      GO TO 10
 250  CALL QAVE(NG,QW)
      GO TO 10
*
*  CALCULATE REYNOLDS No., h, St
*
 300  IF (IFLAG.EQ.1) THEN
      WRITE(6,*)' MUST COMPUTE (1) FIRST'
      GO TO 10
      ENDIF
      WRITE(6,'(A,I1,A)')' Gauge # = ',NG,'  Continue with this
     &gauge? (Y or N)'
      READ(5,'(A1)')ANS
      IF (ANS.EQ.'N'.OR.ANS.EQ.'n') THEN
```

```
         WRITE(6,*)'Note: only theoretical results may be correct'
 350     WRITE(6,*)'ENTER GAUGE #'
         READ(5,*) NG
       ENDIF
       WRITE(6,*)'ENTER Turbulence Level  Tu  IN %  [ 0. or 9.5]'
       READ(5,*) TU
*  Re,x (Theor. and Exper.)
       REX=RHO*U2*X(NG)/MU
*  THEORETICAL St, h, q
       STTH=(0.0287/REX**.2/PR**.4)*(1.+5.*TU/100.)
       HTH=STTH*RHO*U2*CP
       QTH=HTH*(TAW-TW)
*  EXPERIMENTAL/MEASURED h, St
       H=QW/(TAW-TW)
       ST=H/RHO/U2/CP
*
*   OUTPUT RESULTS
*
       WRITE(6,903)NG,REX*1E-6,STTH*1E3,HTH,QTH/1E3,QW/1E3,H,ST*1E3
       WRITE(13,903)NG,REX*1E-6,STTH*1E3,HTH,QTH/1E3,QW/1E3,H,ST*1E3
 903   FORMAT(/,T2,'Gage',T8,'Rex',T16,'St,th',T24,'h,th',T32,'q,th',
      &T40,'qw,avg',T48,'h',T56,'St',/,' No.',T7,'(x1E-6)',T16,
      &'(x1E3)',T24,'W/m^2/K',T32,'kW/m^2',T40,'kW/m^2',T48,'W/m^2',
      &T56,'(x1E3)',//,T2,I1,T8,F6.4,T16,F6.3,T24,F6.1,T32,F6.2,T40,
      &F6.2,T48,F6.1,T56,F6.3,/)
       WRITE(6,*)'Again with SAME q, new gauge number or Tu? (Y or N)'
       READ(5,'(A1)')ANS
       IF (ANS.EQ.'Y'.OR.ANS.EQ.'y') GOTO 350
       GO TO 10
*
*   FILM COOLING PARAMETERS/RESULTS
*
 400   IF(IFLAG.EQ.1)THEN
       WRITE(6,*)'PLEASE SELECT (1) BEFORE RUNNING THIS'
       GO TO 10
       ENDIF
 450   WRITE(6,*)'choked flow for Pc > ',(P2/.5283-Patm)/6894.757,' psig'
       WRITE(6,*)'ENTER COOLING PRESS. MEASURED DURING AVE q CALC (psig)'
       READ(5,*)PCE
       WRITE(6,*)' COOLING STAG. TEMP = ',T0C,'K.  Change? <Y,N>'
       READ(5,'(A1)')ANS
         IF(ANS.EQ.'Y'.OR.ANS.EQ.'y')THEN
            WRITE(6,*)' ENTER FILM COOLING CHAMBER TEMP  Tc (deg K)'
            READ(5,*) T0C
         ENDIF
       PC=PCE*6894.757 + Patm              !Convert to Pa, abs
       IF(PC.LT.P2) THEN
          PRINT*,' WARNING: Pc < P2 => NO COOLING FLOW. Change Pc? <Y,N>'
          READ(5,'(A1)')ANS
          IF (ANS.EQ.'Y'.OR.ANS.EQ.'y') GOTO 450
          GOTO 10
       ENDIF
       IF(P2.LE.0.52828*PC) THEN
          WRITE(6,*)' COOLING FLOW IS CHOKED!'
          WRITE(13,*)' COOLING FLOW IS CHOKED!'
          UC=(2.*GAM4*RA*T0C/(GAM4+1.))**.5
          RHOC=PC/RA/T0C*(2./(GAM4+1.))**(1./(GAM4-1.))
          TC=0.83333*T0C
       ELSE
          UC=(2.*RA*T0C*GAM4/(GAM4-1.)*(1-(P2/PC)**((GAM4-1.)/GAM4)))**.5
```

```
         RHOC=PC/RA/T0C*(P2/PC)**(1./GAM4)
         TC=T0C*(P2/PC)**((GAM4-1.)/GAM4)
       ENDIF
       DR=RHOC/RHO2
       VR=UC/U2
       MB=DR*VR
       IR=MB*VR
       WRITE(13,*)' FOR Pc = ',PC/1000.,'kPa  chamber Tc= ',T0C,'K'
       WRITE(6,*)' Uc =',UC,' m/s  rhoc =',RHOC,' kg/m^3  Tc =',TC,' K'
       WRITE(6,*)'Density Ratio DR=',DR,'  Velocity Ratio VR=',VR
       WRITE(6,*)'Blowing Ratio Mb=',MB,'  Momentum Flux Ratio I=',IR
       WRITE(13,*)'Density Ratio DR=',DR,'  Velocity Ratio VR=',VR
       WRITE(13,*)'Blowing Ratio Mb=',MB,'  Momentum Flux Ratio I=',IR
       WRITE(6,'(/,A)')' TRY ANOTHER COOLING PRESSURE or TEMP? (Y or N)'
       READ(5,'(A1)') ANS
       IF (ANS.EQ.'Y'.OR.ANS.EQ.'y') GOTO 450
       GOTO 10
 500   WRITE(6,*)'OUTPUT IS IN FILE ',OUTPUT
       STOP
       END
*
*
*  FUNCTIONS/SUBROUTINE FOR PROPERTY/GAUGE VALUES
*
       REAL FUNCTION MUA(T)
C      FROM SUTHERLAND-LAW FOR ABSOLUTE VISCOSITY OF AIR (White, 1991:28)
       MUA= 1.716E-5*(T/273.)**(1.5)*(384./(T+111.))
       END
*
*
       REAL FUNCTION MUHE(T)
C      LINEAR FIT OF VISCOSITY FOR He FROM (KAYS AND CRAWFORD, 1980:391)
       MUHE= 4.4E-8*T + 6.7E-6
       END
*
*
       REAL FUNCTION KA(T)
C      FROM SUTHERLAND-LAW FOR THERMAL CONDUCTIVITY OF AIR (White,'91:31)
       KA= 0.0241*(T/273.)**1.5*(467./(T+194.))
       END
*
*
       REAL FUNCTION KHE(T)
C      LINEAR FIT OF THERMAL CONDUCTIVITY FOR He FROM (K&C, 1980:391)
       KHE= 3.4E-5*T + 0.0053
       END
*
*
       SUBROUTINE MUMIX(TR,P1,PA,PHE,MWA,MWHE,MU)
C      DILUTE MIXTURE VISCOSITY , APPROX. FROM (WHITE, 1991:35)
C        WITH MOLE FRACTION = PARTIAL PRESSURE
       REAL MWA, MWHE, MU, MUA, MUHE
       PHIHA=(1.+(MUHE(TR)/MUA(TR))**.5*(MWA/MWHE)**.25)**2./
      & (8.+8.*MWHE/MWA)**.5
       PHIAH=(1.+(MUA(TR)/MUHE(TR))**.5*(MWHE/MWA)**.25)**2./
      & (8.+8.*MWA/MWHE)**.5
       MU=PHE/P1*MUHE(TR)/(PA/P1*PHIHA+PHE/P1)+PA/P1*MUA(TR)/(PHE/P1*
      &PHIAH+PA/P1)                    !Note: mu = mu(air) if pHe = 0
       RETURN
       END
```

```
*
*
      SUBROUTINE KMIX(TR,P1,PA,PHE,MWA,MWHE,K)
C     DILUTE MIXTURE THERMAL CONDUCTIVITY, similar to above subr.
      REAL K, KHE, KA, KPHIHA, KPHIAH, MWA, MWHE
      KPHIHA=(1.+(KHE(TR)/KA(TR))**.5*(MWA/MWHE)**.25)**2./
     & (8.+8.*MWHE/MWA)**.5
      KPHIAH=(1.+(KA(TR)/KHE(TR))**.5*(MWHE/MWA)**.25)**2./
     & (8.+8.*MWA/MWHE)**.5
      K=PHE/P1*KHE(TR)/(PA/P1*KPHIHA + PHE/P1)+PA/P1*KA(TR)/(PHE/P1*
     & KPHIAH + PA/P1)                    !Note: k = k(air) if pHe = 0
      RETURN
      END
*
*
      REAL FUNCTION X(NG)
      IF (NG.EQ.1) X=0.05477
      IF (NG.EQ.2) X=0.05675
      IF (NG.EQ.3) X=0.05874
      IF (NG.EQ.4) X=0.06072
      IF (NG.EQ.5) X=0.06668
      IF (NG.EQ.6) X=0.07164
      IF (NG.EQ.7) X=0.08156
      END
*
*************************************************************************
*  AVERAGE HEAT FLUX SUBROUTINE                                         *
*************************************************************************
*
      SUBROUTINE QAVE(NG,QAVG)
*  WRITTEN FOR SHOCK-TUBE FLAT-PLATE HEAT-TRANSFER WITH FILM COOLING
*  TO CALCULATE AN AVERAGE HEAT FLUX FROM THE THIN-FILM RESISTANCE
*  GAUGE/HEAT FLUX ELECTRICAL ANALOG OUTPUT VOLTAGE
*
* VARIABLES:
*  COUNT    COUNTER FOR NUMBER OF POINTS TO AVERAGE
*  HFC      HEAT FLUX PROPORTIONALITY COEFFICIENT (W/m^2 per Volt)
*              (GAUGE/CIRCUIT DEPENDENT, FROM CALIBRATIONS)
*  QAVG     AVERAGE HEAT FLUX  (W/m^2)
*  Q(I)     HEAT FLUX AT DATA PT I WRT AVG REFERENCE
*  TIME(I)  TIME OF DATA POINT "I"
*  TBEG, TEND  BEGINNING AND ENDING TIMES FOR QAVG (FROM NICOLET SCREEN)
*  TPP      TIME PER POINT OF DATA ACQUIRED
*  TTOT     TOTAL ACQUISITION TIME
*  VSUM     INITIAL REFERENCE (ZERO HEAT FLUX) VOLTAGE SUM
*  VRAVG    AVERAGE REFERENCE VOLTAGE
*  V(I)     HEAT FLUX VOLTAGE AT DATA PT  I
*  VAVG     AVERAGE HEAT FLUX VOLTAGE (FOR SPECIFIED RANGE)
*
*
      IMPLICIT NONE
      REAL Q(10000), TIME(10000), V(10000), SUM, TBEGI, TENDI
      REAL HFC, QAVG, QREF, VAVG, VRAVG, VSUM, TPP, TTOT, TBEG, TEND
      INTEGER I, J, COUNT, NDATA, NG, NREF
      CHARACTER*1 ANS
      CHARACTER*12 INPUT, OUTPUT, QOUT
      CHARACTER*60 HDR1,HDR2
      WRITE(6,*)'THIS IS THE DATA REDUCTION PROGRAM FOR AVE. HEAT FLUX'
      WRITE(6,*)'   (PROGRAM ASSUMES FIRST 20% OF DATA IS REFERENCE)'
 10   WRITE(6,*) 'ENTER FILENAME OF DATA TO READ (.FLT)'
```

```
      READ(5,'(A12)') INPUT
      WRITE(6,*) 'ENTER FILENAME FOR OUTPUT'
      READ(5,'(A12)') OUTPUT
      WRITE(6,*) 'ENTER FILENAME FOR OUTPUT OF Q VS TIME'
      READ(5,'(A12)') QOUT
      OPEN(10,FILE=INPUT,STATUS='UNKNOWN')
      OPEN(11,FILE=OUTPUT,STATUS='UNKNOWN')
      OPEN(12,FILE=QOUT,STATUS='NEW')
      WRITE(6,*) 'ENTER NUMBER OF DATA POINTS ACQUIRED (5000?)'
      READ(5,*) NDATA
      WRITE(6,*) 'ENTER TIME/POINT (in microsec) [ 2? ]'
      READ(5,*) TPP
      TPP= TPP*1.E-6
      TTOT= REAL(NDATA)*TPP         !Total Time
      WRITE(6,*)'ENTER BEGIN,END TIMES FOR HEAT FLUX AVG (msec,msec)'
      READ(5,*) TBEGI,TENDI
      TBEG= TBEGI*.001 + TTOT/10.   !.FLT conver. shifts time values
      TEND= TENDI*.001 + TTOT/10.
      WRITE(6,*)'USE PROGRAMMED VALUES FOR CALIB. COEFF.? (Y or N)'
      READ(5,'(A1)') ANS
      IF (ANS.EQ.'y'.OR.ANS.EQ.'Y') THEN
         WRITE(6,*)'ENTER GAUGE NUMBER'
         READ(5,*) NG
         CALL CAL(HFC,NG)
      ELSE
         WRITE(6,*)'ENTER CALIB. COEFF. FOR GAUGE NO.',NG,'W/m^2/Volt'
         READ(5,*) HFC
      ENDIF
*
*  READ HEADER IN .FLT DATA FILE AND WRITE IT TO OUTPUT FILE
*
      READ(10,900) HDR1,HDR2
 900  FORMAT(2(A60,/))
      WRITE(11,'(1X,A60,/)') HDR1
      WRITE(6,*)'DATA USED IS FROM ',HDR1
*
*  READ DATA AND CALCULATE AVERAGE HEAT FLUX
*
      DO 15 I=1,NDATA-1
      READ(10,*) V(I), TIME(I)
 15   CONTINUE
      VSUM = 0.
      COUNT = 0
      NREF = NINT(TTOT/5./TPP)
      DO 20 I= 1, NREF
         COUNT=COUNT+1
         VSUM=VSUM+V(I)
 20   CONTINUE
      PRINT*,'NUMBER OF REFERENCE POINTS USED=',COUNT
      VRAVG = VSUM/REAL(COUNT)
      QREF=HFC*VRAVG
      COUNT = 0
      SUM = 0.
      DO 30 J= 1, NDATA-1
         IF (TIME(J).GE.TBEG.AND.TIME(J).LE.TEND) THEN
            COUNT=COUNT+1
            SUM=SUM+V(J)
         ENDIF
         Q(J)=HFC*(V(J)-VRAVG)
         WRITE(12,*) TIME(J),Q(J)
```

```
 30   CONTINUE
      VAVG=SUM/REAL(COUNT)-VRAVG
      QAVG=VAVG*HFC
*
*  OUTPUT RESULTS
*
      WRITE(6,*)'CALIBR. COEFF. =',HFC/1000.,'kW/m^2/Volt'
      WRITE(11,*)'Gauge/Circuit CALIB. COEF. =',HFC,'W/m^2/Volt'
      WRITE(6,*)'Ave. Ref. Voltage =',VRAVG,'  q(ref)=',QREF,'W/m^2'
      WRITE(11,*)'Ave. Ref. Volt =',VRAVG,'V   q(ref)=',QREF,'W/m^2'
      WRITE(6,*)'Ave. Volt = ',VAVG
      WRITE(11,*)'Ave. Volt = ',VAVG
      PRINT*,'Tbeg(from .FLT)= ',TBEG,'msec  Tend = ',TEND,'msec'
      WRITE(11,*)'Beg. time = ',TBEGI,'msec  End Time = ',TENDI,'msec'
      WRITE(6,902)' FOR GAUGE #',NG,'qavg = ',QAVG/1000.,'kW/m^2'
      WRITE(11,902)' FOR GAUGE #',NG,'qavg = ',QAVG/1000.,'kW/m^2'
 902  FORMAT(/,A,1X,I1,3X,A,F12.2,1X,A,//)
      WRITE(6,'(/,A)')' COMPUTE ANOTHER q (ave) ? (Y or N)'
      READ(5,'(A1)')ANS
      IF (ANS.EQ.'Y'.OR.ANS.EQ.'y') THEN
         REWIND 10
         GOTO 10
      ENDIF
      WRITE(6,*)'OUTPUT IS IN FILE ',OUTPUT
      WRITE(6,*)'OUTPUT OF time, q (heat flux) IS IN FILE ',QOUT
      RETURN
      END
*
*
      SUBROUTINE CAL(HFC,NG)
      IF(NG.EQ.1) HFC=53710.
      IF(NG.EQ.2) HFC=69715.
      IF(NG.EQ.3) HFC=65647.
      IF(NG.EQ.4) HFC=62668.
      IF(NG.EQ.5) HFC=41949.
      IF(NG.EQ.6) HFC=91732.
      IF(NG.EQ.7) HFC=35521.
      HFC=HFC*(2.*3.1415926536)**.5
      RETURN
      END
```

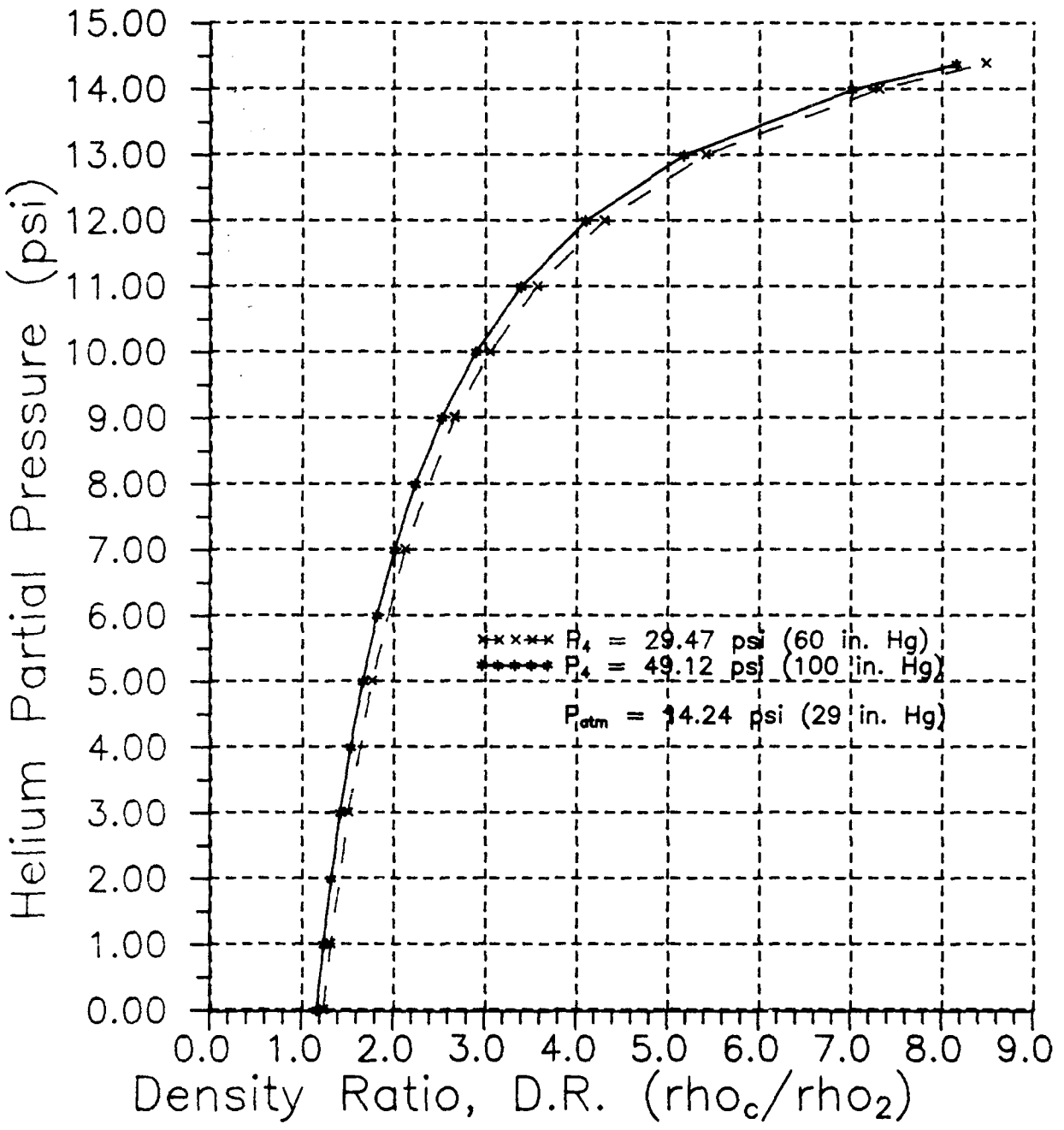


Figure E.1 Calculated Density Ratio Versus Partial Pressure of Helium in Shock Tube for Min. Blowing (from Fortran Program STFCRT)

## Appendix F: Data Summary Worksheets

Worksheets for measured and calculated parameters of all tests included in the presentation of data are included in this appendix, pages F.2 to F.26. Test runs are designated with different symbols. 'T' denotes test (with or without helium in shock tube), 'H' denotes helium used in film cooling test run, 'P' denotes a practice run, 'V' denotes a verification run, and 'X' denotes an extra run without holes covered.

## Test No. T01

($P_4$ = 60" Hg gauge, $P_{atm}$ = 28.92 in Hg, $\gamma_4=\gamma_1$ = 1.400, $R_1=R_4$ = 287 J/kg-K)

**Measured**

| | | | |
|---|---|---|---|
| Driver Pressure | $P_4$ = 300.10 kPa | (88.62 in Hg abs) | |
| Driven Pressure | $P_1$ = 97.93 kPa | (28.92 in Hg abs) | |
| Driver/Driven Temp. | $T_1=T_4$ = 293.15 K | (20.0 deg C) | |
| Shock Velocity | $U_s$ = 412.50 m/sec | | = $\Delta x/\Delta t$ ($\Delta t$ = 1.724 msec) |
| Pressure behind shock | $P_2$ = 149.65 kPa | (21.70 psia) | |

**Calculated**

| | | | |
|---|---|---|---|
| Sonic Velocity | $a_1$ = 343.20 m/sec | | $=(\gamma_1 R_1 T_1)^{1/2}$ |
| Shock Mach Number | $M_s$ = 1.202 | | $=U_s/a_1$ |
| Theoretical Shock Mach No. | $M_{th}$ = 1.268 | | based on $P_4/P_1$, $\gamma_1$, $\gamma_4$, $a_1/a_4$ |
| Temperature behind shock | $T_2=T_\infty$ = 331.02 K | (57.9 deg C) | based on $M_s$, $\gamma_1$ |
| Press. behind shock, Theor. | $P_2=P_\infty$ = 148.75 kPa | (21.574 psia) | based on $M_s$, $\gamma_1$ |
| Density behind shock | $\rho_2=\rho_\infty$ = 1.566 kg/m$^3$ | | $=P_2/R_1 T_2$ |
| Flow Velocity, behind shock | $U_2=U_\infty$ = 105.84 m/sec | | based on $M_s$, $a_1$, $\gamma_1$ |
| Sonic Velocity behind shock | $a_2=a_\infty$ = 364.70 m/sec | | $=(\gamma_1 R_1 T_2)^{1/2}$ |
| Flow Mach No. behind shock | $M_2=M_\infty$ = 0.290 | | $=U_2/a_2$ |
| Reference Temperature | $T^*$ = 313.62 K | (40.47 deg C) | $= 0.5(T_w+T_\infty)+0.039M^2_\infty T_\infty$ |

**Flow Properties** (evaluated at $T^*$)

| | | | |
|---|---|---|---|
| Density | $\rho$ = 1.652 kg/m$^3$ | | $=P_2/R_1 T^*$ |
| Specific Heat | $C_p$ = 1005.0 J/kg-K | | |
| Absolute Viscosity | $\mu$ = 1.911E-5 Pa-sec | | Sutherland-Law |
| Thermal Conductivity | k = 0.02730 W/m$^2$-K | | Sutherland-Law |
| Prandtl Number | Pr = 0.7034 | | $=\mu C_p/k$ |
| Recovery Factor | $r_c$ = 0.8894 | | $=Pr^{1/3}$ |

| | | | |
|---|---|---|---|
| Adiabatic Wall Temperature | $T_{aw}$ = 335.98 K | (62.8 deg C) | $=T_\infty[1+r_c(\gamma_1-1)M_\infty^2/2]$ |
| Measured Avg Wall Temperature | $T_w$ = 294.15 K | (21.0 deg C) | gauge 4 location |

**Results**

| | | | Theoretical (Tu = 9.5%) | | | Measured (4-5 msec) | | |
|---|---|---|---|---|---|---|---|---|
| Gauge No. | X cm | $Re_x$ (x10$^{-6}$) | $St_{th}$ (x10$^3$) | $h_{th}$ W/m$^2$-K | $q_{th}$ kW/m$^2$ | $q_{avg}$ kW/m$^2$ | h W/m$^2$-K | St (x10$^3$) |
| 1 | 5.48 | 0.5012 | 3.530 | 620.4 | 25.95 | 35.97 | 859.9 | 4.893 |
| 2 | 5.68 | 0.5193 | 3.505 | 616.0 | 25.77 | 33.15 | 792.5 | 4.510 |
| 3 | 5.87 | 0.5375 | 3.481 | 611.8 | 25.59 | 31.12 | 744.0 | 4.234 |
| 4 | 6.07 | 0.5556 | 3.458 | 607.8 | 25.42 | 28.44 | 679.9 | 3.869 |
| 5 | 6.67 | 0.6102 | 3.394 | 596.5 | 24.95 | 29.03 | 694.0 | 3.949 |
| 6 | 7.16 | 0.6555 | 3.346 | 588.0 | 24.59 | 31.06 | 742.6 | 4.226 |
| 7 | 8.16 | 0.7465 | 3.260 | 572.9 | 23.96 | 29.28 | 699.9 | 3.983 |

## Test No. T02

($P_4$ = 80" Hg gauge, $P_{atm}$ = 28.92 in Hg, $\gamma_4=\gamma_1$ = 1.400, $R_1=R_4$ = 287 J/kg-K)

**Measured**

| | | | |
|---|---|---|---|
| Driver Pressure | $P_4$ = 367.39 kPa | (108.49 in Hg abs) | |
| Driven Pressure | $P_1$ = 98.07 kPa | (28.96 in Hg abs) | |
| Driver/Driven Temp. | $T_1=T_4$ = 293.15 K | (20.0 deg C) | |
| Shock Velocity | $U_s$ = 435.52 m/sec | | = $\Delta x/\Delta t$ ($\Delta t$ = 1.633 msec) |
| Pressure behind shock | $P_2$ = 167.71 kPa | (24.32 psia) | |

**Calculated**

| | | | |
|---|---|---|---|
| Sonic Velocity | $a_1$ = 343.20 m/sec | | $=(\gamma_1 R_1 T_1)^{1/2}$ |
| Shock Mach Number | $M_s$ = 1.269 | | $=U_s/a_1$ |
| Theoretical Shock Mach No. | $M_{th}$ = 1.326 | | based on $P_4/P_1$, $\gamma_1$, $\gamma_4$, $a_1/a_4$ |
| Temperature behind shock | $T_2=T_\infty$ = 343.35 K | (70.2 deg C) | based on $M_s$, $\gamma_1$ |
| Press. behind shock, Theor. | $P_2=P_\infty$ = 167.90 kPa | (24.35 psia) | based on $M_s$, $\gamma_1$ |
| Density behind shock | $\rho_2=\rho_\infty$ = 1.704 kg/m$^3$ | | $P_2/R_1$-$T_2$ |
| Flow Velocity, behind shock | $U_2=U_\infty$ = 137.57 m/sec | | based on $M_s$, $a_1$, $\gamma_1$ |
| Sonic Velocity behind shock | $a_2=a_\infty$ = 371.43 m/sec | | $=(\gamma_1 R_1 T_2)^{1/2}$ |
| Flow Mach No. behind shock | $M_2=M_\infty$ = .3704 | | $=U_2/a_2$ |
| Reference Temperature | $T^*$ = 320.69 K | (47.5 deg C) | $= 0.5(T_w+T_\infty)+0.039M^2_\infty T_\infty$ |

**Flow Properties** (evaluated at $T^*$)

| | | | |
|---|---|---|---|
| Density | $\rho$ = 1.824 kg/m$^3$ | | $=P_2/R_1$-$T^*$ |
| Specific Heat | $C_p$ = 1005.0 J/kg-K | | |
| Absolute Viscosity | $\mu$ = 1.943E-5 Pa-sec | | Sutherland-Law |
| Thermal Conductivity | k = 0.02784 | W/m$^2$-K | Sutherland-Law |
| Prandtl Number | Pr = 0.7015 | | $=\mu C_p/k$ |
| Recovery Factor | $r_c$ = 0.8886 | | $=Pr^{1/3}$ |

| | | | |
|---|---|---|---|
| Adiabatic Wall Temperature | $T_{aw}$ = 351.72 K | (78.6 deg C) | $=T_\infty[1+r_c(\gamma_1-1)M_\infty^2/2]$ |
| Measured Avg Wall Temperature | $T_w$ = 294.39 K | (21.2 deg C) | gauge 4 location |

**Results** — Theoretical (Tu = 9.5%) — Measured (4-5 msec)

| Gauge No. | X cm | $Re_x$ (x10$^{-6}$) | $St_{th}$ (x10$^3$) | $h_{th}$ W/m$^2$-K | $q_{th}$ kW/m$^2$ | $q_{avg}$ kW/m$^2$ | h W/m$^2$-K | St (x10$^3$) |
|---|---|---|---|---|---|---|---|---|
| 1 | 5.48 | 0.7072 | 3.299 | 831.9 | 47.72 | 60.71 | 1058. | 4.196 |
| 2 | 5.68 | 0.7328 | 3.275 | 826.0 | 47.39 | 52.26 | 911.0 | 3.612 |
| 3 | 5.87 | 0.7585 | 3.253 | 820.3 | 47.06 | 48.90 | 852.4 | 3.380 |
| 4 | 6.07 | 0.7840 | 3.231 | 814.9 | 46.75 | 45.22 | 788.2 | 3.126 |
| 5 | 6.67 | 0.8610 | 3.171 | 799.8 | 45.88 | 49.59 | 864.4 | 3.428 |
| 6 | 7.16 | 0.9250 | 3.126 | 788.4 | 45.23 | 48.56 | 846.5 | 3.357 |
| 7 | 8.16 | 1.0531 | 3.046 | 768.2 | 44.07 | 42.71 | 744.5 | 2.952 |

## Test No. T03

($P_4$ = 100" Hg gauge, $P_{atm}$ = 28.92 in Hg, $\gamma_4=\gamma_1$ = 1.400, $R_1=R_4$ = 287 J/kg-K)

**Measured**

| | | | |
|---|---|---|---|
| Driver Pressure | $P_4$ = 439.71 kPa | (128.37 in Hg abs) | |
| Driven Pressure | $P_1$ = 97.93 kPa | (28.92 in Hg abs) | |
| Driver/Driven Temp. | $T_1=T_4$ = 293.15 K | (20.0 deg C) | |
| Shock Velocity | $U_s$ = 451.27 m/sec | | = $\Delta x/\Delta t$ ($\Delta t$ = 1.576 msec) |
| Pressure behind shock | $P_2$ = 182.53 kPa | (26.47 psia) | |

**Calculated**

| | | | |
|---|---|---|---|
| Sonic Velocity | $a_1$ = 343.20 m/sec | | $=(\gamma_1 R_1 T_1)^{1/2}$ |
| Shock Mach Number | $M_s$ = 1.315 | | $=U_s/a_1$ |
| Theoretical Shock Mach No. | $M_{th}$ = 1.369 | | based on $P_4/P_1$, $\gamma_1$, $\gamma_4$, $a_1/a_4$ |
| Temperature behind shock | $T_2=T_\infty$ = 351.86 K | (78.71 deg C) | based on $M_s$, $\gamma_1$ |
| Press. behind shock, Theor. | $P_2=P_\infty$ = 181.25 kPa | (26.288 psia) | based on $M_s$, $\gamma_1$ |
| Density behind shock | $\rho_2=\rho_\infty$ = 1.795 kg/m$^3$ | | $=P_2/R_1-T_2$ |
| Flow Velocity, behind shock | $U_2=U_\infty$ = 158.61 m/sec | | based on $M_s$, $a_1$, $\gamma_1$ |
| Sonic Velocity behind shock | $a_2=a_\infty$ = 376.00 m/sec | | $=(\gamma_1 R_1 T_2)^{1/2}$ |
| Flow Mach No. behind shock | $M_2=M_\infty$ = 0.4218 | | $=U_2/a_2$ |
| Reference Temperature | $T^*$ = 325.80 K | (52.65 deg C) | $= 0.5(T_w+T_\infty)+0.039M^2_\infty T_\infty$ |

**Flow Properties** (evaluated at $T^*$)

| | | | |
|---|---|---|---|
| Density | $\rho$ = 1.938 kg/m$^3$ | | $=P_2/R_1-T^*$ |
| Specific Heat | $C_p$ = 1006.0 J/kg-K | | |
| Absolute Viscosity | $\mu$ = 1.967E-5 Pa-sec | | Sutherland-Law |
| Thermal Conductivity | k = 0.02823 | W/m$^2$-K | Sutherland-Law |
| Prandtl Number | Pr = 0.7009 | | $=\mu C_p/k$ |
| Recovery Factor | $r_c$ = 0.8883 | | $=Pr^{1/3}$ |

| | | | |
|---|---|---|---|
| Adiabatic Wall Temperature | $T_{aw}$ = 362.98 K | (89.83 deg C) | $=T_\infty[1+r_c(\gamma_1-1)M_\infty^2/2]$ |
| Measured Avg Wall Temperature | $T_w$ = 294.83 K | (21.7 deg C) | gauge 4 location |

| Results | | | Theoretical (Tu = 9.5%) | | | Measured (3.8-4.8 msec) | | |
|---|---|---|---|---|---|---|---|---|
| Gauge No. | X cm | $Re_x$ (x10$^{-6}$) | $St_{th}$ (x10$^3$) | $h_{th}$ W/m$^2$-K | $q_{th}$ kW/m$^2$ | $q_{avg}$ kW/m$^2$ | h W/m$^2$-K | St (x10$^3$) |
| 1 | 5.48 | 0.8561 | 3.176 | 982.3 | 66.92 | 80.29 | 1178. | 3.810 |
| 2 | 5.68 | 0.8870 | 3.154 | 975.3 | 66.45 | 68.95 | 1022. | 3.273 |
| 3 | 5.87 | 0.9181 | 3.132 | 968.6 | 65.99 | 65.09 | 955.4 | 3.089 |
| 4 | 6.07 | 0.9491 | 3.111 | 962.2 | 65.55 | 63.09 | 926.0 | 2.994 |
| 5 | 6.67 | 1.0423 | 3.054 | 944.4 | 64.34 | 69.93 | 1026. | 3.319 |
| 6 | 7.16 | 1.1198 | 3.010 | 930.9 | 63.42 | 68.63 | 107.3 | 3.257 |
| 7 | 8.16 | 1.2748 | 2.933 | 907.1 | 61.80 | 59.34 | 871.0 | 2.817 |

## Test No. T09

($P_4$ = 60" Hg gauge, $P_{atm}$ = 29.30 in Hg, $\gamma_4=\gamma_1$ = 1.400, $R_1=R_4$ = 287 J/kg-K)

**Measured**

| | | | |
|---|---|---|---|
| Driver Pressure | $P_4$ = 302.40 kPa | (89.30 in Hg abs) | |
| Driven Pressure | $P_1$ = 99.22 kPa | (29.30 in Hg abs) | |
| Driver/Driven Temp. | $T_1=T_4$ = 292.15 K | (19.0 deg C) | |
| Shock Velocity | $U_s$ = 411.57 m/sec | | = $\Delta x/\Delta t$ ($\Delta t$ = 1.728 msec) |
| Pressure behind shock | $P_2$ = 149.35 kPa | (21.66 psia) | |

**Calculated**

| | | | |
|---|---|---|---|
| Sonic Velocity | $a_1$ = 342.61 m/sec | | $=(\gamma_1 R_1 T_1)^{1/2}$ |
| Shock Mach Number | $M_s$ = 1.201 | | $=U_s/a_1$ |
| Theoretical Shock Mach No. | $M_{th}$ = 1.267 | | based on $P_4/P_1$, $\gamma_1$, $\gamma_4$, $a_1/a_4$ |
| Temperature behind shock | $T_2=T_\infty$ = 329.71 K | (56.56 deg C) | based on $M_s$, $\gamma_1$ |
| Press. behind shock, Theor. | $P_2=P_\infty$ = 150.43 kPa | (21.818 psia) | based on $M_s$, $\gamma_1$ |
| Density behind shock | $\rho_2=\rho_\infty$ = 1.590 kg/m$^3$ | | $=P_2/R_1$-$T_2$ |
| Flow Velocity, behind shock | $U_2=U_\infty$ = 105.18 m/sec | | based on $M_s$, $a_1$, $\gamma_1$ |
| Sonic Velocity behind shock | $a_2=a_\infty$ = 363.97 m/sec | | $=(\gamma_1 R_1 T_2)^{1/2}$ |
| Flow Mach No. behind shock | $M_2=M_\infty$ = 0.2890 | | $=U_2/a_2$ |
| Reference Temperature | $T^*$ = 312.53 K | (39.38 deg C) | $= 0.5(T_w+T_\infty)+0.039M^2_\infty T_\infty$ |

**Flow Properties** (evaluated at $T^*$)

| | | | |
|---|---|---|---|
| Density | $\rho$ = 1.677 kg/m$^3$ | | $=P_2/R_1$-$T^*$ |
| Specific Heat | $C_p$ = 1005.0 J/kg-K | | |
| Absolute Viscosity | $\mu$ = 1.906E-5 Pa-sec | | Sutherland-Law |
| Thermal Conductivity | k = 0.02722 | W/m$^2$-K | Sutherland-Law |
| Prandtl Number | Pr = 0..7039 | | $=\mu C_p/k$ |
| Recovery Factor | $r_c$ = 0.8895 | | $=Pr^{1/3}$ |

| | | | |
|---|---|---|---|
| Adiabatic Wall Temperature | $T_{aw}$ = 334.61 K | (00.0 deg C) | $=T_\infty[1+r_c(\gamma_1-1)M_\infty^2/2]$ |
| Measured Avg Wall Temperature | $T_w$ = 293.21 K | (20.06 deg C) | gauge 4 location |

**Results**

| | | | Theoretical (Tu = 9.5%) | | | Measured (4-5 msec) | | |
|---|---|---|---|---|---|---|---|---|
| Gauge No. | X cm | $Re_x$ (x10$^{-6}$) | $St_{th}$ (x10$^3$) | $h_{th}$ W/m$^2$-K | $q_{th}$ kW/m$^2$ | $q_{avg}$ kW/m$^2$ | h W/m$^2$-K | St (x10$^3$) |
| 1 | 5.48 | 0.5069 | 3.522 | 624.2 | 25.84 | 37.35 | 902.3 | 5.090 |
| 2 | 5.68 | 0.5252 | 3.497 | 619.8 | 25.66 | 30.47 | 736.1 | 4.153 |
| 3 | 5.87 | 0.5436 | 3.473 | 615.5 | 25.48 | 29.14 | 704.0 | 3.972 |
| 4 | 6.07 | 0.5620 | 3.450 | 611.5 | 25.31 | 28.26 | 682.6 | 3.851 |
| 5 | 6.67 | 0.6171 | 3.386 | 600.1 | 24.84 | 27.38 | 661.5 | 3.732 |
| 6 | 7.16 | 0.6630 | 3.337 | 591.6 | 24.49 | 29.84 | 720.8 | 4.064 |
| 7 | 8.16 | 0.7548 | 3.252 | 576.4 | 23.86 | 27.96 | 675.5 | 3.811 |

## Test No. T10

($P_4$ = 80" Hg gauge, $P_{atm}$ = 29.33 in Hg, $\gamma_4=\gamma_1$ = 1.400, $R_1=R_4$ = 287 J/kg-K)

**Measured**

| | | | |
|---|---|---|---|
| Driver Pressure | $P_4$ = 291.85 kPa | (109.29 in Hg abs) | |
| Driven Pressure | $P_1$ = 99.323 kPa | (29.33 in Hg abs) | |
| Driver/Driven Temp. | $T_1=T_4$ = 291.85 K | (18.7 deg C) | |
| Shock Velocity | $U_s$ = 435.78 m/sec | | = $\Delta x/\Delta t$ ($\Delta t$ = 1.632 msec) |
| Pressure behind shock | $P_2$ = 170.55 kPa | (24.74 psia) | |

**Calculated**

| | | | |
|---|---|---|---|
| Sonic Velocity | $a_1$ = 342.44 m/sec | | $=(\gamma_1 R_1 T_1)^{1/2}$ |
| Shock Mach Number | $M_s$ = 1.273 | | $=U_s/a_1$ |
| Theoretical Shock Mach No. | $M_{th}$ = 1.321 | | based on $P_4/P_1$, $\gamma_1$, $\gamma_4$, $a_1/a_4$ |
| Temperature behind shock | $T_2=T_\infty$ = 342.49 K | (69.3 deg C) | based on $M_s$, $\gamma_1$ |
| Press. behind shock, Theor. | $P_2=P_\infty$ = 171.11 kPa | (24.82 psia) | based on $M_s$, $\gamma_1$ |
| Density behind shock | $\rho_2=\rho_\infty$ = 1.741 kg/m$^3$ | | $=P_2/R_1 T_2$ |
| Flow Velocity, behind shock | $U_2=U_\infty$ = 138.93 m/sec | | based on $M_s$, $a_1$, $\gamma_1$ |
| Sonic Velocity behind shock | $a_2=a_\infty$ = 370.96 m/sec | | $=(\gamma_1 R_1 T_2)^{1/2}$ |
| Flow Mach No. behind shock | $M_2=M_\infty$ = 0.3745 | | $=U_2/a_2$ |
| Reference Temperature | $T^*$ = 319.54 K | (46.39 deg C) | $= 0.5(T_w+T_\infty)+0.039M^2_\infty T_\infty$ |

**Flow Properties** (evaluated at $T^*$)

| | | | |
|---|---|---|---|
| Density | $\rho$ = 1.865 kg/m$^3$ | | $=P_2/R_1 T^*$ |
| Specific Heat | $C_p$ = 1005.5 J/kg-K | | |
| Absolute Viscosity | $\mu$ = 1.938E-5 Pa-sec | | Sutherland-Law |
| Thermal Conductivity | k = 0.02775 W/m$^2$-K | | Sutherland-Law |
| Prandtl Number | Pr = 0.7022 | | $=\mu C_p/k$ |
| Recovery Factor | $r_c$ = 0.8888 | | $=Pr^{1/3}$ |

| | | | |
|---|---|---|---|
| Adiabatic Wall Temperature | $T_{aw}$ = 351.02 K | (77.87 deg C) | $=T_\infty[1+r_c(\gamma_1-1)M_\infty^2/2]$ |
| Measured Avg Wall Temperature | $T_w$ = 292.85 K | (19.7 deg C) | gauge 4 location |

**Results**

| | | | Theoretical (Tu = 9.5%) | | | Measured (3.6-4.6 msec) | | |
|---|---|---|---|---|---|---|---|---|
| Gauge No. | X cm | $Re_x$ (x10$^{-6}$) | $St_{th}$ (x10$^3$) | $h_{th}$ W/m$^2$-K | $q_{th}$ kW/m$^2$ | $q_{avg}$ kW/m$^2$ | h W/m$^2$-K | St (x10$^3$) |
| 1 | 5.48 | 0.7324 | 3.274 | 853.3 | 49.64 | 62.48 | 1074. | 4.121 |
| 2 | 5.68 | 0.7589 | 3.251 | 847.3 | 49.29 | 50.16 | 862.2 | 3.309 |
| 3 | 5.87 | 0.7855 | 3.229 | 841.5 | 48.95 | 48.57 | 834.9 | 3.204 |
| 4 | 6.07 | 0.8120 | 3.208 | 835.9 | 48.63 | 48.43 | 832.5 | 3.195 |
| 5 | 6.67 | 0.8917 | 3.148 | 820.4 | 47.73 | 49.47 | 850.4 | 3.263 |
| 6 | 7.16 | 0.9580 | 3.103 | 808.7 | 47.05 | 52.34 | 899.6 | 3.452 |
| 7 | 8.16 | 1.0906 | 3.024 | 788.0 | 45.84 | 45.64 | 784.6 | 3.011 |

## Test No. T11

($P_4$ = 100" Hg gauge, $P_{atm}$ = 29.27 in Hg, $\gamma_4=\gamma_1$ = 1.400, $R_1=R_4$ = 287 J/kg-K)

**Measured**

| | | | |
|---|---|---|---|
| Driver Pressure | $P_4$ = 437.76 kPa | (129.27 in Hg abs) | |
| Driven Pressure | $P_1$ = 99.255 kPa | (29.31 in Hg abs) | |
| Driver/Driven Temp. | $T_1=T_4$ = 292.25 K | (19.1 deg C) | |
| Shock Velocity | $U_s$ = 448.42 m/sec | | = $\Delta x/\Delta t$ ($\Delta t$ = 1.586 msec) |
| Pressure behind shock | $P_2$ = 180.61 kPa | (26.20 psia) | |

**Calculated**

| | | | |
|---|---|---|---|
| Sonic Velocity | $a_1$ = 342.67 m/sec | | $=(\gamma_1 R_1 T_1)^{1/2}$ |
| Shock Mach Number | $M_s$ = 1.309 | | $=U_s/a_1$ |
| Theoretical Shock Mach No. | $M_{th}$ = 1.367 | | based on $P_4/P_1$, $\gamma_1$, $\gamma_4$, $a_1/a_4$ |
| Temperature behind shock | $T_2=T_\infty$ = 349.67 K | (76.52 deg C) | based on $M_s$, $\gamma_1$ |
| Press. behind shock, Theor. | $P_2=P_\infty$ = 181.87 kPa | (26.38 psia) | based on $M_s$, $\gamma_1$ |
| Density behind shock | $\rho_2=\rho_\infty$ = 1.812 kg/m$^3$ | | $=P_2/R_1 T_2$ |
| Flow Velocity, behind shock | $U_2=U_\infty$ = 155.66 m/sec | | based on $M_s$, $a_1$, $\gamma_1$ |
| Sonic Velocity behind shock | $a_2=a_\infty$ = 374.83 m/sec | | $=(\gamma_1 R_1 T_2)^{1/2}$ |
| Flow Mach No. behind shock | $M_2=M_\infty$ = 0.4153 | | $=U_2/a_2$ |
| Reference Temperature | $T^*$ = 323.69 K | (50.54 deg C) | $= 0.5(T_w+T_\infty)+0.039M^2_\infty T_\infty$ |

**Flow Properties** (evaluated at $T^*$)

| | | | |
|---|---|---|---|
| Density | $\rho$ = 1.957 kg/m$^3$ | | $=P_2/R_1 T^*$ |
| Specific Heat | $C_p$ = 1006.0 J/kg-K | | |
| Absolute Viscosity | $\mu$ = 1.957E-5 Pa-sec | | Sutherland-Law |
| Thermal Conductivity | k = 0.02807 W/m$^2$-K | | Sutherland-Law |
| Prandtl Number | Pr = 0.7015 | | $=\mu C_p/k$ |
| Recovery Factor | $r_c$ = 0.8885 | | $=Pr^{1/3}$ |

| | | | |
|---|---|---|---|
| Adiabatic Wall Temperature | $T_{aw}$ = 360.38 K | (60.23 deg C) | $=T_\infty[1+r_c(\gamma_1-1)M_\infty^2/2]$ |
| Measured Avg Wall Temperature | $T_w$ = 293.01 K | (19.86 deg C) | gauge 4 !ocation |

| Results | | | Theoretical (Tu = 9.5%) | | | Measured (4-5 msec) | | |
|---|---|---|---|---|---|---|---|---|
| Gauge No. | X cm | $Re_x$ (x10$^{-6}$) | $St_{th}$ (x10$^3$) | $h_{th}$ W/m$^2$-K | $q_{th}$ kW/m$^2$ | $q_{avg}$ kW/m$^2$ | h W/m$^2$-K | St (x10$^3$) |
| 1 | 5.48 | 0.8527 | 3.178 | 974.0 | 65.62 | 82.20 | 1220. | 3.980 |
| 2 | 5.68 | 0.8835 | 3.155 | 967.2 | 65.16 | 68.78 | 1021. | 3.331 |
| 3 | 5.87 | 0.9145 | 3.134 | 960.5 | 64.71 | 65.90 | 978.2 | 3.191 |
| 4 | 6.07 | 0.9453 | 3.113 | 954.2 | 64.28 | 64.75 | 961.1 | 3.136 |
| 5 | 6.67 | 1.0381 | 3.055 | 936.5 | 63.09 | 68.90 | 1023. | 3.336 |
| 6 | 7.16 | 1.1153 | 3.012 | 923.1 | 62.19 | 68.39 | 1015. | 3.311 |
| 7 | 8.16 | 1.2698 | 2.934 | 899.5 | 60.60 | 61.58 | 914.0 | 2.982 |

## Test No. T12

($P_4$ = 120" Hg gauge, $P_{atm}$ = 29.27 in Hg, $\gamma_4=\gamma_1$ = 1.400, $R_1=R_4$ = 287 J/kg-K)

**Measured**

| | | | |
|---|---|---|---|
| Driver Pressure | $P_4$ = 503.79 kPa | (119.50 in Hg abs) | |
| Driven Pressure | $P_1$ = 99.250 kPa | (29.31 in Hg abs) | |
| Driver/Driven Temp. | $T_1=T_4$ = 292.35 K | (19.2 deg C) | |
| Shock Velocity | $U_s$ = 464.84 m/sec | | = $\Delta x/\Delta t$ ($\Delta t$ = 1.530 msec) |
| Pressure behind shock | $P_2$ = 196.38 kPa | (28.48 psia) | |

**Calculated**

| | | | |
|---|---|---|---|
| Sonic Velocity | $a_1$ = 342.73 m/sec | | $=(\gamma_1 R_1 T_1)^{1/2}$ |
| Shock Mach Number | $M_s$ = 1.356 | | $=U_s/a_1$ |
| Theoretical Shock Mach No. | $M_{th}$ = 1.408 | | based on $P_4/P_1$, $\gamma_1$, $\gamma_4$, $a_1/a_4$ |
| Temperature behind shock | $T_2=T_\infty$ = 358.52 K | (85.37 deg C) | based on $M_s$, $\gamma_1$ |
| Press. behind shock, Theor. | $P_2=P_\infty$ = 196.37 kPa | (28.48 psia) | based on $M_s$, $\gamma_1$ |
| Density behind shock | $\rho_2=\rho_\infty$ = 1.908 kg/m$^3$ | | $=P_2/R_1\text{-}T_2$ |
| Flow Velocity, behind shock | $U_2=U_\infty$ = 176.67 m/sec | | based on $M_s$, $a_1$, $\gamma_1$ |
| Sonic Velocity behind shock | $a_2=a_\infty$ = 379.54 m/sec | | $=(\gamma_1 R_1 T_2)^{1/2}$ |
| Flow Mach No. behind shock | $M_2=M_\infty$ = 0.4655 | | $=U_2/a_2$ |
| Reference Temperature | $T^*$ = 329.02 K | (55.87 deg C) | $=0.5(T_w+T_\infty)+0.039M^2_\infty T_\infty$ |

**Flow Properties** (evaluated at $T^*$)

| | | | |
|---|---|---|---|
| Density | $\rho$ = 2.079 kg/m$^3$ | | $=P_2/R_1\text{-}T^*$ |
| Specific Heat | $C_p$ = 1006.5 J/kg-K | | |
| Absolute Viscosity | $\mu$ = 1.981E-5 Pa-sec | | Sutherland-Law |
| Thermal Conductivity | k = 0.02847 W/m$^2$-K | | Sutherland-Law |
| Prandtl Number | Pr = 0.7004 | | $=\mu C_p/k$ |
| Recovery Factor | $r_c$ = 0.8881 | | $=Pr^{1/3}$ |

| | | | |
|---|---|---|---|
| Adiabatic Wall Temperature | $T_{aw}$ = 372.31 K | (99.16 deg C) | $=T_\infty[1+r_c(\gamma_1-1)M_\infty^2/2]$ |
| Measured Avg Wall Temperature | $T_w$ = 293.45 K | (20.3 deg C) | gauge 4 location |

**Results**

| | | | Theoretical (Tu = 9.5%) | | | Measured (3.5-4.5 msec) | | |
|---|---|---|---|---|---|---|---|---|
| Gauge No. | X cm | $Re_x$ (x10$^{-6}$) | $St_{th}$ (x10$^3$) | $h_{th}$ W/m$^2$-K | $q_{th}$ kW/m$^2$ | $q_{avg}$ kW/m$^2$ | h W/m$^2$-K | St (x10$^3$) |
| 1 | 5.48 | 1.0155 | 3.070 | 1135. | 89.53 | 106.7 | 1353. | 3.660 |
| 2 | 5.68 | 1.0522 | 3.049 | 1127. | 88.90 | 90.41 | 1146. | 3.100 |
| 3 | 5.87 | 1.0891 | 3.028 | 1120. | 88.29 | 87.27 | 1107. | 2.993 |
| 4 | 6.07 | 1.1258 | 3.008 | 1112. | 87.70 | 83.59 | 1060. | 2.866 |
| 5 | 6.67 | 1.2363 | 2.952 | 1092. | 86.08 | 90.30 | 1145. | 3.097 |
| 6 | 7.16 | 1.3283 | 2.910 | 1076. | 84.85 | 93.13 | 1181. | 3.194 |
| 7 | 8.16 | 1.5122 | 2.835 | 1048. | 82.68 | 79.64 | 1010. | 2.731 |

## Test No. V12

($P_4$ = 120" Hg gauge, $P_{atm}$ = 28.87 in Hg, $\gamma_4=\gamma_1$ = 1.400, $R_1=R_4$ = 287 J/kg-K)

| Measured | | | |
|---|---|---|---|
| Driver Pressure | $P_4$ = 503.56 kPa | (148.70 in Hg abs) | |
| Driven Pressure | $P_1$ = 97.765 kPa | (28.87 in Hg abs) | |
| Driver/Driven Temp. | $T_1=T_4$ = 297.75 K | (24.6 deg C) | |
| Shock Velocity | $U_s$ = 470.37 m/sec | | = $\Delta x/\Delta t$ ($\Delta t$ = 1.512 msec) |
| Pressure behind shock | $P_2$ = 195.05 kPa | (28.29 psia) | |

| Calculated | | | |
|---|---|---|---|
| Sonic Velocity | $a_1$ = 345.88 m/sec | | $=(\gamma_1 R_1 T_1)^{1/2}$ |
| Shock Mach Number | $M_s$ = 1.360 | | $=U_s/a_1$ |
| Theoretical Shock Mach No. | $M_{th}$ = 1.411 | | based on $P_4/P_1$, $\gamma_1$, $\gamma_4$, $a_1/a_4$ |
| Temperature behind shock | $T_2=T_\infty$ = 365.88 K | (92.73 deg C) | based on $M_s$, $\gamma_1$ |
| Press. behind shock, Theor. | $P_2=P_\infty$ = 194.66 kPa | (28.23 psia) | based on $M_s$, $\gamma_1$ |
| Density behind shock | $\rho_2=\rho_\infty$ = 1.854 kg/m$^3$ | | $=P_2/R_1 T_2$ |
| Flow Velocity, behind shock | $U_2=U_\infty$ = 180.07 m/sec | | based on $M_s$, $a_1$, $\gamma_1$ |
| Sonic Velocity behind shock | $a_2=a_\infty$ = 383.42 m/sec | | $=(\gamma_1 R_1 T_2)^{1/2}$ |
| Flow Mach No. behind shock | $M_2=M_\infty$ = 0.4696 | | $=U_2/a_2$ |
| Reference Temperature | $T^*$ = 335.97 K | (62.82 deg C) | $= 0.5(T_w+T_\infty)+0.039M^2_\infty T_\infty$ |

| Flow Properties (evaluated at $T^*$) | | | |
|---|---|---|---|
| Density | $\rho$ = 2.019 kg/m$^3$ | | $=P_2/R_1 T^*$ |
| Specific Heat | $C_p$ = 1007.0 J/kg-K | | |
| Absolute Viscosity | $\mu$ = 2.013E-5 Pa-sec | | Sutherland-Law |
| Thermal Conductivity | k = 0.02899 | W/m$^2$-K | Sutherland-Law |
| Prandtl Number | Pr = 0.6990 | | $=\mu C_p/k$ |
| Recovery Factor | $r_c$ = 0.8875 | | $=Pr^{1/3}$ |

| | | | |
|---|---|---|---|
| Adiabatic Wall Temperature | $T_{aw}$ = 380.20 K | (107.05 deg C) | $=T_\infty[1+r_c(\gamma_1-1)M_\infty^2/2]$ |
| Measured Avg Wall Temperature | $T_w$ = 299.75 K | (26.6 deg C) | gauge 4 location |

| Results | | | Theoretical (Tu = 9.5%) | | | Measured (3.5-4.5 msec) | | |
|---|---|---|---|---|---|---|---|---|
| Gauge No. | X cm | $Re_x$ (x10$^{-6}$) | $St_{th}$ (x10$^3$) | $h_{th}$ W/m$^2$-K | $q_{th}$ kW/m$^2$ | $q_{avg}$ kW/m$^2$ | h W/m$^2$-K | St (x10$^3$) |
| 1 | 5.48 | 0.9891 | 3.089 | 1131. | 90.99 | 109.3 | 1359. | 3.712 |
| 2 | 5.68 | 1.0249 | 3.067 | 1123. | 80.34 | 92.92 | 1155. | 3.155 |
| 3 | 5.87 | 1.0608 | 3.046 | 1115. | 89.72 | 88.85 | 1104. | 3.016 |
| 4 | 6.07 | 1.0966 | 3.026 | 1108. | 89.13 | 88.24 | 1097. | 2.996 |
| 5 | 6.67 | 1.2042 | 2.970 | 1087. | 87.48 | 93.79 | 1166. | 3.184 |
| 6 | 7.16 | 1.2938 | 2.927 | 1072. | 86.23 | 99.39 | 1235. | 3.374 |
| 7 | 8.16 | 1.4730 | 2.853 | 1044. | 84.02 | 83.32 | 1035. | 2.829 |

## Test No. X11

($P_4$ = 100" Hg gauge, $P_{atm}$ = 28.88 in Hg, $\gamma_4=\gamma_1$ = 1.400, $R_1=R_4$ = 287 J/kg-K)
holes uncovered

**Measured**

| | | | |
|---|---|---|---|
| Driver Pressure | $P_4$ = 436.40 kPa | (128.87 in Hg abs) | |
| Driven Pressure | $P_1$ = 97.80 kPa | (28.88 in Hg abs) | |
| Driver/Driven Temp. | $T_1=T_4$ = 297.75 K | (24.6 deg C) | |
| Shock Velocity | $U_s$ = 456.48 m/sec | | = $\Delta x/\Delta t$ ($\Delta t$ = 1.558 msec) |
| Pressure behind shock | $P_2$ = kPa | ( psia) | |

**Calculated**

| | | | |
|---|---|---|---|
| Sonic Velocity | $a_1$ = 345.88 m/sec | | $=(\gamma_1 R_1 T_1)^{1/2}$ |
| Shock Mach Number | $M_s$ = 1.320 | | $=U_s/a_1$ |
| Theoretical Shock Mach No. | $M_{th}$ = 1.370 | | based on $P_4/P_1$, $\gamma_1$, $\gamma_4$, $a_1/a_4$ |
| Temperature behind shock | $T_2=T_\infty$ = 358.33 K | (85.18 deg C) | based on $M_s$, $\gamma_1$ |
| Press. behind shock, Theor. | $P_2=P_\infty$ = 182.50 kPa | (26.47 psia) | based on $M_s$, $\gamma_1$ |
| Density behind shock | $\rho_2=\rho_\infty$ = 1.775 kg/m$^3$ | | $=P_2/R_1$-$T_2$ |
| Flow Velocity, behind shock | $U_2=U_\infty$ = 162.12 m/sec | | based on $M_s$, $a_1$, $\gamma_1$ |
| Sonic Velocity behind shock | $a_2=a_\infty$ = 379.44 m/sec | | $=(\gamma_1 R_1 T_2)^{1/2}$ |
| Flow Mach No. behind shock | $M_2=M_\infty$ = 0.4273 | | $=U_2/a_2$ |
| Reference Temperature | $T^*$ = 331.56 K | (58.41 deg C) | $= 0.5(T_w+T_\infty)+0.039M^2_\infty T_\infty$ |

**Flow Properties** (evaluated at $T^*$)

| | | | |
|---|---|---|---|
| Density | $\rho$ = 1.918 kg/m$^3$ | | $=P_2/R_1$-$T^*$ |
| Specific Heat | $C_p$ = 1007.0 J/kg-K | | |
| Absolute Viscosity | $\mu$ = 1.993E-5 Pa-sec | | Sutherland-Law |
| Thermal Conductivity | k = 0.02866 | W/m$^2$-K | Sutherland-Law |
| Prandtl Number | Pr = 0.7002 | | $=\mu C_p/k$ |
| Recovery Factor | $r_c$ = 0.8880 | | $=Pr^{1/3}$ |

| | | | |
|---|---|---|---|
| Adiabatic Wall Temperature | $T_{aw}$ = 369.94 K | (96.79 deg C) | $=T_\infty[1+r_c(\gamma_1-1)M_\infty^2/2]$ |
| Measured Avg Wall Temperature | $T_w$ = 299.70 K | (26.55deg C) | gauge 4 location |

**Results** — Theoretical (Tu = 9.5%) — Measured (3.6-7 msec)

| Gauge No. | X cm | $Re_x$ (x10$^{-6}$) | $St_{th}$ (x10$^3$) | $h_{th}$ W/m$^2$-K | $q_{th}$ kW/m$^2$ | $q_{avg}$ kW/m$^2$ | h W/m$^2$-K | St (x10$^3$) |
|---|---|---|---|---|---|---|---|---|
| 1 | 5.48 | 0.8544 | 2.155 | 674.7 | 47.39 | 94.00 | 1338. | 4.275 |
| 2 | 5.68 | 0.8853 | 2.140 | 669.9 | 47.05 | 101.2 | 1441. | 4.602 |
| 3 | 5.87 | 0.9163 | 2.125 | 665.3 | 46.73 | 90.54 | 1289. | 4.118 |
| 4 | 6.07 | 0.9472 | 2.111 | 660.9 | 46.42 | 78.33 | 1115. | 3.562 |
| 5 | 6.67 | 1.0402 | 2.072 | 648.7 | 45.56 | 88.36 | 1258. | 4.018 |
| 6 | 7.16 | 1.1176 | 2.042 | 639.4 | 44.91 | 82.77 | 1178. | 3.764 |
| 7 | 8.16 | 1.2723 | 1.990 | 623.0 | 43.76 | 72.54 | 1033. | 3.299 |

## Test No. T13

($P_4$ = 100" Hg gauge, $P_{atm}$ = 29.47 in Hg, $\gamma_4$= 1.400, $\gamma_1$ = 1.496, $R_1$= 492.5, $R_4$ = 287 J/kg-K)
helium added

**Measured**

| | | | |
|---|---|---|---|
| Driver Pressure | $P_4$ = 437.59 kPa | (129.22 in Hg abs) | |
| Driven Pressure | $P_1$ = 99.079 kPa | (29.258 in Hg abs) | |
| Driver/Driven Temp. | $T_1$=$T_4$ = 295.35 K | (22.2 deg C) | |
| Shock Velocity | $U_s$ = 587.77 m/sec | | = $\Delta x/\Delta t$ ($\Delta t$ = 1.210 msec) |
| Partial Pressure of Helium | $P_{He}$ = 47.960 kPa | (6.956 psi) | |

**Calculated**

| | | | |
|---|---|---|---|
| Sonic Velocity | $a_1$ = 466.46 m/sec | | $=(\gamma_1 R_1 T_1)^{1/2}$ |
| Shock Mach Number | $M_s$ = 1.260 | | $=U_s/a_1$ |
| Theoretical Shock Mach No. | $M_{th}$ = 1.306 | | based on $P_4/P_1$, $\gamma_1$, $\gamma_4$, $a_1/a_4$ |
| Temperature behind shock | $T_2$=$T_\infty$ = 354.10 K | (80.95 deg C) | based on $M_s$, $\gamma_1$ |
| Press. behind shock, Theor. | $P_2$=$P_\infty$ = 168.89 kPa | (24.49 psia) | based on $M_s$, $\gamma_1$ |
| Density behind shock | $\rho_2$=$\rho_\infty$ = 0.9685 kg/m$^3$ | | $=P_2/R_1$-$T_2$ |
| Flow Velocity, behind shock | $U_2$=$U_\infty$ = 174.37 m/sec | | based on $M_s$, $a_1$, $\gamma_1$ |
| Sonic Velocity behind shock | $a_2$=$a_\infty$ = 510.75 m/sec | | $=(\gamma_1 R_1 T_2)^{1/2}$ |
| Flow Mach No. behind shock | $M_2$=$M_\infty$ = 0.3414 | | $=U_2/a_2$ |
| Prandtl Number | Pr = 0.6807 | | $4\gamma_1/(7.08\gamma_1-1.8)$ |
| Recovery Factor | $r_c$ = 0.8796 | | $=Pr^{1/3}$ |
| Reference Temperature | $T^*$ = 335.11 K | (61.96 deg C) | $= 0.5(T_w+T_\infty)+.22r_c(\gamma_1-1)M^2_\infty T_\infty/2$ |

**Flow Properties** (evaluated at $T^*$)

| | | | |
|---|---|---|---|
| Density | $\rho$ = 1.023 kg/m$^3$ | | $=P_2/R_1$-$T^*$ |
| Specific Heat | $C_p$ = 1485.7 J/kg-K | | |
| Absolute Viscosity | $\mu$ = 2.156E-5 Pa-sec | | Sutherland and Curve Fit (K and C) |
| Thermal Conductivity | k = 0.02703 | W/m$^2$-K | Sutherland and Curve Fit (K and C) |

| | | | |
|---|---|---|---|
| Adiabatic Wall Temperature | $T_{aw}$ = 363.11 K | (89.96 deg C) | $=T_\infty[1+r_c(\gamma_1-1)M_\infty^2/2]$ |
| Measured Avg Wall Temperature | $T_w$ = 298.12 K | (24.97 deg C) | gauge 1, 4, 6, 7 locations |

| Results | | | Theoretical (Tu = 9.5%) | | | Measured (3-3.5 msec) | | |
|---|---|---|---|---|---|---|---|---|
| Gauge No. | X cm | $Re_x$ (x10$^{-6}$) | $St_{th}$ (x10$^3$) | $h_{th}$ W/m$^2$-K | $q_{th}$ kW/m$^2$ | $q_{avg}$ kW/m$^2$ | h W/m$^2$-K | St (x10$^3$) |
| 1 | 5.48 | 0.4533 | 3.649 | 967.5 | 62.88 | 90.93 | 1399. | 5.278 |
| 2 | 5.68 | 0.4697 | 3.624 | 960.7 | 62.43 | 73.78 | 1135. | 4.282 |
| 3 | 5.87 | 0.4862 | 3.599 | 954.1 | 62.00 | 69.90 | 1076. | 4.057 |
| 4 | 6.07 | 0.5025 | 3.575 | 947.8 | 61.59 | 65.16 | 1003. | 3.782 |
| 5 | 6.67 | 0.5519 | 3.509 | 930.2 | 60.45 | 70.55 | 1086. | 4.095 |
| 6 | 7.16 | 0.5929 | 3.459 | 916.9 | 59.59 | 71.58 | 1102. | 4.155 |
| 7 | 8.16 | 0.6750 | 3.370 | 893.5 | 58.06 | 62.22 | 957.4 | 3.611 |

Test No. P09

($P_4$ = 60" Hg gauge, $P_{atm}$ = 29.27 in Hg, $\gamma_4$= 1.400, $\gamma_1$ = 1.512, $R_1$= 544.24, $R_4$ = 287 J/kg-K)
helium added

Measured

| | | | |
|---|---|---|---|
| Driver Pressure | $P_4$ = 301.96 kPa | (89.17 in Hg abs) | |
| Driven Pressure | $P_1$ = 98.95 kPa | (29.22 in Hg abs) | |
| Driver/Driven Temp. | $T_1$=$T_4$ = 292.45 K | (19.3 deg C) | |
| Shock Velocity | $U_s$ = 567.15 m/sec | | = $\Delta x/\Delta t$ ($\Delta t$ = 1.254 msec) |
| Partial Pressure of Helium | $P_{He}$ = 54.26 kPa | (7.87 psi) | |

Calculated

| | | | |
|---|---|---|---|
| Sonic Velocity | $a_1$ = 490.60 m/sec | | $=(\gamma_1 R_1 T_1)^{1/2}$ |
| Shock Mach Number | $M_s$ = 1.156 | | $=U_s/a_1$ |
| Theoretical Shock Mach No. | $M_{th}$ = 1.216 | | based on $P_4/P_1$, $\gamma_1$, $\gamma_4$, $a_1/a_4$ |
| Temperature behind shock | $T_2$=$T_\infty$ = 328.54 K | (55.39 deg C) | based on $M_s$, $\gamma_1$ |
| Press. behind shock, Theor. | $P_2$=$P_\infty$ = 139.02 kPa | (20.16 psia) | based on $M_s$, $\gamma_1$ |
| Density behind shock | $\rho_2$=$\rho_\infty$ = 0.7775 kg/m$^3$ | | $=P_2/R_1$-$T_2$ |
| Flow Velocity, behind shock | $U_2$=$U_\infty$ = 113.64 m/sec | | based on $M_s$, $a_1$, $\gamma_1$ |
| Sonic Velocity behind shock | $a_2$=$a_\infty$ = 519.99 m/sec | | $=(\gamma_1 R_1 T_2)^{1/2}$ |
| Flow Mach No. behind shock | $M_2$=$M_\infty$ = 0.2185 | | $=U_2/a_2$ |
| Prandtl Number | Pr = 0.6792 | | $4\gamma_1/(7.08\gamma_1-1.8)$ |
| Recovery Factor | $r_c$ = 0.8790 | | $=Pr^{1/3}$ |
| Reference Temperature | $T^*$ = 314.48 K | (40.88 deg C) | $= 0.5(T_w+T_\infty)+.22r_c(\gamma_1-1)M^2_\infty T_\infty/2$ |

Flow Properties (evaluated at $T^*$)

| | | | |
|---|---|---|---|
| Density | $\rho$ = 0.8122 kg/m$^3$ | | $=P_2/R_1$-$T^*$ |
| Specific Heat | $C_p$ = 1606.8 J/kg-K | | |
| Absolute Viscosity | $\mu$ = 2.077E-5 Pa-sec | Sutherland and Curve Fit (K and C) | |
| Thermal Conductivity | k = 0.02515 W/m$^2$-K | Sutherland and Curve Fit (K and C) | |

| | | | |
|---|---|---|---|
| Adiabatic Wall Temperature | $T_{aw}$ = 332.07 K | (58.92 deg C) | $=T_\infty[1+r_c(\gamma_1-1)M_\infty^2/2]$ |
| Measured Avg Wall Temperature | $T_w$ = 293.35 K | (20.20 deg C) | gauge 1, 4, 6, 7 locations |

Results — Theoretical (Tu = 9.5%) — Measured (3-4 msec)

| Gauge No. | X cm | $Re_x$ (x10$^{-6}$) | $St_{th}$ (x10$^3$) | $h_{th}$ W/m$^2$-K | $q_{th}$ kW/m$^2$ | $q_{avg}$ kW/m$^2$ | h W/m$^2$-K | St (x10$^3$) |
|---|---|---|---|---|---|---|---|---|
| 1 | 5.48 | 0.2433 | 4.137 | 613.5 | 23.76 | 43.68 | 1128. | 7.606 |
| 2 | 5.68 | 0.2521 | 4.107 | 609.1 | 23.59 | 35.63 | 920.1 | 6.204 |
| 3 | 5.87 | 0.2610 | 4.079 | 604.9 | 23.43 | 31.35 | 809.6 | 5.459 |
| 4 | 6.07 | 0.2698 | 4.052 | 601.0 | 23.27 | 31.70 | 818.6 | 5.520 |
| 5 | 6.67 | 0.2963 | 3.977 | 589.8 | 22.84 | 32.05 | 827.7 | 5.581 |
| 6 | 7.16 | 0.3183 | 3.920 | 581.4 | 22.51 | 31.85 | 822.5 | 5.546 |
| 7 | 8.16 | 0.3624 | 3.820 | 566.5 | 21.94 | 28.68 | 740.7 | 4.944 |

$q_o$ (heat flux reference, no film cooling) determination for film cooling comparison

For $P_4$ = 80 in Hg runs (air only) take the average of the average heat flux for tests T02 and T10 at the later test time (6.3 to 7.2 msec).

For $P_4$ = 100 in Hg run (air/He) only Test T13 is used, at the later test time.

| Gauge No. | Test T02, $q_{avg}$ $kW/m^2$ | Test T10, $q_{avg}$ | Test T13, $q_{avg}$ (5.4 - 5.7 msec) | $q_o$ (air) | x/d |
|---|---|---|---|---|---|
| 1 | 63.55 | 64.17 | 91.9 | 63.86 | 3.9 |
| 2 | 55.93 | 53.73 | 78.3 | 54.83 | 5.9 |
| 3 | 52.62 | 51.48 | 77.9 | 52.05 | 7.8 |
| 4 | 48.19 | 52.99 | 71.5 | 50.59 | 9.8 |
| 5 | 57.14 | 58.87 | 79.7 | 58.01 | 15.6 |
| 6 | 52.91 | 55.74 | 77.6 | 54.33 | 20.5 |
| 7 | 48.05 | 48.39 | 63.8 | 48.22 | 30.3 |

## Film Cooling Test (T14)

($P_4$ = 80" Hg gauge, $P_{atm}$ = 28.92 in Hg, $\gamma_4=\gamma_1$ = 1.400, $R_1=R_4$ = 287 J/kg-K)

Pressure Regulator Setting 13.0 psig

**Measured**

| | | | |
|---|---|---|---|
| Driver Pressure | $P_4$ = 367.05 kPa | (108.39 in Hg abs) | |
| Driven Pressure | $P_1$ = 97.934 kPa | (28.92 in Hg abs) | |
| Driver/Driven Temp. | $T_1=T_4$ = 297.05 K | (23.9 deg C) | |
| Shock Velocity | $U_s$ = 439.01 m/sec | | = $\Delta x/\Delta t$ ($\Delta t$ =1.620 msec) |
| Pressure behind shock | $P_2$ = 167.92 kPa | (24.36 psia) | |

**Calculated**

| | | |
|---|---|---|
| Sonic Velocity | $a_1$ = 345.48 m/sec | $=(\gamma_1 R_1 T_1)^{1/2}$ |
| Shock Mach Number | $M_s$ = 1.271 | $=U_s/a_1$ |
| Theoretical Shock Mach No. | $M_{th}$ = 1.322 | based on $P_4/P_1$, $\gamma_1$, $\gamma_4$, $a_1/a_4$ |
| Temperature behind shock | $T_2=T_\infty$ = 348.24 K | based on $M_s$, $\gamma_1$ |
| Press. behind shock, Theor. | $P_2=P_\infty$ = 168.16 kPa (24.39 psia) | based on $M_s$, $\gamma_1$ |
| Density behind shock | $\rho_2=\rho_\infty$ = 1.6823 kg/m$^3$ | $=P_2/R_1T_2$ |
| Flow Velocity, behind shock | $U_2=U_\infty$ = 139.28 m/sec | based on $M_s$, $a_1$, $\gamma_1$ |
| Sonic Velocity behind shock | $a_2=a_\infty$ = 374.06 m/sec | $=(\gamma_1 R_1 T_2)^{1/2}$ |
| Flow Mach No. behind shock | $M_2=M_\infty$ = 0.3723 | $=U_2/a_2$ |

**Results**

| $P_c$ psia | $T_c$ K | $\rho_c$ kg/m$^3$ | $U_c$ m/sec | D.R. $\rho_c/\rho_\infty$ | V.R. $U_c/U_\infty$ | $M_b$ DR*VR |
|---|---|---|---|---|---|---|
| 24.69 | 296.02 | 1.979 | 45.578 | 1.176 | 0.327 | 0.385 |

| | Gauge Location | | | | | | |
|---|---|---|---|---|---|---|---|
| | 1 | 2 | 3 | 4 | 5 | 6 | 7 |
| Measured $q_{avg}$ kW/m$^2$ | 64.01 | 68.58 | 62.08 | 55.48 | 65.41 | 59.11 | 52.55 |
| $q/q_o$ | 1.002 | 1.251 | 1.193 | 1.097 | 1.128 | 1.088 | 1.090 |
| $x/d\ (V.R.)^{-4/5}$ | 17.29 | 26.16 | 34.58 | 43.45 | 69.16 | 90.89 | 134.33 |

## Film Cooling Test (T15)

($P_4$ = 80" Hg gauge, $P_{atm}$ = 28.93 in Hg, $\gamma_4=\gamma_1$ = 1.400, $R_1=R_4$ = 287 J/kg-K)

Pressure Regulator Setting 16.0 psig

Measured

| | | | |
|---|---|---|---|
| Driver Pressure | $P_4$ = 367.42 kPa | (108.50 in Hg abs) | |
| Driven Pressure | $P_1$ = 97.968 kPa | (28.93 in Hg abs) | |
| Driver/Driven Temp. | $T_1=T_4$ = 927.05 K | (23.9 deg C) | |
| Shock Velocity | $U_s$ = 439.01 m/sec | | = $\Delta x/\Delta t$ ($\Delta t$ = 1.620 msec) |
| Pressure behind shock | $P_2$ = 168.23 kPa | (24.399 psia) | |

Calculated

| | | |
|---|---|---|
| Sonic Velocity | $a_1$ = 345.48 m/sec | $=(\gamma_1 R_1 T_1)^{1/2}$ |
| Shock Mach Number | $M_s$ = 1.271 | $=U_s/a_1$ |
| Theoretical Shock Mach No. | $M_{th}$ = 1.323 | based on $P_4/P_1$, $\gamma_1$, $\gamma_4$, $a_1/a_4$ |
| Temperature behind shock | $T_2=T_\infty$ = 348.24 K | based on $M_s$, $\gamma_1$ |
| Press. behind shock, Theor. | $P_2=P_\infty$ = 168.22 kPa | based on $M_s$, $\gamma_1$ |
| Density behind shock | $\rho_2=\rho_\infty$ = 1.6829 kg/m$^3$ | $=P_2/R_1-T_2$ |
| Flow Velocity, behind shock | $U_2=U_\infty$ = 139.28 m/sec | based on $M_s$, $a_1$, $\gamma_1$ |
| Sonic Velocity behind shock | $a_2=a_\infty$ = 374.06 m/sec | $=(\gamma_1 R_1 T_2)^{1/2}$ |
| Flow Mach No. behind shock | $M_2=M_\infty$ = 0.3723 | $=U_2/a_2$ |

Results

| $P_{0c}$ psia | $T_c$ K | $\rho_c$ kg/m$^3$ | $U_c$ m/sec | D.R. $\rho_c/\rho_\infty$ | V.R. $U_c/U_\infty$ | $M_b$ DR*VR |
|---|---|---|---|---|---|---|
| 25.47 | 293.42 | 1.997 | 85.44 | 1.187 | 0.6135 | 0.7281 |

| | Gauge Location | | | | | | |
|---|---|---|---|---|---|---|---|
| | 1 | 2 | 3 | 4 | 5 | 6 | 7 |
| Measured $q_{avg}$ kW/m$^2$ | 57.59 | 61.58 | 57.68 | 50.81 | 61.66 | 55.63 | 50.43 |
| $q/q_o$ | 0.902 | 1.123 | 1.108 | 1.004 | 1.063 | 1.024 | 1.046 |
| $x/d\ (V.R.)^{-4/3}$ | 7.481 | 11.318 | 14.963 | 18.799 | 29.925 | 39.325 | 58.124 |

## Film Cooling Test (T16)

($P_4$ = 80" Hg gauge, $P_{atm}$ = 28.92 in Hg, $\gamma_4=\gamma_1$ = 1.400, $R_1=R_4$ = 287 J/kg-K)

Pressure Regulator Setting 20.0 psig

**Measured**

| | | | |
|---|---|---|---|
| Driver Pressure | $P_4$ = 367.39 kPa | (103.49 in Hg abs) | |
| Driven Pressure | $P_1$ = 97.93 kPa | (28.92 in Hg abs) | |
| Driver/Driven Temp. | $T_1=T_4$ = 297.05 K | (23.9 deg C) | |
| Shock Velocity | $U_s$ = 437.93 m/sec | | = $\Delta x/\Delta t$ ($\Delta t$ = 1.624 msec) |
| Pressure behind shock | $P_2$ = 167.20 kPa | (24.25 psia) | |

**Calculated**

| | | | |
|---|---|---|---|
| Sonic Velocity | $a_1$ = 345.48 m/sec | | $=(\gamma_1 R_1 T_1)^{1/2}$ |
| Shock Mach Number | $M_s$ = 1.268 | | $=U_s/a_1$ |
| Theoretical Shock Mach No. | $M_{th}$ = 1.323 | | based on $P_4/P_1$, $\gamma_1$, $\gamma_4$, $a_1/a_4$ |
| Temperature behind shock | $T_2=T_\infty$ = 347.66 K | (74.53 deg C) | based on $M_s$, $\gamma_1$ |
| Press. behind shock, Theor. | $P_2=P_\infty$ = 167.26 kPa | (24.253 psia) | based on $M_s$, $\gamma_1$ |
| Density behind shock | $\rho_2=\rho_\infty$ = 1.6761 kg/m$^3$ | | $=P_2/R_1$-$T_2$ |
| Flow Velocity, behind shock | $U_2=U_\infty$ = 137.83 m/sec | | based on $M_s$, $a_1$, $\gamma_1$ |
| Sonic Velocity behind shock | $a_2=a_\infty$ = 373.75 m/sec | | $=(\gamma_1 R_1 T_2)^{1/2}$ |
| Flow Mach No. behind shock | $M_2=M_\infty$ = 0.3688 | | $=U_2/a_2$ |

**Results**

| $P_{0c}$ psia | $T_c$ K | $\rho_c$ kg/m$^3$ | $U_c$ m/sec | D.R. $\rho_c/\rho_\infty$ | V.R. $U_c/U_\infty$ | $M_b$ DR*VR |
|---|---|---|---|---|---|---|
| 26.46 | 289.76 | 2.011 | 121.04 | 1.200 | 0.8782 | 1.054 |

| | Gauge Location | | | | | | |
|---|---|---|---|---|---|---|---|
| | 1 | 2 | 3 | 4 | 5 | 6 | 7 |
| Measured $q_{avg}$ kW/m$^2$ | 44.82 | 46.35 | 45.38 | 44.27 | 53.92 | 52.12 | 41.76 |
| $q/q_o$ | 0.702 | 0.845 | 0.872 | 0.875 | 0.930 | 0.959 | 0.866 |
| $x/d\ (V.R.)^{-4/3}$ | 4.637 | 7.016 | 9.275 | 11.653 | 18.55 | 24.376 | 36.029 |

## Film Cooling Test (T17)

($P_4$ = 80" Hg gauge, $P_{atm}$ = 28.91 in Hg, $\gamma_4=\gamma_1$ = 1.400, $R_1=R_4$ = 287 J/kg-K)

Pressure Regulator Setting 30.0 psig

Measured

| | | |
|---|---|---|
| Driver Pressure | $P_4$ = 367.355 kPa | (0108.48 in Hg abs) |
| Driven Pressure | $P_1$ = 97.90 kPa | (28.91 in Hg abs) |
| Driver/Driven Temp. | $T_1=T_4$ = 297.05 K | (23.9 deg C) |
| Shock Velocity | $U_s$ = 437.39 m/sec | = $\Delta x/\Delta t$ ($\Delta t$ = 1.626 msec) |
| Pressure behind shock | $P_2$ = 167.40 kPa | (24.28 psia) |

Calculated

| | | |
|---|---|---|
| Sonic Velocity | $a_1$ = 345.48 m/sec | $=(\gamma_1 R_1 T_1)^{1/2}$ |
| Shock Mach Number | $M_s$ = 1.266 | $=U_s/a_1$ |
| Theoretical Shock Mach No. | $M_{th}$ = 1.323 | based on $P_4/P_1$, $\gamma_1$, $\gamma_4$, $a_1/a_4$ |
| Temperature behind shock | $T_2=T_\infty$ = 347.36 K | based on $M_s$, $\gamma_1$ |
| Press. behind shock, Theor. | $P_2=P_\infty$ = 166.74 kPa (00.000 psia) | based on $M_s$, $\gamma_1$ |
| Density behind shock | $\rho_2=\rho_\infty$ = 1.6723 kg/m$^3$ | $=P_2/R_1$-$T_2$ |
| Flow Velocity, behind shock | $U_2=U_\infty$ = 137.08 m/sec | based on $M_s$, $a_1$, $\gamma_1$ |
| Sonic Velocity behind shock | $a_2=a_\infty$ = 373.59 m/sec | $=(\gamma_1 R_1 T_2)^{1/2}$ |
| Flow Mach No. behind shock | $M_2=M_\infty$ = 0.3669 | $=U_2/a_2$ |

Results

| $P_{0c}$ psia | $T_c$ K | $\rho_c$ kg/m$^3$ | $U_c$ m/sec | D.R. $\rho_c/\rho_\infty$ | V.R. $U_c/U_\infty$ | $M_b$ DR*VR |
|---|---|---|---|---|---|---|
| 28.14 | 284.47 | 2.042 | 159.00 | 1.221 | 1.160 | 1.416 |

| | Gauge Location | | | | | | |
|---|---|---|---|---|---|---|---|
| | 1 | 2 | 3 | 4 | 5 | 6 | 7 |
| Measured $q_{avg}$ kW/m$^2$ | 51.37 | 51.44 | 47.84 | 46.50 | 55.46 | 53.26 | 44.71 |
| $q/q_o$ | 0.804 | 0.938 | 0.919 | 0.919 | 0.956 | 0.980 | 0.927 |
| $x/d\ (V.R.)^{-4/3}$ | 3.200 | 4.4841 | 6.400 | 8.042 | 12.80 | 16.82 | 24.86 |

## Film Cooling Test (T18)

($P_4$ = 80" Hg gauge, $P_{atm}$ = 28.88 in Hg, $\gamma_4=\gamma_1$ = 1.400, $R_1=R_4$ = 287 J/kg-K)

Pressure Regulator Setting 40.0 psig

Measured

| | | | |
|---|---|---|---|
| Driver Pressure | $P_4$ = 367.48 kPa | (108.45 in Hg abs) | |
| Driven Pressure | $P_1$ = 97,788 kPa | (28.88 in Hg abs) | |
| Driver/Driven Temp. | $T_1=T_4$ = 297.05 K | (23.9 deg C) | |
| Shock Velocity | $U_s$ = 437.93 m/sec | | = $\Delta x/\Delta t$ ($\Delta t$ = 1.624 msec) |
| Pressure behind shock | $P_2$ = 167.08 kPa | (24.23 psia) | |

Calculated

| | | | |
|---|---|---|---|
| Sonic Velocity | $a_1$ = 345.48 m/sec | | $=(\gamma_1 R_1 T_1)^{1/2}$ |
| Shock Mach Number | $M_s$ = 1.268 | | $=U_s/a_1$ |
| Theoretical Shock Mach No. | $M_{th}$ = 1.323 | | based on $P_4/P_1$, $\gamma_1$, $\gamma_4$, $a_1/a_4$ |
| Temperature behind shock | $T_2=T_\infty$ = 347.66 K | (74.51deg C) | based on $M_s$, $\gamma_1$ |
| Press. behind shock, Theor. | $P_2=P_\infty$ = 167.03 kPa | (24.226 psia) | based on $M_s$, $\gamma_1$ |
| Density behind shock | $\rho_2=\rho_\infty$ = 1.674 kg/m$^3$ | | $=P_2/R_1T_2$ |
| Flow Velocity, behind shock | $U_2=U_\infty$ = 137.83 m/sec | | based on $M_s$, $a_1$, $\gamma_1$ |
| Sonic Velocity behind shock | $a_2=a_\infty$ = 373.75 m/sec | | $=(\gamma_1 R_1 T_2)^{1/2}$ |
| Flow Mach No. behind shock | $M_2=M_\infty$ = 0.3688 | | $=U_2/a_2$ |

Results

| $P_{0c}$ psia | $T_c$ K | $\rho_c$ kg/m$^3$ | $U_c$ m/sec | D.R. $\rho_c/\rho_\infty$ | V.R. $U_c/U_\infty$ | $M_b$ DR*VR |
|---|---|---|---|---|---|---|
| 29.72 | 280.20 | 2.077 | 184.03 | 1.241 | 1.335 | 1.657 |

| | Gauge Location | | | | | | |
|---|---|---|---|---|---|---|---|
| | 1 | 2 | 3 | 4 | 5 | 6 | 7 |
| Measured $q_{avg}$ kW/m$^2$ | 54.03 | 59.23 | 52.09 | 45.97 | 51.03 | 52.73 | 41.67 |
| $q/q_o$ | 0.846 | 1.080 | 1.001 | 0.909 | 0.880 | 0.971 | 0.864 |
| $x/d\ (V.R.)^{-4/3}$ | 2.653 | 4.013 | 5.305 | 6.666 | 10.610 | 13.943 | 20.609 |

## Film Cooling Test (T19)

($P_4$ = 80" Hg gauge, $P_{atm}$ = 28.88 in Hg, $\gamma_4=\gamma_1$ = 1.400, $R_1=R_4$ = 287 J/kg-K)

Pressure Regulator Setting 50.0 psig

Measured

| | | | |
|---|---|---|---|
| Driver Pressure | $P_4$ = 367.25 kPa | (108.45 in Hg abs) | |
| Driven Pressure | $P_1$ = 97.799 kPa | (28.88 in Hg abs) | |
| Driver/Driven Temp. | $T_1=T_4$ = 297.05 K | (23.9 deg C) | |
| Shock Velocity | $U_s$ = 437.93 m/sec | | = $\Delta x/\Delta t$ ($\Delta t$ =1.624 msec) |
| Pressure behind shock | $P_2$ = 165.79 kPa | (24.05 psia) | |

Calculated

| | | | |
|---|---|---|---|
| Sonic Velocity | $a_1$ = 345.48 m/sec | | $=(\gamma_1 R_1 T_1)^{1/2}$ |
| Shock Mach Number | $M_s$ = 1.268 | | $=U_s/a_1$ |
| Theoretical Shock Mach No. | $M_{th}$ = 1.323 | | based on $P_4/P_1$, $\gamma_1$, $\gamma_4$, $a_1/a_4$ |
| Temperature behind shock | $T_2=T_\infty$ = 347.66 K | (74.51deg C) | based on $M_s$, $\gamma_1$ |
| Press. behind shock, Theor. | $P_2=P_\infty$ = 167.03 kPa | (24.226 psia) | based on $M_s$, $\gamma_1$ |
| Density behind shock | $\rho_2=\rho_\infty$ = 1.674 kg/m$^3$ | | $=P_2/R_1 T_2$ |
| Flow Velocity, behind shock | $U_2=U_\infty$ = 137.83 m/sec | | based on $M_s$, $a_1$, $\gamma_1$ |
| Sonic Velocity behind shock | $a_2=a_\infty$ = 373.75 m/sec | | $=(\gamma_1 R_1 T_2)^{1/2}$ |
| Flow Mach No. behind shock | $M_2=M_\infty$ = 0.3688 | | $=U_2/a_2$ |

Results

| $P_{0c}$ psia | $T_c$ K | $\rho_c$ kg/m$^3$ | $U_c$ m/sec | D.R. $\rho_c/\rho_\infty$ | V.R. $U_c/U_\infty$ | $M_b$ DR*VR |
|---|---|---|---|---|---|---|
| 32.79 | 272.57 | 2.136 | 222.34 | 1.276 | 1.613 | 2.058 |

| | Gauge Location | | | | | | |
|---|---|---|---|---|---|---|---|
| | 1 | 2 | 3 | 4 | 5 | 6* | 7 |
| Measured $q_{avg}$ kW/m$^2$ | 64.77 | 68.62 | 60.30 | 46.86 | 48.95 | 49.55 | 39.82 |
| $q/q_o$ | 1.014 | 1.251 | 1.159 | 0.926 | 0.844 | 0.912 | 0.826 |
| x/d (V.R.)$^{-4/3}$ | 2.061 | 3.119 | 4/123 | 5.180 | 8.246 | 10.836 | 16.016 |

## Film Cooling Test (T20)

($P_4$ = 81" Hg gauge, $P_{atm}$ = 29.30 in Hg, $\gamma_4=\gamma_1$ = 1.400, $R_1=R_4$ = 287 J/kg-K)

Pressure Regulator Setting 60.0 psig

**Measured**

| | | |
|---|---|---|
| Driver Pressure | $P_4$ = 372.03 kPa | (109.86 in Hg abs) |
| Driven Pressure | $P_1$ = 99.221 kPa | (29.30 in Hg abs) |
| Driver/Driven Temp. | $T_1=T_4$ = 294.25 K | (21.1 deg C) |
| Shock Velocity | $U_s$ = 435.78 m/sec | = $\Delta x/\Delta t$ ($\Delta t$ = 1.632 msec) |
| Pressure behind shock | $P_2$ = kPa | ( psia) |

**Calculated**

| | | |
|---|---|---|
| Sonic Velocity | $a_1$ = 343.85 m/sec | $=(\gamma_1 R_1 T_1)^{1/2}$ |
| Shock Mach Number | $M_s$ = 1.267 | $=U_s/a_1$ |
| Theoretical Shock Mach No. | $M_{th}$ = 1.322 | based on $P_4/P_1$, $\gamma_1$, $\gamma_4$, $a_1/a_4$ |
| Temperature behind shock | $T_2=T_\infty$ = 344.34 K | based on $M_s$, $\gamma_1$ |
| Press. behind shock, Theor. | $P_2=P_\infty$ = 169.40 kPa | based on $M_s$, $\gamma_1$ |
| Density behind shock | $\rho_2=\rho_\infty$ = 1.7139 kg/m$^3$ | $=P_2/R_1 T_2$ |
| Flow Velocity, behind shock | $U_2=U_\infty$ = 137.09 m/sec | based on $M_s$, $a_1$, $\gamma_1$ |
| Sonic Velocity behind shock | $a_2=a_\infty$ = 371.96 m/sec | $=(\gamma_1 R_1 T_2)^{1/2}$ |
| Flow Mach No. behind shock | $M_2=M_\infty$ = 0.3685 | $=U_2/a_2$ |

**Results**

| $P_{0c}$ psia | $T_c$ K | $\rho_c$ kg/m$^3$ | $U_c$ m/sec | D.R. $\rho_c/\rho_\infty$ | V.R. $U_c/U_\infty$ | $M_b$ DR*VR |
|---|---|---|---|---|---|---|
| 36.05 | 263.06 | 2.238 | 247.69 | 1.306 | 1.807 | 2.359 |

| | Gauge Location 1 | 2 | 3 | 4 | 5 | 6 | 7 |
|---|---|---|---|---|---|---|---|
| Measured $q_{avg}$ kW/m$^2$ | 71.54 | 68.18 | 59.52 | 53.62 | 56.91 | 57.22 | 41.85 |
| $q/q_o$ | 1.120 | 1.243 | 1.144 | 1.060 | 0.981 | 1.053 | 0.868 |
| $x/d\ (V.R.)^{-4/3}$ | 1.772 | 2.681 | 3.544 | 4.453 | 7.088 | 9.314 | 13.767 |

## Film Cooling Test (H01)

($P_4$ = 100" Hg gauge, $P_{atm}$ = 28.83 in Hg, $\gamma_4$= 1.400, $\gamma_1$ = 1.498, $R_1$= 499.04, $R_4$ = 287 J/kg-K)
Helium added

Pressure Regulator Setting 13.0 psig

Measured

| | | |
|---|---|---|
| Driver Pressure | $P_4$ = 434.41 kPa | (128.28 in Hg abs) |
| Driven Pressure | $P_1$ = 97.63 kPa | (28.83 in Hg abs) |
| Driver/Driven Temp. | $T_1=T_4$ = 296.55 K | (23.4 deg C) |
| Shock Velocity | $U_s$ = 593.66 m/sec | = $\Delta x/\Delta t$ ($\Delta t$ = 1.198 msec) |
| Pressure behind shock | $P_2$ = 166.80 kPa | (24.192 psia) |
| Partial Pressure of Helium | $P_{He}$ = 6.98 psi | |

Calculated

| | | |
|---|---|---|
| Sonic Velocity | $a_1$ = 470.846 m/sec | $=(\gamma_1 R_1 T_1)^{1/2}$ |
| Shock Mach Number | $M_s$ = 1.2608 | $=U_s/a_1$ |
| Theoretical Shock Mach No. | $M_{th}$ = 1.306 | based on $P_4/P_1$, $\gamma_1$, $\gamma_4$, $a_1/a_4$ |
| Temperature behind shock | $T_2=T_\infty$ = 355.92 K | based on $M_s$, $\gamma_1$ |
| Press. behind shock, Theor. | $P_2=P_\infty$ = 166.67 kPa (24.174 psia) | based on $M_s$, $\gamma_1$ |
| Density behind shock | $\rho_2=\rho_\infty$ = 0.9384 kg/m$^3$ | $=P_2/R_1$-$T_2$ |
| Flow Velocity, behind shock | $U_2=U_\infty$ = 176.29 m/sec | based on $M_s$, $a_1$, $\gamma_1$ |
| Sonic Velocity behind shock | $a_2=a_\infty$ = 515.83 m/sec | $=(\gamma_1 R_1 T_2)^{1/2}$ |
| Flow Mach No. behind shock | $M_2=M_\infty$ = 0.3418 | $=U_2/a_2$ |

Results

| $P_{0c}$ psia | $T_c$ K | $\rho_c$ kg/m$^3$ | $U_c$ m/sec | D.R. $\rho_c/\rho_\infty$ | V.R. $U_c/U_\infty$ | $M_b$ DR*VR |
|---|---|---|---|---|---|---|
| 24.84 | 294.26 | 1.973 | 67.81 | 2.103 | 0.385 | 0.809 |

| | Gauge Location | | | | | | |
|---|---|---|---|---|---|---|---|
| | 1 | 2 | 3 | 4 | 5 | 6 | 7 |
| Measured $q_{avg}$ kW/m$^2$ | 79.3 | 85.0 | 79.5 | 73.6 | 85.5 | 78.0 | 66.4 |
| $q/q_o$ | 0.863 | 1.086 | 1.021 | 1.029 | 1.073 | 1.005 | 1.040 |
| $x/d\ (V.R.)^{-4/3}$ | 13.93 | 21.07 | 27.85 | 34.99 | 55.70 | 73.19 | 108.18 |

## Film Cooling Test (H02)

($P_4$ = 100" Hg gauge, $P_{atm}$ = 28.87 in Hg, $\gamma_4$= 1.400, $\gamma_1$ = 1.498, $R_1$= 499.82, $R_4$ = 287 J/kg-K)

Helium added

Pressure Regulator Setting 16.0 psig

Measured

| | | |
|---|---|---|
| Driver Pressure | $P_4$ = 435.896 kPa | (128.72 in Hg abs) |
| Driven Pressure | $P_1$ = 97.867 kPa | (28.90 in Hg abs) |
| Driver/Driven Temp. | $T_1$=$T_4$ = 296.55 K | (23.4 deg C) |
| Shock Velocity | $U_s$ = 592.67 m/sec | = $\Delta x/\Delta t$ ($\Delta t$ = 1.200 msec) |
| Pressure behind shock | $P_2$ = 167.49 kPa | (24.293 psia) |
| Partial Pressure of Helium | $P_{He}$ = 7.01 psi | |

Calculated

| | | |
|---|---|---|
| Sonic Velocity | $a_1$ = 471.207 m/sec | $=(\gamma_1 R_1 T_1)^{1/2}$ |
| Shock Mach Number | $M_s$ = 1.2578 | $=U_s/a_1$ |
| Theoretical Shock Mach No. | $M_{th}$ = 1.306 | based on $P_4/P_1$, $\gamma_1$, $\gamma_4$, $a_1/a_4$ |
| Temperature behind shock | $T_2$=$T_\infty$ = 355.26 K | based on $M_s$, $\gamma_1$ |
| Press. behind shock, Theor. | $P_2$=$P_\infty$ = 166.19 kPa | based on $M_s$, $\gamma_1$ |
| Density behind shock | $\rho_2$=$\rho_\infty$ = 0.9361 kg/m$^3$ | $=P_2/R_1$-$T_2$ |
| Flow Velocity, behind shock | $U_2$=$U_\infty$ = 174.56 m/sec | based on $M_s$, $a_1$, $\gamma_1$ |
| Sonic Velocity behind shock | $a_2$=$a_\infty$ = 515.75 m/sec | $=(\gamma_1 R_1 T_2)^{1/2}$ |
| Flow Mach No. behind shock | $M_2$=$M_\infty$ = 0.3385 | $=U_2/a_2$ |

Results

| $P_{0c}$ psia | $T_c$ K | $\rho_c$ kg/m$^3$ | $U_c$ m/sec | D.R. $\rho_c/\rho_\infty$ | V.R. $U_c/U_\infty$ | $M_b$ DR*VR |
|---|---|---|---|---|---|---|
| 25.34 | 292.47 | 1.980 | 90.57 | 2.115 | 0.519 | 1.097 |

| | Gauge Location | | | | | | |
|---|---|---|---|---|---|---|---|
| | 1 | 2 | 3 | 4 | 5 | 6 | 7 |
| Measured $q_{avg}$ kW/m$^2$ | 71.5 | 72.7 | 69.0 | 64.8 | 82.1 | 71.7 | 68.8 |
| $q/q_o$ | 0.778 | 0.928 | 0.886 | 0.965 | 1.030 | 0.924 | 1.078 |
| x/d (V.R.)$^{-4/3}$ | 9.353 | 14.15 | 18.71 | 23.50 | 37.41 | 49.16 | 72.67 |

## Film Cooling Test (H03)

($P_4$ = 100" Hg gauge, $P_{atm}$ = 28.96 in Hg, $\gamma_4$= 1.400, $\gamma_1$ = 1.498, $R_1$= 497.75, $R_4$ = 287 J/kg-K)

Helium added

Pressure Regulator Setting 20.0 psig

### Measured

| | | | |
|---|---|---|---|
| Driver Pressure | $P_4$ = 437.525 kPa | (129.201 in Hg abs) | |
| Driven Pressure | $P_1$ = 98.057 kPa | (28.96 in Hg abs) | |
| Driver/Driven Temp. | $T_1$=$T_4$ = 296.55 K | (23.4 deg C) | |
| Shock Velocity | $U_s$ = 591.68 m/sec | | = $\Delta x/\Delta t$ ($\Delta t$ = 1.202 msec) |
| Pressure behind shock | $P_2$ = 167.20 kPa | (24.25 psia) | |
| Partial Pressure of Helium | $P_{He}$ = 6.989 psi | | |

### Calculated

| | | |
|---|---|---|
| Sonic Velocity | $a_1$ = 470.228 m/sec | $=(\gamma_1 R_1 T_1)^{1/2}$ |
| Shock Mach Number | $M_s$ = 1.2583 | $=U_s/a_1$ |
| Theoretical Shock Mach No. | $M_{th}$ = 1.307 | based on $P_4/P_1$, $\gamma_1$, $\gamma_4$, $a_1/a_4$ |
| Temperature behind shock | $T_2$=$T_\infty$ = 355.32 K | based on $M_s$, $\gamma_1$ |
| Press. behind shock, Theor. | $P_2$=$P_\infty$ = 166.67 kPa | based on $M_s$, $\gamma_1$ |
| Density behind shock | $\rho_2$=$\rho_\infty$ = 0.9422 kg/m$^3$ | $=P_2/R_1$-$T_2$ |
| Flow Velocity, behind shock | $U_2$=$U_\infty$ = 174.55 m/sec | based on $M_s$, $a_1$, $\gamma_1$ |
| Sonic Velocity behind shock | $a_2$=$a_\infty$ = 514.72 m/sec | $=(\gamma_1 R_1 T_2)^{1/2}$ |
| Flow Mach No. behind shock | $M_2$=$M_\infty$ = 0.3391 | $=U_2/a_2$ |

### Results

| $P_{0c}$ psia | $T_c$ K | $\rho_c$ kg/m$^3$ | $U_c$ m/sec | D.R. $\rho_c/\rho_\infty$ | V.R. $U_c/U_\infty$ | $M_b$ DR*VR |
|---|---|---|---|---|---|---|
| 26.14 | 289.99 | 2.002 | 114.8 | 2.125 | 0.6579 | 1.398 |

| | Gauge Location | | | | | | |
|---|---|---|---|---|---|---|---|
| | 1 | 2 | 3 | 4 | 5 | 6 | 7 |
| Measured $q_{avg}$ kW/m$^2$ | 64.8 | 72.7 | 65.3 | 64.8 | 80.3 | 75.1 | 64.5 |
| $q/q_o$ | 0.705 | 0.928 | 0.838 | 0.906 | 1.008 | 0.968 | 1.010 |
| $x/d\ (V.R.)^{-4/3}$ | 6.816 | 10.31 | 13.63 | 17.13 | 27.26 | 35.83 | 52.95 |

## Film Cooling Test (H04)

($P_4$ = 101" Hg gauge, $P_{atm}$ = 28.98 in Hg, $\gamma_4$= 1.400, $\gamma_1$ = 1.494, $R_1$= 497.92, $R_4$ = 287 J/kg-K)
Helium added

Pressure Regulator Setting 30.0 psig

**Measured**

| | | |
|---|---|---|
| Driver Pressure | $P_4$ = 439.49 kPa | (129.82 in Hg abs) |
| Driven Pressure | $P_1$ = 98.138 kPa | (28.98 in Hg abs) |
| Driver/Driven Temp. | $T_1$=$T_4$ = 296.55 K | (23.4 deg C) |
| Shock Velocity | $U_s$ = 585.83 m/sec | = $\Delta x/\Delta t$ ($\Delta t$ = 1.214 msec) |
| Pressure behind shock | $P_2$ = 170.05 kPa | (24.663 psia) |
| Partial Pressure of Helium | $P_{He}$ = 6.802 psi | |

**Calculated**

| | | |
|---|---|---|
| Sonic Velocity | $a_1$ = 464.99 m/sec | $=(\gamma_1 R_1 T_1)^{1/2}$ |
| Shock Mach Number | $M_s$ = 1.2599 | $=U_s/a_1$ |
| Theoretical Shock Mach No. | $M_{th}$ = 1.310 | based on $P_4/P_1$, $\gamma_1$, $\gamma_4$, $a_1/a_4$ |
| Temperature behind shock | $T_2$=$T_\infty$ = 355.34 K | based on $M_s$, $\gamma_1$ |
| Press. behind shock, Theor. | $P_2$=$P_\infty$ = 167.20 kPa | based on $M_s$, $\gamma_1$ |
| Density behind shock | $\rho_2$=$\rho_\infty$ = 0.9644 kg/m$^3$ | $=P_2/R_1$-$T_2$ |
| Flow Velocity, behind shock | $U_2$=$U_\infty$ = 173.81 m/sec | based on $M_s$, $a_1$, $\gamma_1$ |
| Sonic Velocity behind shock | $a_2$=$a_\infty$ = 509.00 m/sec | $=(\gamma_1 R_1 T_2)^{1/2}$ |
| Flow Mach No. behind shock | $M_2$=$M_\infty$ = 0.3415 | $=U_2/a_2$ |

**Results**

| $P_{0c}$ psia | $T_c$ K | $\rho_c$ kg/m$^3$ | $U_c$ m/sec | D.R. $\rho_c/\rho_\infty$ | V.R. $U_c/U_\infty$ | $M_b$ DR*VR |
|---|---|---|---|---|---|---|
| 28.433 | 283.37 | 2.056 | 162.7 | 2.132 | 0.9363 | 1.996 |

| | Gauge Location | | | | | | |
|---|---|---|---|---|---|---|---|
| | 1 | 2 | 3 | 4 | 5 | 6 | 7 |
| Measured $q_{avg}$ kW/m$^2$ | 73.9 | 69.6 | 69.5 | 63.8 | 76.9 | 73.5 | 63.8 |
| $q/q_o$ | 0.804 | 0.889 | 0.892 | 0.892 | 0.965 | 0.947 | 1.00 |
| $x/d\ (V.R.)^{-4/3}$ | 4.258 | 6.441 | 8.515 | 10.70 | 17.03 | 22.38 | 33.08 |

## Film Cooling Test (H06)

($P_4$ = 101" Hg gauge, $P_{atm}$ = 29.00 in Hg, $\gamma_4$= 1.400, $\gamma_1$ = 1.495, $R_1$= 490.25, $R_4$ = 287 J/kg-K)

Helium added

Pressure Regulator Setting 40.0 psig

**Measured**

| | | |
|---|---|---|
| Driver Pressure | $P_4$ = 438.32 kPa | (129.44 in Hg abs) |
| Driven Pressure | $P_1$ = 98.195 kPa | (28.997 in Hg abs) |
| Driver/Driven Temp. | $T_1$=$T_4$ = 296.55 K | (23.4 deg C) |
| Shock Velocity | $U_s$ = 583.91 m/sec | = $\Delta x/\Delta t$ ($\Delta t$ = 1.218 msec) |
| Pressure behind shock | $P_2$ = 168.66 kPa | (24.462 psia) |
| Partial Pressure of Helium | $P_{He}$ = 6.85 psi | |

**Calculated**

| | | |
|---|---|---|
| Sonic Velocity | $a_1$ = 466.22 m/sec | $=(\gamma_1 R_1 T_1)^{1/2}$ |
| Shock Mach Number | $M_s$ = 1.2524 | $=U_s/a_1$ |
| Theoretical Shock Mach No. | $M_{th}$ = 1.309 | based on $P_4/P_1$, $\gamma_1$, $\gamma_4$, $a_1/a_4$ |
| Temperature behind shock | $T_2$=$T_\infty$ = 353.74 K | based on $M_s$, $\gamma_1$ |
| Press. behind shock, Theor. | $P_2$=$P_\infty$ = 165.10 kPa | based on $M_s$, $\gamma_1$ |
| Density behind shock | $\rho_2$=$\rho_\infty$ = 0.9520 kg/m$^3$ | $=P_2/R_1$-$T_2$ |
| Flow Velocity, behind shock | $U_2$=$U_\infty$ = 169.63 m/sec | based on $M_s$, $a_1$, $\gamma_1$ |
| Sonic Velocity behind shock | $a_2$=$a_\infty$ = 509.13 m/sec | $=(\gamma_1 R_1 T_2)^{1/2}$ |
| Flow Mach No. behind shock | $M_2$=$M_\infty$ = 0.3332 | $=U_2/a_2$ |

**Results**

| $P_{0c}$ psia | $T_c$ K | $\rho_c$ kg/m$^3$ | $U_c$ m/sec | D.R. $\rho_c/\rho_\infty$ | V.R. $U_c/U_\infty$ | $M_b$ DR*VR |
|---|---|---|---|---|---|---|
| 29.81 | 277.91 | 2.065 | 190.17 | 2.169 | 1.121 | 2.431 |

| | Gauge Location | | | | | | |
|---|---|---|---|---|---|---|---|
| | 1 | 2 | 3 | 4 | 5 | 6 | 7 |
| Measured $q_{avg}$ kW/m$^2$ | 77.1 | 81.9 | 75.3 | 62.6 | 72.8 | 65.1 | 60.5 |
| $q/q_o$ | 0.839 | 1.046 | 0.967 | 0.876 | 0.913 | 0.839 | 0.948 |
| $x/d\ (V.R.)^{-4/3}$ | 3.349 | 5.067 | 6.698 | 8.416 | 13.40 | 17.60 | 26.02 |

## Film Cooling Test (H05)

($P_4$ = 101" Hg gauge, $P_{atm}$ = 28.99 in Hg, $\gamma_4$= 1.400, $\gamma_1$ = 1.495, $R_1$= 484.93, $R_4$ = 287 J/kg-K)

Helium added

Pressure Regulator Setting 50.0 psig

Measured

| | | |
|---|---|---|
| Driver Pressure | $P_4$ = 438.32 kPa | (129.437 in Hg abs) |
| Driven Pressure | $P_1$ = 98.181 kPa | (28.99 in Hg abs) |
| Driver/Driven Temp. | $T_1$=$T_4$ = 296.55 K | (23.4 deg C) |
| Shock Velocity | $U_s$ = 585.83 m/sec | = $\Delta x/\Delta t$ ($\Delta t$ = 1.214 msec) |
| Pressure behind shock | $P_2$ = 170.23 kPa | (24.69 psia) |
| Partial Pressure of Helium | $P_{He}$ = 6.842 psi | |

Calculated

| | | |
|---|---|---|
| Sonic Velocity | $a_1$ = 466.05 m/sec | $=(\gamma_1 R_1 T_1)^{1/2}$ |
| Shock Mach Number | $M_s$ = 1.2570 | $=U_s/a_1$ |
| Theoretical Shock Mach No. | $M_{th}$ = 1.309 | based on $P_4/P_1$, $\gamma_1$, $\gamma_4$, $a_1/a_4$ |
| Temperature behind shock | $T_2$=$T_\infty$ = 354.76 K | based on $M_s$, $\gamma_1$ |
| Press. behind shock, Theor. | $P_2$=$P_\infty$ = 166.41 kPa | based on $M_s$, $\gamma_1$ |
| Density behind shock | $\rho_2$=$\rho_\infty$ = 0.9575 kg/m$^3$ | $=P_2/R_1$-$T_2$ |
| Flow Velocity, behind shock | $U_2$=$U_\infty$ = 172.39 m/sec | based on $M_s$, $a_1$, $\gamma_1$ |
| Sonic Velocity behind shock | $a_2$=$a_\infty$ = 509.74 m/sec | $=(\gamma_1 R_1 T_2)^{1/2}$ |
| Flow Mach No. behind shock | $M_2$=$M_\infty$ = 0.3382 | $=U_2/a_2$ |

Results

| $P_{0c}$ psia | $T_c$ K | $\rho_c$ kg/m$^3$ | $U_c$ m/sec | D.R. $\rho_c/\rho_\infty$ | V.R. $U_c/U_\infty$ | $M_b$ DR*VR |
|---|---|---|---|---|---|---|
| 32.34 | 272.78 | 2.125 | 218.59 | 2.200 | 1.268 | 2.815 |

| | Gauge Location | | | | | | |
|---|---|---|---|---|---|---|---|
| | 1 | 2 | 3 | 4 | 5 | 6 | 7 |
| Measured $q_{avg}$ kW/m$^2$ | 90.0 | 93.4 | 89.0 | 69.6 | 78.4 | 77.6 | 60.4 |
| $q/q_o$ | 0.979 | 1.193 | 1.142 | 0.973 | 0.984 | 1.000 | 0.947 |
| $x/d\ (V.R.)^{-4/3}$ | 2.842 | 4.299 | 5.683 | 7.141 | 11.37 | 14.94 | 22.08 |

## Bibliography


Ammari, H. D., et al. "The Effect of Density Ratio on the Heat Transfer Coefficient From a Film-Cooled Flat Plate," ASME Journal of Turbomachinery, 112: 444-450 (July 1990).

Bird, R. Byron, et al. Transport Phenomena. New York: John Wiley and Sons, Inc., 1960.

Eckert, E. R. G. "Engineering Relations for Friction and Heat Transfer to Surfaces in High Velocity Flow," Journal of the Aeronautical Sciences: 585-587 (August 1955).

Forth, C. J. P., and T. V. Jones. "Scaling Parameters in Film-Cooling," Proceedings of the Eighth International Heat Transfer Conference. 1271-1276. San Francisco: Hemisphere Publishing Corporation, 1986.

Gaydon, A. G., and I. R. Hurle. The Shock Tube in High-Temperature Chemical Physics. New York: Reinhold Publishing Corporation, 1963.

Glass, I. I. Shock Tubes, Part I: Theory and Performance of Simple Shock Tubes. UTIA Review No. 12. Toronto: University of Toronto Institute of Aerophysics, 1958.

Goldstein, R. J., et al. "Film Cooling," Advances in Heat Transfer, 7. New York: Academic Press, 1971.

Gul, Flt Lt Rakhman. Transient Heat Transfer Measurements on a Film Cooled Flat Plate in a Shock Tube. MS Thesis, AFIT/GAE/ENY/91M-4. School of Engineering, Air Force Institute of Technology (AU), Wright-Patterson AFB OH, March 1991 (AD-A319472).

Hall, J. Gordon. Shock Tubes, Part II: Production of Strong Shock Waves; Shock Tube Applications, Design, and Instrumentation. UTIA Review No. 12. Toronto: University of Toronto Institute of Aerophysics, 1958.

Hill, Philip G. and Carl R. Peterson. Mechanics and Thermodynamics of Propulsion (Second Edition). New York: Addison-Wesley Publishing Company, 1992.

Incropera, Frank P. and David P. DeWitt. Fundamentals of Heat Transfer. New York: John Wiley and Sons, Inc., 1981.

John, James E. A. Gas Dynamics (Second Edition). Boston: Allyn and Bacon Inc., 1984.

Jumper, Major Geoffrey W. Film Cooling Effectiveness on a Flat Plate in High Free-stream Turbulence Using a Single Row of 30 Degree Slant-hole Injectors. MS Thesis, AFIT/GAE/AA/87D-7. School of Engineering, Air Force Institute of Technology (AU), Wright-Patterson AFB OH, December 1987 (AD-A190500).

Jurgelewicz, Capt Scott A. Investigation of Heat Transfer With Film Cooling to a Flat Plate in a Shock Tube. MS Thesis, AFIT/GAE/ENY/89D-17. School of Engineering, Air Force Institute of Technology (AU), Wright-Patterson AFB OH, December 1989 (AD-A216379).

Kays, William M. and Michael E. Crawford. Convective Heat and Mass Transfer (Second Edition). New York: McGraw-Hill Book Company, Inc., 1980.

MacMullin, R., et al. "Free-Stream Turbulence From A Circular Wall Jet on a Flat Plate Heat Transfer and Boundary Layer Flow," ASME Journal of Turbomachinery, 111: 78-86 (January 1989).

Mehendale, A. B., et al. "Influence of High Mainstream Turbulence on Leading Edge Heat Transfer," ASME Journal of Heat Transfer, 113: 843-850 (November 1991).

Mirels, Harold. "Boundary Layer Behind Shock or Thin Expansion Wave Moving into Stationary Fluid," NACA TN 3712, 1956.

Scott, C. J. "Transient Experimental Techniques," Measurements in Heat Transfer (Second Edition). Edited by Ernst R. G. Eckert and Richard J. Goldstein. Washington: Hemisphere Publishing Corporation, 1976.

Suo, Mikio. "Turbine Cooling," Aerothermodynamics of Aircraft Engine Components. Edited by Gordon C. Oates. AIAA Education Series. New York: American Institute of Aeronautics and Astronautics, Inc., 1985.

Pederson, D. R., et al. "Film Cooling With Large Density Differences Between the Mainstream and the Secondary Fluid Measured by the Heat-Mass Transfer Analogy," ASME Journal of Heat Transfer, 99: 620-627 (November 1977).

Pietrzyk, J. R., et al. "Effects of Density Ratio on the Hydrodynamics of Film Cooling," ASME Journal of Turbomachinery, 112: 437-443 (July 1990).

Rivir, R. B., et al. "Visualization of Film Cooling Flows Using Laser Sheet Light," Paper No. AIAA-87-1914. New York: American Institute of Aeronautics and Astronautics, 1987.

Rockwell, Capt Richard K. Transient Heat Transfer Measurements on a Flat Plate in Turbulent Flow Using an Electrical Analog. MS Thesis, AFIT/GAE/ENY/89D-31. School of Engineering, Air Force Institute of Technology (AU), Wright-Patterson AFB OH, December 1989 (AD-A216286).

Schlichting, Hermann, Boundary-Layer Theory (Seventh Edition). New York: McGraw-Hill Book Company, Inc., 1979.

Schultz, D.L. and Jones, T.V. Heat Transfer Measurements in Short Duration Hypersonic Facilities. AGARDograph AG-165, February, 1973.

Simonich, J. C. and Bradshaw, P. "Effect of Free Stream Turbulence on Heat Transfer Through a Turbulent Boundary Layer," ASME Journal of Heat Transfer, 100: 671-677 (November 1978).

White, Frank M. Viscous Fluid Flow (Second Edition). New York: McGraw-Hill, Inc., 1991.

## Vita

Captain Thomas A. Eads was born on 10 June 1962 in Salt Lake City, Utah, the son of William A., Sr. and Vivian M. Eads and 9th of 11 children. He graduated from Granger High School in 1980, receiving a 4-year Air Force ROTC scholarship, and attended Brigham Young University, Provo, Utah for one year then Utah State University (USU) in Logan for one year. He completed AFROTC Field Training at McClellan AFB, California then served a mission for The Church of Jesus Christ of Latter-Day Saints for 18 months in Ecuador, South America. Returning to USU, he married Penni Daun Sparks on December 21, 1984. He graduated with a Bachelor of Science degree in Mechanical Engineering, Cum Laude, in March 1988. He had also graduated from the LDS Institute of Religion. As an AFROTC Distinguished Graduate he was commissioned in January 1988. In September 1988 he was assigned as Officer-In-Charge, Mechanical Engineering at the 90th Strategic Missile Wing, Technical Engineering Branch, F. E. Warren AFB, Wyoming, working with the Minuteman and Peacekeeper Missile Systems. He entered the School of Engineering, Air Force Institute of Technology, in May 1991.

Permanent Address: 85 E. 100 N. Dingle, ID 83233

# REPORT DOCUMENTATION PAGE

Form Approved
OMB No. 0704-0188



| 1. AGENCY USE ONLY (Leave blank) | 2. REPORT DATE | 3. REPORT TYPE AND DATES COVERED |
|---|---|---|
| | 30 Nov 92 | Final |

**4. TITLE AND SUBTITLE**

Shock Tube Study of the Effects of Large Density Differences and Blowing Ratio on Heat Transfer to a Film-Cooled Flat Plate

**5. FUNDING NUMBERS**

**6. AUTHOR(S)**

Thomas A. Eads, Capt, USAF

**7. PERFORMING ORGANIZATION NAME(S) AND ADDRESS(ES)**

AFIT/ENY
Wright-Patterson AFB OH 45431

**8. PERFORMING ORGANIZATION REPORT NUMBER**

AFIT/GAE/ENY/92D-25

**9. SPONSORING/MONITORING AGENCY NAME(S) AND ADDRESS(ES)**

Aero Propulsion and Power Directorate
WL/POTC
Wright-Patterson AFB OH 45431

**10. SPONSORING/MONITORING AGENCY REPORT NUMBER**

**11. SUPPLEMENTARY NOTES**

**12a. DISTRIBUTION/AVAILABILITY STATEMENT**

Approved for public release; distribution unlimited.

**12b. DISTRIBUTION CODE**

**13. ABSTRACT** *(Maximum 200 words)*

The effects of coolant-to-mainstream density ratio (D.R.) and mass flux (blowing) ratio ($M_b$) on flat plate heat transfer were investigated in a shock tube. The round-nosed plate has a single row of holes inclined 35 deg downstream with two-diameter lateral spacing and hole length of three diamters. Mixing helium with air in the shock tube produced a D.R. range of 1.2 to 2.1. The parameters studied approach those of film-cooled turbine components. For an $M_b$ range of 0.4 to 3 and 10% mainstream turbulence, heat flux was measured with thin-film heat flux gauges located 4 to 30 hole diameters downstream of the cooling holes using an electrical analog. Various flow conditions were produced over the flat plate. The "steady" portion of turbulent flow heat transfer data compared within 20% of the theoretical flat plate solution. Ratios of heat flux with cooling to heat flux without cooling versus $M_b$ and D.R. were determined. Analysis of the results showed film cooling heat transfer is correlated by coolant-to-mainstream velocity ratio. Effectiveness of cooling was reduced by the high mainstream turbulence.

**14. SUBJECT TERMS**

Film Cooling, Free-stream Turbulence, Heat Transfer, Shock Tube, Turbulent Flow, Density Ratio, Blowing Ratio, Flat Plate, Gas Turbine

**15. NUMBER OF PAGES**

181

**16. PRICE CODE**

| 17. SECURITY CLASSIFICATION OF REPORT | 18. SECURITY CLASSIFICATION OF THIS PAGE | 19. SECURITY CLASSIFICATION OF ABSTRACT | 20. LIMITATION OF ABSTRACT |
|---|---|---|---|
| UNCLASSIFIED | UNCLASSIFIED | UNCLASSIFIED | UL |